Hair Cell Regeneration in the Cristae of the Mouse Vestibular System

Amber D. Slowik

A dissertation

submitted in partial fulfillment of the

requirements for the degree of

Doctor of Philosophy

University of Washington

2015

Reading Committee:

Olivia Bermingham-McDonogh, Chair

David Raible

Bruce Tempel

Program Authorized to Offer Degree:

Neuroscience

University of Washington

Abstract

Hair Cell Regeneration in the Cristae of the Mouse Vestibular System

Amber D. Slowik

Chair of the Supervisory Committee:
Professor Olivia Bermingham-McDonogh
Department of Biological Structure

The sensory modalities of hearing and balance are mediated by the six sensory organs of the inner ear that are each comprised of the same two main cell types, support cells and mechanosensory hair cells. Loss of the sensory hair cells from these organs causes permanent hearing loss and/or balance disorders, as there is currently no therapeutic treatment for hair cell loss. In developing organs, hair cells can be generated through the transdifferentiation of support cells caused by inhibition of the Notch signaling pathway, which is normally required to determine and maintain the precise ratio of hair cells and support cells through lateral inhibition. Although the efficacy of this method declines as the organs mature and Notch signaling is downregulated, previous research has shown that the Notch downstream effector, Hes5, is present in the adult cristae, suggesting that Notch signaling may be active and that the cristae of the adult mouse may retain some regenerative ability. In this dissertation, I tested this hypothesis and showed that Notch signaling is active in the peripheral region of the adult cristae and, using hair cell counts and lineage tracing, that supernumerary hair cells can be generated through inhibition of Notch signaling *in vitro*.

Further, through an analysis of the spatial distribution of hair cell birth in the developing cristae, I showed that there is a correlation between the regions that maintain regenerative competence in the adult and the last regions to exit the cell cycle. In addition, to aid future regenerative studies, I identified a new support cell marker that can be used to lineage trace support cells and have used this marker to characterize spontaneous hair cell regeneration in the adult cristae *in vivo*. I also created standard protocols for lesioning hair cells *in vivo* in two common mouse strains using the known ototoxin 3,3'-Iminodipropionitrile (IDPN) and for quantifiably assaying vestibular behavior in mice with varying degrees of hair cell lesion. Together, this work establishes the previously uncharacterized mouse cristae as an additional model for studying the mechanisms of hair cell regeneration and provides some of the tools necessary for future studies.

TABLE OF CONTENTS

Page

List of Figures v

List of Tables vii

Glossary viii

Acknowledgements xi

Chapter One: Introduction 1

1.1 The Inner Ear 2
1.1.1 Inner Ear Deficits 6
1.1.2 Spontaneous Hair Cell Regeneration 8
1.2 The Canonical Notch Signaling Pathway 9
1.3 The Role of Notch Signaling in Inner Ear Development 12
1.3.1 Lateral Induction 12
1.3.2 Lateral Inhibition 14
1.4 The Role of Notch Signaling in Regeneration of the Inner Ear 18
1.4.1 Regeneration Through Inner Ear Stem Cells 18
1.4.2 Regeneration Through Lateral Induction 19
1.4.3 Regeneration Through Lateral Inhibition 24
1.4.3.1 Organ of Corti 25
1.4.3.2 Utricle 26
1.4.3.3 Crista Ampullaris 29

Chapter Two: Hair Cell Regeneration Through Notch Inhibition in Vitro 31

2.1 Introduction 32
2.2 Results 33
2.2.1 The Cristae Ampullaris 33
2.2.2 Organotypic Cultures of Postnatal and Adult Cristae 35
2.2.3 Notch Signaling is Active in Adult Cristae 38
2.2.4 DAPT-Treatment Increases Total Hair Cell Number 40
2.2.5 New Hair Cells Arise Through Transdifferentiation 48

Page

Chapter Two: Hair Cell Regeneration Through Notch Inhibition in Vitro (cont.)

2.3 Discussion 55
2.3.1 New Evidence for Hair Cell Regeneration in the Cristae 55
2.3.2 The Role of Damage in Notch-Mediated Hair Cell Regeneration 56
2.3.3 Morphological Changes Observed During Transdifferentiation 58
2.3.4 Regional Differences in Hair Cell Regeneration 60

Chapter Three: Spontaneous Hair Cell Regeneration in Vivo 63

3.1 Introduction 64
3.2 Results 66
3.2.1 Screen for Cre Recombinases Expressed in the Inner Ear 66
3.2.2 Recombination in Dcx-CreER Mice is Exclusively in Support Cells 69
3.2.3 Immunolabeling for Endogenous Dcx Expression 70
3.2.4 Characterizing Spontaneous Regeneration After Damage Using the Dcx-CreER Mice 73
3.3 Discussion 78
3.3.1 New Cre recombinase-expressing mouse lines for crista and inner ear studies 78
3.3.2 Spontaneous hair cell regeneration after damage 80

Chapter Four: The Spatial Distribution of Hair Cell Birth in the Cristae 83

4.1 Introduction 84
4.2 Results 86
4.2.1 BrdU Injections to Birthdate Hair Cells 86
4.2.2 Hair Cell Birth on the Medial to Lateral Axis 90
4.2.3 Hair Cell Birth on the Longitudinal X-Axis 94
4.2.4 Differentiation of Hair Cells in Embryonic Inner Ears 97
4.2.5 Support Cell Birth Follows a Similar Pattern 100
4.3 Discussion 102
4.3.1 The Spatial Pattern of Development in the Cristae 102
4.3.2 Regional Differences in Hair Cell Regeneration 104

Page

Chapter Five: Behavioral Assay of Vestibular Deficit in Mice 109

5.1 Introduction 110
5.2 Results 111
5.2.1 Strain differences in hair cell number and efficacy of IDPN lesion ... 111
5.2.2 Measuring vestibular deficit in IDPN-lesioned mice: vestibulo-ocular reflex (VOR) 114
5.2.3 Measuring vestibular deficit in IDPN-lesioned mice: open field test and swim test 117
5.3 Discussion 122

Chapter Six: Discussion and Future Directions 125

6.1 Perspective 126
6.1.1 Spontaneous Hair Cell Regeneration 126
6.1.2 Induced Hair Cell Regeneration 127
6.2 Conclusions 130
6.3 Future Work 133

Chapter Seven: Materials and Methods 139

7.1 Animals and Genotyping 140
7.2 Injections of Pharmacological Agents 143
7.3 Organotypic Cristae Cultures 144
7.4 Immunofluoresence 145
7.5 Paintfill of the Embryonic Inner Ear 148
7.6 Imaging and Processing of Image Files 148
7.7 Analysis of Fluorescent Intensity 149
7.8 Manual Cell Counting 149
7.9 Identifying Lineage-Traced Hair Cells 150
7.10 Normalization of Cristae Position 150
7.11 Analysis of Spatial Patterns of Development 152
7.12 Analysis of Mouse Behavior Using Video Tracking 152
7.13 Quantitative Real-Time Polymerase Chain Reaction 154
7.14 Graphs, Tables, and Statistical Analyses 155

Page

Bibliography **157**

Appendix One: Screen for Cre Recombinases Expressed in the Inner Ear *A1*

A1.1 Screen for Cre Recombinases Expressed in the Inner Ear A2
A1.1.1 Cre Recombinases Expressed Ubiquitously A3
A1.1.2 Cre Recombinases With Interesting Expression A5
A1.1.3 Cre Recombinases Expressed in Hair Cells A8
A1.1.4 Cre Recombinases Expressed in Support Cells A9

Appendix Two: Supplemental Movies *A15*

Movie 1.1 The three-dimensional inner ear A16

Movie 2.1 The three-dimensional crista ampullaris A16
Movie 2.2 Examples of transitional cells: cell 1 ..... A16
Movie 2.3 Examples of transitional cells: cell 2 ..... A17
Movie 2.4 Examples of transitional cells: cell 3 ..... A17

LIST OF FIGURES

Page

Chapter One: Introduction

1.1 The inner ear 2
1.2 Canonical Notch signaling 10
1.3 Notch signaling in the inner ear 13
1.4 Competency for regeneration through Atoh1 overexpression decreases with age 17
1.5 Summaries of regenerative competence through Notch manipulation 20

Chapter Two: Hair Cell Regeneration Through Notch Inhibition in Vitro

2.1 The crista ampullaris 34
2.2 Organotypic cristae cultures 36
2.3 Notch signaling is active in the postnatal and adult cristae 39
2.4 DAPT-treatment increases total hair cell number in postnatal and adult cristae 41
2.5 Hair cells appear to arise through transdifferentiation in postnatal cristae 43
2.6 Most support cells transdifferentiate after DAPT-treatment in postnatal cristae 45
2.7 Hair cells do not arise through proliferation 47
2.8 PLP/CreER lineage trace of support cell fate 49
2.9 Notch inhibition induces transdifferentiation of support cells to hair cells 50
2.10 Examples of lineage-traced transitional cells 52

Chapter Three: Spontaneous Hair Cell Regeneration in Vivo

3.1 Mouse lines with useful expression of Cre recombinase in the crista 67
3.2 Doublecortin antibody staining in Math1-GFP cristae 70
3.3 Support cells recombine in tamoxifen-treated adult Dcx-CreER;Ai14 mice 72
3.4 Spontaneous regeneration in adult CBA/CaJ males after IDPN lesion 74
3.5 Adult Dcx-CreER;Ai14 mice have very little spontaneous regeneration in vivo 76

Chapter Four: The Spatial Distribution of Hair Cell Birth

4.1 Birthdating hair cells using embryonic injections of BrdU 87
4.2 Qualitative group data for all three cristae 89
4.3 Hair cell birth shifts from the medial to lateral regions with age 91
4.4 The pattern of hair cell birth largely does not occur along the longitudinal x-axis 95
4.5 Expression of the hair cell markersMyo6 and Gfi1 in the E14.5 inner ear 98
4.6 Support cells in E12.5 posterior cristae show a similar pattern as hair cells 101
4.7 Summary of the pattern of cell cycle exit in the cristae 106

Page

Chapter Five: Behavioral Assay of Vestibular Deficit in Mice

5.1 Differences in hair cell number and IDPN efficacy in C57BL/6 and CBA/CaJ mice 112
5.2 Measuring the vestibulo-ocular reflex after IDPN lesion 115
5.3 Hyperactivity and circling scale with degree of vestibular deficit in the open field test 118
5.4 Swimming ability decreased with vestibular deficit in a swim test 120

Appendix One: Screen for Cre Recombinases Expressed in the Inner Ear

A1.1 Cre recombinase strains ubiquitously expressed in the inner ear A4
A1.2 Cre recombinase strains with interesting expression patterns A6
A1.3 Cre recombinase strains expressed in hair cells A8
A1.4 Cre recombinase strains expressed in support cells A10

LIST OF TABLES

Page

Table 2.1 Quantification of Gfi1$^+$ hair cells in cristae explants cultured for 5 DIV 42

Table 4.1 The total number of BrdU+ hair cells by age in each crista type 88

Table 4.2 Numerical summary of the number and percentage of BrdU+ hair cells along the z-axis 92

Table 4.3 Statistical summary of the number and percentage of BrdU$^+$ hair cells along the z-axis 93

Table 4.4 Summary of the number of BrdU$^+$ hair cells along the longitudinal x-axis 96

Table 5.1 Numerical summary of the number of Gfi1+ hair cells at varying ages in CBA/CaJ and C57BL/6 mice 113

Table 5.2 Numerical summary of the number and percentage of Gfi1+ hair cells at varying IDPN concentrations 114

Table 7.1 Summary of mouse strains used 140

Table 7.2 Summary of antibodies used.....147

Table 7.3 Summary of qPCR primers used 153

Table A1.1 Summary of the cellular expression of various Cre recombinase mouse lines A2

GLOSSARY

*	Denotes statistical significance where $p \leq 0.05$, unless otherwise noted
**	Denotes statistical significance where $p \leq 0.01$, unless otherwise noted
***	Denotes statistical significance where $p \leq 0.001$, unless otherwise noted
****	Denotes statistical significance where $p \leq 0.0001$, unless otherwise noted
3D	Three-dimensional
4-OHT	4-Hydroxytamoxifen
bHLH	basic helix loop helix transcription factor
bp	Base pairs
BrdU	5-bromo-2'-deoxyuridine, a thymidine analogue
CreER	An inducible Cre recombinase made by fusing the Estrogen receptor to Cre
CreERT2	A second generation version of the CreER inducible fusion protein
DAPT	N-[N-(3,5-Difluorophenacetyl)-L-alanyl]-S-phenylglycine t-butyl ester
DIV	Days *in vitro*
DMSO	Dimethylsulfoxide, a common vehicle for drug delivery
E	Embryonic day (i.e. embryonic day 13 is E13)
EdU	5-Ethynyl-2´-deoxyuridine, a thymidine analogue
ESR	Ectopic sensory region
FACS	Fluorescence activated cell sorting
g	Grams
GER	Greater epithelial ridge
GFP	Green fluorescent protein (also eGFP for enhanced GFP)
ID	Interdental region
IDPN	3,3'-Iminodiproprionitrile
IHC	Inner hair cell
IHC	Immunohistochemistry
ip	Intraperitoneal (a type of injection into the abdominal cavity)
IRES	Internal ribosome entry site
kg	Kilogram

LER	Lesser epithelial ridge
mg	Milligram
mGFP	Membrane bound green fluorescent protein (also mG)
MIP	Maximum intensity projection
mL	Milliliter
mmol	Millimolar
mTomato	Membrane bound Tomato, a red fluorescent protein (also mT)
n	The number of samples
nGFP	Nuclear green fluorescent protein (has a nuclear localization signal)
NICD	Notch intracellular domain
ns	Not significant
OHC	Outer hair cell
P	Postnatal day (i.e. postnatal day 30 is P30)
PBS	Phosphate-buffered saline
RM	Reissner's membrane
qRT-PCR	Quantitative real-time polymerase chain reaction (qPCR/RT-qPCR/RT-PCR)
SC	Support cell
SD	Standard deviation
SE	Standard error of the difference, statistical term related to data values
SE	Sensory epithelium
SEM	Standard error of the mean (statistics)
SEM	Scanning electron microscopy (technique)
TC	Transitioning cell, generally a cell undergoing transdifferentiation
μm	Micrometer (a measure of distance)
μM	Micromolar (a measure of concentration)

ACKNOWLEDGEMENTS

Looking back at my time in graduate school, it's amazing to realize just how many people have helped me along the way. I want to begin by thanking my mentor, Olivia Bermingham-McDonogh. I learned a lot from her and for that I am truly grateful. I also owe a huge debt to my fellow labmates, Toshi Hayashi, Byron Hartman, Vidhya Munnamalai, and Cat Ray, not only for teaching me everything I needed to know, but also for being my friends and making work such an enjoyable place to be. Cat especially kept everything organized and made sure I had everything I needed and Vidhya made sure that I stayed on track and helped me keep my sanity through the stresses of graduate school. I also had the privilege of working with many undergraduates who helped me a great deal, including Katena Koemmpel, Kayla Ritchie, Filippo Artoni, Colby Lea, Dingxiang Luo, and Heather Zebroski.

I also want to thank Jen Chao, Tom Reh, and the members of their labs for all of their advice and support. I especially want to thank Anna La Torre, Deepak Lamba, Yumi Ueki, and Russ Taylor for their help with my projects and Joe Brezinski, Laura Chipman, Jonathan Choi, Francis Concepcion, Kristen Cox, Sean Georgi, Jule Gust, Lauren Hood, Akina Hoshino, Anu Jayabalu, Kaitlen Knight, Drew McUsic, Paul Nakamura, Julia Pollak, Kristin Sternhagen, Jenny Thomas, Matt Wilken, Stefanie Wohl, and Aya Yanagida for their advice and friendship. They made the lab a truly enjoyable place to be and I am very grateful to them for giving me the sense of community and camaraderie that is hard to find in a smaller lab.

My supervisory committee, including Phil Horner, Dave Raible, Billie Swalla, and Bruce Temple, was an amazing asset throughout my time as a graduate student and I can't thank each member enough for their help and support over the years. I know that there are many fantastic faculty at the University of Washington, but I really feel like I had one of the best and most dedicated committees out there.

I also had a lot of support from my various programs and affiliations. Ron Seifert and the Lynn and Mike Garvey Imaging Core in the Institute for Stem Cell and Regenerative Medicine were a great resource that allowed me to take such beautiful images. Linda Robinson provided mice and I'm especially grateful for how amazing she was at her job as her plug dates were always spot on. Ann Wilkinson, Lucia Wisdom, and the Neuroscience Graduate Program made sure that I stayed on track and got everything done on time. Ann especially kept me in line and helped me whenever I needed it. The Cellular and Molecular Biology Training Grant and the Neurobiology Training Grant not only funded my time here, but also helped me to grow as a scientist and a communicator.

Lastly, I'd like to thank all of my friends and family, including some of those already mentioned. They not only supported me and loved me, but they got me through the rough patches and helped to remind me that there's more to my life than my experiments that more often than not were not working.

I think that the most important part of getting my doctorate wasn't the degree, but the realization that so many people believed in me so much. Without each of these people and probably even more, I wouldn't have made it this far. I wish that there were more words to express how grateful I am to all of them, but I'll end with the only words I have. Thank you.

C H A P T E R O N E

INTRODUCTION

Modified and expanded from
Slowik and Bermingham-McDonogh (2013b)

1.1 THE INNER EAR

The mammalian inner ear is composed of six distinct sensory organs that contribute to the sensory modalities of hearing and balance (Figure 1.1A, Supplemental Movie 1.1). The cochlea, containing the sensory organ of Corti, is the only organ of the auditory system (Figure 1.1B, blue), while the vestibular system contains two distinct types of sensory organs, the cristae ampullaris (Figure 1.1B, orange) and the maculae, including the utricular macula and the saccular macula (Figure 1.1B, green). All of the inner ear organs are designed to respond to different types of sensory stimuli and are otherwise fairly similar at the cellular and mechanistic levels. Each organ is comprised of two main cell types that are derived from the same progenitor lineage (Fekete*, et al.,* 1998, Jiang*, et al.,* 2013). The mechanosensory hair

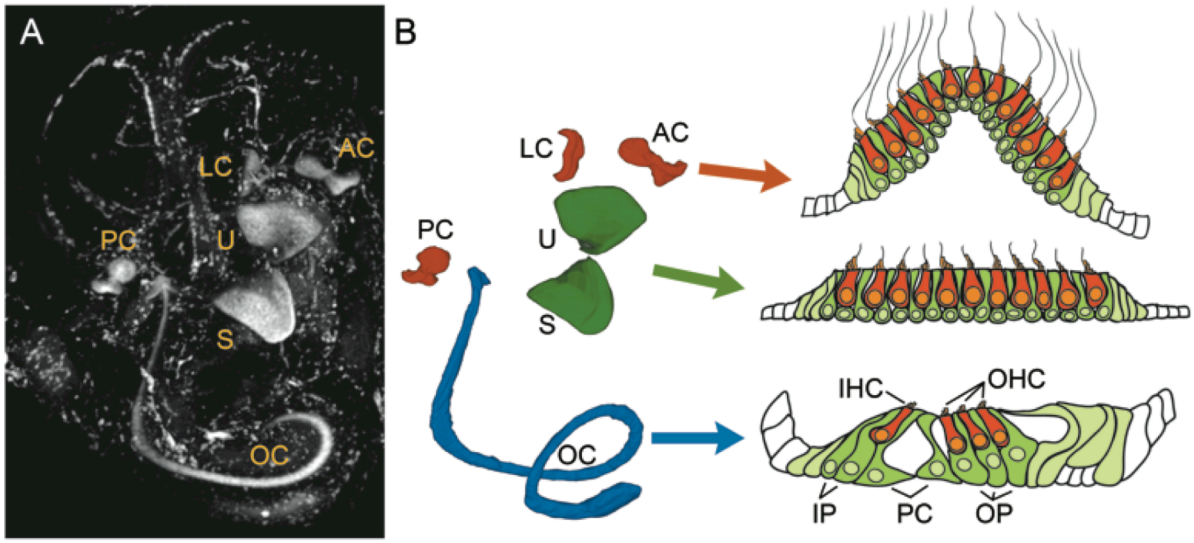

Figure 1.1 The inner ear. **A)** Immunolabeling for Sox2 in an intact E15.5 inner ear shows the location of the sensory organs. LC – lateral crista, AC- anterior crista, PC – posterior crista, U – utricle, S – saccule, OC – organ of Corti. **B)** A color coded model of the position of the Sox2-labeled sensory organs shown in A created by 3-dimensionally rendering tracings of the Sox2 regions in the individual confocal slices. In each of the inner ear organs, hair cells (orange) are arranged above the support cell layer (green). In the organ of Corti, the hair cells and support cells are highly specialized with obvious functional and morphological differences. In the vestibular system, these differences are not as pronounced. IHC – inner hair cell, OHC – outer hair cell, IP – inner phalangeal cell, PC – pillar cell, OP – outer phalangeal cell (Deiters' cell).

cells (Figure 1.1B, orange cells) transduce hearing and balance information through actin-rich stereocilia located on their apical surface. Non-selective mechanosensitive ion channels located at the tips of the stereocilia open in response to direction-specific deflections of the stereocilia allowing for a rapid influx of ions, mainly potassium and calcium, into the cell. This influx causes the cell to depolarize and ultimately results in the release of the neurotransmitter glutamate and the subsequent firing of the neurons in either the spiral ganglion of the auditory system or Scarpa's ganglion of the vestibular system (Fettiplace and Hackney, 2006, Hudspeth, 2008, Kazmierczak and Muller, 2012).

Although the hair cells in each organ are very similar and express a core set of hair cell machinery, there are two distinct types of hair cells in each system. These hair cell types vary in many ways including in their locations, gene expression, nerve innervation, cell shape, stereocilia bundle properties, ultrastructural features, etc. (reviewed in Eatock, *et al.,* 1998). In the cochlea, the inner hair cells (IHCs) and outer hair cells (OHCs) serve distinct functions, which will be discussed below. In the vestibular system, though, it is not clear how the two hair cell types, classified as either type I or type II, differ functionally.

In addition to the hair cells, each organ also contains support cells (Figure 1.1B, green cells). As their name suggests, support cells function in a variety of supportive roles (reviewed in Monzack and Cunningham, 2013) including: structural support, trophic support of the hair cells and the ganglion neurons (Montcouquiol, *et al.,* 1998, Stankovic, *et al.,* 2004, Sugawara, *et al.,* 2005, Gomez-Casati, *et al.,* 2010b, Zuccotti, *et al.,* 2012), development of the patterning and mapping of the organs (Tritsch, *et al.,* 2007, Tritsch and Bergles, 2010), clearance of the neurotransmitter glutamate to prevent excitotoxicity (Furness and Lehre,

1997, Furness and Lawton, 2003, Glowatzki, *et al.,* 2006), potassium recycling to maintain the ionic gradients necessary for the endocochlear potential (Boettger, *et al.,* 2002, Spiess, *et al.,* 2002, Boettger, *et al.,* 2003, Jagger and Forge, 2006), mediation of hair cell death (Gale, *et al.,* 2004, Lahne and Gale, 2008, Lahne and Gale, 2010), phagocytosis and ejection of dying hair cells, and subsequent scar formation to maintain the reticular lamina (Forge, 1985, Cotanche, *et al.,* 1987, Cotanche and Dopyera, 1990, Marsh, *et al.,* 1990, Raphael and Altschuler, 1991, Stone and Cotanche, 1992, Meiteles and Raphael, 1994, Li, *et al.,* 1995, Hirose, *et al.,* 1999, Gale, *et al.,* 2002, Ahmad, *et al.,* 2003, Hirose, *et al.,* 2004, Hordichok and Steyger, 2007, Bird, *et al.,* 2010).

In the cochlea, the support cells are highly differentiated and specialized with distinct morphologies and positions. Inner phalangeal cells surround the inner hair cells, while outer phalangeal cells, also known as Deiters' cells, surround the outer hair cells. In addition, the tunnel of Corti, which is created by the highly specialized inner and outer pillar cells, separates the inner and outer hair cell rows. The support cells of the vestibular system, on the other hand, do not have any specific classifications, as they appear to have a more homogeneous appearance and lack the obvious morphological specializations seen in the auditory system. However, different subpopulations of support cells can be identified by their expression of distinct markers (Hartman, *et al.,* 2009, Gomez-Casati, *et al.,* 2010a) and it is likely that they do have some specialized functions.

In each organ, hair cells and support cells are arranged in a mosaic such that hair cells are surrounded by support cells and rarely are in contact with other hair cells. Further, the cells are organized into pseudostratified layers where hair cell nuclei are always located

apically to the support cell nuclei, which rest near the basement membrane (Figure 1.1B). In the organ of Corti, the hair cells are arranged into rows with one row of inner hair cells that are the primary detectors of sound and three rows of outer hair cells that function primarily as the cochlear amplifier to increase amplitude and frequency sensitivity through a positive feedback mechanism. These rows of hair cells form a tonotopic map along the length of the spiraling cochlea such that higher frequencies are detected by the hair cells in the base of the cochlea and lower frequencies are detected by hair cells in the apex.

In the vestibular system, the two types of organs each have separate functions that together provide the precise information on the location and the movement of the head necessary for balance. The two maculae, the saccule and the utricle, are linear acceleration detectors, which are primarily used for gravity sensation. They sense linear acceleration using heavy calcium carbonate crystals, known as otoconia, that rest on a membrane (known as the otolithic membrane) overlying the hair cells (Figure 1.1B, green). Further, the stereocilia on these hair cells are arranged in specific orientations throughout the organs to allow for detection of linear acceleration in different directions. The three cristae ampullaris detect rotational velocity and acceleration caused by head motions. They are positioned at the base of the semicircular canals and have their stereocilia embedded in a gelatinous membrane known as the cupulla. Fluid motion through the canals caused by rotational head movements results in bidirectional displacements of the cupulla, which allows the cristae to detect these head movements in the three cardinal planes, one for each canal ampulla (Figure 1.1B, orange).

1.1.1 INNER EAR DEFICITS

While there are many causes for inner ear deficits, the focus of this work will be on those caused by hair cell loss. In the organ of Corti, loss of hair cells results in hearing loss, while in the vestibular system it results in balance disorders and vertigo. In both the auditory and vestibular organs, hair cell loss has been correlated with age (Richter*,* 1980, Soucek*, et al.,* 1987, Wright*, et al.,* 1987, Merchant*, et al.,* 2000, Rauch*, et al.,* 2001, Lopez*, et al.,* 2005). For the cochlea in particular, this hair cell loss is in part due to environmental causes such as noise exposure. Other causes for hair cell loss include genetic deficits, such as in Ménière's disease, and drug-related ototoxicity, from drugs such as aminoglycoside antibiotics or chemotherapy drugs such as cisplatin.

For hearing loss, there are many successful therapeutic options available including hearing aids to replace the function of lost outer hair cells by amplifying sound and cochlear implants to replace the function of lost inner hair cells by stimulating the spiral ganglion nerve fibers directly. For vestibular deficits caused by hair cell loss, there are no current effective treatments. Instead, severe vestibular impairment is treated by lesioning the organs and allowing the other ear and/or the cerebellum to compensate for the lost sensory input.

Although hearing deficits gain more public attention than vestibular deficits, perhaps due to the devastating effects of hearing loss on language acquisition and communication and due to the prevalence of hearing aids and cochlear implants in the population, balance disorders and vertigo also pose a very significant health problem. In the elderly, it is thought that balance disorders may account for half of the accidental deaths due to falls. In the 1989 Report of the Task Force on the National Strategic Plan of the National Institute for

Deafness and Communication Disorders (NIDCD) it was estimated that over 90 million Americans aged 17 and over have experienced balance or dizziness problems, resulting in approximately $500 million spent on balance related physician costs in 1976. More recently, in the 2008 National Health Interview Survey conducted by the CDC, 11.4% of all respondents reported a problem with dizziness or balance within the last twelve months. In those aged 65 and above, this incidence was increased to 19.6%, accounting for approximately 7 million people (Lin and Bhattacharyya, 2012). From studies conducted worldwide as well as from meta-analyses, it appears that the prevalence of balance disorders and vertigo could range from 21-30% overall (Neuhauser, *et al.,* 2008, Mendel, *et al.,* 2010) and 36-45% in the elderly (Gopinath, *et al.,* 2009, de Moraes, *et al.,* 2011), which is at a similar level to the incidence of hearing loss in those same populations (Morton, 1991). In addition, balance dysfunction and vertigo have been linked to a decrease in quality of life, characterized by increased sick leave, medical consultations, interruptions to daily life, and increased levels of anxiety, stress, and depression (Neuhauser, *et al.,* 2008, Gopinath, *et al.,* 2009, Mendel, *et al.,* 2010, Lin and Bhattacharyya, 2012).

Approximately a third of all cases of balance dysfunction have a peripheral origin in the vestibular system (Kroenke, *et al.,* 2000, Uno, *et al.,* 2001, Neuhauser, *et al.,* 2008, Gopinath, *et al.,* 2009, Yin, *et al.,* 2009). Many of these cases of peripheral vestibulopathy involve inflammation or displacement of the otoliths and are readily treatable. However, there is no current effective treatment for approximately 19% of those with balance dysfunction where the cause is either unknown or due to a loss of the sensory hair cells from the vestibular organs (Kroenke, *et al.,* 2000). While multiple therapeutic strategies to treat

hair cell loss are currently under investigation, including protection and repair of hair cells as well as vestibular prostheses similar to cochlear implants (Dai*, et al.,* 2011, Lewis*, et al.,* 2013, Phillips*, et al.,* 2014), regenerative therapies would provide the ability to replace already lost hair cells.

1.1.2 SPONTANEOUS HAIR CELL REGENERATION

Robust hair cell regeneration is found in all non-mammalian vertebrates that have been studied thus far (reviewed in Warchol*,* 2011), including fish (Corwin*,* 1981, Corwin*,* 1983, Popper and Hoxter*,* 1984, Popper and Hoxter*,* 1990, Faucher*, et al.,* 2009), amphibians (Lewis and Li*,* 1973, Corwin*,* 1985, Baird*, et al.,* 1993, Baird*, et al.,* 1996, Baird*, et al.,* 2000, Taylor and Forge*,* 2005), reptiles (Avallone*, et al.,* 2003, Avallone*, et al.,* 2008), and birds (Jorgensen and Mathiesen*,* 1988, Roberson*, et al.,* 1992, Weisleder and Rubel*,* 1993, Kil*, et al.,* 1997, Stone*, et al.,* 1999, Stone and Rubel*,* 1999, Matsui*, et al.,* 2000). In these systems, new hair cells are generated either in response to damage or as part of a continuous turnover process to maintain the sensory organs.

In mammals, while there have been some promising results, previous studies have found only limited levels of regeneration in the adult vestibular system. In the saccule and utricle, spontaneous regeneration of hair cells after lesion with aminoglycoside antibiotics has been shown *in vitro* and *in vivo* in the guinea pig (Forge*, et al.,* 1993, Warchol*, et al.,* 1993, Rubel*, et al.,* 1995, Yamane*, et al.,* 1995, Li and Forge*,* 1997, Forge*, et al.,* 1998, Walsh*, et al.,* 2000), gerbil (Ogata*, et al.,* 1999), bat (Kirkegaard and Jorgensen*,* 2000), rat (Meza*, et al.,* 1996, Zheng and Gao*,* 1997, Berggren*, et al.,* 2003, Oesterle*, et al.,* 2003, Taura*, et al.,* 2006), and mouse (Kawamoto*, et al.,* 2009, Lin*, et al.,* 2011, Golub*, et al.,* 2012). In the cristae, all

evidence for spontaneous hair cell regeneration after lesion comes from the chinchilla (Lopez*, et al.,* 1997, Lopez*, et al.,* 1998), where there is also some evidence for proliferating support cells (Tanyeri*, et al.,* 1995) as well as re-innervation of new hair cells by nerve terminals (Lopez*, et al.,* 2003).

Though spontaneous regeneration in the mammalian adult is limited, it may be possible to generate new hair cells through manipulation of the developmental pathways involved in hair cell differentiation. One very promising pathway is Notch signaling (see below), which is necessary during inner ear development for both the specification of the sensory organs ("prosensory") and at a later stage of development for their patterning ("lateral inhibition"). In addition, Notch signaling has been linked to regenerative potential in other systems where adult neurogenesis is possible (Stump*, et al.,* 2002, Aguirre*, et al.,* 2010, Imayoshi*, et al.,* 2010, Lugert*, et al.,* 2010), including the subventricular zone (Givogri*, et al.,* 2006, Andreu-Agullo*, et al.,* 2009, Carlen*, et al.,* 2009) and the hippocampal progenitor zone (Breunig*, et al.,* 2007, Ables*, et al.,* 2010, Ehm*, et al.,* 2010).

1.2 THE CANONICAL NOTCH SIGNALING PATHWAY

The Notch signaling pathway was initially discovered in Drosophila where it earned its name from a mutation that caused notches in the wings of the flies (Wharton*, et al.,* 1985). From this humble beginning, Notch is now recognized as a highly evolutionarily conserved pathway important in the development of most organ systems in many species, including mammals (reviewed in Andersson*, et al.,* 2011).

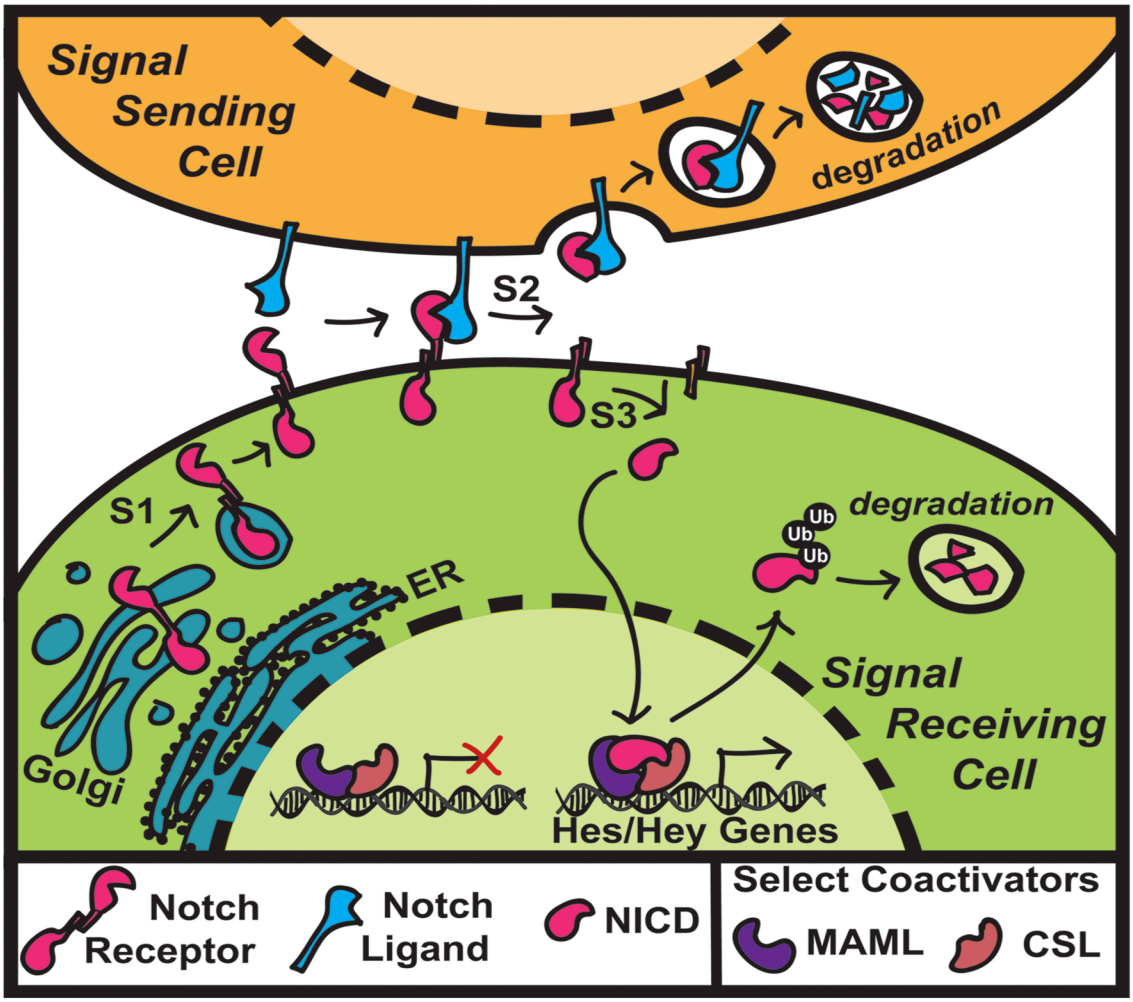

Figure 1.2 Canonical Notch signaling. In the canonical Notch signaling pathway, there are three main proteolytic cleavage events. The furin-mediated S1 cleavage is required to generate the mature form of the Notch receptor, which is then expressed on the cell membrane. Notch ligands expressed on neighboring cells bind to the receptor, which causes a conformational change in the extracellular domain of the receptor. This allows ADAM metalloproteases to perform the extracellular S2 cleavage. The freed extracellular domain bound to the ligand is endocytosed and ultimately degraded by the signal sending cell. The Notch extracellular truncation then undergoes a regulated cleavage at the S3 site by the γ-secretase complex. This cleavage releases the Notch intracellular domain (NICD), which then translocates to the nucleus and forms an active transcriptional complex with CSL and MAML. This leads to the transcription of various Notch effector genes such as the Hes/Hey genes.

In mammals, there are four different Notch receptors, Notch1-4, and five canonical Notch ligands, Jagged1/2 and Dll1/3/4 (Figure 1.2)(Kopan and Ilagan*,* 2009, D'Souza*, et al.,* 2010, reviewed in Andersson*, et al.,* 2011). The Notch receptor is a transmembrane protein with an extracellular domain for ligand binding and an intracellular cytoplasmic domain. Activation of Notch signaling occurs through a series of proteolytic cleavages at different sites on the receptor, known as S1-S3. The S1 cleavage is mediated by furin-like convertases that generate the mature bipartite heterodimeric receptor that consists of an extracellular domain non-covalently bonded to a transmembrane and intracellular domain. Upon binding of the receptor to a ligand, the receptor undergoes conformational changes that expose the S2 cleavage site on the extracellular domain to ADAM metalloproteases. This cleavage results in the release of the extracellular domain, which is then endocytosed and degraded by the ligand-expressing cell along with the bound ligand. The remaining domain, known as the Notch extracellular truncation, then undergoes an intracellular S3 cleavage by the γ-secretase complex, which releases the Notch intracellular domain (NICD) from the membrane. Once released, the NICD translocates into the nucleus and forms an active transcriptional complex with CSL (RBPj-κ) and mastermind-like (MAML) that can recruit additional co-activators and drive transcription of target effector genes, such as the *Hes* and *Hey* genes.

There are many layers of regulation that can occur at each of these different steps along the pathway. Indeed, considering the breadth of function of Notch in different organs and different developmental stages, these would be required in order to generate such diversity from what appears to be a very straightforward pathway. For example, in addition to regulation at each of the proteolytic cleavages, the pathway can be regulated through

modification of the Notch receptors. Glycosylation by Pofut1 and Fringe proteins can change the responsiveness of the receptors to different ligands while the presence of Numb proteins can promote the degradation of the receptors through ubiquitination. Further, the NICD itself can also be regulated through modifications, including phosphorylation, hydroxylation, acetylation, and ubiquitination (reviewed in Andersson*, et al.,* 2011, Moretti and Brou*,* 2013). Thus, this basic signaling pathway very quickly becomes more complicated as the co-expression of specific components and regulators of the pathway in specific domains at different times can greatly change the cellular context of this signaling. Although this work will largely be dealing with a very basic version of Notch signaling as outlined in Figure 1.2, it is important to keep in mind that many of these regulatory mechanisms are likely present even though it is currently unclear how they might be altering Notch signaling in the contexts of inner ear development and regeneration.

1.3 THE ROLE OF NOTCH SIGNALING IN INNER EAR DEVELOPMENT

1.3.1 LATERAL INDUCTION

The earliest known role of Notch signaling in the development of the sensory organs of the inner ear is in the specification of the regions that will become the various sensory organs, i.e. the prosensory domains. This phenomenon is generally referred to as prosensory specification (Kiernan*, et al.,* 2001, Brooker*, et al.,* 2006, Kiernan*, et al.,* 2006, Hayashi*, et al.,* 2008, Pan*, et al.,* 2010, Basch*, et al.,* 2011, Yamamoto*, et al.,* 2011, Hao*, et al.,* 2012) (reviewed in Cotanche and Kaiser*,* 2010, Murata*, et al.,* 2012, Kiernan*,* 2013). In brief, an early loss of Notch signaling either in Notch mutants or through pharmacological inhibition results in absent or smaller sensory domains with an overall decrease in both hair cells and support

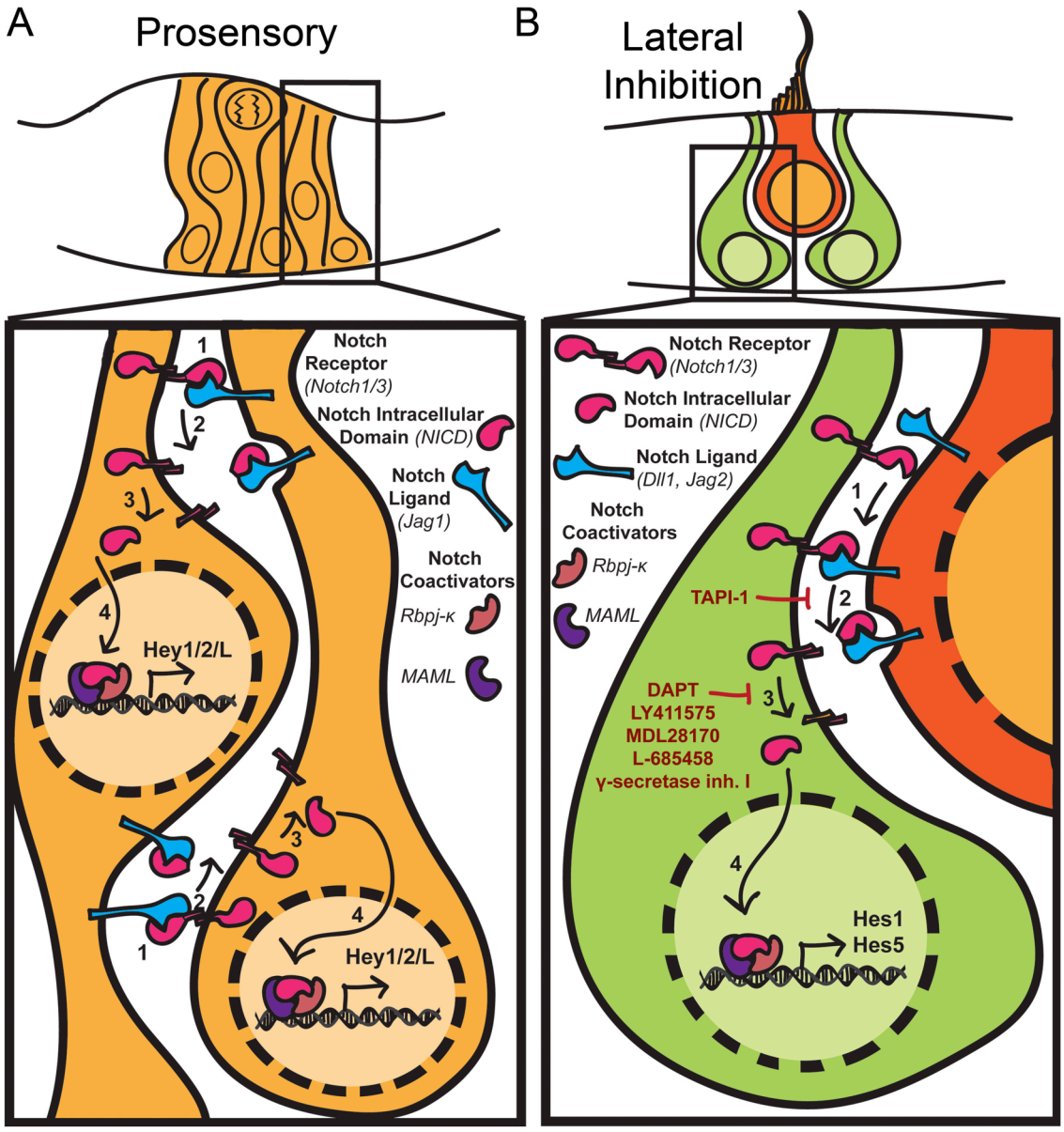

Figure 1.3 Notch signaling in the inner ear. **A)** During the development of the prosensory domains, progenitors express the Notch ligand Jag1 and have reciprocal signaling such that Notch is broadly activated throughout the prosensory domain. In these progenitors, Notch signaling appears to act through the Hey family of Notch effectors as inhibition of Notch signaling during the prosensory phase results in a down-regulation of Hey1 and Hey2. **B)** Later in development, as hair cells differentiate they begin to express the Notch ligands Dll1 and Jag2. These ligands then bind to the Notch receptors on the surrounding cells, where Notch signaling is then activated. Here Notch signaling appears to largely act through Hes1 and Hes5 in order to inhibit the proneural bHLH, Atoh1, and prevent the cells from differentiating into hair cells. Through this mechanism, hair cells, become surrounded by support cells, forming a mosaic-like pattern in each of the sensory organs. Common inhibitors of the S2 and S3 cleavages are depicted in red.

cells. Since initially the expression of markers for the prosensory domain appear normal, it seems that Notch signaling is required in these early stages to establish the proper domain size and/or to maintain the prosensory domains (Figure 1.3A). This could in part be mediated through Notch-induced proliferation of the sensory progenitors as was shown in a study generating ectopic sensory regions through transient NICD overexpression (Pan*, et al.,* 2013). This phenomenon has been called "lateral induction," similar to the classic role of Notch signaling described below called lateral inhibition. When Notch ICD is experimentally activated in non-sensory regions of the inner ear, cells with the activated Notch, as well as their immediate neighbors, acquire a sensory identity. These neighboring cells are therefore thought to acquire a sensory identity via "lateral induction."

1.3.2 LATERAL INHIBITION

The more classic role of Notch signaling, lateral inhibition, occurs after prosensory specification and is important in establishing the mosaic-like pattern of hair cells and support cells where hair cells are surrounded by support cells and, in general, do not contact one another in the mature organs (Figure 1.1B). This role has been well established in embryonic and early postnatal animals in both the auditory system (Lanford*, et al.,* 1999, Zhang*, et al.,* 2000, Zheng*, et al.,* 2000, Zine*, et al.,* 2001, Kiernan*, et al.,* 2005, Brooker*, et al.,* 2006, Yamamoto*, et al.,* 2006, Takebayashi*, et al.,* 2007, Hayashi*, et al.,* 2008, Doetzlhofer*, et al.,* 2009, Zhao*, et al.,* 2011, Du*, et al.,* 2013, Korrapati*, et al.,* 2013, Mizutari*, et al.,* 2013) and the vestibular system (Zheng*, et al.,* 2000, Zine*, et al.,* 2001, Collado*, et al.,* 2011, Du*, et al.,* 2013) (reviewed in Cotanche and Kaiser*,* 2010, Murata*, et al.,* 2012, Kiernan*,* 2013). For lateral inhibition, Notch signaling acts through effectors to inhibit proneural basic helix loop

helix (bHLHs) transcription factors. This in turn keeps Notch expressing cells from differentiating into neuronal cell types. In the inner ear, developing hair cells express the Notch ligands Delta1 (Dll1) and Jagged2 (Jag2) that bind to the Notch receptors on the surrounding cells (Figure 1.3B). The resulting release of the NICD in these cells ultimately leads to the up-regulation of the effectors Hes1 and Hes5, which results in the inhibition of the bHLH transcription factor Atoh1 (also known as Math1 in mice), which is essential for hair cell formation.

Atoh1 is the earliest known hair cell marker and its expression begins a transcriptional cascade necessary for hair cell differentiation (Bermingham*, et al.,* 1999, Chen*, et al.,* 2002). Developmentally, most but not all inner ear cells that express Atoh1 will go on to become hair cells. This has been demonstrated using both Atoh1 lineage tracing and Atoh1 overexpression. Using an inducible *Cre* recombinase strategy to lineage trace Atoh1-expressing cells, Driver*, et al.* (2013) found that in embryonic day 13 (E13) cochleae cultured for 1 day *in vitro* (DIV, E13+1DIV), 70% of lineage-traced cells that had expressed Atoh1 became hair cells. This number increased to 98.5% in E17+1DIV cochleae. Further, misexpression of Atoh1 into competent regions both in and near the developing sensory organs, such as the greater epithelial ridge (GER) and Kölliker's organ can induce ectopic hair cells that mature and can even become innervated by nerve fibers (Zheng and Gao*,* 2000, Zheng*, et al.,* 2000, Shou*, et al.,* 2003, Woods*, et al.,* 2004, Gubbels*, et al.,* 2008, Kelly*, et al.,* 2012, Liu*, et al.,* 2012a).

The ability of Atoh1 to cause an irreversible hair cell fate choice, either in development or in overexpression studies, is likely linked to the level of Atoh1 expression

and its ability to autoregulate its own promoter (Helms*, et al.,* 2000). In the immature cochlea, the transdifferentiation of pillar cells and Deiters' cells induced by overexpression of Atoh1 required activation of endogenous Atoh1 expression, likely through activation of this autoregulatory feedback mechanism (Liu*, et al.,* 2012a). In addition, Atoh1 has several known enhancer sites (Helms and Johnson*,* 1998, Helms*, et al.,* 2000) as well as multiple known repressors and activators under the control of multiple signaling pathways (reviewed in Mulvaney and Dabdoub*,* 2012).

Modulation of Notch signaling can alter the fate of Atoh1-expressing cells. For example, in the study by Driver*, et al.* (2013), inhibition of Notch signaling using the γ-secretase inhibitor, N-[N-(3,5-Difluorophenacetyl)-L-alanyl]-S-phenylglycine t-butyl ester (DAPT), resulted in more lineage-traced hair cells, while Notch activation using Dll1-Fc shifted the fate of the lineage-traced cells from that of hair cells to support cells. Further, overexpression of the Notch effector Hes1 with Atoh1 in early postnatal cochleae reduces or abolishes the increase in ectopic hair cells seen with Atoh1 overexpression alone (Zheng*, et al.,* 2000). Conversely, DAPT treatment after Atoh1 overexpression in cultured cochleae from postnatal day 2 (P2) mice results in even more ectopic hair cells than Atoh1 or DAPT treatment alone (Kelly*, et al.,* 2012).

These effects are also seen in the zebrafish inner ear and the chicken basilar papilla. In the developing zebrafish, overexpression of the NICD results in a loss of Atoh1a and Atoh1b expression, thereby blocking hair cell formation (Millimaki*, et al.,* 2007). In the post hatch chick, DAPT treatment increases the number of Atoh1-expressing cells and ultimately the number of hair cells expressing Myosin6 (Myo6) (Lewis*, et al.,* 2012).

Since Atoh1 expression possesses the ability to induce hair cell differentiation even in non-sensory regions, many groups are investigating the use of Atoh1 overexpression to regenerate hair cells (reviewed in Mulvaney and Dabdoub, 2012). However, thus far there has been limited success using this method in mature organs since the ability to generate ectopic hair cells through Atoh1 overexpression appears to be limited not only regionally but also temporally; for example, Atoh1 overexpression in P14 mouse cochleae does not induce ectopic hair cells as it does in younger organs (Figure 1.4) (Kelly, *et al.,* 2012, Liu, *et al.,* 2012a).

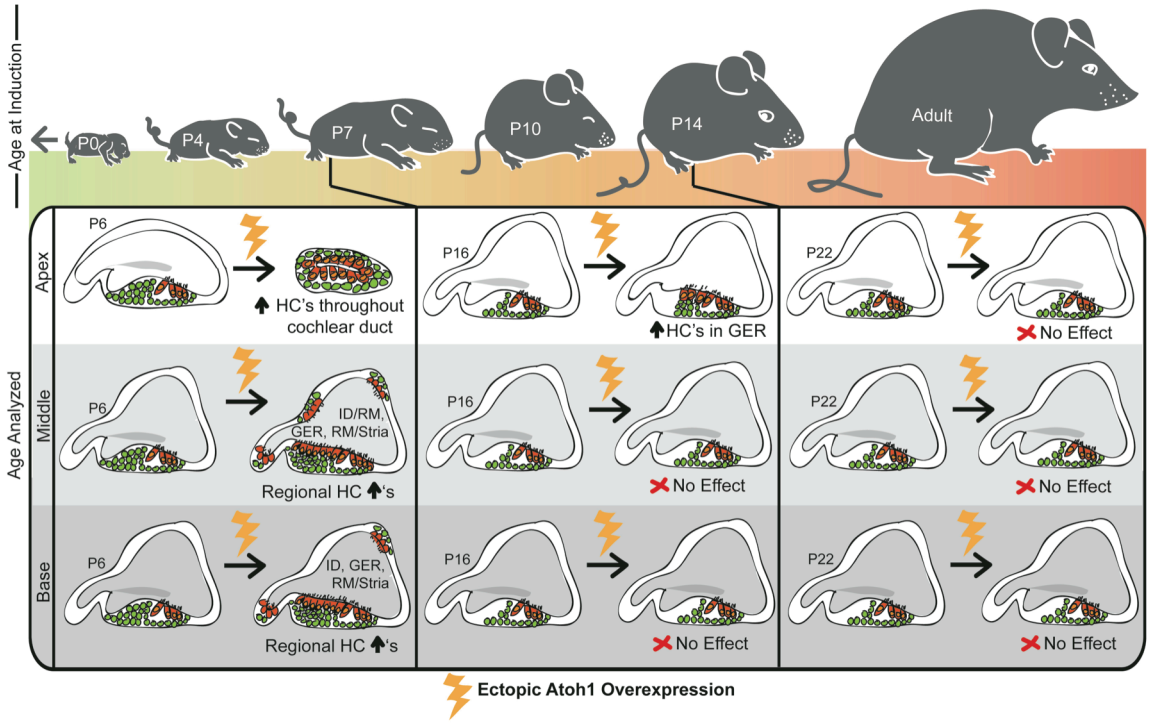

Figure 1.4 The ability to generate hair cells through Atoh1 overexpression is gradually lost as the inner ear matures. Atoh1 overexpression in the very apical portion of neonatal animals can induce ectopic hair cells throughout the entire cochlear duct, while in the middle and basal regions ectopic hair cells are induced in specific areas near the sensory domain. After a week of age, ectopic hair cells are only generated in the GER of the apical portion of the cochlea and later, Atoh1 overexpression either ectopically or in support cells specifically has no effect.

1.4 THE ROLE OF NOTCH SIGNALING IN REGENERATION OF THE INNER EAR

The importance of Notch signaling in defining the development of the sensory epithelium and in determining the precise ratio of hair cells and support cells has naturally led to speculation that it may play a role during regeneration. Several labs have used different approaches to manipulate Notch signaling in order to regenerate hair cells (Hori*, et al.,* 2007, Savary*, et al.,* 2008, Hartman*, et al.,* 2010, Pan*, et al.,* 2010, Basch*, et al.,* 2011, Collado*, et al.,* 2011, Jeon*, et al.,* 2011, Lin*, et al.,* 2011, Liu*, et al.,* 2012b, Jung*, et al.,* 2013, Mizutari*, et al.,* 2013, Pan*, et al.,* 2013). These approaches include (1) modulation of Notch signaling in the culturing and differentiation of inner ear stem cells in order to increase hair cell yield, (2) activation of Notch signaling in order to promote the formation of ectopic sensory regions in normally non-sensory regions within the inner ear, and (3) inhibition of Notch signaling to disrupt lateral inhibition, thereby relieving the inhibition on Atoh1 by Notch effectors and allowing Notch-expressing support cells to transdifferentiate into hair cells.

1.4.1 REGENERATION THROUGH INNER EAR STEM CELLS

Since Notch signaling has several important developmental roles *in vivo,* it is not surprising that it would be important in the growth and differentiation of inner ear stem and progenitor cells. In the *in vivo* cochlea, Pan*, et al.* (2013) showed that Notch signaling plays a role in the proliferation of sensory progenitors. By transiently overexpressing the NICD, they found that ectopic sensory regions formed in non-sensory areas near the cochlea. Using

expression of eGFP to lineage trace the cells that had overexpressed NICD, they found that the eGFP-positive regions were larger in the NICD-expressing cochleae than the controls and that they also expressed pHistone-H3, a marker of mitosis. Overall, this suggested that the NICD-overexpressing cells were proliferating. A similar result was observed in progenitors isolated from early postnatal mouse cochleae and treated with Jagged1-Fc to activate Notch signaling. Treatment with Jagged1-Fc resulted in more secondary inner ear spheres and overall larger spheres than in controls. In addition, it increased the capacity for self-renewal of the progenitors and ultimately resulted in increased numbers of Myo7a-positive hair cells after differentiation (Savary*, et al.,* 2008). Further, consistent with Notch signaling's role in lateral inhibition, inhibition of Notch signaling with the γ-secretase inhibitor L-685458 in inner ear spheres created from early postnatal utricles increased the number of hair cells expressing Myo7a and the Atoh1-nGFP reporter. These hair cells were generated at the expense of support cells, identified by their expression of $p27^{Kip1}$, Sox2, and Jag1 (Jeon*, et al.,* 2011). Therefore, it appears as if Notch may be able to increase hair cell yield in stem cell differentiation by 1) increasing the proliferation and self-renewal of the stem cells to increase overall yield and by 2) increasing the proportion of cells that differentiate as hair cells as opposed to support cells.

1.4.2 REGENERATION THROUGH LATERAL INDUCTION

As noted above, the phenomenon of lateral induction and prosensory specification by Notch signaling has provided an additional approach to use this receptor to promote hair cell regeneration. This approach aims to regenerate hair cells by producing ectopic sensory regions complete with both hair cells and support cells. By overexpressing the NICD,

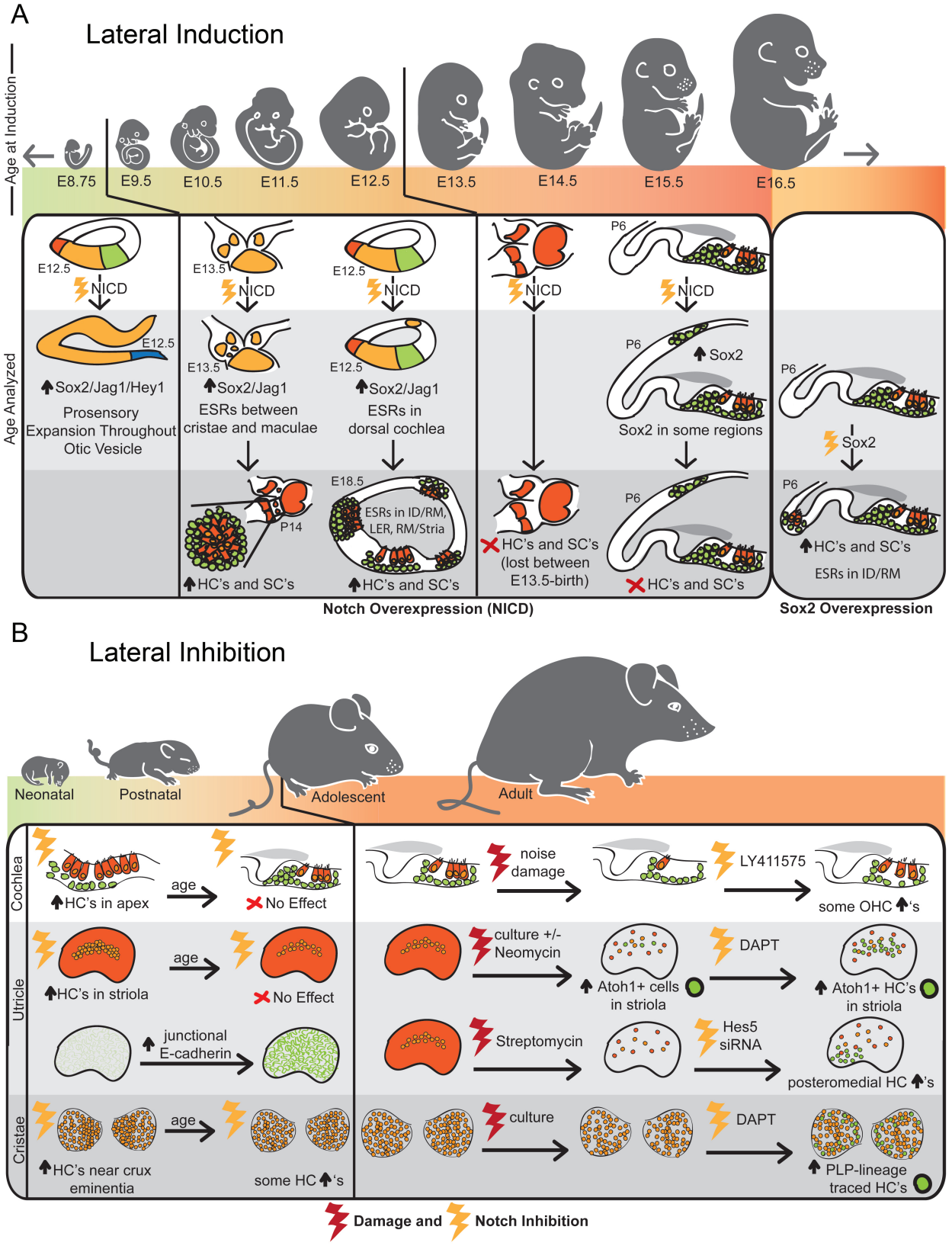
A
Lateral Induction
Age at Induction
E8.75
E9.5
E10.5
E11.5
E12.5
E13.5
E14.5
E15.5
E16.5
Age Analyzed
NICD
Sox2/Jag1/Hey1
Prosensory Expansion Throughout Otic Vesicle
Sox2/Jag1
ESRs between cristae and maculae
ESRs in dorsal cochlea
HC's and SC's
ESRs in ID/RM, LER, RM/Stria
HC's and SC's (lost between E13.5-birth)
Sox2
Sox2 in some regions
HC's and SC's
ESRs in ID/RM
Notch Overexpression (NICD)
Sox2 Overexpression
B
Lateral Inhibition
Neonatal
Postnatal
Adolescent
Adult
Cochlea
Utricle
Cristae
HC's in apex
age
No Effect
noise damage
LY411575
some OHC 's
HC's in striola
culture +/- Neomycin
Atoh1+ cells in striola
DAPT
Atoh1+ HC's in striola
junctional E-cadherin
Streptomycin
Hes5 siRNA
posteromedial HC 's
HC's near crux eminentia
some HC 's
culture
PLP-lineage traced HC's
Damage and Notch Inhibition

Figure 1.5 Summaries of the regenerative competence of the inner ear organs in response to Notch activation for lateral induction (A) and Notch inhibition for lateral inhibition (B). **A)** The ability to form ectopic sensory regions in response to Notch activation (NICD overexpression) is gradually lost embryonically and occurs in a similar developmental timeframe as the normal prosensory formation. With age, the competence of the otic cells is restricted to specific regions near the sensory organs until it is completely lost by E16.5. Overexpression of Sox2 at this same age, however, can induce ectopic sensory regions, though still only in specific areas. **B)** While supernumerary hair cells can be generated much later using Notch inhibition, each of the inner ear organs exhibits a declining competence for hair cell regeneration during postnatal maturation. In the cochlea and utricle, it appears that Notch signaling has no effect in adolescent mice without significant damage to the organs. However, with damage, each of the organs does appear to have a modest capacity for hair cell generation in the adult.

ectopic sensory patches can be generated in non-sensory regions of both the developing cochlear duct (Pan*, et al.,* 2010, Liu*, et al.,* 2012b, Pan*, et al.,* 2013) and the developing vestibular system (Hartman*, et al.,* 2010, Liu*, et al.,* 2012b). The ectopic patches that form express normal markers for hair cells and support cells. Further, the hair cells in these ectopic patches can mature and develop stereocilia bundles, acquire innervation by Tuj1-positive neurites, express synaptic markers, and develop Calretinin-positive calyces (Hartman*, et al.,* 2010, Liu*, et al.,* 2012b, Pan*, et al.,* 2013). However, the ability to induce these ectopic sensory regions appears to be limited to a specific early period in development.

Using Notch overexpression, initially, every cell in the otic vesicle is competent to become prosensory in response to Notch. Constitutive overexpression of the NICD using Foxg1-Cre, which is expressed as early as E8.75, results in an expansion of the prosensory domains throughout the entire otic vesicle (Hartman*, et al.,* 2010, Pan*, et al.,* 2010). Later in development, between E9.5 and E11.5, this competence is then restricted regionally to specific zones near the normal sensory areas, including between the maculae and cristae in the vestibular system and along the entire length of the cochlea in the interdental region, Reissner's membrane, the LER, and the region of the stria vascularis (Pan*, et al.,* 2010, Liu*, et al.,* 2012b, Pan*, et al.,* 2013). Even later in development, between E13.5 and E16.5, Notch overexpression can induce ectopic Sox2 expression, but does not result in the formation of ectopic sensory regions (Basch*, et al.,* 2011, Liu*, et al.,* 2012b, Pan*, et al.,* 2013). Interestingly, overexpression of Sox2 itself, which is directly downstream of Notch (Ehm*, et al.,* 2010), is able to produce ectopic sensory regions at E16.5, past the limit for NICD overexpression (Pan*, et al.,* 2013). However, ectopic sensory regions were only generated in specific areas,

such as the interdental region, suggesting that the competence for Sox2-induction may also be decreasing with age.

The decrease in the ability to generate ectopic sensory regions through either NICD- or Sox2-overexpression may be a reflection of the changing role of Notch signaling in inner ear development during this same period. While it is not currently clear how this change is being mediated in the inner ear mechanistically, it does appear that different Notch ligands are involved in the two processes. Jag1 is expressed early in the prosensory domains and its loss results in a decrease in outer hair cells in the cochlea and in smaller or absent vestibular organs (Lanford*, et al.,* 1999, Kiernan*, et al.,* 2001, Brooker*, et al.,* 2006, Kiernan*, et al.,* 2006, Murata*, et al.,* 2006, Pan*, et al.,* 2010, Basch*, et al.,* 2011, Hao*, et al.,* 2012, Murata*, et al.,* 2012). Later, as hair cells differentiate, Dll1 and Jag2 are expressed in hair cells and loss of these genes results in a lateral inhibition phenotype with supernumerary hair cells generated at the expense of support cells (Lanford*, et al.,* 1999, Kiernan*, et al.,* 2005, Brooker*, et al.,* 2006). This is particularly interesting as it has been shown that glycosylation of the Notch receptor by Pofut1 and then subsequently by Fringe proteins can reduce the responsiveness of the Notch receptor to Jag1 while potentiating its interactions with Dll1 (Hicks*, et al.,* 2000, Kato*, et al.,* 2010). In the cochlea, Lunatic fringe (Lfng) is present in the support cells at the appropriate time to increase their responsiveness to the Dll1-expressing hair cells (Zhang*, et al.,* 2000, Korrapati*, et al.,* 2013). Further, Pofut1 conditional knockouts do not show a prosensory phenotype, but later exhibit supernumerary hair cells consistent with a loss of Notch signaling's lateral inhibition role (Basch*, et al.,* 2011). This is probably not the only regulatory change occurring as there also appears to be differences in the effectors

transcribed in response to Notch signaling as well as specific expression of different effectors in different cell types and regions (Yamamoto*, et al.,* 2006, Takebayashi*, et al.,* 2007, Hayashi*, et al.,* 2008, Doetzlhofer*, et al.,* 2009, Collado*, et al.,* 2011, Lin*, et al.,* 2011, Jung*, et al.,* 2013, Korrapati*, et al.,* 2013, Mizutari*, et al.,* 2013). These types of transcriptional changes could be due to posttranslational modifications to the NICD, which we are only now beginning to understand. For example, it has been shown that phosphorylation of the ICD of the Notch2 receptor can inhibit its ability to induce specific effectors, such as Hes1 (Espinosa*, et al.,* 2003). This type of mechanism could be partly responsible for the inability of the NICD-overexpression to induce sufficient Sox2 levels for full sensory specification.

While overall, this approach to generating hair cells has been very promising, in order for this strategy to be viable for hair cell regeneration in mature organs, it will be important to determine the mechanisms that limit the spatial and temporal competence of the inner ear regions, which is likely linked to the mechanisms mediating the change between prosensory specification and lateral inhibition.

1.4.3 REGENERATION THROUGH LATERAL INHIBITION

The third approach that has been used to regenerate hair cells by modulating Notch signaling is in some ways analogous to the mechanism for hair cell regeneration and turnover that is found in nonmammalian vertebrates. For example, in the vestibular organs of the chick, hair cells are continuously being replaced, or turned over (Roberson*, et al.,* 1992). In this system, support cells require Notch signaling in order to maintain their support cell phenotype and Notch inhibition induces support cells to proliferate and to differentiate into hair cells. In other organs, such as the chick basilar papilla and the zebrafish lateral line,

Notch signaling is not maintained in the healthy, mature organ and is therefore not required to maintain the support cell fate. In these healthy organs, Notch inhibition has no effect on hair cell or support cell numbers. Instead, Notch pathway genes are up-regulated in response to damage and then subsequent Notch inhibition leads to an overproduction of hair cells. In fish this increase in hair cells is due to increased support cell proliferation (Ma*, et al.,* 2008), while in birds the increase in hair cells after Notch inhibition occurs via transdifferentiation of the support cells into hair cells (Daudet*, et al.,* 2009).

1.4.3.1 Organ of Corti

In the mammalian organ of Corti, Notch signaling is still active in newborn mice, and inhibition of Notch with γ-secretase inhibitors leads to an increase in hair cell numbers via transdifferentiation from support cells. However, Notch ligands are down-regulated within the first few days after birth (Hartman*, et al.,* 2007) and the organ of Corti loses its ability to generate supernumerary hair cells in response to Notch inhibition (Lanford*, et al.,* 1999, Zine*, et al.,* 2001, Murata*, et al.,* 2006, Yamamoto*, et al.,* 2006, Hayashi*, et al.,* 2008, Doetzlhofer*, et al.,* 2009, Hartman*, et al.,* 2009, Basch*, et al.,* 2011, Zhao*, et al.,* 2011). Nevertheless, in more mature cochlea, some reports suggest that the Notch pathway can be up-regulated in response to damage. While Hartman*, et al.* (2009) failed to find evidence for expression of a Notch pathway reporter (using transgenic mice expressing eGFP under the *Hes5* promoter) after damage with a high dose of the ototoxic aminoglycoside antibiotic kanamycin (1g/kg) followed by furosemide (400 mg/kg), Mizutari*, et al.* (2013) reported that hair cell damage from exposure to 8-16 kHz octave band noise induced *Hes5* expression as shown by RT-qPCR. Further, in guinea pig cochleae damaged with kanamycin (500 mg/kg)

followed by ethacrynic acid, Hori*, et al.* (2007) showed an increase in Jagged1 in support cells while both Jagged1 and Notch1 were up-regulated in inner sulcus cells.

If Notch signaling is re-established after certain types of damage in the cochlea, then the approaches to stimulate hair cell regeneration through Notch inhibition and transdifferentiation might be effective in this organ. Support for this possibility comes from two studies. Notch inhibition using the γ-secretase inhibitor LY411575 causes an increase in outer hair cells derived from support cells in the noise damaged cochlea, consistent with transdifferentiation (Mizutari*, et al.,* 2013). In addition, in the guinea pig, occasional ectopic hair cells were found in the inner sulcus after 14 days of Notch inhibition with the γ-secretase inhibitor, MDL28170 (Hori*, et al.,* 2007). Therefore, under the appropriate damage conditions, some mammalian species are able to express Notch signaling components after hair cell damage, and the modulation of Notch signaling could provide an approach to stimulate hair cell transdifferentiation leading to some functional recovery from the damage.

1.4.3.2 Utricle

While Notch signaling is not found in the mature undamaged cochlea, Hartman*, et al.* (2009) found that Hes5-eGFP (from the transgenic mice) and *Hes5* mRNA (by *in situ* hybridization) are expressed in the undamaged vestibular organs of adult mice. In the mature utricle, Hes5 is expressed in some of the support cells of the medial posterior region, suggesting that Notch inhibition may be able to induce these support cells to transdifferentiate. While this suggests that the mature utricle may possess the ability to generate supernumerary hair cells in response to Notch inhibition without damage, this

remains untested since the studies to date have all included a damage component, either by design or due to the damage incurred during culture of the utricle *in vitro*. It is then also unclear whether Notch components are further up-regulated after hair cell damage, though it has been shown in cultured utricles that DAPT treatment results in decreased expression of *Hes1*, *Hey1*, and *HeyL* as compared to DMSO controls (Lin*, et al.,* 2011).

Despite agreement that Notch signaling continues in the vestibular system into adulthood, there are conflicting results as to whether inhibitors of Notch can stimulate hair cell transdifferentiation from support cells in the mouse utricle. Collado*, et al.* (2011) reported no evidence for hair cell regeneration (Myosin7a-positive and E- cadherin-negative cells) in utricles explanted from P16 and older Swiss Webster mice cultured with 50 uM DAPT for up to 10 days *in vitro*. Conversely, Lin*, et al.* (2011) found an increase in Atoh1-positive cells overall and in Atoh1-positive cells that also expressed Myo7a and phalloidin in the striolar and juxtastriolar regions of utricles explanted from 6-9 week old Swiss Webster mice cultured with 50 uM DAPT for up to 18 days *in vitro*. From these results, the authors infer that Notch inhibition is not only increasing the number of cells that express Atoh1, but is also promoting the differentiation of these cells into mature hair cells. This is similar to the result in the postnatal cochlea where overexpression of Atoh1 in conjunction with DAPT treatment generated more hair cells than either Atoh1-up-regulation or DAPT treatment alone (Kelly*, et al.,* 2012). Lastly, using a streptomycin lesion paradigm followed by treatment with *Hes5* siRNA in utricles of 3-4 week old CD1 mice, Jung*, et al.* (2013) found an increase in Myo7a-positive hair cells in the treated utricles *in vivo* 3 weeks after lesioning. These

regenerated hair cells were located in the medial posterior utricle, which is appropriately where Hartman*, et al.* (2009) showed that Hes5 is expressed in the mature utricle.

While both of these studies demonstrate that the mature utricle has the capacity for modest hair cell regeneration after damage, these studies displayed stark differences in the regions of regeneration and the changes in Notch effectors. The study by Jung*, et al.* (2013) is consistent with Notch signaling acting through Hes5 to maintain the support cell fate. Hes5 is normally expressed in the posteromedial utricle in the adult and therefore it is not surprising that treatment with *Hes5* siRNA would result in the generation of hair cells in this same region. This raises the question of whether damage was even necessary in order to induce generation of the hair cells through this method. In contrast, Lin*, et al.* (2011) found hair cell increases in the striolar and juxtastriolar regions of the utricle. After damage, Atoh1 was spontaneously induced largely in these regions and subsequent DAPT treatment resulted in more differentiated hair cells in these regions as well. In addition, Lin*, et al.* (2011) did not find significant levels of *Hes5* expression in their damaged utricles, by RT-qPCR, but did see significant decreases in the expression of *Hes1*, *Hey1*, and *HeyL* after DAPT treatment. Therefore, it would be interesting to examine whether Hes1 and Hes5 are playing specific roles in the various regions of the undamaged and damaged mature utricle and to what extent varying degrees of hair cell damage are important. These and differences in methodology and the criteria for whether a hair cell was newly regenerated may account for the differences in results between studies including that of Collado*, et al.* (2011) where no regeneration was found.

1.4.3.3 Crista Ampullaris

Unlike the utricle, where Hes5 is expressed in only a small subset of support cells, the support cells in the peripheral region of the cristae have robust Hes5 expression, higher than in any other organ of the mature inner ear (Hartman*, et al.,* 2009). This suggests that Notch signaling may still be active in the adult cristae and that it may be required for maintaining the support cell phenotype through lateral inhibition. If this were the case, then inhibition of Notch signaling in these organs would likely result in some hair cell regeneration through transdifferentiation of Notch-expressing support cells.

In this dissertation, I tested this hypothesis and characterized the regenerative potential of the adult cristae *in vitro*. In addition, I laid the groundwork for future investigations into hair cell regeneration in the mouse cristae. My data shows that supernumerary hair cells can be generated through inhibition of Notch signaling *in vitro*, thus showing that Notch signaling does play a role in maintaining the support cell phenotype in a subset of peripheral support cells in the adult cristae. Further, it shows that there is a correlation between the regions that maintain regenerative competence in the adult and the last regions to exit the cell cycle through an analysis of the spatial distribution of hair cell birth in the developing cristae. For future studies, I have identified a new support cell marker that can be used to lineage trace support cells and have used this marker to characterize spontaneous hair cell regeneration in the adult cristae *in vivo*. In addition, I have established standard protocols for lesioning hair cells *in vivo* in two common mouse strains using the known ototoxin 3,3'-Iminodipropionitrile (IDPN) and for quantifiably assaying vestibular behavior in mice with varying degrees of hair cell lesion. Together, this work establishes the

previously uncharacterized mouse cristae as an additional model for studying mammalian hair cell regeneration. By better understanding the similarities and differences between not only regenerative and non-regenerative species, but also between the different organs of the inner ear, we can better understand not only why mammals possess a much lower regenerative capacity, but how we can safely stimulate regeneration in these systems.

C H A P T E R T W O

HAIR CELL REGENERATION THROUGH NOTCH INHIBITION *IN VITRO*

Modified and expanded from
Slowik and Bermingham-McDonogh (2013a)

2.1 INTRODUCTION

Many studies have attempted to regenerate hair cells through inhibition of Notch signaling in the cochlea (Lanford*, et al.,* 1999, Zine*, et al.,* 2001, Murata*, et al.,* 2006, Yamamoto*, et al.,* 2006, Hori*, et al.,* 2007, Hayashi*, et al.,* 2008a, Doetzlhofer*, et al.,* 2009, Hartman*, et al.,* 2009, Basch*, et al.,* 2011, Zhao*, et al.,* 2011, Mizutari*, et al.,* 2013) and the utricle (Collado*, et al.,* 2011, Lin*, et al.,* 2011, Jung*, et al.,* 2013). However, despite evidence for robust expression of Notch signaling components in the adult cristae, namely the downstream Notch effector Hes5, no studies have characterized the role of Notch signaling in the mature cristae. In fact, Hes5 is expressed more highly in the cristae than in any other mature organ of the inner ear (Hartman*, et al.,* 2009), including the cochlea, where Notch signaling components are downregulated postnatally (Hartman*, et al.,* 2007), and the utricle where Hes5 is restricted regionally and only expressed in a small subset of support cells in those regions (Hartman*, et al.,* 2009). The presence of Notch signaling effectors in the mature cristae suggests that Notch signaling is active in the majority of peripheral support cells and is likely important in maintaining the fate of those support cells through lateral inhibition. This would be similar to the vestibular organs of the chick where hair cells are continuously replaced (Roberson*, et al.,* 1992) and Notch signaling is required through lateral inhibition to maintain the correct ratio of hair cells and support cells. In these systems where Notch signaling is required for the maintenance of the support cell fate, it is possible to generate supernumerary hair cells through inhibition of Notch signaling without damage.

In order to determine if Notch signaling is required to maintain the support cell fate through lateral inhibition in the mature cristae, I carried out a series of experiments to

determine if Notch is active in the mature cristae and if it can be inhibited to generate hair cells. To inhibit Notch signaling I used the γ-secretase inhibitor, DAPT. In order to easily administer DAPT and other reagents in these preliminary studies, I first developed a method to maintain cristae *in vitro.* Using this culture system, I found that five days of DAPT-treatment resulted in a down-regulation of the Notch effectors *Hes1* and *Hes5* and also an increase in the total number of cells expressing the early hair cell marker, Gfi1. Hes5, as reported by Hes5-eGFP, was down-regulated specifically in peripheral support cells. Using lineage tracing with PLP/CreER;mTmG mice, I found that these hair cells arose through transdifferentiation of support cells in cristae explanted from mice up to ten weeks of age. These transdifferentiated cells arose without proliferation and were capable of taking on a hair cell morphology, migrating to the correct cell layer, and assembling what appears to be a stereocilia bundle with a long kinocilium. Overall, these data show that Notch signaling is active in the mature cristae and suggest that it may be important in maintaining the support cell fate in a subset of peripheral support cells.

2.2 RESULTS

2.2.1 THE CRISTA AMPULLARIS

The three cristae are situated at the bases of the three semicircular canals (Figure 2.1A-A'). In mice, the anterior and posterior cristae are separated into two hemicristae by a hair cell-free region called the eminentia cruciatum (Figure 2.1B,D-D')(Desai*, et al.,* 2005a). The lateral crista does not have an eminentia cruciatum and is instead one continuous sensory structure (Figure 2.1C). In addition, I found that the lateral crista had significantly fewer hair cells than anterior or posterior cristae (data not shown) and so excluded it from

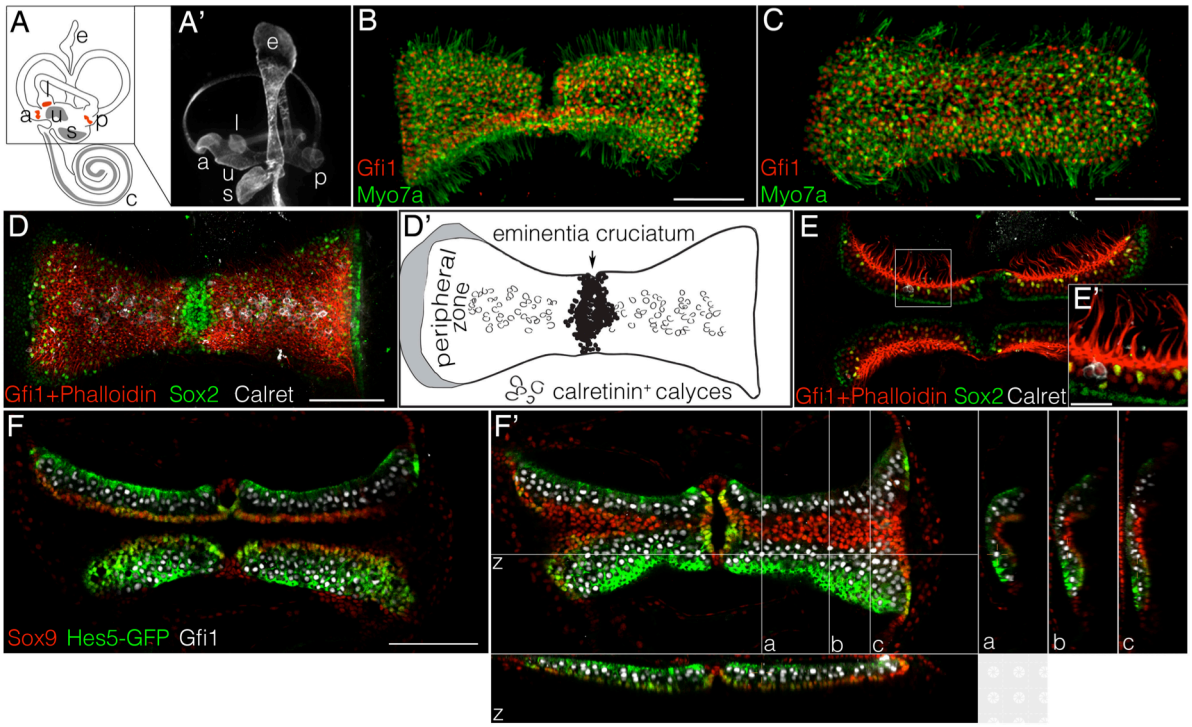

Figure 2.1 The crista ampullaris. **A-A')** The three cristae (red) are located at the bases of the semicircular canals shown in a diagram of the inner ear (A) and in a paint-fill of an E14.5 vestibular system (A'). a – anterior crista, l – lateral crista, p – posterior crista, u – utricle, s – saccule, c – cochlea, e – endolymphatic sac. **B-C)** Maximum intensity projections of adult whole mount cristae labeled with the hair cell markers Myo7a (cytoplasmic, green) and Gfi1 (nuclear, red). The eminentia cruciatum divides the anterior (B) and posterior cristae into two saddle-shaped hemicristae. **C)** The sensory epithelium of the lateral crista is continuous. Scale bars – 100 µm. **D-D')** Sox2 (green) labels support cells, a subset of type II hair cells, and non-sensory cells in the planum semilunatum (shaded grey in D') and eminentia cruciatum. The sensory epithelium contains $Gfi1^{+}$ hair cells (red nuclei) with phalloidin-stained (red) stereocilia bundles. The central zone is defined by the $Calretinin^{+}$ (white) calyx afferents that contact type I hair cells, while the remaining Calretinin-negative region is the peripheral zone. Scale bar – 100 µm. **E-E')** The layering of the support cells and hair cells of the sensory epithelium is visible in a single z-plane depicting a cross-sectional view of the cristae from D. Scale bar in E' is 25 µm. **F)** This layering can also be seen in cristae explanted from Hes5-eGFP mice labeled with Sox9 (red) and Gfi1 (white). Scale bar – 100 µm. **F')** The three-dimensional structure of this same cristae can be seen in z-projections through the confocal stacks at the labeled lines (a, b, c, z). Sox9 is also expressed throughout the ampulla, which flattened onto the sensory epithelium of the cristae during mounting and culturing (c). z-depth – 75.5 µm.

analyses involving hair cell counts. For this study I used the regional boundaries defined by Desai*, et al.* (2005a) where the central zone is the region containing the Calretinin-positive calyx afferents that innervate type I hair cells (Figure 2.1D-D') and the remaining sensory region is the peripheral zone. While simplified, these boundaries define the regions of interest to this work, as I use transgenic mouse strains (Hes5-eGFP and PLP/CreER) that limit my analyses to the Calretinin-negative peripheral zone.

As in the other sensory organs of the inner ear, the cristae are organized into layers of hair cells ($Gfi1^{+}$) and support cells ($Sox2^{+}$, $Sox9^{+}$, Hes5-$eGFP^{+}$)(Figure 2.1E-F') that specifically in the cristae are folded into complex, highly three-dimensional structures. For example, in the anterior and posterior cristae, each hemicristae is saddle-shaped (Figure 2.1F'; Supplemental Movie 2.1). As reported previously, there is a subset of hair cells throughout the epithelium that also express Sox2 (yellow cells in Figure 2.1E-E')(Hume*, et al.,* 2007, Oesterle*, et al.,* 2008). Similar to the staining seen in the utricle, this subset of cells does not appear to be innervated by Calretinin-positive calyces and is generally located closer to the apical surface of the sensory epithelium (Figure 1E')(Desai*, et al.,* 2005b). Together, these data suggest that these Sox2-expressing cells belong to the type II subclass of hair cells, though it is not clear whether every type II hair cell expresses Sox2.

2.2.2 ORGANOTYPIC CULTURES OF POSTNATAL AND ADULT CRISTAE

To test for a role of Notch signaling in the transdifferentiation of support cells in the cristae, I developed a method for maintaining cristae *in vitro*. In brief, cristae were dissected from the capsule (Figure 2.1A), mechanically separated from the semicircular canals, and

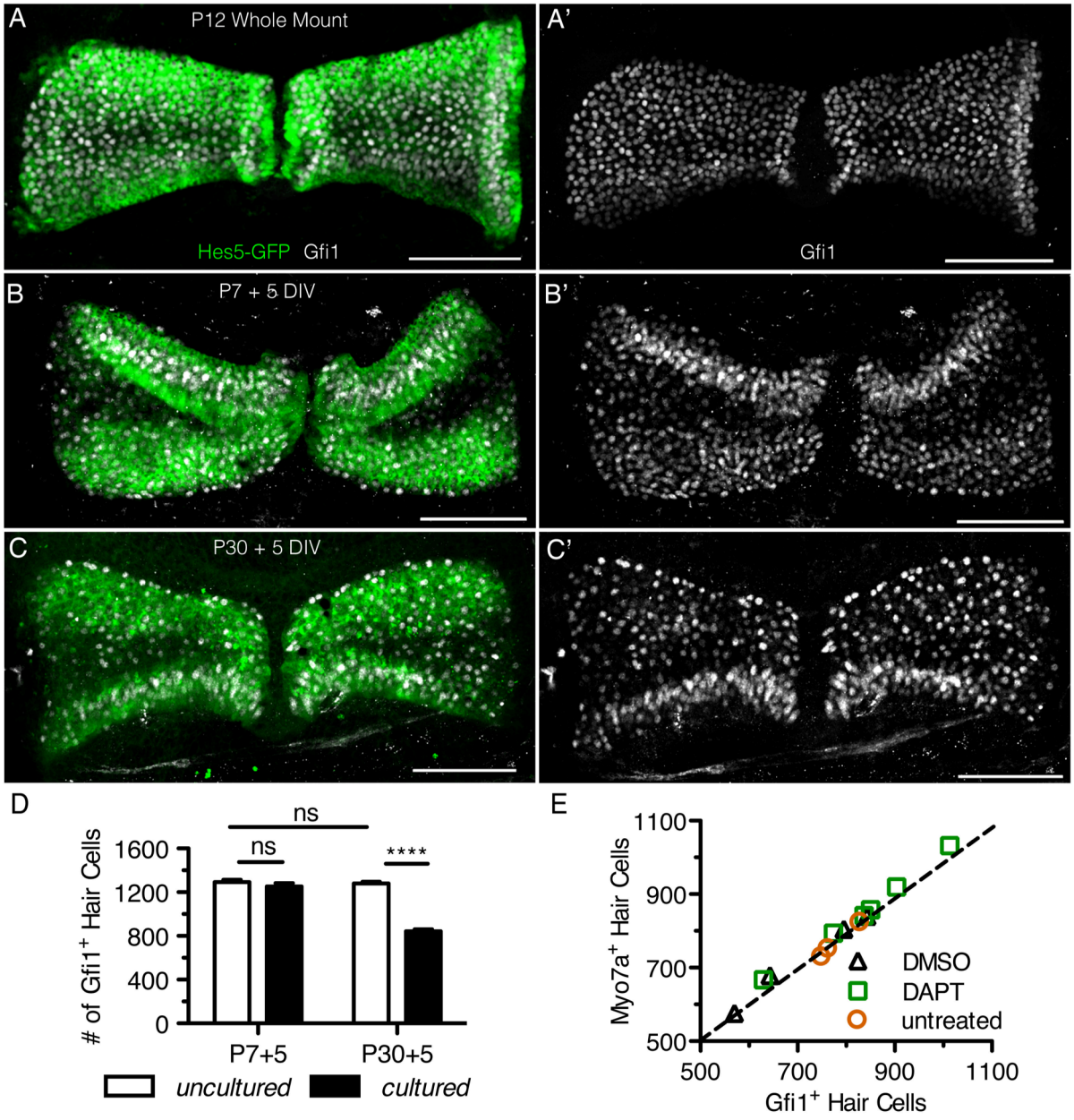

Figure 2.2 Organotypic cristae cultures. **A,A′,B,B′)** Maximum intensity projections of cristae explanted from P7 and P12 Hes5-GFP mice and labeled with Gfi1 (white) show that after 5 days in vitro (DIV) cristae maintained their overall morphology compared to uncultured littermate controls (B,B′ compared to A,A′). **C,C′)** Cristae cultured from P30 adults also maintained their normal morphology. Scale bars 100 µm. **D)** P7+5 DIV cristae maintained similar levels of Gfi1+ hair cells (n=11) compared to P12 littermates (n=9; t=0.9590, df=18, p=0.35), while P30+5 DIV explants had a significantly reduced number of hair cells (n=10) compared to P35 littermates (n=9; t=19.1571, df=17, p < 0.0001). Error bars depict standard error of the mean (SEM). Two-tailed unpaired Student's t test where ns denotes p>0.05 and **** denotes p≤0.0001. **E)** In P30+5 DIV cristae, the hair cell counts obtained using an antibody to Gfi1 were comparable to those using an antibody to Myo7a regardless of culture cond itions (DMSO, n=4, DAPT, n=6, untreated, n=3).

cultured with the ampulla intact on culture membrane inserts at the gas-liquid interface. Cristae were cultured for five days *in vitro* (DIV), fixed, and then labeled with antibodies to assess the survival of hair cells and the overall morphology of the sensory epithelium. Postnatal ages were used in addition to the mature ages for comparison purposes, as the survival and plasticity of inner ear organs is generally greater at younger ages. To facilitate accurate hair cell counts, I used the nuclear hair cell marker Gfi1. Gfi1 is expressed in both the developing (Wallis*, et al.,* 2003, Hertzano*, et al.,* 2004, Yang*, et al.,* 2010) and mature (Figure 2.1B-C) vestibular system. In the adult, counts of $Gfi1^+$ cells were nearly identical to counts with the more commonly used cytoplasmic marker, Myo7a (Hasson*, et al.,* 1995), under all culture conditions tested (Figure 2.2E).

After five DIV, both postnatal (P7) and adult (P30) cristae maintained their overall morphology compared to control cristae freshly dissected from similarly staged animals (Figure 2.2B-B' and 2.2C-C' compared to 2.2A-A'). The overall shape of the sensory epithelium was maintained, including the separation of the epithelium into the two distinct hemicristae by the eminentia cruciatum. In addition, in cultures from transgenic mice expressing eGFP under the *Hes5* promoter (Hes5-eGFP), the expression of eGFP (green) in the peripheral zone and immunostaining with the hair cell markers Gfi1 (white) and Myo7a (data not shown) were similar to control explants (Figure 2.2A-C'). However, there was a slight difference in the appearance of the cultured cristae in maximum intensity projections. This was due to the flattening and folding of the highly three-dimensional tissue onto the culture membrane. The degree of folding varied from explant to explant, but most commonly appeared as in Figure 2.2B-B' and 2.2C-C'.

In addition to morphology, I assessed the overall hair cell survival after five DIV at both P7 and P30 (Figure 2.2D). In the P7 explants, nearly all the hair cells survived the five-day culture period, with 1253.4±30.8 (n=11) $Gfi1^+$ hair cells in cultured explants, compared with 1291.4±22.3 (n=9) in littermate controls (t=0.9590, df=18, p=0.35). By contrast, in the P30 explants, there was significant hair cell loss after five DIV, with 843.5±17.2 (n=10) $Gfi1^+$ hair cells in cultured explants, compared to 1280.7±14.5 (n=9) in littermate controls (t=19.1571, df=17, p<0.0001) (Figure 2.2D). This loss appears to be due to culture survivability and is not related to age-dependent hair cell loss, as there was no significant difference in hair cell number between the P7 and P30 uncultured explants (t=0.4044, df=16, p=0.69). Overall, at P30, there was a 34.1% loss due to culture, which is consistent with that seen in other adult cultures of vestibular organs (e.g. Lin*, et al.,* 2011). Generally, this loss appeared as an overall thinning of the hair cell density throughout the sensory epithelium (Figure 2.2C'); however, occasionally there was an almost complete loss of the hair cells in the more central regions.

2.2.3 NOTCH SIGNALING IS ACTIVE IN ADULT CRISTAE

Previously, the Bermingham-McDonogh lab suggested that Notch signaling is active in the peripheral support cells of the adult cristae based on an analysis of the Notch effector Hes5 in Hes5-eGFP reporter mice and on *Hes5* expression examined by *in situ* hybridization (Hartman*, et al.,* 2009). To provide additional evidence that the Hes5 expression seen in the adult is a result of active Notch signaling, cristae from postnatal (P7, P12, P14) and adult (P30) Hes5-eGFP mice were explanted and treated with the γ-secretase inhibitor, DAPT, to pharmacologically inhibit Notch signaling. The postnatal ages were used for comparison,

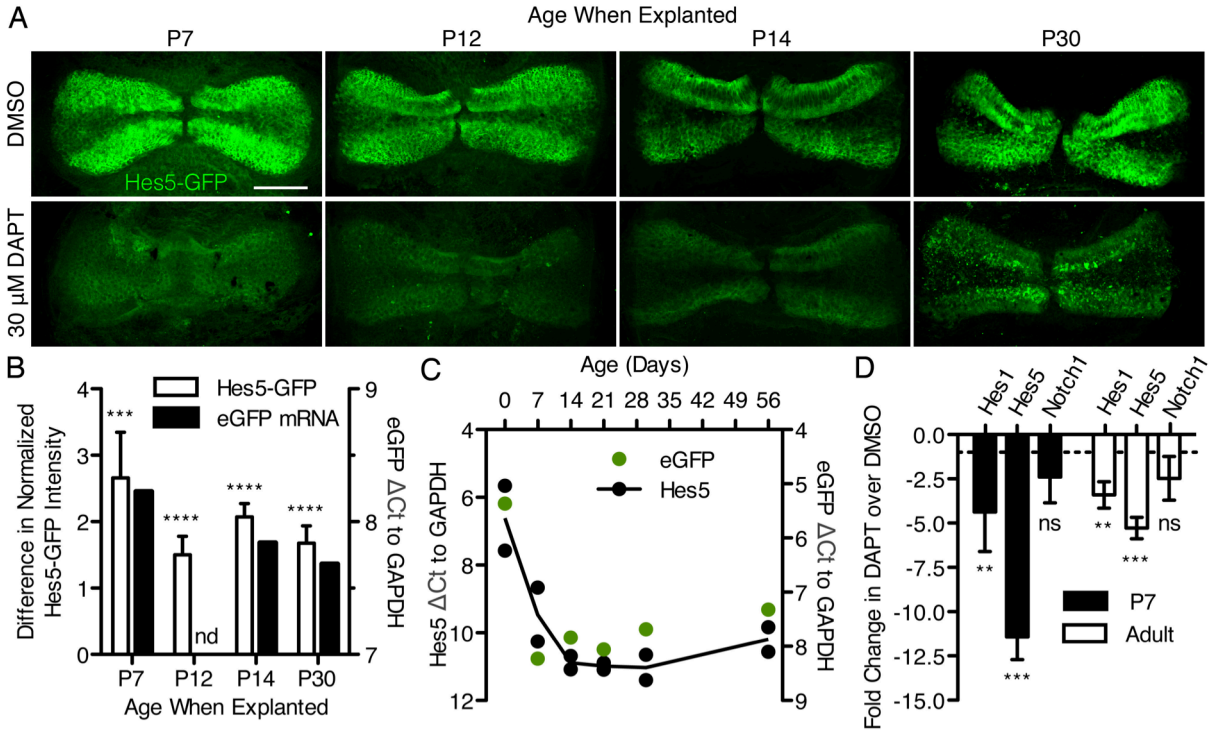

Figure 2.3 Notch signaling is active in the postnatal and adult cristae. **A)** Hes5-eGFP was expressed in the support cells along the peripheral edges of the cristae at all ages in DMSO controls and was down-regulated by 30 µM DAPT after 5 DIV. Scale bar 100 µm. **B)** Quantification of the Hes5-eGFP fluorescence intensity showed significant reduction with DAPT treatment at all ages (white bars, n=[DMSO; DAPT]; P7 [10; 8], −2.66± 0.69, t=3.868, df=16, p=0.00068; P12 [10; 12], −1.50±0.27, t=5.467, df=20, p<0.0001; P14 [12; 12], −2.07±0.20, t=10.30, df=22, p< 0.0001; P30 [19; 13], −1.68±0.26, t=6.453, df=30, p<0.0001). Error bars depict standard error of the difference (SE). The difference in fluorescent intensity showed a similar trend with age as the gene expression of eGFP assayed by RT-qPCR (black bars; P7, 8.226; P12, no data (nd); P14, 7.840; P30, 7.682). **C)** RT-qPCR analysis of uncultured cristae showed that endogenous Hes5 (black points) is downregulated postnatally but maintains similar levels of expression between late postnatal and adult ages (8 weeks). Each point represents a single biological replicate, while the black line shows the average of the two replicates (P0, 6.613±1.356; P7, 9.463±1.124; P14, 10.884±0.280; P21, 10.988±0.143; P30, 11.025±0.530; P56, 10.198± 0.511). Error on reported values is standard deviation (SD). The expression of eGFP from the Hes5-eGFP transgene in these same organs showed a similar trend to that of Hes5 (green points; P0, 5.364; P7, 8.226; P14, 7.840; P21, 8.060; P30, 7.682; P56, 7.320). **D)** RT-qPCR analysis of cristae explanted from P7 and adult (8–10 weeks) mice showed a significant reduction in Hes1 (P7: −4.38±1.28, t=3.8060, df=4, p=0.0095; adult: −3.40±0.43, t=3.5309, df=4, p=0.012) and Hes5 (P7: −11.42±0.75, t= 11.4975, df=4, p=0.00016; adult: −5.28±0.35, t=6.7954, df=4, p= 0.0012) gene expression in DAPT treated cristae over DMSO controls after 5 DIV with no change in Notch1 expression (P7: −2.38±0.85, t= 2.0646, df=4, p=0.054; adult: −2.47±0.72, t=1.8732, df=4, p=0.067). Error bars depict SEM. One-tailed unpaired Student's t test where ns – p>0.025, * - p≤0.025, ** - p≤0.0125, *** - p≤0.00125, **** - p≤0.0001.

since the ability to generate supernumerary hair cells through Notch inhibition is lost after P12 in the utricle (Collado*, et al.,* 2011). After five DIV with 30 μM DAPT, the Hes5-eGFP expression specific to the support cells of the peripheral zone was down-regulated compared to the DMSO controls in all of the ages examined (Figure 2.3A). In the P30 explants, there was some remaining fluorescent signal due to the autofluorescence of dead and dying cells, indicative of the decreased survivability of the adult explants. Quantification of the difference in Hes5-eGFP fluorescence intensity between DAPT- and DMSO-treated cristae shows that this down-regulation was significant at all ages examined (white bars, Figure 2.3B). Further, the degree of this downregulation showed a similar trend with age to the expression of *eGFP* in uncultured cristae from Hes5-eGFP mice assayed by RT-qPCR (black bars, Figure 3B). Overall, in the uncultured cristae it appeared that *Hes5* gene expression was highly downregulated postnatally, but remained relatively stable after P7 and into the adult ages (black circles, Figure 2.3C). The expression of *eGFP* from the *Hes5-eGFP* reporter showed an identical trend (green circles, Figure 2.3C). In addition, RT-qPCR analysis of cristae explanted from P7 and adult (8-10 week) mice and cultured for five DIV, showed that the Notch effectors *Hes1* and *Hes5* were significantly down-regulated in DAPT-treated cristae over DMSO controls, with no change in the expression of the Notch receptor, *Notch1* (Figure 2.3D). Overall, these data show that Notch signaling is active in the adult cristae, albeit possibly at a lower level than in early postnatal animals.

2.2.4 DAPT-TREATMENT INCREASES TOTAL HAIR CELL NUMBER

The presence of active Notch signaling in the adult cristae supports the hypothesis that Notch signaling may still be necessary to maintain the support cell phenotype in mature

cristae and that Notch inhibition would lead to the generation of supernumerary hair cells. To test this, postnatal (P7, P12, P14) and adult (P30) explants were cultured for five DIV with 30 μM DAPT or DMSO as a vehicle control (Figure 2.4). Cristae were analyzed by counting the total number of Gfi1$^+$ hair cells. This concentration of DAPT is lower than that used in similar studies in the utricle (Collado*, et al.,* 2011, Lin*, et al.,* 2011) and was

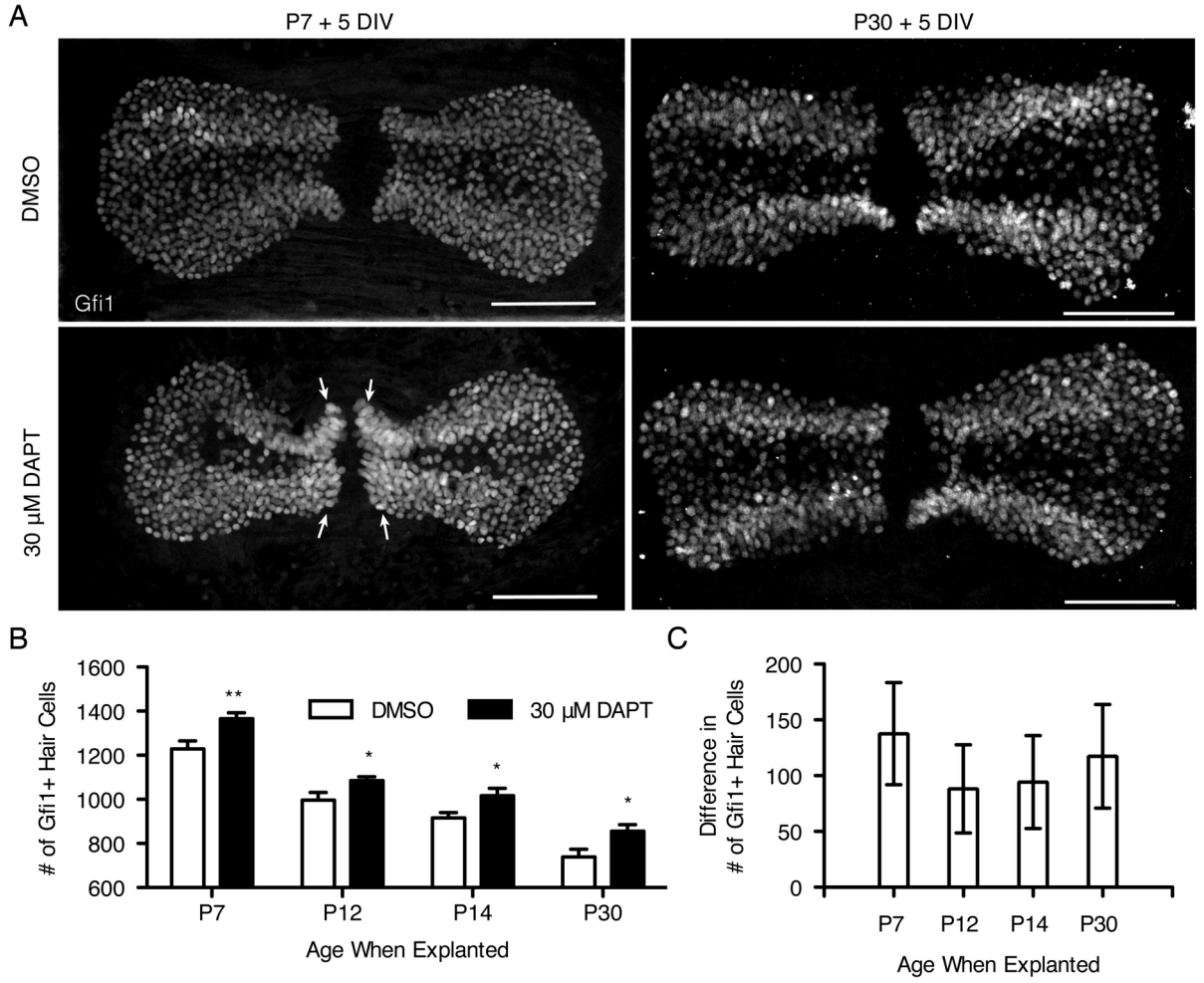

Figure 2.4 DAPT-treatment increases total hair cell number in postnatal and adult cristae. **A)** Maximum intensity projections of Gfi1$^+$ hair cells in explants from P7 and P30 mice after 5 DIV with 30 μm DAPT or DMSO. Scale bars 100 μm. Arrows point to regions of increased hair cell density. **B)** At each age examined, the total number of Gfi1$^+$ hair cells was significantly increased in DAPT-treated cristae versus DMSO controls (Table 2.1). Note that the scale on the y-axis begins at 600. Error bars depict SEM. One-tailed unpaired Student's t test where * - $p \leq 0.025$ and ** - $p \leq 0.0125$. **C)** The difference in hair cell number between treated and control cristae was similar at all ages. Error bars depict SE.

chosen based on a concentration curve performed on P7 explants cultured for five DIV with 1 μM, 10 μM, or 30 μM DAPT with DMSO as a vehicle control. This is in contrast to the postnatal cochlea where 5 μM DAPT is sufficient to inhibit lateral inhibition (Hayashi*, et al.,* 2008a). To determine efficacy, the difference in the total number of Gfi1$^+$ hair cells between DAPT- and DMSO-treated cristae was used. Only the explants treated with 30 μM DAPT showed a statistically significant increase in hair cell number over the DMSO controls (DMSO - 1153±37.29 (n=10), 1 μM - 1222±76.05 (n=3), 10 μM - 1157±38.15 (n=4), 30 μM - 1380±89.79 (n=7); means reported with SEM; one-way ANOVA where $F(4,20)$=3.223, p=0.0445 with Tukey-Kramer post-test [α=0.05]).

TABLE 2.1

Quantification of Gfi1$^+$ hair cells in cristae explants cultured for 5 DIV

Explant Age and Treatment	n	Mean (±SEM)	Difference between means (± SE)	p-value (Df, t)[a]
P7				
DMSO	15	1228(±36.79)	-137.6(±45.79)	0.0028 (28, 3.005)
DAPT	15	1366(±27.26)		
P12				
DMSO	15	996.5(±35.37)	-88.13(±39.5)	0.0169 (28, 2.231)
DAPT	15	1085(±17.58)		
P14				
DMSO	11	922.5(±24.82)	-94.35(±41.62)	0.0176 (19, 2.267)
DAPT	10	1017(±34.10)		
P30				
DMSO	22	738.9(±35.07)	-117.3(±46.4)	0.0078 (39, 2.528)
DAPT	19	856.2(±29.01)		

2-way ANOVA	F-value	p-value
Effect of DAPT	$F_{1,114}$ = 21.85	<0.0001
Effect of Age	$F_{3,114}$ = 92.57	<0.0001
Interaction	$F_{3,114}$ = 0.23	0.8722

SEM - Standard error of the mean, SE - Standard error of the difference

[a] p-values from one-tailed unpaired student's t-tests with degrees of freedom and t-value

Overall, there was a highly statistically significant effect of DAPT on total hair cell number (Table 2.1). In addition, there was also a statistically significant effect of age on total hair cell number as the survivability of the explants decreased with increasing age (Figure 2.2D, Table 2.1). However, there was no differential effect of DAPT-treatment with age as

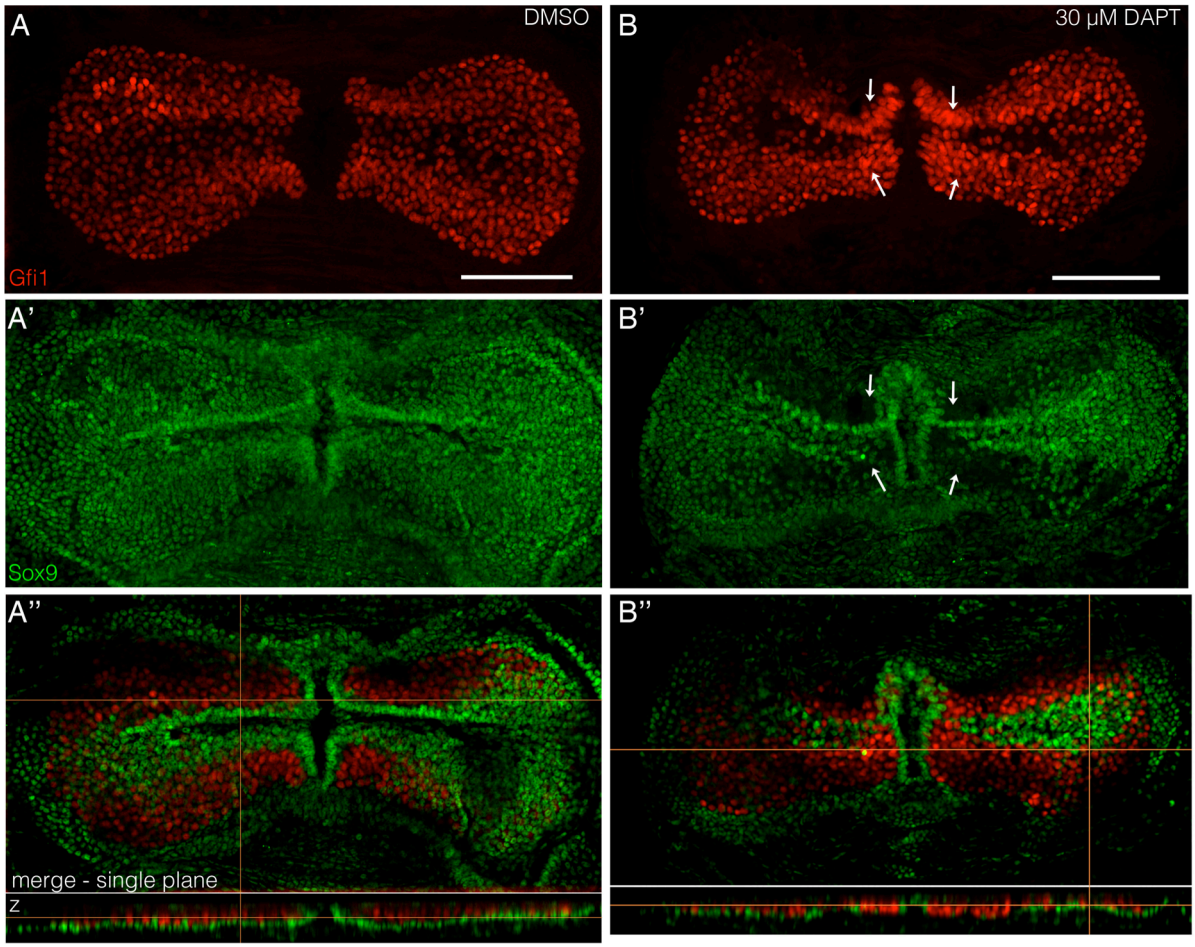

Figure 2.5 Hair cells appear to arise through transdifferentiation in postnatal cristae. **A,A',B,B')** Maximum intensity projections of P7+5 DIV cristae treated with either DMSO (A,A') or 30 μm DAPT (B,B') stained with Gfi1 for hair cells (A,B, red) and Sox9 for support cells (A',B', green). In DAPT-treated cristae, the $Sox9^{+}$ support cell layer (B', green) was disrupted near the eminentia cruciatum as compared to DMSO-treated controls where the Sox9 layer was continuous (A', green)(arrows point to regions of increased hair cell density and decreased support cell density). **A",B")** This can also be seen in z projections through the sensory epithelium (at the yellow lines) where in controls the green support cell layer was continuous beneath the red hair cells (A"), but in DAPT-treated cristae it was disrupted (B"). This obvious disruption is not seen in adult explants. Scale bars 100 μm.

the interaction between them was not significant (Table 2.1). At each individual age tested, there was a significant increase in the number of hair cells in DAPT-treated cristae relative to their aged-matched controls (Table 2.1, Figure 2.4B). In the P7 explants, there was a noticeable increase in the hair cell density in the regions near the eminentia cruciatum (Figure 2.4A and 2.5B; white arrows) that was accompanied by a loss of $Sox9^+$ support cells in the same regions (Figure 2.5B', white arrows). In the adult explants (P30), the increase in hair cells was not as apparent in the maximum intensity projections; nevertheless, there was a consistent and statistically significant increase in the number of hair cells in the DAPT-treated explants, even at P30 (Figure 2.4B). This increase in hair cell number was approximately the same at all of the ages tested (Table 2.1, Figure 2.4C), which is consistent with the relatively stable levels of *Hes5* gene expression, and therefore Notch signaling levels, at these same ages (Figure 2.3C).

In the other organs of the inner ear, the amount of support cells that undergo transdifferentiation in response to Notch inhibition decreases during development, as the levels of active Notch signaling in these organs also decrease (Lanford*, et al.,* 1999, Zhang*, et al.,* 2000, Zheng*, et al.,* 2000, Zine*, et al.,* 2001, Kiernan*, et al.,* 2005, Brooker*, et al.,* 2006, Yamamoto*, et al.,* 2006, Takebayashi*, et al.,* 2007, Hayashi*, et al.,* 2008a, Doetzlhofer*, et al.,* 2009, Collado*, et al.,* 2011, Zhao*, et al.,* 2011, Du*, et al.,* 2013, Korrapati*, et al.,* 2013, Mizutari*, et al.,* 2013). Since in the cristae the expression of *Hes5* is higher at birth than at P7 or in the adult (Figure 2.3C), it is likely that more hair cells would be generated in response to Notch inhibition in early postnatal cristae. To test this I explanted cristae from P1 and P4 mice and cultured them for three DIV with 30 μM DAPT or DMSO as a vehicle control. For analysis,

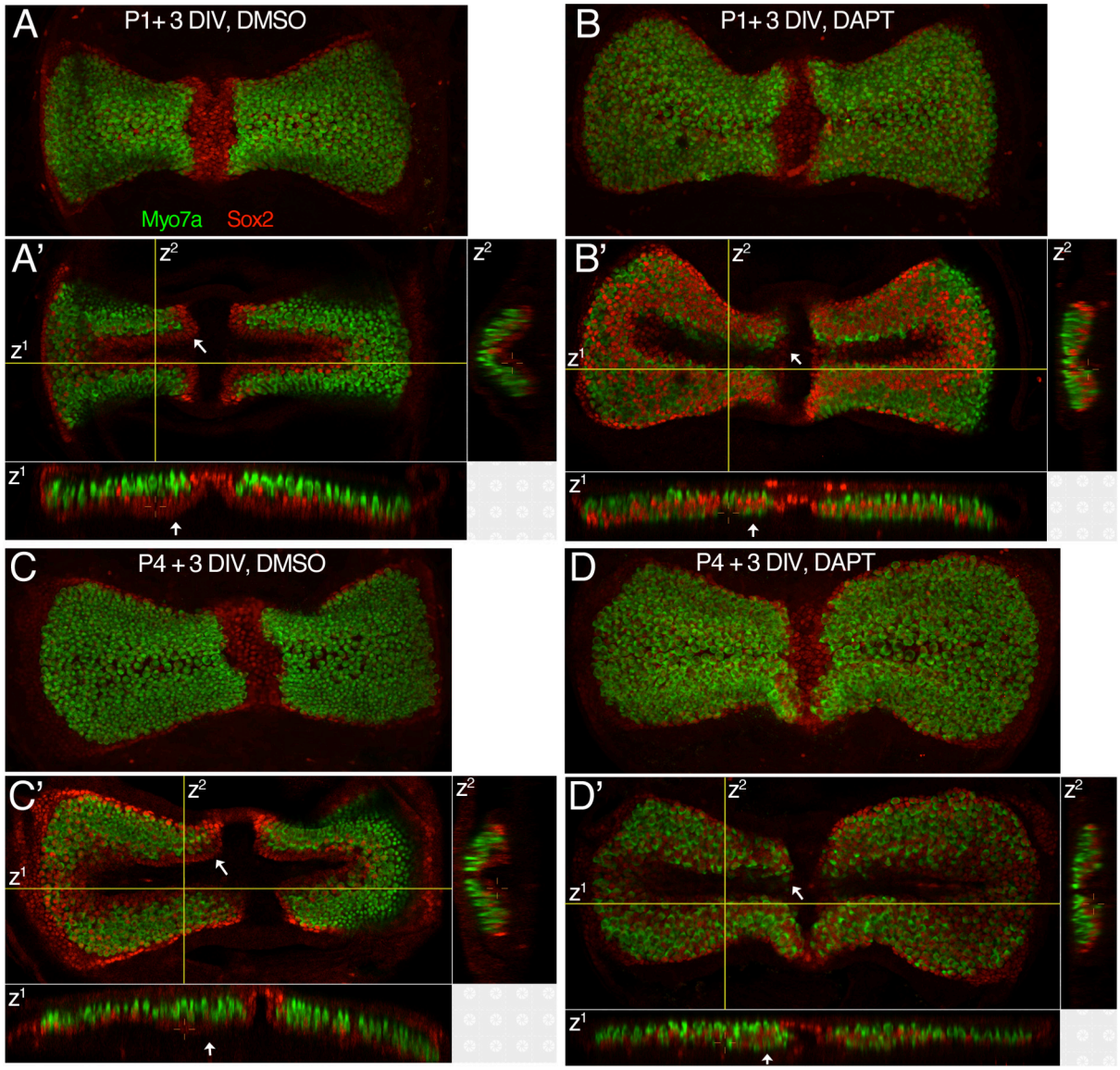

Figure 2.6 Most support cells transdifferentiate after DAPT-treatment in postnatal cristae. Cristae were explanted from P1 and P4 mice and cultured for 3 DIV. Cristae are labeled with Myo7a (green) and Sox2 (red) and are shown in maximum intensity projections (A,B,C,D) and in single slice views (A', B',C',D'). In the slice views, yellow lines indicate the location of the two slice projections (z^1 and z^2) shown to the right and bottom of each image. **A-D)** There is no qualitative difference in the appearance of DAPT- and DMSO-treated cristae in the maximum intensity projections at either P1 (A versus B) or P4 (C versus D). **A',C')** In the DMSO-treated cristae at both P1 (A') and P4 (C'), the layering of the support cells and hair cells is preserved (white arrows point to areas where the layer of red support cell nuclei can be seen beneath the green hair cell layer). **B',D')** In the cristae treated with 30 μM DAPT, the layering is disrupted since most of the Sox2-expressing support cells have transdifferentiated and now express the hair cell marker Myo7a (green), in addition to Sox2 (red).

cristae were labeled for hair cells with Myo7a (green) and for support cells with Sox2 (red) (Figure 2.6). Though there was no visible difference in the appearance of the treated versus control cristae in maximum intensity projections (Figure 2.6A,B,C,D), slice views of the cristae showed that the majority of the support cells underwent transdifferentiation in response to Notch inhibition at both early postnatal ages. In the DMSO-treated cristae, there was a clear layer of Sox2-expressing support cells (red) beneath the hair cell layer (green) (Figure 2.6A',C', indicated by white arrows). This can be seen in both a single slice view of the cristae and in slice projections (white arrows). In the DAPT-treated cristae, there is no obvious layering of the hair cells and support cells. Instead, the sensory epithelium looks like one continuous layer of cells expressing both Myo7a (green) and Sox2 (red) (Figure 2.6B',D'). Sox2 is expressed by support cells and a subset of type II hair cells in the mature cristae (Figure 2.1E,E') and is expressed briefly in immature hair cells of the other inner ear organs (Hume*, et al.,* 2007, Dabdoub*, et al.,* 2008, Hayashi*, et al.,* 2008b, Munnamalai*, et al.,* 2012). Therefore, the continued expression of Sox2 in these cells could be due to a failure to downregulate Sox2, or could just be a normal part of hair cell development.

The hair cell increases in the later postnatal and mature cristae did not appear to be due to cell proliferation. Culturing for five DIV with continuous 5 μM 5-Ethynyl-2´-deoxyuridine (EdU), a thymidine analogue, did not result in EdU uptake by $Gfi1^+$ hair cells in either DAPT- or DMSO-treated cristae, despite numerous EdU^+ cells in the surrounding non-sensory tissue (Figure 2.7). In addition, the majority of support cells appeared to be negative for EdU labeling. It is still possible, however, that there was a low level of support cell proliferation, as I did not label the support cells to test for this and instead identified

them based on their position in the sensory epithelium and their nuclear morphology. The data shown in Figure 2.7 are examples of P30 explants, though I found the same results at P7 and P14. Overall, this suggests that any newly generated hair cells did not arise through proliferation, but through direct transdifferentiation.

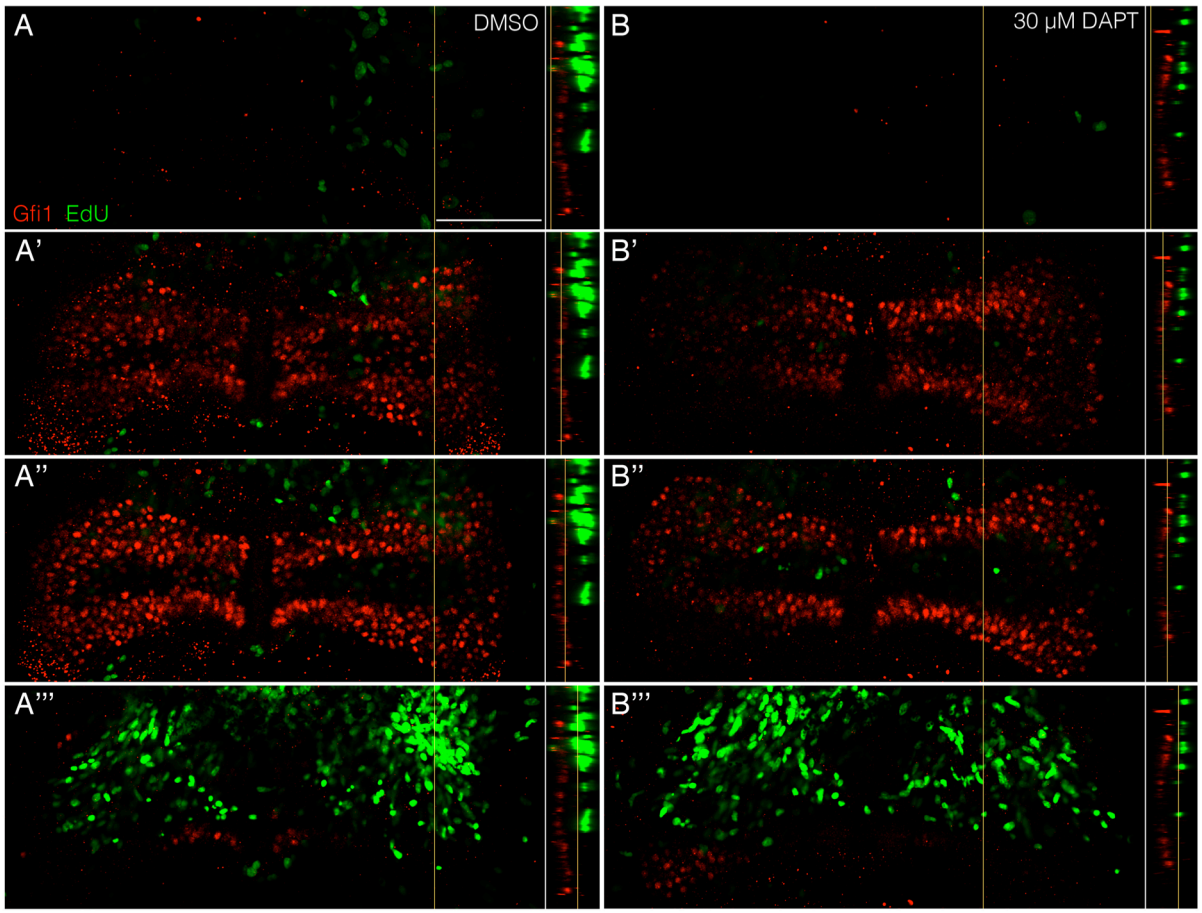

Figure 2.7 Hair cells do not arise through proliferation. **A-A''', B-B''')** Hair cells did not uptake EdU (green), despite the presence of EdU throughout the entire culture period in either DMSO- (A-A''') or 30 μm DAPT- (B-B''') treated P30 + 5 DIV cristae shown in single slice views at different z depths in the sensory epithelium labeled with Gfi1 (red). Z slice projections are shown to the right of the image indicating the location of the slice relative to the sensory epithelium in the z dimension. In both conditions, while many cells beneath the sensory epithelium were positive for EdU (A''', B'''), no $Gfi1^{+}$ hair cells had EdU labeling, as indicated by the lack of yellow cells in A', A'', B', and B''.

2.2.5 NEW HAIR CELLS ARISE THROUGH TRANSDIFFERENTIATION

In order to directly demonstrate that the hair cell increases I observed were due to support cell transdifferentiation and not from hair cell survival or repair, I used a lineage tracing strategy to label support cells prior to DAPT-treatment (Figure 2.8A). For these experiments, I used animals that had reached sexual maturity (8-10 weeks) as I felt that they better represented mature adults. The analysis of *Hes5* gene expression, both with age and with DAPT-treatment, suggested that Notch signaling was still active at this age (Figure 2.3C-D). Further, the 8-10 week old control cristae cultured for 7 DIV from this experiment had a similar number of $Gfi1^+$ hair cells (836.2±41.52, n=5) as the cultured P30+5 DIV explants (Figure 2.2D, 843.5±17.2, n=10). This suggests that even though the adult explants do not survive as well in culture as younger explants, their survivability does not continue to decline with age, but stabilizes between at least P30 and P56-70. To label support cells, I used PLP/CreER mice expressing an inducible *Cre* recombinase under the proteolipid protein 1 (PLP) promoter crossed to mTmG reporter mice that express membrane-bound Tomato (mTomato) prior to recombination and membrane-bound GFP (mGFP) after *Cre*-mediated recombination (Doerflinger*, et al.,* 2003, Muzumdar*, et al.,* 2007, Gomez-Casati*, et al.,* 2010). Upon tamoxifen treatment, the support cells and Schwann cells that express the *PLP* transgene expressed GFP in a dose dependent manner (Figure 2.8B-B"). By replacing the media with fresh 5 μM 4-Hydroxytamoxifen (4-OHT) each day of the two day recombination period, it was possible to recombine almost all of the peripheral support cells (Figure 2.8B"). However, with this recombination efficiency it was impossible to distinguish

between a hair cell expressing mGFP and an unlabeled hair cell surrounded by support cells expressing mGFP. Using a single treatment of 5 µM 4-OHT with no media change during the two days of recombination, there was a lower recombination efficiency overall (Figure 2.8C-C', with and without Gfi1). With this recombination efficiency, the morphology and

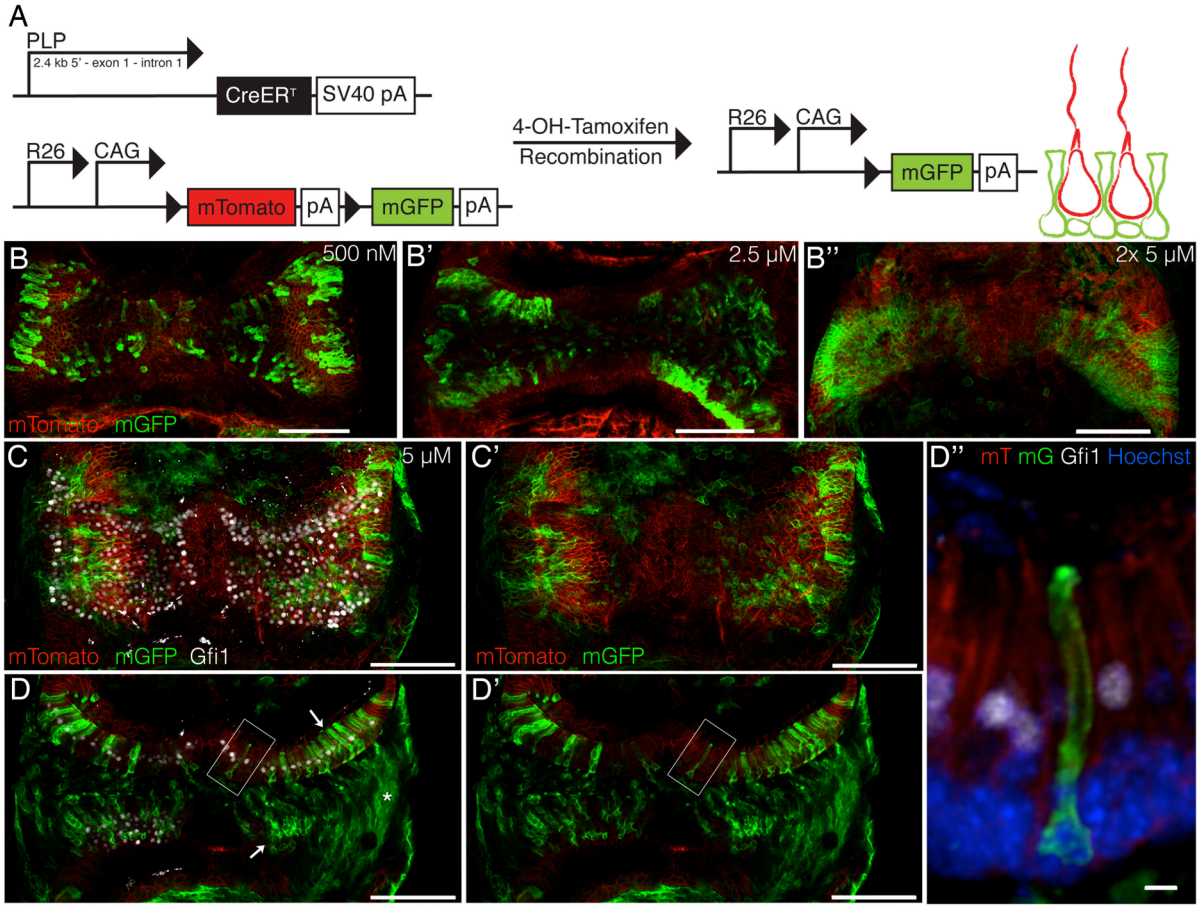

Figure 2.8 PLP/CreER lineage trace of support cell fate. **A)** Mice expressing a tamoxifen-inducible *Cre* recombinase under the PLP promoter were crossed to mTmG reporter mice that express a floxed-stop membrane-bound Tomato followed by a membrane-bound GFP driven by a CAGs promoter in the *ROSA26* locus. **B-B")** Tamoxifen-induced recombination was dose dependent. Most support cells in the peripheral region expressed GFP after two days of 5 µM 4-OHT treatment with a media change on the second day. **C-C')** Fewer support cells expressed GFP after two days of 5 µM 4-OHT treatment with no media changes, shown with (C) and without (C') Gfi1 (white) in maximum intensity projections. **D-D')** Single z-slices of the crista in C-C' show recombination in support cells (arrows) and Schwann cells (asterisk). **D")** A zoomed image of the boxed region in D-D' shows an example of a recombined support cell. All scale bars are 100 µm except for in D" where it is 5 µm.

layering of individual cells when viewed in single z-planes was clearly visible (Figure 2.8D-D", arrows indicate regions of support cell recombination, asterisk indicates a region of Schwann cell recombination).

To verify that the *Cre* recombinase was not expressed in hair cells, cristae were explanted from 8-10 week old PLP/CreER;mTmG mice and treated with 5 μM 4-OHT for two DIV to induce recombination. Recombination control cristae were fixed directly after

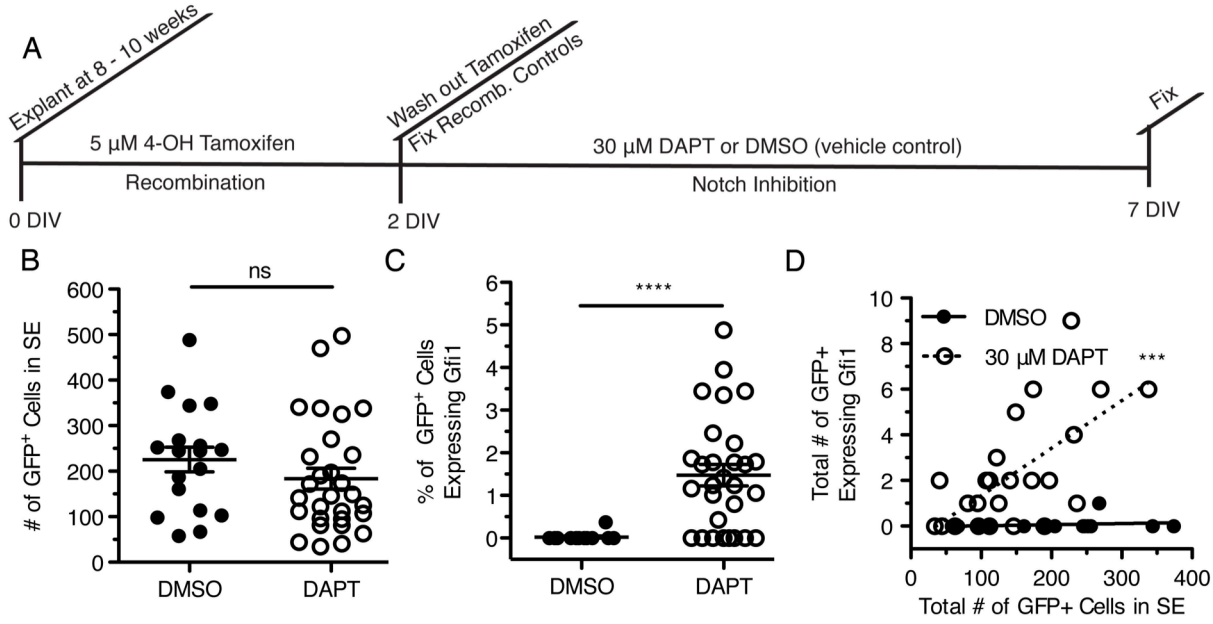

Figure 2.9 Notch inhibition induces transdifferentiation of support cells to hair cells. **A)** Cristae were explanted from 8 to 10 week old PLP/CreER;mTmG mice and cultured for 2 DIV with a single dose of 5 μm 4-OHT. Recombination control cristae were fixed after 2 days and remaining cristae were washed and treated with either 30 μM DAPT or DMSO for 5 additional days with daily media changes. **B)** The number of GFP^+ cells in the sensory epithelium was similar between treatment groups (DMSO, 225.6±27.3, n=18, DAPT, 183.8±22.0, n=29) (t=1.155, df=45, p=0.25). Error bars depict SEM. **C)** There was a significant increase in the percentage of GFP^+ cells in the SE expressing Gfi1 in DAPT-treated cristae versus DMSO controls (DMSO, 0.023±0.023, n=16; DAPT, 1.47±0.25, n=29) (t=4.286, df=43, p=0.00010). Error bars depict SEM. Two-tailed unpaired Student's t-test where ns denotes $p>0.05$ and **** denotes $p\leq0.0001$. **D)** Overall, in the DAPT-treated cristae the number of GFP^+ cells expressing Gfi1 correlated with the recombination efficiency of the explants (r^2=0.6520, n=25, p=0.00041). The DMSO controls showed no significant correlation (r^2=0.1873, n=16, p=0.49). Pearson's correlation where *** denotes $p\leq0.001$.

these two days and analyzed. Out of nine recombination control cristae, no hair cell recombination was observed despite significant support cell recombination comparable to the number of GFP^+ cells in the sensory epithelium quantified in Figure 2.9B.

To determine whether the additional hair cells observed with DAPT-treatment were derived from support cells, I explanted cristae from 8-10 week old PLP/CreER;mTmG mice and treated them with 5 μM 4-OHT for two DIV to induce recombination, as described above. After two DIV, the media was replaced with either 30 μM DAPT or DMSO as a vehicle control for an additional five DIV (Figure 2.9A). Both treated and control cristae had similar levels of recombination (Figure 2.9B). In the DMSO-treated controls there were 225.6±27.3 (n=18) recombined $mGFP^+$ cells in the sensory epithelium, compared to 183.8±22.0 (n=29) $mGFP^+$ cells in the DAPT-treated cristae (t=1.155, df=45, p=0.25). Further, in the DAPT-treated cristae, I found many examples of GFP^+ cells in the sensory epithelium expressing Gfi1, which will be referred to as transitioning cells (TC). Overall, there were significantly more TCs in DAPT-treated cristae compared to controls (Figure 2.9C)(t=4.286, df=43, p=0.00010). In addition, the number of TCs found in an explant correlated with the degree of *Cre*-mediated recombination in support cells (Figure 2.9D)(r^2=0.6520, n=25, p=0.00041). Most DAPT-treated cristae had at least one TC, and in one case there were as many as nine. By contrast, there was only a single TC in all of the DMSO control explants (Figure 2.9D), which may be a result of spontaneous regeneration as there were no TCs in the two-day recombination controls.

The TCs derived from support cells showed a range of morphologies. Most of the TCs were similar to the representative example shown in Figure 2.10A-C. These cells were

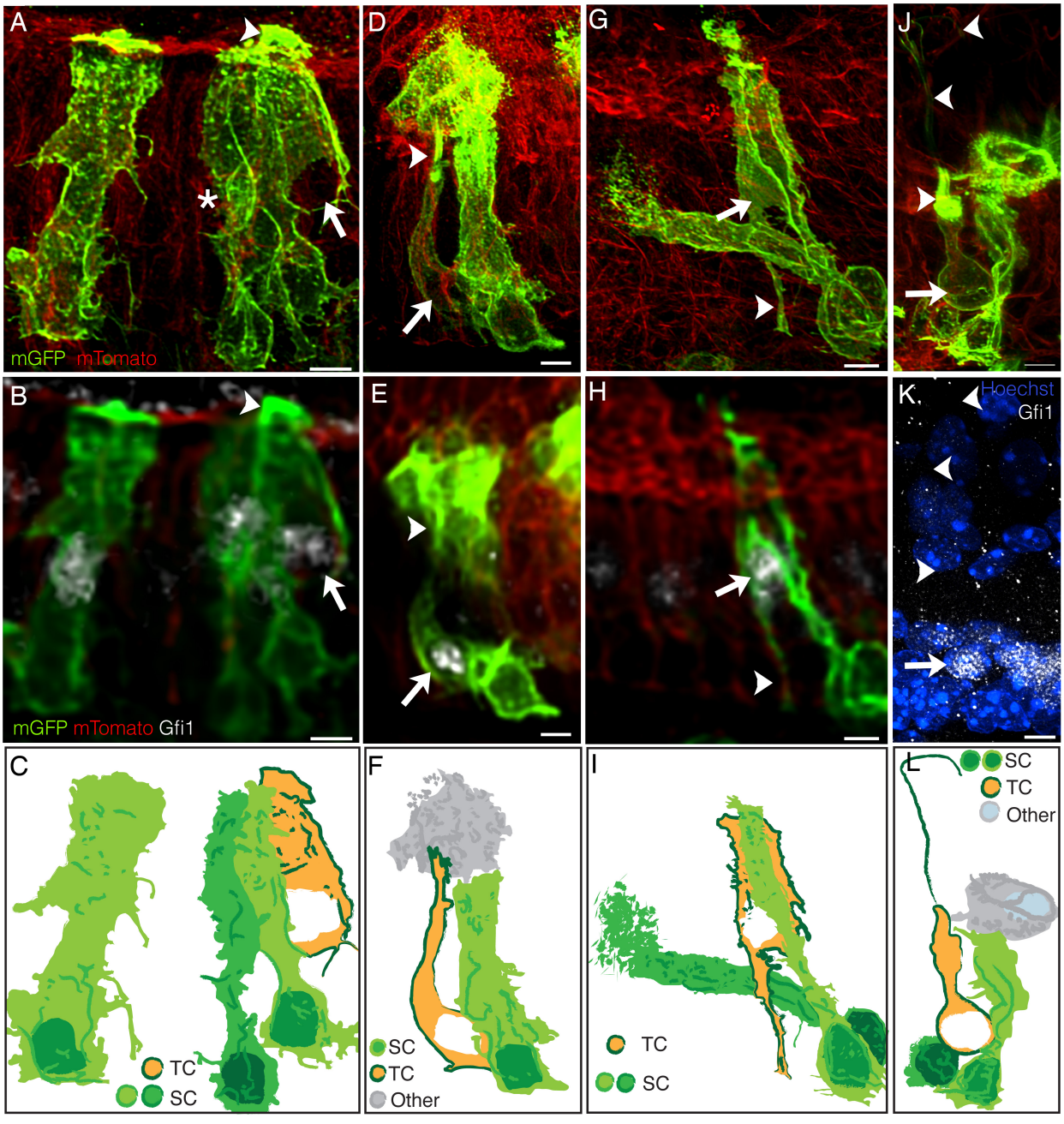
A
D
G
J
mGFP mTomato
B
E
H
K
Hoechst
Gfi1
mGFP mTomato Gfi1
C
F
I
L
TC
SC
SC
TC
Other
TC
SC
SC
TC
Other

Figure 2.10 Examples of lineage-traced transitional cells. Two views of the cells are shown, one at 60x (A,D,G,J,K) and the other at 20x (B,E,H), due to bleaching of the Gfi1 staining at the higher magnification. All scale bars, 5 μm. **A,B,C)** An example of a lineage traced cell representative of the majority of observed TCs. This cell was located in the hair cell layer, expressed Gfi1 (arrow), and had a taller apical mGFP labeling than surrounding support cells (SC) (arrowhead). A diagram of this cell (C) also shows several GFP^+ support cells near the hair cell, one of which partially enveloped an unlabeled hair cell (dark green cell, asterisk in A). **D,E,F)** A lineage traced cell with a morphology intermediate between a hair cell and a support cell. This cell expressed Gfi1 (arrow) and also had a taller apical mGFP labeling (arrowhead). This cell, however, was not in the hair cell layer, nor was it attached to the basement membrane. A diagram of this cell (F) also shows several GFP^+ non-sensory cells (other) and a GFP^+ support cell surrounding the TC. **G–I)** Another lineage traced TC had a traditional hair cell morphology and Gfi1 expression (arrow), but also had a trailing foot attached to the basement membrane (arrowhead). A diagram of this cell (I) also shows two GFP^+ support cells. **J–L)** The last example TC had a typical hair cell morphology, a kinocilium (arrowhead in J), and Gfi1 expression (arrow in K). A diagram of this cell (L) also shows a GFP^+ non-sensory cell and two GFP^+ support cells surrounding the hair cell.

found in the hair cell layer and had an immature hair cell morphology including a large, rounded nucleus and longer apical projections than the surrounding GFP^+ support cells (arrowhead, Figure 2.10A-C). There were several instances, however, where I observed more intermediate morphologies between that of a support cell and a hair cell. For example, one such cell had an elongated body typical of a support cell, but appeared to be lifting off of the basement membrane and in the process of translocating to the hair cell layer (Figure 2.10D-F; Supplemental Movie 2.2). The apical projection of this cell was thinner than the other labeled support cells and it had intense apical mGFP labeling with an appearance unlike other hair cells or support cells (arrowhead in Figure 2.10D-E). In addition, there were TCs located in the hair cell layer with hair cell morphologies that maintained contact with the basement membrane through thin, foot-like projections (arrowhead, Figure 2.10G-I; Supplemental Movie 2.3). In one instance, there was a TC that appeared to have a more mature morphology that was characteristic of a 'normal' hair cell. This TC was in the hair cell layer with a hair cell appearance, including a large rounded nucleus and a thin apical neck. In addition to having what appears to be a stereocilia bundle like the majority of the TCs, this cell also had a clear kinocilium extending from its apical surface (arrowheads, Figure 2.10J-L; Supplemental Movie 2.4). This was the most mature-looking cell that I observed, perhaps suggesting that this cell was one of the first to transdifferentiate and thus had more time to reach maturity.

Overall, these data suggest that Notch signaling plays a role in maintaining the support cell phenotype in a subset of support cells in the mature cristae. Upon DAPT-treatment, these support cells can transdifferentiate into hair cells that express the hair cell

marker Gfi1, translocate to the hair cell layer, and take on a hair cell morphology, which in one case included a long kinocilium.

2.3 DISCUSSION

2.3.1 NEW EVIDENCE FOR HAIR CELL REGENERATION IN THE CRISTAE

These results demonstrate that Notch signaling is active in the mature mammalian cristae and may be important for maintaining the support cell fate in a subset of peripheral support cells. Culturing postnatal and adult cristae from Hes5-eGFP reporter mice with the γ-secretase inhibitor, DAPT, decreased the expression of the Notch effectors *Hes5* and *Hes1*. Hes5, as reported by Hes5-eGFP, was down-regulated specifically in peripheral support cells. DAPT-treatment resulted in an increase in the total number of $Gfi1^+$ hair cells at a similar rate in both the mature and postnatal cristae. New hair cells arose without proliferation, as no hair cells incorporated EdU even though it was present throughout the entire culture period. Instead, lineage tracing in adult cristae showed hair cells arose through transdifferentiation of PLP-expressing support cells. These transdifferentiated cells expressed the early hair cell marker Gfi1 and were capable of displaying hair cell morphologies, migrating to the correct cell layer, and assembling a stereocilia bundle with a kinocilium.

Previous work in the mature chinchilla cristae provided evidence for spontaneous hair cell regeneration after damage (Tanyeri*, et al.,* 1995, Lopez*, et al.,* 1997, Lopez*, et al.,* 1998, Lopez*, et al.,* 2003). These studies found a partial recovery in hair cell number and innervation over time without a concomitant decrease in support cells. While this was

suggestive of proliferative regeneration, the limitations of the chinchilla system prevented further analysis. Here, in addition to providing further evidence for hair cell regeneration in the mature mammalian cristae, I show that hair cells arise through transdifferentiation of support cells using lineage tracing with PLP/CreER;mTmG mice. This is the first evidence for direct transdifferentiation from support cells to hair cells in the mature mammalian vestibular system. Though I cannot discount a role for some hair cell survival or repair, the use of lineage tracing with the PLP/CreER;mTmG mice shows that at least a portion of the hair cell increases are due to support cell transdifferentiation. In addition, while I attribute these increases to Notch inhibition based on the downregulation of Notch effectors such as Hes5 and Hes1, other pathways could also be involved. The Notch receptor is not the only target for γ-secretase, and therefore Notch might not be the only pathway whose inhibition is contributing to the regeneration observed through γ-secretase inhibition with DAPT. The γ-secretase complex is involved in a process called regulated intramembrane proteolysis (RIP) that has over ninety known substrates including Notch receptors and ligands, amyloid precursor protein (APP), Ephs/Ephrins, Interleukin receptors, cadherins, and Erb/Neuregulins (reviewed in Haapasalo and Kovacs, 2011).

2.3.2 THE ROLE OF DAMAGE IN NOTCH-MEDIATED HAIR CELL REGENERATION

In other systems where hair cells can be generated through transdifferentiation following Notch inhibition, Notch signaling is either continuously active in the organs and required to maintain the mosaic pattern of support cells and hair cells or Notch signaling components are upregulated in response to damage. Several studies have suggested that hair

cell damage may be required for Notch-mediated regeneration in the adult utricle (Wang*, et al.,* 2010, Lin*, et al.,* 2011, Jung*, et al.,* 2013), consistent with what has been shown in the zebrafish lateral line and the chick basilar papilla (Ma*, et al.,* 2008, Daudet*, et al.,* 2009). Although my experiments were performed *in vitro* and, therefore, involved some hair cell death due to the damage from culturing the organs, I believe that cristae differ from the utricle in that they do not require damage for hair cell regeneration. In the mature undamaged utricle, Hes5 is only expressed in a small subset of support cells in the posteromedial region, whereas in the mature undamaged cristae Hes5 is expressed in all of the peripheral support cells (Hartman*, et al.,* 2009). In the utricle, it therefore makes sense that many support cells would need to upregulate Notch signaling in response to damage before Notch can be inhibited in order to generate hair cells. In the cristae, however, since Notch signaling is normally present in the majority of peripheral support cells, it may be playing an ongoing role in maintenance of the support cell fate and may not require a damage-induced upregulation of Notch signaling for hair cell regeneration.

Further evidence for this hypothesis comes from the comparison between hair cell regeneration at the adult and postnatal ages. At P7, the total number of hair cells increased in response to Notch inhibition with no damage to the cristae evident from culturing. This suggests that the level of Notch signaling present in the P7 cristae is sufficient for maintenance of the support cell fate through lateral inhibition. Further, an RT-qPCR analysis of the mRNA expression levels of *Hes5* and *eGFP* (from the *Hes5-eGFP* transgene) showed that *Hes5* is expressed at similar levels in uncultured cristae of postnatal and adult mice. This is consistent with the immunofluorescence data from the Hes5-eGFP transgenic mice, which

also shows a downregulation of Hes5-eGFP in response to Notch inhibition in both postnatal and adult cristae at a similar level. Therefore, while I cannot preclude the possibility that damage is necessary for DAPT-induced hair cell generation, I believe that the ongoing presence, expression levels, and responsiveness of Hes5 to Notch inhibition suggests that Notch may be important in the quiescent, undamaged cristae. However, since Hes5 is expressed at a lower level at P7 and in the adult than in earlier postnatal animals, suggesting lower levels of Notch signaling, it is still possible that further damage could stimulate additional regeneration.

2.3.3 MORPHOLOGICAL CHANGES OBSERVED DURING TRANSDIFFERENTIATION

In the lineage tracing experiments using the PLP/CreER;mTmG mice, there were several interesting morphological changes in the transdifferentiating cells. These changes were similar to those noted in the initial reports on transdifferentiation in the mature regenerating organs of bullfrogs (Baird*, et al.,* 1996, Steyger*, et al.,* 1997), chicks (Raphael*, et al.,* 1994, Adler and Raphael*,* 1996, Adler*, et al.,* 1997), bats (Kirkegaard and Jorgensen*,* 2000) and guinea pigs (Li and Forge*,* 1997). Since hair cell regeneration occurs in most vertebrate species, it is perhaps unsurprising that these different species show similar changes as cells transition between the distinct morphologies of support cells and hair cells. Most of these studies reported transdifferentiating cells with morphologies intermediate between those of support cells and hair cells. Like support cells, these cells were elongated and spanned the entire sensory epithelium. However, these cells also had enlarged, basally located nuclei and immature stereocilia bundles, suggesting that they were becoming hair cells. In my data, most

of the cells appeared to be in later stages of transdifferentiation. Most of the cells had typical hair cell morphologies, were located in the hair cell layer, and appeared to have longer apical processes. However, there were two types of cells that appeared to be in earlier stages almost identical to those previously reported. The first cell was located near the planum semilunatum and had a transitional morphology between a hair cell and a support cell. Further, this cell was separated from the basement membrane, appearing to be translocating its nucleus to the hair cell layer. This is similar to other studies in the chick basilar papilla where it appeared that detachment from the basement membrane occurred early, prior to or during translocation of the nucleus (Raphael*, et al.,* 1994, Adler*, et al.,* 1997). The second cell, located near the eminentia cruciatum, had a characteristic hair cell morphology and layering, but maintained contact with the basement membrane through a thin foot-like projection. This is similar to the study by Li and Forge (1997) in the guinea pig utricle where it appeared that transitioning cells maintained contact with the basement membrane until later stages of transdifferentiation. These basal projections are also seen in other cases where hair cells are generated through overexpression of cyclin D1 or Atoh1 (Loponen*, et al.,* 2011, Lewis*, et al.,* 2012). Although I did not have the same subcellular resolution as the thin sections used in most of these previous experiments, the membrane-bound GFP allowed me to observe nearly identical intermediate morphologies in whole mount explants. Whether these different morphological changes represent distinct mechanisms, it is interesting that support cell transdifferentiation may proceed through similar intermediate morphologies in the chick basilar papilla, the guinea pig utricle, and the mouse cristae.

2.3.4 REGIONAL DIFFERENCES IN HAIR CELL REGENERATION

While the morphological changes occurring during transdifferentiation may be similar between species, the regenerative ability of mammals, whether spontaneous or through manipulations such as Notch inhibition, is much lower than all other vertebrates studied (reviewed in Warchol*,* 2011). This suggests that only a subset of support cells remain competent to form hair cells in the mature mammalian vestibular system. The role for additional factors, such as other signaling pathways or further regulation downstream of Notch signaling is apparent in my data, since only a fraction of the peripheral support cells that express Hes5 and down-regulate it in response to Notch inhibition undergo transdifferentiation. However, determining the identity of these factors and why they only affect certain support cells ultimately requires a better understanding of vestibular support cells and their markers. Here I show that some of the support cells capable of transdifferentiating express the PLP transgene, as was also shown in the postnatal utricle (Collado*, et al.,* 2011). In addition, in P7 explants the support cells near the eminentia cruciatum are the most responsive to Notch inhibition. Though there is no obvious difference in Hes5 expression or down-regulation in this region, more hair cells were generated here with a concomitant loss in support cells following Notch inhibition. This is similar to a result found by Lopez*, et al.* (1997) studying spontaneous hair cell regeneration after damage in the mature chinchilla crista, where hair cells regenerated along this same gradient, from the crux eminentia to the planum semilunatum. However, in the experiments using mature PLP/CreER;mTmG mice, there were lineage-traced hair cells throughout the peripheral zone of the cristae, both near the eminentia cruciatum and the planum

semilunatum. Therefore, while the PLP-transgene limited the analysis to the peripheral zone, at least within this region there was not a particular area of regenerative competence in the adult. Even if this regenerative gradient only occurs postnatally, it is still an interesting finding since the crux eminentia of the crista and the striola of the utricle are the only places where the zinc finger gene GATA-3 is expressed (Karis*, et al.,* 2001). GATA proteins have been shown to act cooperatively with NICD-CSL at the promoter level (Neves*, et al.,* 2007) and in the inner ear, it has been suggested that GATA-3 expression could be important for hair cell regeneration through downstream signaling targets such as Wnt (Alvarado*, et al.,* 2009).

In the mature regenerating utricle, there does appear to be regional regeneration (Collado*, et al.,* 2011, Lin*, et al.,* 2011, Golub*, et al.,* 2012, Jung*, et al.,* 2013), though there is no consensus on which regions are competent for regeneration as the regionalization found varied between studies. Similar to the utricle, there were some regional differences in hair cell regeneration in the crista. Though this analysis was largely limited to the peripheral region, since both Hes5 and PLP are expressed only in peripheral support cells, I did not see any significant qualitative evidence of hair cell regeneration in the central zone. The central zone of the cristae shares many characteristics with the striola of the utricle and generally exhibited the highest degree of hair cell death in the cultures, with occasional loss of all of the hair cells in this region. There did not appear to be any increase in hair cells in this region in the DAPT-treated cultures as opposed to those treated with DMSO. This would be more similar to the study by Jung*, et al.* (2013) where most of the hair cell increases are in the regions that maintain Hes5 expression in the mature organ. In addition, there was a larger

decrease in *Hes5* expression in response to Notch inhibition than of *Hes1*. Studies showing hair cell regeneration in the striolar region of the utricle have reported decreases in *Hes1* expression during the regenerative process (Collado*, et al.,* 2011, Lin*, et al.,* 2011). It would be interesting to know in what cells Hes1 is being expressed in the mature cristae and, again, whether it and Hes5 have unique roles in both the undamaged and damaged cristae.

CHAPTER THREE

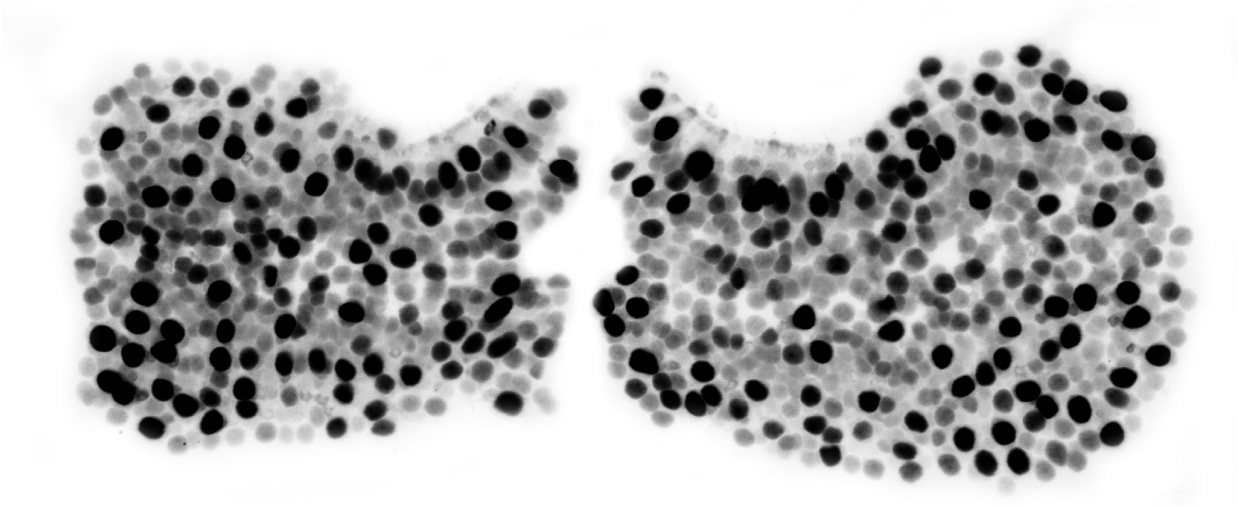

SPONTANEOUS HAIR CELL REGENERATION *IN VIVO*

3.1 INTRODUCTION

Since the *in vitro* results demonstrating that the adult cristae have some regenerative capacity in response to Notch inhibition were very promising, I next wanted to validate these results *in vivo*. In addition to validation, performing experiments in live animals is necessary to assess behavioral recovery and to determine if the hair cells can reintegrate into the neural circuitry. In previous studies of regeneration, new hair cells were able to reintegrate by recruiting nerve fibers and forming synaptic connections. These new hair cells were generated through a variety of methods, including through spontaneous regeneration after damage (Lopez*, et al.,* 2003), overexpression of Atoh1 (Kawamoto*, et al.,* 2003, Gubbels*, et al.,* 2008, Kelly*, et al.,* 2012, Liu*, et al.,* 2012a), and through induction of ectopic patches through activation of Notch signaling (Hartman*, et al.,* 2010, Liu*, et al.,* 2012b, Pan*, et al.,* 2013). In my *in vitro* cultures, the cristae were isolated and maintained without the neurons of Scarpa's ganglion, making it impossible to assay for these signs of reintegration.

In order to assess for reinnervation, it is important to be able to distinguish newly generated hair cells from pre-existing and repaired hair cells. For this, lineage-tracing of the support cells is the easiest and most accurate method since new hair cells mostly arise through transdifferentiation of support cells. For my previous experiments, I used the PLP/CreER mice (Doerflinger*, et al.,* 2003, Gomez-Casati*, et al.,* 2010) for lineage tracing, which allowed for a successful identification of transdifferentiating support cells, but limited the analysis to the peripheral region of the cristae, where PLP/CreER is expressed. For future experiments, an analysis of the entire cristae would be better, but would require a mouse line expressing an inducible Cre recombinase in all of the support cells. Although

many Cre-expressing mouse lines useful for inner ear work have been described (reviewed in Cox*, et al.,* 2012), there are no known inducible Cre lines with robust support cell expression and no hair cell expression except for the PLP/CreER mice.

In order to identify a suitable mouse line expressing an inducible Cre recombinase for *in vivo* experiments, I performed a screen of various Cre-expressing mouse lines with known expression in the nervous system in collaboration with Dr. Julie Harris of the Allen Institute for Brain Science. I characterized the expression of these lines in the inner ear and from this screen identified several promising lines for future inner ear work and one promising candidate specifically for lineage tracing support cells for studying hair cell regeneration. I confirmed the endogenous expression of this gene in the cristae using immunohistochemistry and confirmed that this line recombines in support cells and no hair cells both *in vitro* and *in vivo*. Further, I used this line of mice to characterize spontaneous regeneration of hair cells after damage in the mouse *in vivo* using lineage tracing.

Previous studies of spontaneous hair cell regeneration after damage in the cristae were performed in the chinchilla, where the lack of genetic tools requires the use of secondary measures to identify regenerating hair cells, such as the presence of immature hair bundles, the presence of hair cells after a complete lesion, and the identification of intermediate transitional morphologies (Tanyeri*, et al.,* 1995, Lopez*, et al.,* 1997, Lopez*, et al.,* 1998, Lopez*, et al.,* 2003). Although these measures are indicative of hair cell regeneration, only lineage tracing can definitively show that a hair cell has transdifferentiated from a support cell and is, therefore, a result of regeneration and not incomplete lesion or repair.

3.2 RESULTS

3.2.1 SCREEN FOR CRE RECOMBINASES EXPRESSED IN THE INNER EAR

In order to screen for inner ear expression of Cre-expressing mouse lines, I examined the expression of Cre recombinase in adult inner ear capsules provided by Dr. Julie Harris at the Allen Institute for Brain Science. The Cre-expressing mouse lines screened had known expression in the nervous system and were crossed to the Ai14 reporter mouse line. Ai14 mice express a floxed-stop tdTomato under the CAG promoter in the *ROSA26* locus (Madisen*, et al.,* 2010) and exhibit robust expression of tdTomato throughout the cell upon Cre-mediated removal of the floxed-stop element. All mice screened were approximately eight weeks old at the time of sacrifice and for each line only one mouse was screened. For mice expressing non-inducible Cre recombinases, it is not possible from the samples obtained to determine when recombination occurred or whether recombination occurred in the labeled cells or in a progenitor cell. For the mice expressing inducible Cre recombinases, five doses of tamoxifen (5.0 mg/25 g mouse) were administered via oral gavage, with the last dose given two days prior to sacrifice.

From the screen, I identified seven mouse lines with potentially useful expression in the inner ear. Two lines, Calb2-IRES-Cre and Otof-Cre, showed specific expression in hair cells (Figure 3.1A,B), and five lines showed expression mainly in support cells, including Wfs1-Tg2-CreERT2, Glast-CreER (transgenic and knock-in), Cralbp-CreER, and Dcx-CreER (Figure 3.1C-F').

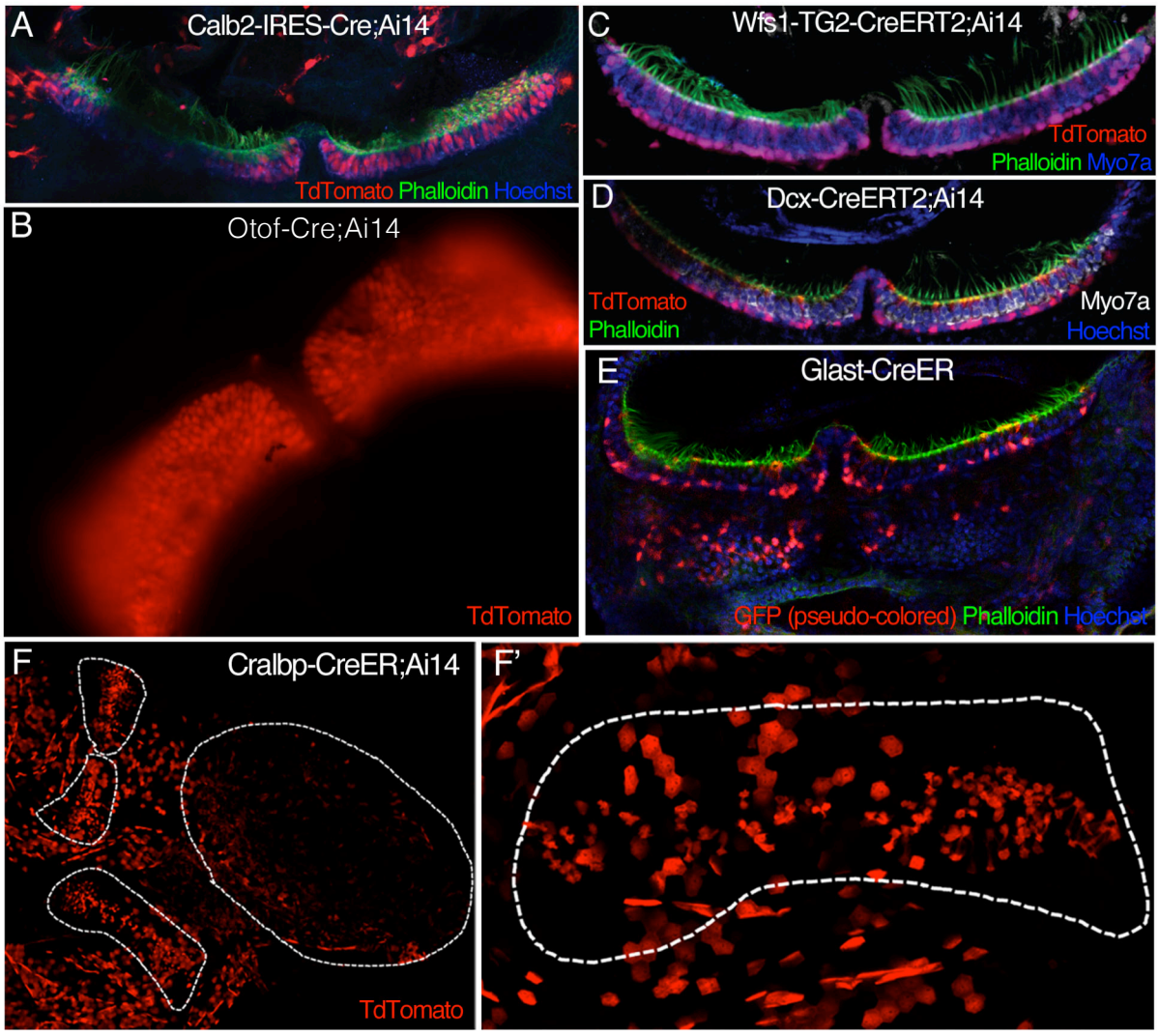

Figure 3.1 Mouse lines with useful expression of Cre recombinase in the crista. **A)** Adult Calb2-IRES-Cre;Ai14 mice show recombination in almost all hair cells in the cristae (dark area in A is shadowed by pigment) as well as in some non-sensory cells. **B)** Adult Otof-Cre;Ai14 mice show recombination in all hair cells in the cristae. **C)** Adult Wfs-TG2-CreERT2;Ai14 mice show recombination mainly in support cells, but also in some hair cells and non-sensory cells. **D)** Adult Dcx-CreERT2;Ai14 mice show recombination almost exclusively in the support cells. **E)** Adult Glast-CreER knockin mice show recombination in a scattering of support cells throughout the sensory epithelium. **F-F')** P14 Cralbp-CreER;Ai14 mice show recombination in many non-sensory cells of the ampulla and canals, with less recombination occurring around the utricle. In addition, they show recombination in many support cells located in the central zone of the cristae. White dotted lines indicate the location of the sensory epithelia, including the two cristae and the utricle.

The Calb2-IRES-Cre knock-in mice express Cre recombinase in most of the hair cells in the cristae, in addition to some non-sensory cells and neuronal like cells (Figure 3.1A). The Otof-Cre knock-in mice, on the other hand, express Cre recombinase exclusively in all of the hair cells of the cristae (Figure 3.1B). Since the Otof-Cre mice express Cre recombinase in only the hair cells in the cristae, as compared to Calb2-IRES-Cre mice, which have some expression in other cells, the Otof-Cre mice would be a better line for restricting expression to hair cells for experiments involving FACS or genetic lesion.

The Cralbp-CreER transgenic mice express Cre recombinase in many non-sensory epithelial cells throughout the ampulla and the semicircular canals, characterized by their honeycomb shape (Figure 3.1F,F'). In addition, these mice express Cre recombinase in a subset of support cells found in the central region of the cristae, which directly complements the PLP-Cre/ER mice that express Cre recombinase in a subset of support cells found in the peripheral zone. Together, these two strains can be used characterize differences between these two regions and support cell populations.

The Wfs1-TG2-CreERT2 transgenic mice express Cre recombinase in support cells in the cristae throughout the entire sensory epithelium at a high efficiency (Figure 3.1C). However, these mice also have a low rate of hair cell recombination, which makes them unusable for lineage tracing for regeneration studies. These mice may still be useful though for experiments involving FACS, as they can be used to label almost all of the support cells with no regional restriction and only a small amount of hair cell contamination.

The Dcx-CreER transgenic mice (Figure 3.1D) and the Glast-CreER transgenic and knock-in mice (Figure 3.1E) express Cre recombinase almost exclusively in support cells

throughout the entire sensory epithelium. While none of these mouse lines show any recombination in hair cells, they all have significantly lower recombination efficiencies than the Wfs1-TG2-CreERT2 mice. However, the lack of hair cell recombination makes these mice excellent for lineage tracing for regeneration studies and FACS.

Since the Dcx-CreER transgenic mice have a higher recombination efficiency than the Glast-CreER mice, I decided to further assess the suitability of the Dcx-CreER mice for lineage tracing support cells. For more information on the screen I performed and the various mice lines screened, including their expression in the cochlea and their endogenous expression, see Appendix 1.

3.2.2 RECOMBINATION IN DCX-CreER MICE IS EXCLUSIVELY IN SUPPORT CELLS

To confirm the expression of the Dcx-CreER transgene in the support cells, I obtained the Dcx-CreER mice from the Mutant Mouse Regional Resource Centers (MMRRC), crossed them to the Ai14 mouse line, and induced recombination with tamoxifen in eight week old mice both *in vivo* and *in vitro*. Tamoxifen was administered *in vivo* using a single intraperitoneal (ip) injection of tamoxifen (3.0 mg/25 g mouse) and *in vitro* by adding 5 μM 4-OHT to the media. For *in vitro* experiments, the cristae explants were cultured for two DIV with two media changes containing fresh tamoxifen per day. For both *in vivo* and *in vitro* experiments, cristae were fixed two days after the initial tamoxifen treatment, immunolabeled for Myo7a and Sox2, and analyzed for recombination. In total, sixteen cristae were analyzed and no hair cell recombination was observed in either the *in vivo* or the *in vitro* conditions. Instead, consistent with the results of the initial screen, only

support cells and non-sensory cells immediately adjacent to the sensory epithelium underwent recombination (Figure 3.2A-C'").

3.2.3 IMMUNOLABELING FOR ENDOGENOUS DCX EXPRESSION

In the nervous system, Dcx is expressed in developing neurons (Francis*, et al.,* 1999, Gleeson*, et al.,* 1999, Tanaka*, et al.,* 2004) and in regions of the adult brain where there is ongoing neurogenesis, including in the subventricular zone and in the subgranular zone (Nacher*, et al.,* 2001, Brown*, et al.,* 2003, Rao and Shetty*,* 2004, Couillard-Despres*, et al.,* 2005). In the inner ear, the expression of Dcx has not been described. Since Dcx is normally expressed in neuronal cell types, it is possible that the expression of the Dcx-CreER transgene in the support cells of the crista is due to the transgene not faithfully reporting on

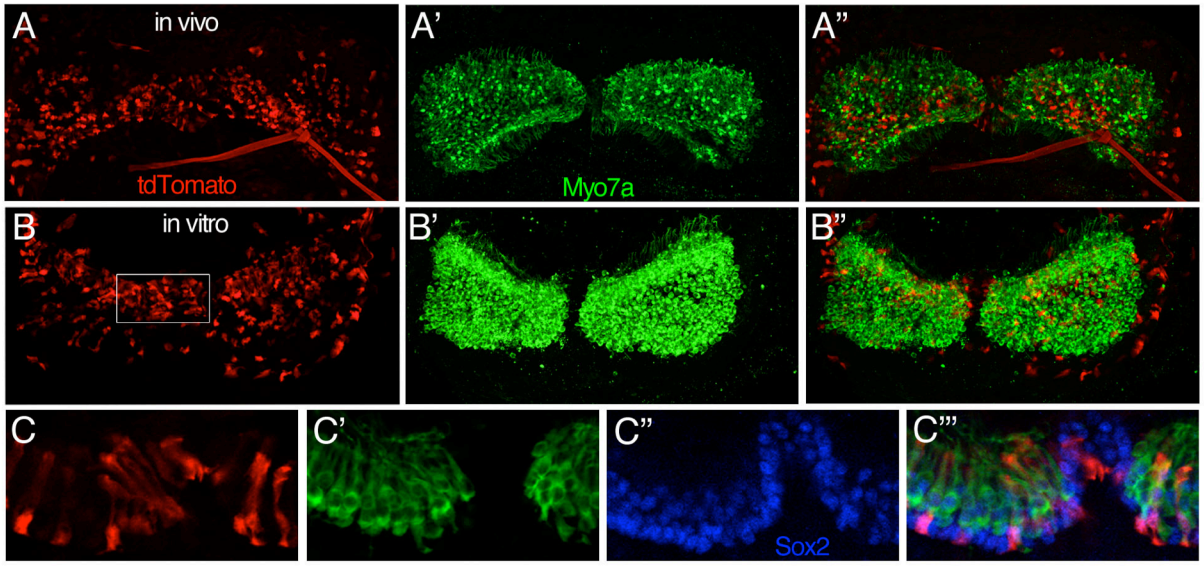

Figure 3.2 Support cells recombine in adult Dcx-CreER;Ai14 mice. **A-A") ** Whole mount cristae explanted from eight week old mice given a single injection of tamoxifen (3.0 mg/25 g mouse) two days prior to sacrifice show robust tdTomato expression in support cells (A,merge in A") in the sensory region labeled by Myo7a (A', merge in A"). **B-B") ** Cristae explanted from eight week old mice and cultured for 2 DIV with 4 media changes of fresh 5 uM 4-OHT also show robust tdTomato expression in support cells. Images in A-B" are maximum intensity projections. **C-C'") ** A zoomed inset of the boxed region in B shown in a single slice depicts the morphology and the layering of the tdTomato+ support cells. Sox2, expressed in support cell nuclei and some hair cell nuclei is also shown (C").

the endogenous expression of Dcx. To address this, I assayed the endogenous expression of Dcx in the cristae of P11 Math1-GFP mice using an antibody against Dcx. Surprisingly, the Dcx antibody labeling in the cristae was specific to the sensory epithelium (Figure 3.3A-B'", red), consistent with the expression of the Dcx-CreER transgene. A higher magnification view of the Dcx immunolabeling reveals that the strongest Dcx labeling is above the circumferential F-actin bands at the junctions between support cells labeled here by Phalloidin (Figure 3.3C-C'", white). In addition, there is a lower level of labeling in the cytoplasm of the support cells (Figure 3.3C), most evident by the lack of staining where the hair cells are located. These same regions lacking immunolabeling can be seen in the lower magnification view (Figure 3.3A,B), where they appear as holes in the immunolabeling. These holes appear because support cells send processes through the hair cell layer to the apical surface and tightly interdigitate between hair cells (Figure 2.1F). The apical portion of the support cells, therefore, appears as tight rings around the hair cells with holes in the center. Control cristae stained at the same time, under the same conditions, and with the same secondary antibodies did not show this labeling.

Overall, therefore, the consistency of the Dcx immunolabeling with the expression of the Dcx-CreER transgene suggests that Dcx may be expressed in the support cells of the cristae. However, without further control experiments such as immunolabeling of cristae deficient in Dcx, I cannot definitively say whether Dcx is endogenously expressed in support cells. A study comparing the gene expression of hair cells versus support cells using laser microdissection and microarray did not find a greater than 5-fold enrichment of Dcx in the support cells versus the hair cells of the cristae (Cristobal*, et al.,* 2005). However, it is

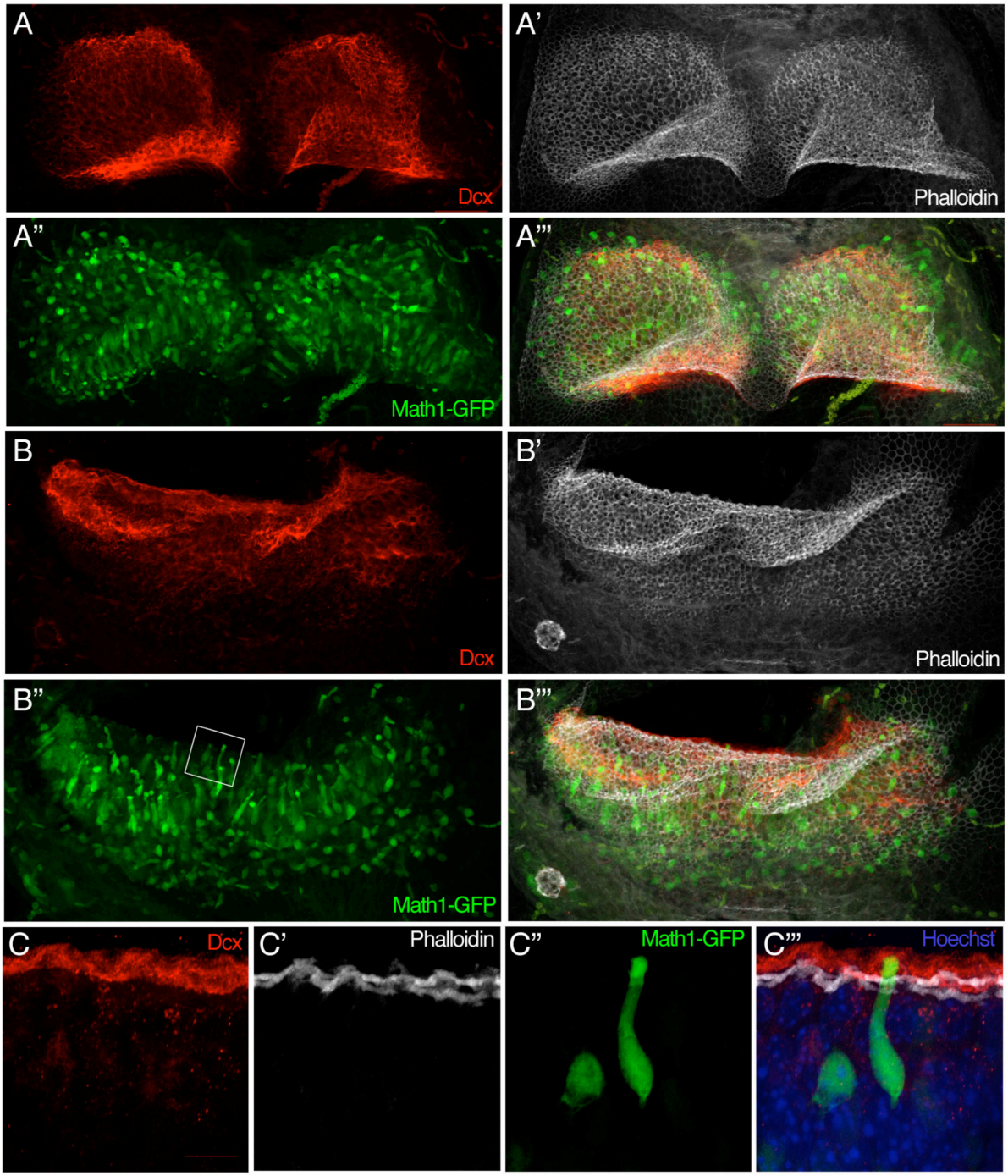

Figure 3.3 Doublecortin antibody staining in Math1-GFP cristae. **A-B''')** P11 transgenic mice expressing GFP under the Math1 promoter were immunolabeled for Doubelcortin (Dcx, red) and F-actin (Phalloidin, white) in anterior (A-A''') and horizontal (B-B''') cristae. **C-C''')** A higher magnification of the boxed region in B" showing the localization of Dcx mainly above the circumferential F-actin bands at the junctions between support cells (labeled with Phalloidin).

possible that this assay was not sensitive enough to detect the Dcx expression or that the Dcx result is a false negative, since so many genes were screened in this analysis. Despite the lack of microarray evidence for Dcx expression in support cells, this result bears further investigation.

3.2.4 CHARACTERIZING SPONTANEOUS REGENERATION AFTER DAMAGE USING THE DCX-CreER MICE

Whether or not support cells endogenously express Dcx, the Dcx-CreER transgene appears to faithfully lineage trace support cells in the adult cristae both *in vivo* and *in vitro* (Chapter 3.2.2). To test the use of this line for lineage tracing support cells to assay for hair cell regeneration, I used the Dcx-CreER mice to characterize spontaneous hair cell regeneration after damage in the adult cristae. In order to lesion the hair cells, I used the known ototoxin 3,3'-Iminodipropionitrile (IDPN). The mechanism through which IDPN lesions hair cells has not been elucidated; however, the effect of IDPN on vestibular hair cells, namely in the cristae, has been well documented qualitatively (Soler-Martin*, et al.,* 2007).

Using the previously published dose of 24 mmol/kg IDPN, I found quantitatively in a single mouse that the hair cells lesioned as expected for nitriles (Figure 3.4A). The cristae were the most affected by nitrile lesion with a 69.6-84.1% lesion. There were 225/236 $Gfi1^+$ hair cells in the posterior cristae, 412/430 hair cells in the anterior cristae and 295/324 hair cells in the horizontal cristae, compared to an average of 1413±102 hair cells in all cristae as published by Desai*, et al.* (2005a) (Figure 3.4A, white circle). In the utricle, more hair cells were lost; however, the utricle has more than twice the number of hair cells as the cristae.

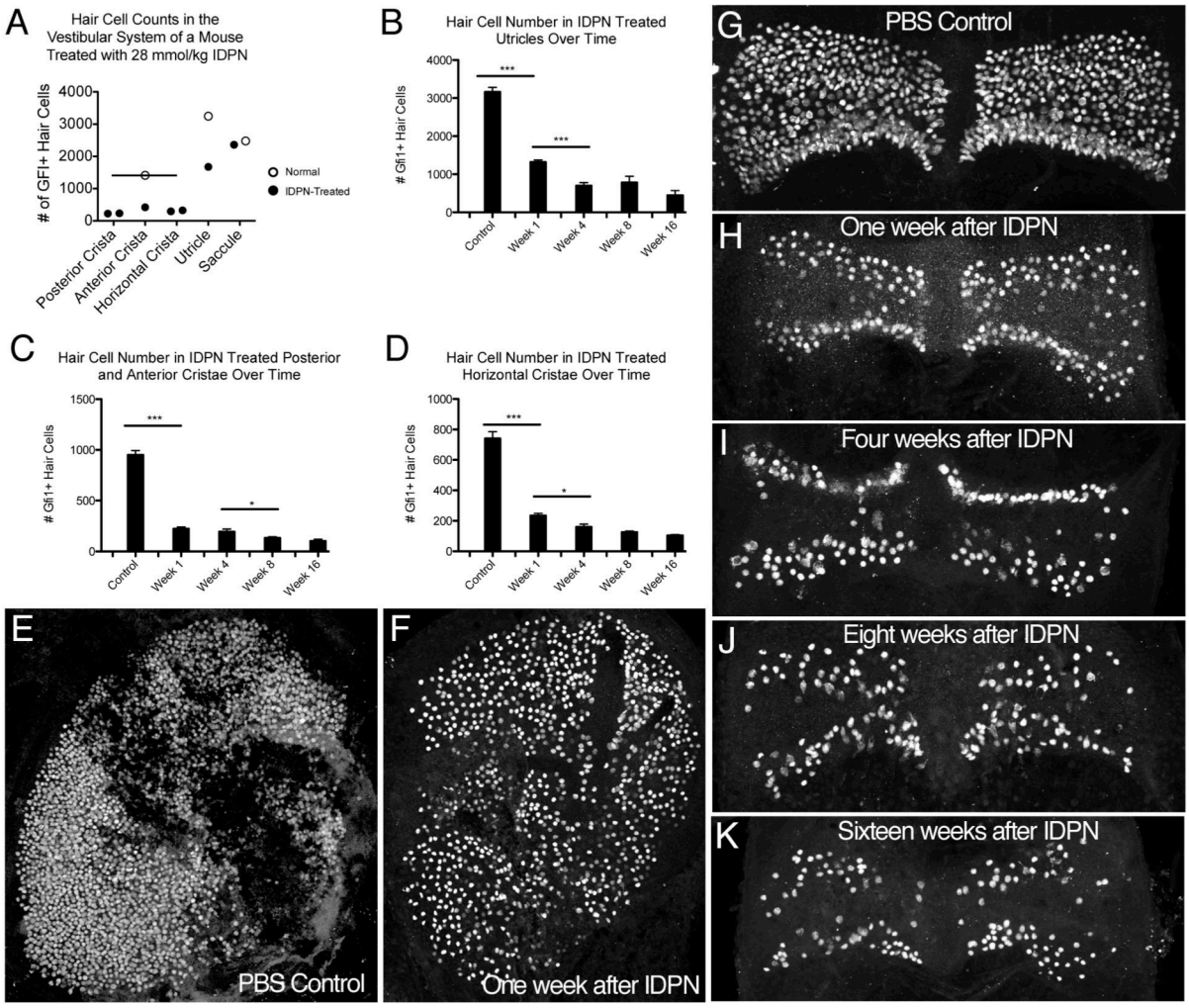

Figure 3.4 Spontaneous regeneration in adult CBA/CaJ males after IDPN lesion. **A)** In a single animal treated with 24 mmol/kg IDPN, the vestibular organs are affected in the order of most to least: cristae, utricle, saccule (black circles compared to white circles, which are the mean number of hair cells found in that organ published by Desai*, et al.* (2005a), Desai*, et al.* (2005b) **B-D)** The number of Gfi1+ hair cells in controls and one, four, eight, and sixteen weeks after lesion in utricles (B), anterior and posterior cristae (APC)(C), and horizontal cristae (HC)(D). Statistical analyses were standard Student's t-tests. Error bars depict SEM. **E)** Control utricles from mice injected with PBS have 3159.0±123.2 (*n*=6) hair cells. **F)** One week after IDPN-treatment, utricles have 1319±56.11 (*n*=9) hair cells. Although not shown, four weeks after lesion utricles have 698.6±83.44 (*n*=5) hair cells. Eight weeks after, utricles have 782.2±163.3 (*n*=5) hair cells. Sixteen weeks after, utricles have 446.0±124.7 (*n*=5) hair cells. **G)** Control cristae have 948.9±45.08 (*n*=17) hair cells in APC (shown) and 740.6±45.18 (*n*=16) hair cells in HC (not shown). **H)** One week after IDPN-treatment, APC have 223.6±16.68 (*n*=34) hair cells, while HC have 233.4±15.15 (*n*=19) hair cells. **I)** Four weeks after IDPN, APC have 194.9±25.42 (*n*=24) hair cells and HC have 159.7±17.81 (*n*=7) hair cells. **J)** Eight weeks after IDPN, APC have 131.4±11.6 (*n*=21) hair cells and HC have 125.8±7.42 (*n*=8) hair cells. **K)** Sixteen weeks after IDPN, APC have 102.0±16.94 (*n*=11) hair cells and HC have 102.5±6.41 (*n*=4) hair cells. Kayla Ritchie, an undergraduate, collected data in panels B-K.

Therefore, even though the IDPN-treated utricles had 1644/1706 hair cells compared to the expected number of 3246±58 as published by Desai*, et al.* (2005b) (Figure 3.4A, white circle), this represents only a 47.4/49.4% lesion. As expected based on previous reports, the saccule was the least affected, with only a 4.7% lesion, or 2361 hair cells as opposed to an expected number of 2477±37 hair cells as published by Desai*, et al.* (2005b) (Figure 3.4A, white circle).

An undergraduate, Kayla Ritchie, pioneered the use of IDPN to lesion hair cells in the Bermingham-McDonogh lab. She gave male CBA/CaJ mice older than 8 weeks of age intraperitoneal (ip) injections with 24 mmol/kg IDPN or PBS as a vehicle control. She then collected cristae at one week, four weeks, eight weeks, or sixteen weeks after IDPN-treatment, immunolabeled the cristae for Gfi1 to label hair cells, and counted the number of hair cells in treated versus control cristae. After one week, the number of hair cells in each organ decreased significantly, consistent with a successful lesion. In the utricle, there were 3159±123.2 (n=6) hair cells in controls versus 1319±56.11 (n=9) hair cells in lesioned utricles (58.3% lesion, t=15.24, df=13, p<0.0001). In posterior and anterior cristae, there were 948.9±45.08 (n=17) hair cells in controls and 223.6±16.68 (n=34) hair cells in lesioned cristae (76.4% lesion, t=18.38, df=49, p<0.0001). In horizontal cristae, there were 740.6±45.18 (n=16) hair cells in controls and 233.4±15.15 (n=19) hair cells in lesioned cristae (68.5% lesion, t=11.39, df=33, p<0.0001). In the following weeks, however, the number of hair cells did not increase, as predicted if spontaneous regeneration were occurring. Instead, there was a significant decrease in the total number of hair cells in each of the vestibular organs (Figure 3.4B-K). The fact that the total number of hair cells in the vestibular organs continued to significantly decrease after the initial lesion suggested that

there might be ongoing degeneration of hair cells in these organs. If present, this would require a more robust analysis such as lineage tracing to detect.

Therefore, to more definitively characterize spontaneous hair cell regeneration after

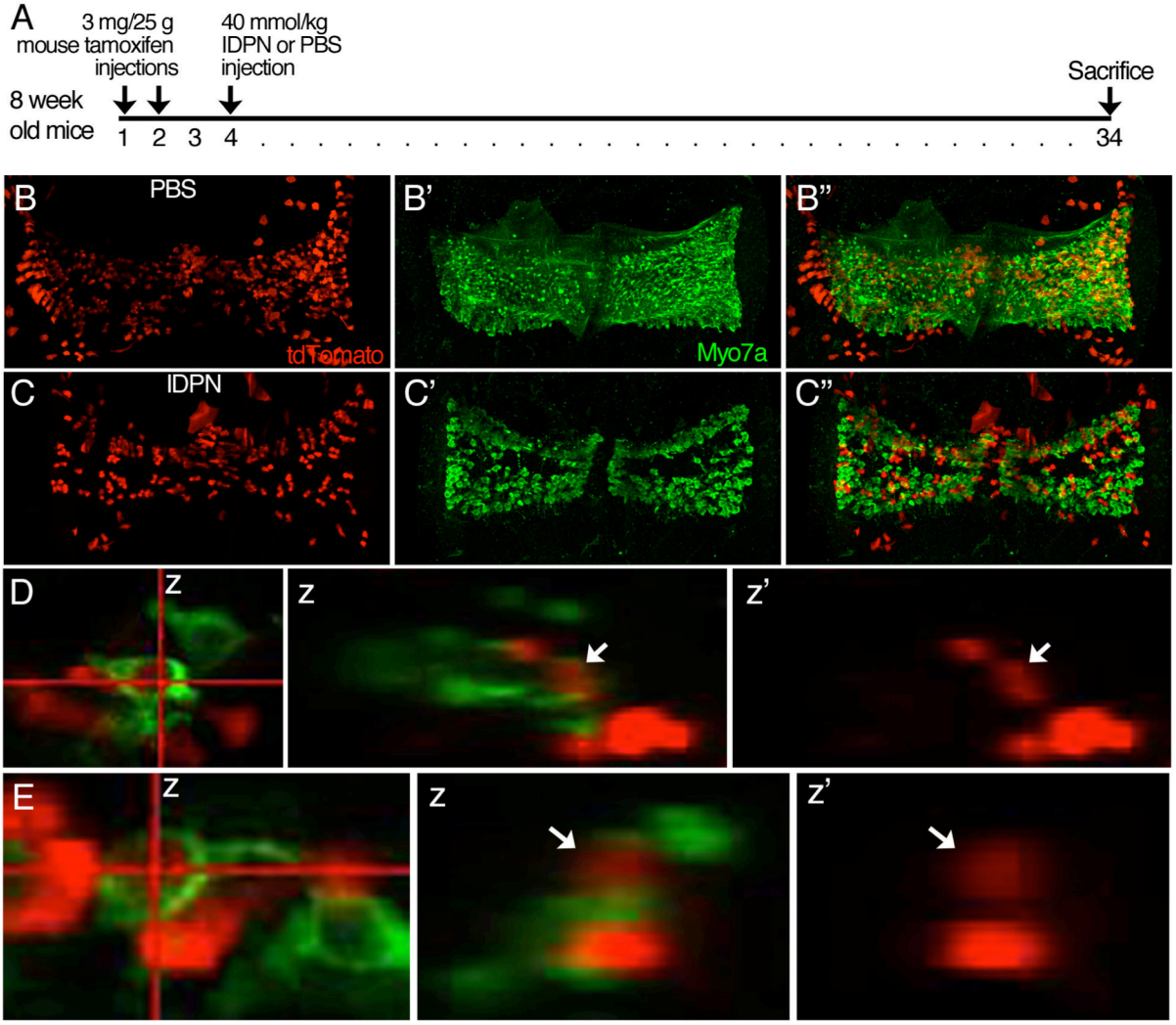

Figure 3.5 Adult Dcx-CreER;Ai14 mice have very little spontaneous regeneration in vivo. **A)** A schematic of the experimental design. Eight-week old Dcx-CreER;Ai14 mice were injected twice daily with tamoxifen (3 mg/25 g mouse), allowed to rest a day, and then injected with 40 mmol/kg IDPN to lesion their cristae. Control mice were injected with PBS. One month after lesion, the cristae were explanted, immunolabaled with Myo7a (green), and wholemounted. **B-B") ** Maximum intensity projections of an example of a control crista. **C-C") ** Maximum intensity projections of an example of a lesioned cristae. Very few hair cells are derived from tdTomato-expressing support cells, as evident by the lack of yellow, double-labeled cells. **D-E)** Examples of two cells derived from tdTomato-expressing lineaged traced support cells. Red lines indicate locations of slice projections showing both Myo7a and tdTomato (z) and tdTomato alone (z').

damage using lineage tracing, I gave eight week old Dcx-CreER;Ai14 mice two daily ip injections of tamoxifen (3.0 mg/25 g mouse), which is sufficient to induce support cell recombination at this age (Chapter 3.2.2). After a day of rest, I lesioned the hair cells by administering 40 mmol/kg IDPN or PBS as a vehicle control via ip injection (Figure 3.5A). This higher dose of IDPN was required to lesion the hair cells in the C57BL/6 mice, which is the strain background for the Dcx-CreER;Ai14 mice (see Chapter 5.2). Thirty days after IDPN-treatment, I harvested the cristae, immunolabeled them with Myo7a for hair cells (Figure 3.5, green), and analyzed them for cells expressing both Myo7a and tdTomato. The IDPN-treatment resulted in approximately a 50% lesion (Figure 3.5B' vs C'), which is most obvious in the central region where the majority of the hair cells are missing (Figure 3.5C'). However, despite a sufficient lesion, very few Myo7a-expressing hair cells were derived from lineage traced support cells. Out of nine lesioned cristae analyzed, only two such cells were found (Figure 3.5D,E), while no Myo7a$^+$/tdTomato$^+$ cells were found in the control cristae (n=5).

This data suggests a very low level of spontaneous regeneration after damage and is consistent with the results *in vitro* where one example of a PLP/CreER;mTmG lineage traced support cell was observed in the DMSO controls (Figure 2.9C). That cell was also likely a result of spontaneous regeneration due to the damage of culturing the adult cristae, which results in approximately a 34.1% lesion (Figure 2.2D). Overall, this data demonstrates that the Dcx-CreER mice can be used to lineage trace support cells and more importantly that they can be used to detect even very low levels of spontaneous regeneration. This method allows for regeneration to be analyzed definitively and independently of total hair cell

number, which can be affected by degeneration, hair cell repair, and incomplete and/or inconsistent lesion.

3.3 DISCUSSION

3.3.1 NEW CRE RECOMBINASE-EXPRESSING MOUSE LINES FOR CRISTAE AND INNER EAR STUDIES

Here I have characterized and identified several Cre recombinase-expressing mouse lines that can be used to study both the cristae and the inner ear. In addition, I have demonstrated the use of one of these lines for studying hair cell regeneration using lineage tracing. In a screen of Cre-expressing mouse lines with known expression in the nervous system, I characterized two mouse lines where the gene was known to be expressed in hair cells and two mouse lines with suspected expression in support cells, both of which had been previously uncharacterized. More importantly, from this screen I identified two new mouse lines with previously unknown and unsuspected expression in support cells.

Otof-Cre is an excellent Cre-expressing mouse line for recombining all hair cells in the cristae and inner hair cells in the cochlea. Since it is a non-inducible Cre, it would best be used in combination with tet-on/off systems using a floxed (r)tTA, where the (r)tTA would be expressed only in Otoferlin-expressing cells and the administration of doxycycline would grant temporal control over the expression of target genes or reporters. Many other options for hair cell recombination have been described, however, including: Atoh1-Cre knock-in mice (Yang*, et al.,* 2010b), Atoh1-Cre transgenic mice (Matei*, et al.,* 2005), Atoh1-CreER transgenic mice (Machold and Fishell*,* 2005, Chow*, et al.,* 2006), Gfi1-Cre knock-in mice

(Yang, *et al.,* 2010a), Pou4f3-Cre transgenic mice (Sage, *et al.,* 2006), and Prestin-Cre transgenic mice (Li, *et al.,* 2004, Tian, *et al.,* 2004) (reviewed in Cox, *et al.,* 2012).

Similarly, for specific support cell recombination, there are many available mouse lines in the cochlea, including: Fgfr3-iCreER transgenic mice (Rivers, *et al.,* 2008, Young, *et al.,* 2010, Cox, *et al.,* 2012), Prox1-eGFP/Cre knock-in mice (Srinivasan, *et al.,* 2010, Liu, *et al.,* 2012b), Sox2-Cre transgenic mice (Hayashi and McMahon, 2002), and Sox2-CreER transgenic mice (Kang and Hebert, 2012) (reviewed in Cox, *et al.,* 2012). However, in the vestibular system, the only known mouse line for specific support cell recombination are the PLP/CreER mice (Doerflinger, *et al.,* 2003, Gomez-Casati, *et al.,* 2010). Although Sox2 is a good marker for support cells for immunohistochemistry, it is also expressed in a subset of type II hair cells in the vestibular organs (Hume, *et al.,* 2007, Oesterle, *et al.,* 2008), which makes it unsuitable for lineage tracing.

Here I have identified and characterized several mouse strains with Cre recombinase expression in support cells that complement the PLP/CreER mice, which express Cre recombinase only in peripheral support cells (Gomez-Casati, *et al.,* 2010, Slowik and Bermingham-McDonogh, 2013). The Cralbp-CreER transgenic mice express Cre recombinase in the central support cells, which is a direct complement to the PLP/CreER mice. The Glast-CreER knock-in and transgenic mice, Dcx-CreER mice, and the Wfs1-TG2-CreERT2 mice each express Cre recombinase in support cells throughout the entire sensory epithelium, although at varying degrees of efficiency. The Glast-CreER mice, both the transgenic and the knock-in, are the least efficient, while the Wfs1-TG2-CreERT2 mice are the most efficient. However, the Wfs1-TG2-CreERT2 mice also have a small degree of

hair cell recombination. For some applications like FACS this might be acceptable; however, for lineage tracing to assay for hair cell regeneration, the Dcx-CreER mice are the best since they do not recombine in any hair cells and have a better recombination efficiency than Glast-CreER mice.

3.3.2 SPONTANEOUS HAIR CELL REGENERATION AFTER DAMAGE

Using the Dcx-CreER;Ai14 mice, I provide direct evidence for a very low level of spontaneous hair cell regeneration after damage in the mature cristae *in vivo* using support cell lineage tracing. Previous studies demonstrating evidence for spontaneous hair cell regeneration after damage, including in the utricle and saccule (Forge*, et al.,* 1993, Warchol*, et al.,* 1993, Rubel*, et al.,* 1995, Yamane*, et al.,* 1995, Meza*, et al.,* 1996, Li and Forge*,* 1997, Zheng and Gao*,* 1997, Forge*, et al.,* 1998, Ogata*, et al.,* 1999, Kirkegaard and Jorgensen*,* 2000, Walsh*, et al.,* 2000, Berggren*, et al.,* 2003, Oesterle*, et al.,* 2003, Taura*, et al.,* 2006, Kawamoto*, et al.,* 2009, Lin*, et al.,* 2011, Golub*, et al.,* 2012) and in the chinchilla cristae (Tanyeri*, et al.,* 1995, Lopez*, et al.,* 1997, Lopez*, et al.,* 1998, Lopez*, et al.,* 2003), have not used lineage tracing to identify newly generated hair cells. Instead, these studies have relied on secondary measures including the presence of immature hair bundles, the presence of hair cells after a complete lesion, and the identification of intermediate transitional morphologies to identify new hair cells. My report of hair cell regeneration through Notch inhibition *in vitro* was actually the first study to definitively show support cell transdifferentiation in the adult vestibular system using lineage tracing (Slowik and Bermingham-McDonogh*,* 2013).

The data presented here on spontaneous hair cell regeneration after damage in the mouse *in vivo* suggests that the level of spontaneous hair cell regeneration in the mouse is

much lower than that reported in the chinchilla. This could be due to species differences in the ability to regenerate hair cells between mice and chinchillas, or this could also be due to technical differences. It is possible that the level of spontaneous hair cell regeneration after damage is higher in the mouse than my data suggests. The recombination efficiency of the Dcx-CreER;Ai14 mice is approximately 50% of support cells, even with higher concentrations of tamoxifen, more doses of tamoxifen, or the use of 4-OHT, the active form of tamoxifen, in culture. While this could be related to the expression of the transgene and inefficient recombination, it is also possible that the Dcx-CreER transgene is only being expressed in a subset of support cells scattered throughout the entire sensory epithelium. Further, it is also possible that this hypothetical subset of support cells could have a lower regenerative capacity than the hypothetical non-Dcx-expressing population of support cells. This could account for a lower apparent rate of regeneration in my lineage tracing study, but would require a more thorough analysis of the endogenous expression of Dcx to determine whether Dcx is expressed by all support cells or only a subset of them.

An additional possibility is that the degree of hair cell regeneration was overestimated in the chinchilla work. Since the methods used to analyze the chinchilla were not direct, it is possible that some of their observed regeneration is actually due to hair cell repair or incomplete lesion. The use of lineage tracing and my *in vitro* work would suggest that this latter possibility is more likely. *In vitro*, while I did not use any pharmacological agent to damage the hair cells, I incurred damage to the adult cristae through culturing. In my damaged adult cristae treated with DMSO, which had a lesion of approximately 34.1%, I

observed very little spontaneous hair cell regeneration using the PLP/CreER;mTmG lineage trace.

C H A P T E R F O U R

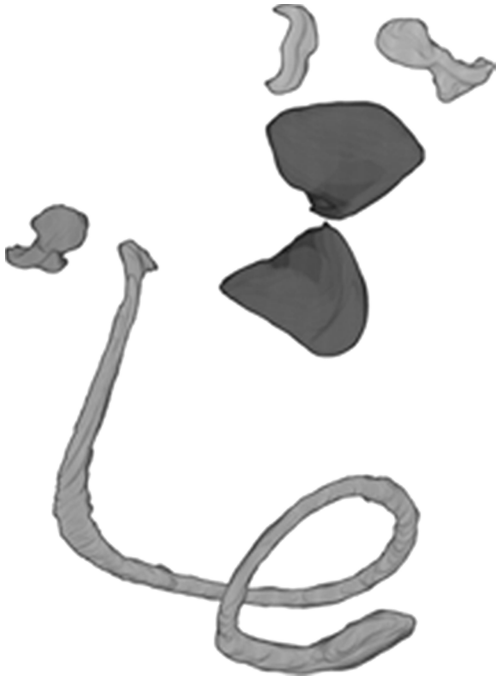

THE SPATIAL DISTRIBUTION OF HAIR CELL BIRTH IN THE CRISTAE

4.1 INTRODUCTION

Studies of the development of the sensory organs, particularly the specification of the sensory regions and the cues governing the differentiation of the various cell types, have suggested several potential strategies to stimulate hair cell regeneration in the inner ear sensory organs. For example, hair cells can be produced through the transdifferentiation of support cells following inhibition of Notch signaling (Hori et al., 2007; Lin et al., 2011; Jung et al., 2013; Mizutari et al., 2013; Slowik and Bermingham-McDonogh, 2013), which developmentally determines the precise ratio of support cells and hair cells through lateral inhibition (Lanford et al., 1999; Zhang et al., 2000; Zheng et al., 2000; Zine et al., 2001; Kiernan et al., 2005; Yamamoto et al., 2006; Takebayashi et al., 2007). However, just as in other neural systems, the level of regeneration is low and the determinants for the regenerative competence of individual support cells are poorly understood.

Here, I define the spatial patterns of hair cell development in order to better understand the increasing limitations on regenerative ability as the inner ear matures. Developmentally, almost every support cell in the inner ear can be induced to transdifferentiate (Lanford et al., 1999; Zine et al., 2001; White et al., 2006; Yamamoto et al., 2006; Hayashi et al., 2008; Collado et al., 2011; Zhao et al., 2011; Burns et al., 2012a); however, later, only an increasingly restricted subset of cells retains the ability to transdifferentiate. For example, as the cochlea matures, hair cell regeneration is increasingly restricted until it primarily occurs in the apical turn (Zheng and Gao, 2000; Yamamoto et al., 2006; Doetzlhofer et al., 2009; Kelly et al., 2012; Liu et al., 2012; Shi et al., 2013; Bramhall et al., 2014; Cox et al., 2014; Liu et al., 2014; Walters et al., 2014; Li et al., 2015). The fact that

the apical turn is the last region in the cochlea to differentiate and mature (Sher, 1971; Lim and Anniko, 1985; Lanford et al., 2000; Chen et al., 2002; Woods et al., 2004) suggests that there is a correlation between relative maturity and regenerative ability in the cochlea. In the adult cristae there are also regional differences in hair cell regeneration and in the expression of Notch signaling components (Lopez et al., 1997; Slowik and Bermingham-McDonogh, 2013). In particular, peripheral support cells maintain active Notch signaling and can transdifferentiate in response to Notch inhibition in the adult. Since the peripheral region maintains some regenerative ability into adulthood, I hypothesized that, similar to the cochlea, the relative maturity and regenerative ability of a region would be linked in the cristae and that the peripheral region would differentiate last during development.

Here, I present new data in the mouse characterizing the spatial pattern of cell cycle exit for hair cells in all three cristae (posterior, anterior, and horizontal) using embryonic injections of BrdU. My data confirms in all three cristae of the mouse the previous results found in the rat horizontal cristae (Sans and Chat, 1982), where hair cell birth begins in the central region and shifts with age towards the periphery or lateral edges. This pattern correlates with the regions that maintain active Notch signaling and possess some regenerative capacity in response to Notch inhibition in the adult mouse cristae. In addition, I provide evidence for an earlier gradient of hair cell differentiation along the longitudinal axis from the crux eminentia to the planum semilunatum by analyzing early hair cell markers in E14.5 inner ears. This data in particular suggests that hair cell differentiation closely follows cell cycle exit in the developing cristae, unlike the cochlea where terminal mitosis is uncoupled from hair cell differentiation.

4.2 RESULTS

4.2.1 BRDU INJECTIONS TO BIRTHDATE HAIR CELLS

In order to determine the spatial pattern of hair cell development in the mouse cristae, cells were birthdated with a single embryonic injection of 5-bromo-2'-deoxyuridine (BrdU) and analyzed once the animals reached one month of age (Figure 4.1A). The embryonic ages for injection were chosen to highlight specific stages of crista development based on data from a birthdating study of the inner ear in which a similar experimental paradigm was performed using tritiated-thymidine (Ruben, 1967). According to this study, embryonic day 9.5 (E9.5) is well before the onset of cell cycle exit for hair cells in the cristae, making it a good baseline control. The onset of hair cell birth is covered by the injection at E12.5 while the injection at E15.5 occurs after the peak of hair cell birth. The peak of cell birth was deliberately avoided because many of the regions of the cristae would likely have hair cells born during that time. The last injection at E17.5 occurs after most of the hair cells are born and identifies the regions of the cristae that are the last to exit the cell cycle (Figure 4.1B).

Examples of the BrdU labeling in the posterior cristae are shown in Figure 4.1E-H. In the cristae that received the BrdU injection at E9.5, there were no BrdU-positive hair cells in the sensory epithelium and very few BrdU-positive cells in the surrounding tissue (Figure 4.1E). The BrdU injection at E12.5 resulted in substantial numbers of BrdU-positive hair cells in the central regions of the cristae (Figure 4.1F). When the BrdU injection was given three days later, at E15.5, the labeled hair cells were predominantly located in the peripheral

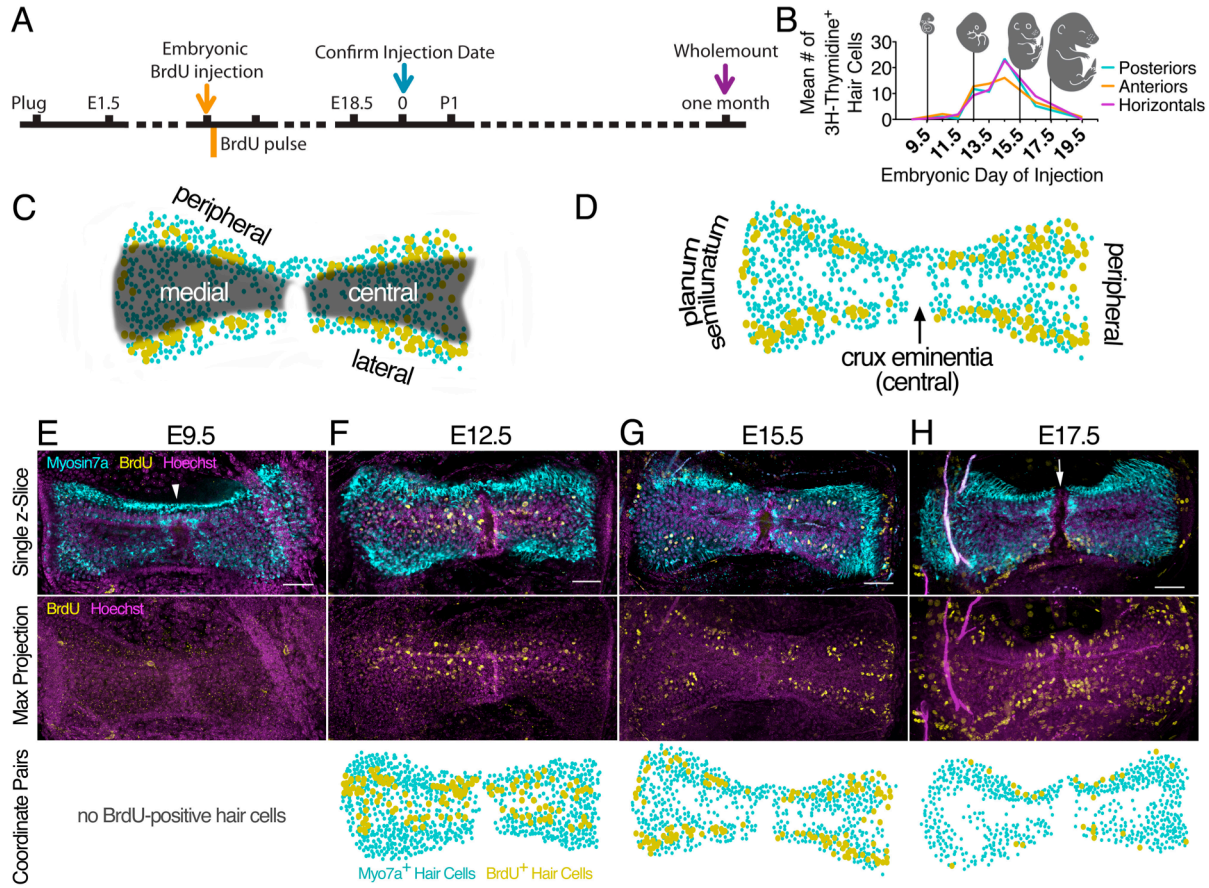

Figure 4.1 Birthdating hair cells using embryonic injections of BrdU. **A**) A diagram of the experimental paradigm. Swiss Webster females were plug-dated and given a single ip injection of BrdU (1.25 mg/25 g mouse) between the 9th and 18th days of their gestation. The age of the embryos on the date of injection was determined by the plug date and verified by the date of birth. The cristae of the mice that had received the BrdU pulse embryonically were whole mounted and immunolabeled once the mice were one month old. **B**) The age of the embryos at time of injection shown against a replotting of data from a birthdating study of the inner ear by Ruben (1967) showing when hair cells in each of the three cristae exit the cell cycle. **C**) A plot of the Myo7a-positive hair cells and the BrdU-positive hair cells in a posterior crista (from panel G, includes the 'bridge' of hair cells spanning the normally non-sensory region) showing the regions referred to as central/medial (grey band) and peripheral/lateral. **D**) The same plot from panel C indicating the central and peripheral regions referred to in analyses of the longitudinal axis. Central refers to the regions near the crux eminentia while peripheral refers to the regions near the planum semilunatum. E-H) Cristae for each age were immunolabeled for BrdU (yellow), hair cells (Myosin7a, cyan) and nuclei (Hoechst 33342, magenta). Examples of posterior cristae from each age are shown in three different views. The single z-slice shows the amount of BrdU labeling within the sensory epithelium, which is not always apparent from the maximum intensity projections below. In this view, the white arrowhead points to an incomplete crux eminentia as compared to a complete crux eminentia indicated by the white arrow. This can best be seen in panel F where there are very few BrdU-positive hair cells even though there are many BrdU-positive cells in general. The last view is a x,y-plot of the coordinate pairs for the Myosin7a-positive hair cells (cyan) and the BrdU+ hair cells (yellow) exported from the standard cell counter plugin in ImageJ.

regions of the cristae (Figure 4.1G). Lastly, injections at E17.5 resulted in few BrdU-positive cells in the sensory epithelium (as seen in the single z-slice), though there were many labeled cells in the surrounding tissue (as seen in the maximum intensity projection)(Figure 4.1H). While examining the posterior cristae, I noticed that a minority of the posterior cristae had an incomplete crux eminentia with hair cells spanning the entire length of the cristae on one side (Figure 4.1E arrowhead vs Figure 4.1H arrow). Normally, the crux eminentia of the posterior and anterior cristae is a completely hair cell free region that divides the cristae into two separate hemicristae. This incomplete crux eminentia occurred at a frequency of approximately 1:3-4 and may be unique to Swiss Webster mice, as I have not observed this phenomenon in C57BL/6 or CBA/CaJ mice. Further, the incomplete crux appears early in development, as immunolabeling of E14.5 inner ears with the nuclear hair cell marker, Gfi1, also shows an incomplete crux eminentia in a similar subset of posterior cristae (data not shown).

The summaries of the qualitative trends for both the number and the spatial pattern of BrdU-labeled cells for each age of BrdU injection are shown in Figure 4.2. The total number of BrdU-positive hair cells labeled at each age agreed with previous data using tritiated-thymidine (Ruben, 1967) (Table 4.1)(Figure 4.2A, colored dots plotted against

TABLE 4.1

The total number of BrdU+ hair cells by age in each crista type

	Posterior Cristae			Anterior Cristae			Horizontal Cristae		
	mean	SEM	n	mean	SEM	n	mean	SEM	n
E9.5	0.00	± 0.00	6	0.00	± 0.00	6	0.00	± 0.00	5
E12.5	135.75	± 7.32	12	173.50	± 7.01	4	94.00	± 15.24	4
E15.5	111.00	± 7.49	6	147.20	± 10.81	5	146.50	± 10.83	6
E17.5	40.75	± 5.20	4	74.33	± 5.61	3	69.00	± 5.51	3

SEM - Standard error of the mean

Ruben's data shown by the grey shaded area). The spatial patterns of hair cell birth can be seen in the normalized group data from a select number of crista for each age and crista type (posterior, anterior, and horizontal) shown in Figure 4.2B-D. The grey dots represent all of the Myosin7a-positive cells for all cristae of that type (posterior, anterior, or horizontal)

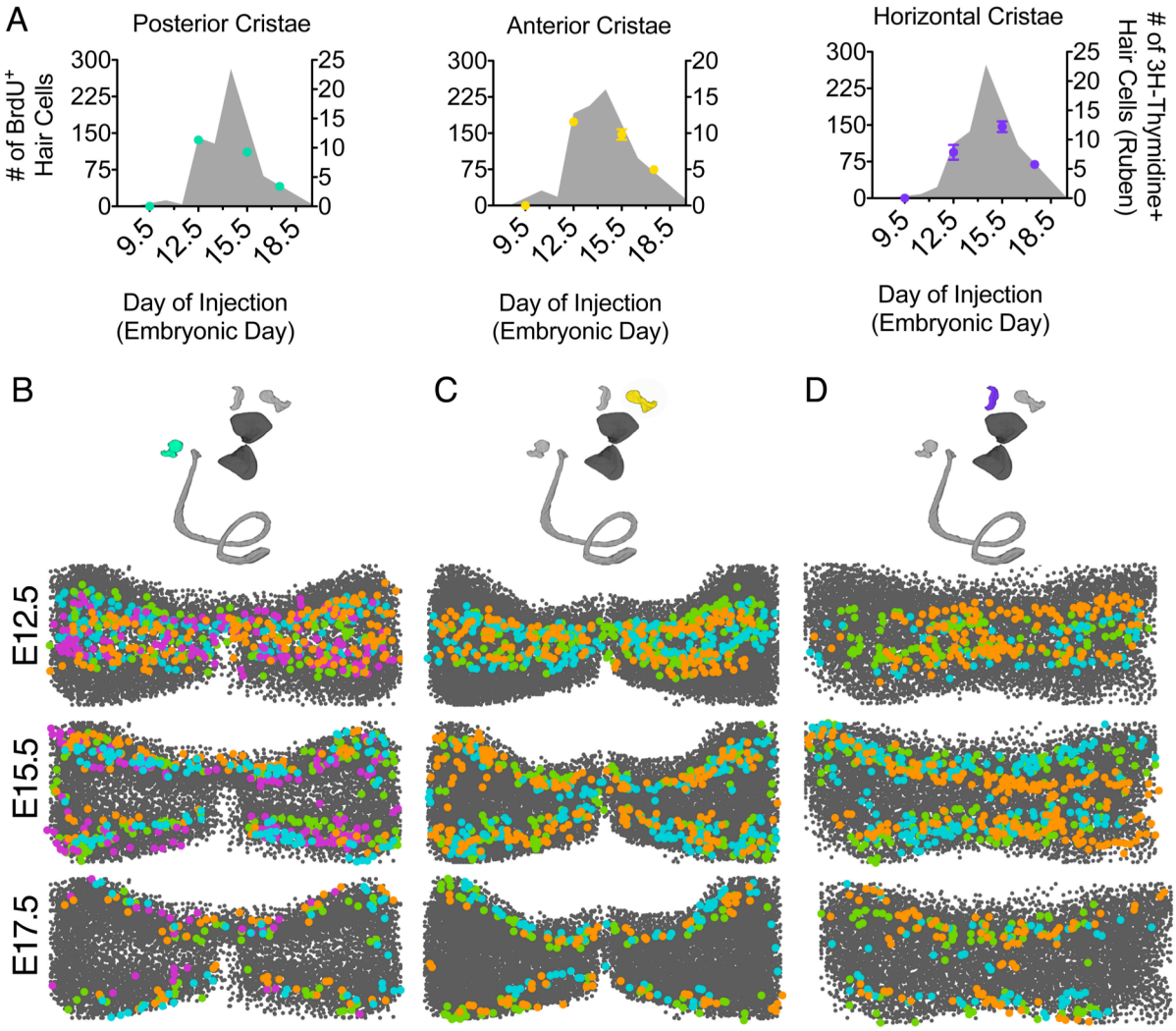

Figure 4.2 Qualitative group data for all three cristae. **A)** The number of BrdU-positive hair cells for each cristae type (colored circles) follows the same trend with age as published by Ruben (1967) using tritiated-thymidine (grey fill, replotted from original publication). Error bars depict standard error of the mean (SEM). **B-D**) Plots of example data for each age for the posterior (B), anterior (C), and horizontal (D) cristae show the overall trends of hair cell birth. The grey points show all of the Myosin7a-positive hair cells from the cristae of that type (posterior, anterior, or horizontal) irrespective of age, while the colored points represent data from a single crista of that type and age.

irrespective of age, while the colored dots represent data from an individual crista of that age and type. For example, in Figure 4.2B, the grey background is identical for each of the three ages because it encompasses the hair cell data for all posterior cristae. The colored data for each crista is then overlaid on top to allow for a comparison of the spatial patterns in posterior cristae between ages. Qualitatively, it appears that hair cells are born in the more central regions in all three cristae types at E12.5 and cell generation shifts to the more peripheral regions at both E15.5 and E17.5 (Figure 4.2B-D).

4.2.2 HAIR CELL BIRTH ON THE MEDIAL TO LATERAL AXIS

To quantitatively analyze the shift in regional hair cell development from the medial to lateral regions of the cristae, I performed an analysis along the z-axis. Due to the highly curved shape of the cristae, I found that this axis provided a better spatial representation of the medial and lateral regions than an analysis of the y-axis for all three cristae types (Figure 4.3A-B). Because this analysis is used to digitally "unfold" or flatten the cristae, I refer to the top of the cristae as being medial and the bottom as being lateral. For this analysis, I divided the cristae into four evenly distributed bins along the z-axis using the Myosin7a-positive hair cells and counted the number of BrdU-positive hair cells in each bin.

In each cristae type, the quantitative analysis supports the qualitative assessment that there is a medial to lateral progression of hair cell birth during development. In the posterior cristae, the hair cells born at E12.5 were found largely in the most medial bins (Figure 4.3C). At E15.5, hair cell birth shifted more peripherally into the more intermediate bins, indicated by the decrease in BrdU-positive hair cells in the medial bins and the concomitant increase in BrdU-positive hair cells in the lateral bins (Tables 4.2 and 4.3)(Figure 4.3F,I). At E17.5, the

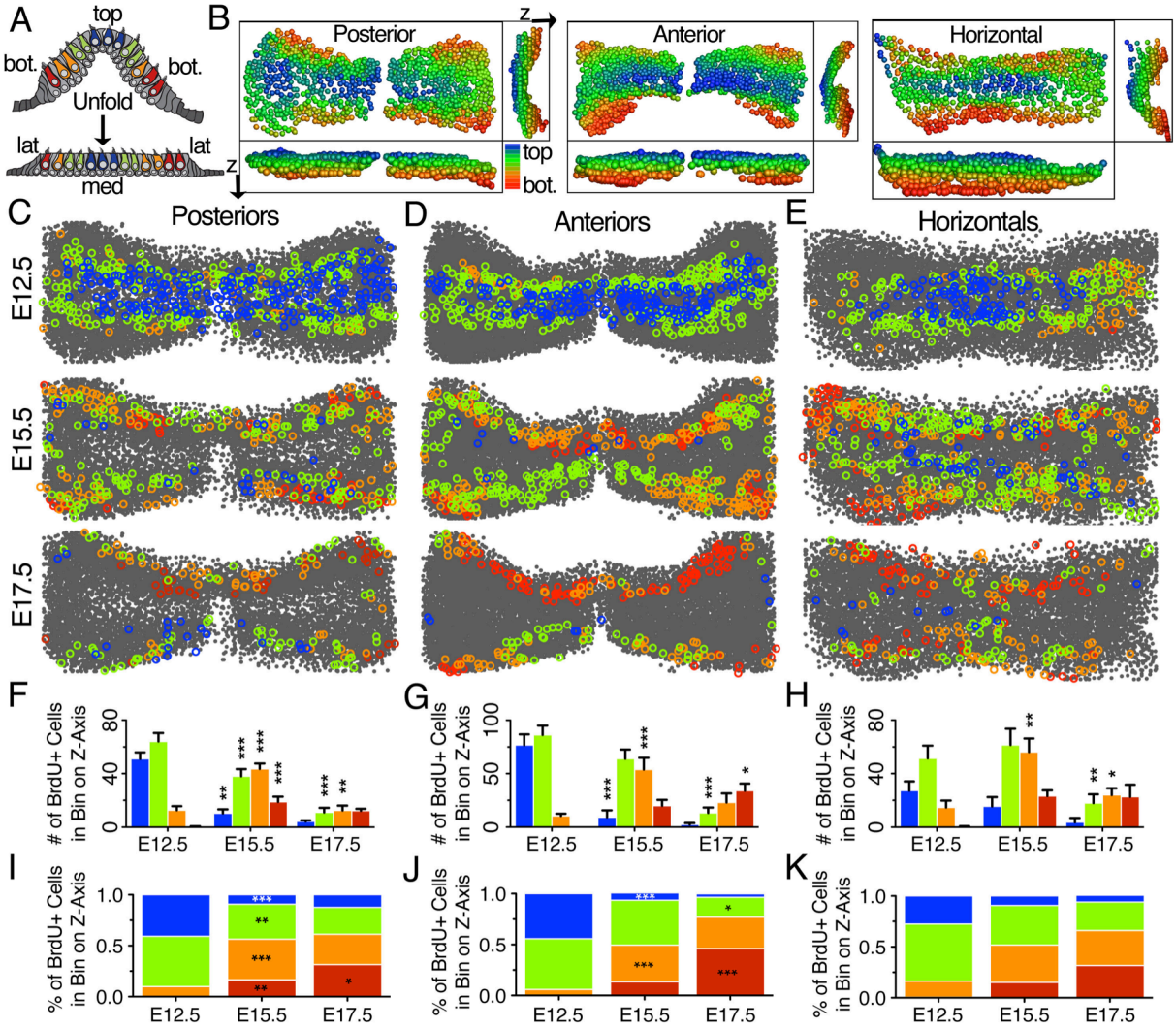

Figure 4.3 Hair cell birth shifts from the medial to lateral regions with age. **A)** In order to analyze the medial to lateral gradient, cristae were divided into four evenly distributed bins along the z-axis using the Myosin7a-positive hair cells shown in grey. The number of BrdU-positive hair cells (shown by color based on z-depth with cooler colors at the top of the cristae and warmer colors at the bottom) was counted for each bin. **B)** Plots of the cristae color-coded for z-depth show that this analysis produces a nice medial to lateral map for each of the three cristae types. **C-E)** The same plots from Figure 4.2A-C showing example data for each age for the posterior (C), anterior (D), and horizontal (E) cristae here color coded for z-bin in the color order from top to bottom of blue, green, orange, red. **F-H)** Graphs of the mean number of BrdU-positive hair cells in each bin show the pattern of hair cell birth with age in the posterior (F), anterior (G), and horizontal (H) cristae. Error bars depict SEM. **I-K)** Graphs depicting the distribution of BrdU-positive hair cells in each bin as a percentage of the total number of BrdU-positive hair cells in that cristae. Asterisks in panels F-K indicate significance from two-way ANOVAs with Bonferroni post-tests comparing the bins of E12.5 to E15.5 and of E15.5 to E17.5 ($p<0.05$ - *, $p<0.01$ - **, $p< 0.001$ - ***).

overall number of BrdU-positive hair cells was decreased, with significant reductions in the number of hair cells in the intermediate bins and a significant increase in the percentage of BrdU-positive hair cells in the most lateral bin (Tables 4.2 and 4.3)(Figure 4.3F,I).

The anterior cristae showed a very similar trend. At E12.5, the majority of the BrdU-positive hair cells were in the medial bins (Figure 4.3D). At E15.5, there was a decrease in the BrdU-positive hair cells in the most medial bin and an increase in the BrdU-positive hair cells in the lateral bin (Tables 4.2 and 4.3)(Figure 4.3G,J). At E17.5, there was a shift from the intermediate to the lateral regions with a significant decrease in cells in the medial bin and a significant increase in cells in the most lateral bin (Tables 4.2 and 4.3)(Figure 4.3G,J).

Lastly, the horizontal cristae showed a similar trend to both the anterior and posterior

TABLE 4.2

Numerical summary of the number and percentage of $BrdU^+$ hair cells along the z-axis

POSTERIOR CRISTAE

		E12.5 (n=9)			E15.5 (n=6)			E17.5 (n=4)		
		mean [# (%)]		SEM [# (%)]	mean [# (%)]		SEM [# (%)]	mean [# (%)]		SEM [# (%)]
Bin color[1]	red	0.44 (0.3)	±	0.24 (0.2)	18.83 (16.47)	±	3.89 (2.6)	12.25 (31.45)	±	1.44 (2.7)
	orange	12.67 (9.56)	±	3.03 (2.2)	43.67 (39.99)	±	3.99 (3.9)	12.50 (29.87)	±	3.52 (5.8)
	green	64.11 (49.43)	±	6.28 (3.0)	38.00 (34.26)	±	5.47 (4.3)	11.00 (26.32)	±	3.39 (6.2)
	blue	51.11 (40.7)	±	4.85 (3.9)	10.33 (9.28)	±	3.00 (2.8)	4.25 (12.36)	±	0.85 (4.4)

ANTERIOR CRISTAE

		E12.5 (n=4)			E15.5 (n=5)			E17.5 (n=3)		
		mean [# (%)]		SEM [# (%)]	mean [# (%)]		SEM [# (%)]	mean [# (%)]		SEM [# (%)]
Bin color[1]	red	0.00 (0.00)	±	0.00 (0.0)	20.00 (13.41)	±	5.48 (3.2)	34.00 (46.09)	±	6.66 (6.1)
	orange	10.50 (5.94)	±	2.02 (1.0)	54.00 (36.05)	±	10.90 (5.9)	23.00 (30.88)	±	8.51 (10.3)
	green	86.25 (49.95)	±	8.66 (5.3)	64.00 (44.05)	±	8.57 (5.6)	13.33 (19.56)	±	4.98 (7.8)
	blue	76.75 (44.12)	±	10.05 (5.2)	9.20 (6.50)	±	6.48 (4.6)	2.33 (3.48)	±	1.45 (2.1)

HORIZONTAL CRISTAE

		E12.5 (n=4)			E15.5 (n=4)			E17.5 (n=3)		
		mean [# (%)]		SEM [# (%)]	mean [# (%)]		SEM [# (%)]	mean [# (%)]		SEM [# (%)]
Bin color[1]	red	0.50 (0.48)	±	0.29 (0.3)	23.25 (15.07)	±	4.19 (2.8)	22.67 (31.65)	±	9.06 (11.7)
	orange	14.75 (15.74)	±	5.11 (5.1)	56.25 (36.69)	±	10.05 (7.2)	24.00 (34.55)	±	5.00 (5.8)
	green	51.50 (56.25)	±	9.51 (9.1)	61.50 (38.80)	±	12.06 (6.3)	18.00 (27.81)	±	6.51 (11.9)
	blue	27.25 (27.53)	±	6.91 (5.5)	15.50 (9.45)	±	6.96 (4.0)	3.67 (5.99)	±	3.18 (5.4)

- Number, % - Percentage

[1] The red bin represents the most lateral region and the blue bin represents the most medial region

cristae, but in general, had fewer BrdU-labeled hair cells and less significant effects. This could be due in part to the fact that the horizontal cristae have fewer hair cells in the adult than the other two cristae types. Nonetheless, at E12.5, the majority of BrdU-positive hair cells were still found within the more medial bins (Figure 4.3E). At E15.5, there was a significant increase in the number of BrdU-positive hair cells in the lateral bin. At E17.5, the overall level of hair cell birth was significantly reduced, specifically in the intermediate bins (Tables 4.2 and 4.3)(Figure 4.3H,K).

TABLE 4.3

Statistical summary of the number and percentage of $BrdU^+$ hair cells along the z-axis

POSTERIOR CRISTAE

- Bins: $F_{3,48} = 17.69$ $p < 0.0001$ Age: $F_{2,16} = 23.63$ $p < 0.0001$ Interaction: $F_{6,48} = 23.46$ $p < 0.0001$

% - Bins: $F_{3,48} = 13.51$ $p < 0.0001$ Age: F2,16 = 0.00 $p = 1.00$ Interaction: $F_{6,48} = 20.98$ $p < 0.0001$

		E12.5 vs E15.5 (#)	E12.5 vs E15.5 (%)	E15.5 vs E17.5 (#)	E15.5 vs E17.5 (%)
Bin color[1]	red	t=3.198, p<0.01	t=3.555, p<0.01	*ns*	t=2.690, p<0.05
	orange	t=5.392, p<0.001	t=6.693, p<0.001	*t=4.426*, p<0.001	*ns*
	green	t=4.542, p<0.001	t=3.337, p<0.01	t=3.834, p<0.01	*ns*
	blue	t=7.093, p<0.001	t=6.911, p<0.001	*ns*	*ns*

ANTERIOR CRISTAE

- Bins: $F_{3,27} = 9.84$ $p = 0.0001$ Age: $F_{2,9} = 26.01$ $p = 0.0002$ Interaction: $F_{6,27} = 14.70$ $p < 0.0001$

% - Bins: $F_{3,27} = 6.41$ $p = 0.002$ Age: F2,9 = -2.77 $p = 1.00$ Interaction: $F_{6,27} = 13.53$ $p < 0.0001$

		E12.5 vs E15.5 (#)	E12.5 vs E15.5 (%)	E15.5 vs E17.5 (#)	E15.5 vs E17.5 (%)
Bin color[1]	red	*ns*	*ns*	*ns*	t=4.308, p<0.001
	orange	t=4.268, p<0.001	t=4.321, p<0.001	t=2.794, p<0.05	*ns*
	green	*ns*	*ns*	t=4.567, p<0.001	t=3.228, p<0.05
	blue	t=6.628, p<0.001	t=5.398, p<0.001	*ns*	*ns*

HORIZONTAL CRISTAE

- Bins: $F_{3,24} = 8.59$ $p = 0.0005$ Age: $F_{2,8} = 14.95$ $p = 0.0020$ Interaction: $F_{6,24} = 4.01$ $p = 0.0064$

% - Bins: $F_{3,24} = 7.98$ $p = 0.0007$ Age: F2,8 = -2.00 $p = 1.00$ Interaction: $F_{6,24} = 4.05$ $p = 0.0061$

		E12.5 vs E15.5 (#)	E12.5 vs E15.5 (%)	E15.5 vs E17.5 (#)	E15.5 vs E17.5 (%)
Bin color[1]	red	*ns*	*ns*	*ns*	*ns*
	orange	t=4.063, p<0.01	*ns*	*t=2.923*, p<0.05	*ns*
	green	*ns*	*ns*	t=3.943, p<0.01	*ns*
	blue	*ns*	*ns*	*ns*	*ns*

- Number, % - Percentage, p-values come from a two-way ANOVA with Bonferroni post-tests

[1] The red bin represents the most lateral region and the blue bin represents the most medial region

4.2.3 HAIR CELL BIRTH ON THE LONGITUDINAL X-AXIS

To analyze the distribution of hair cell birth on the longitudinal axis, cristae were divided into ten evenly spaced bins using the list of Myosin7a-positive hair cells and the number of BrdU-positive hair cells in each bin was counted (Figure 4.4A, summarized in Table 4.4). For the posterior cristae, at E12.5, hair cell birth was evenly distributed along the longitudinal axis (Figure 4.4B, green). At E15.5, there was a significant decrease in the number of hair cells born in the middle bin spanning the crux eminentia (Figure 4.4B, yellow). At E17.5, there was a significant reduction in the number of hair cells born in the remaining regions of the cristae, such that the levels along the longitudinal axis were again evenly distributed (Figure 4.4B, purple). Overall, the spatial patterns of hair cell birth along the longitudinal axis are not very strong during these ages of development; however, in the posterior cristae the decrease in hair cell birth begins in the regions near the central crux eminentia at E15.5 and progresses to the regions near the peripheral planum semilunatum at E17.5. This "off wave" of hair cell birth along the longitudinal axis is indicative of an earlier wave of hair cell birth along this axis.

A similar pattern of hair cell birth along the longitudinal axis was present in the anterior cristae. At E12.5, hair cell birth was fairly evenly distributed along the longitudinal axis, with a slight reduction in the two middle bins that is likely due to the position of the crux eminentia, which is always present and complete in anterior cristae (Figure 4.4C, green). Similar to posterior cristae, the number of hair cells born in the anterior cristae decreased at E15.5 and E17.5. In addition, the anterior cristae appeared to have a similar "off wave"

pattern to the posterior cristae, where the middle bins decreased at E15.5 and the peripheral bins decreased at E17.5 (Figure 4.4C, yellow and purple).

The horizontal cristae, which do not have a crux eminentia, showed a unique pattern of hair cell birth along the longitudinal axis that swept from one side of the cristae to the

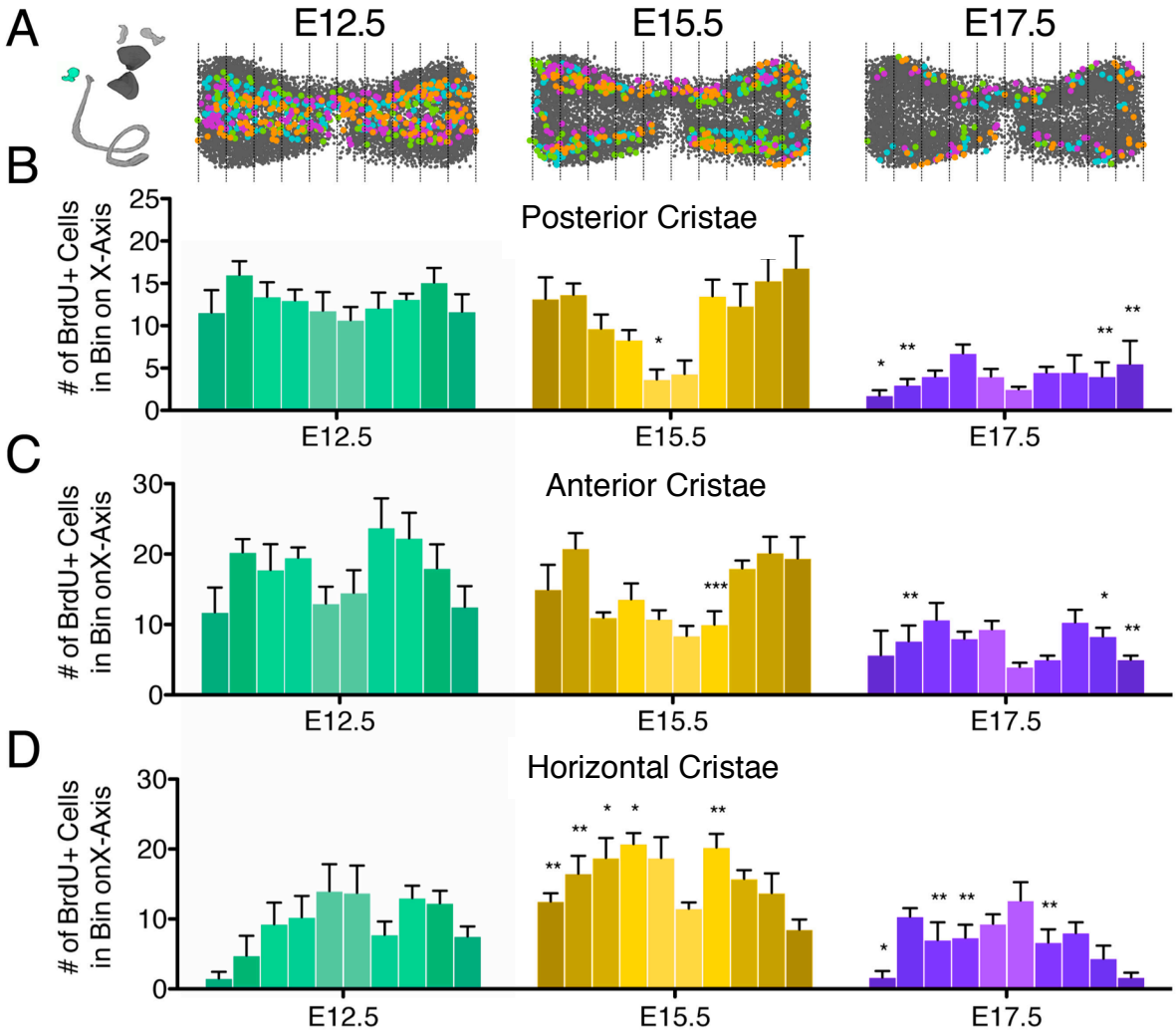

Figure 4.4 The pattern of hair cell birth largely does not occur along the longitudinal x-axis. **A)** To analyze the gradient along the longitudinal x-axis, cristae were divided into ten evenly distributed bins based on the x-values of the Myosin7a-positive hair cells shown in grey. The number of BrdU-positive hair cells (colored points, where each color represents data from an individual crista) were then counted for each bin. **B-D)** Graphs of the mean number of BrdU-positive hair cells in each bin show the pattern of hair cell birth with age in the posterior (B), anterior (C), and horizontal (D) cristae. Error bars depict SEM and asterisks indicate significance from two-way ANOVAs with Bonferroni post-tests comparing the bins of E12.5 to E15.5 and of E15.5 to E17.5 ($p<0.05$ - *, $p<0.01$ - **, $p< 0.001$ - ***).

other, unlike the posterior and anterior cristae that swept from the crux eminentia to the peripheral planum semilunatum. At E12.5, hair cell birth was unevenly distributed towards

TABLE 4.4

Summary of the number of $BrdU^+$ hair cells along the longitudinal axis

POSTERIOR CRISTAE

Bins: $F_{9,144} = 2.74$ $p = 0.0055$ Age: $F_{2,16} = 24.08$ $p < 0.0001$ Interaction: $F_{18,144} = 1.81$ $p = 0.0296$

	E12.5 (n = 9)			E15.5 (n=6)			E17.5 (n=4)		
	mean	±	SEM	mean	±	SEM E12.5 vs E15.5	mean	±	SEM E15.5 vs E17.5
Bin Number[1] 1	11.56	±	2.66	13.17	±	2.54 *ns*	1.75	±	0.63 t=3.548, p<0.01
2	16.00	±	1.63	13.67	±	1.31 *ns*	3.00	±	0.71 *t=3.315*, p<0.05
3	13.44	±	1.68	9.67	±	1.67 *ns*	4.00	±	0.71 *ns*
4	13.00	±	1.25	8.33	±	1.15 *ns*	6.75	±	1.03 *ns*
5	11.78	±	2.18	3.67	±	1.17 t=3.087, p<0.05	4.00	±	0.91 *ns*
6	10.67	±	1.56	4.33	±	1.56 *ns*	2.50	±	0.29 *ns*
7	12.11	±	1.80	13.50	±	1.95 *ns*	4.50	±	0.65 *ns*
8	13.11	±	0.70	12.33	±	2.60 *ns*	4.50	±	2.02 *ns*
9	15.11	±	1.72	15.33	±	2.64 *ns*	4.00	±	1.68 t=3.522, p<0.01
10	11.67	±	2.07	16.83	±	3.78 *ns*	5.50	±	2.72 t=3.522, p<0.01

ANTERIOR CRISTAE

Bins: $F_{9,81}$ =3.04 $p = 0.0035$ Age: $F_{2,9} = 25.52$ p =0.0002 Interaction: $F_{18,81} = 2.22$ $p = 0.0082$

	E12.5 (n = 4)			E15.5 (n=5)			E17.5 (n=3)		
	mean	±	SEM	mean	±	SEM E12.5 vs E15.5	mean	±	SEM E15.5 vs E17.5
Bin Number[1] 1	11.75	±	3.50	15.00	±	3.49 *ns*	5.67	±	3.48 *ns*
2	20.25	±	1.89	20.80	±	2.18 *ns*	7.67	±	2.19 t=3.585, p<0.01
3	17.75	±	3.66	11.00	±	0.71 *ns*	10.67	±	2.40 *ns*
4	19.50	±	1.44	13.60	±	2.25 *ns*	8.00	±	1.00 *ns*
5	13.00	±	2.38	10.80	±	1.24 *ns*	9.33	±	1.20 *ns*
6	14.50	±	3.23	8.40	±	1.40 *ns*	4.00	±	0.58 *ns*
7	23.75	±	4.17	10.00	±	1.90 t=4.086, p<0.001	5.00	±	0.58 *ns*
8	22.25	±	3.61	18.00	±	1.10 *ns*	10.33	±	1.76 *ns*
9	18.00	±	3.39	20.20	±	2.27 *ns*	8.33	±	1.20 t=3.239, p<0.05
10	12.50	±	2.96	19.40	±	3.04 *ns*	5.00	±	0.58 t=3.931, p<0.01

HORIZONTAL CRISTAE

Bins: $F_{9,72}$ =5.92 $p < 0.0001$ Age: $F_{2,8} = 14.38$ p =0.0022 Interaction: $F_{18,72} = 2.5$ $p = 0.0033$

	E12.5 (n = 4)			E15.5 (n=4)			E17.5 (n=3)		
	mean	±	SEM	mean	±	SEM E12.5 vs E15.5	mean	±	SEM E15.5 vs E17.5
Bin Number[1] 1	1.50	±	0.96	12.50	±	1.19 t=3.552, p<0.01	1.67	±	0.88 t=3.239, p<0.05
2	4.75	±	2.84	16.50	±	2.53 t=3.794, p<0.01	10.33	±	1.20 *ns*
3	9.25	±	3.09	18.75	±	2.84 t=3.068, p<0.05	7.00	±	2.52 t=3.513, p<0.01
4	10.25	±	3.07	20.75	±	1.55 t=3.391, p<0.05	7.33	±	1.86 t=4.011, p<0.01
5	14.00	±	3.85	18.75	±	2.96 *ns*	9.33	±	1.33 *ns*
6	13.75	±	3.88	11.50	±	0.87 *ns*	12.67	±	2.60 *ns*
7	7.75	±	1.89	20.25	±	1.93 t=4.037, p<0.01	6.67	±	1.86 t=4.061, p<0.01
8	13.00	±	1.78	15.75	±	1.25 *ns*	8.00	±	1.53 *ns*
9	12.25	±	1.80	13.75	±	2.78 *ns*	4.33	±	1.86 *ns*
10	7.50	±	1.44	8.50	±	1.44 *ns*	1.67	±	0.67 *ns*

SEM - Standard error of the mean, p-values from a two-way ANOVA with Bonferroni post-tests

[1] Bin 1 is the left-most bin and bin 10 is the right-most bin.

one side of the cristae, shown as the right side (Figure 4.4D, green). At E15.5, the bins representing the left side of the cristae increased such that hair cell birth was fairly evenly distributed at this age. At E17.5, there was a significant reduction of the rightward bins. Ultimately, these increases and decreases appear to create a slight wave of cell cycle exit from what is depicted as the right side of the cristae to the left.

4.2.4 DIFFERENTIATION OF HAIR CELLS IN EMBRYONIC INNER EARS

In the cochlea, the terminal mitoses of hair cells are uncoupled from their differentiation. In the apical turn, hair cells exit the cell cycle around E12.5, but do not begin to differentiate until E16.5, four days later. To determine if the pattern of differentiation followed the pattern of cell cycle exit in the cristae, E14.5 inner ears were examined for the expression of the early hair cell markers, Gfi1 and Myo6 (Figure 4.5).

For both the posterior and the anterior cristae, hair cell differentiation appeared to begin in the region nearest to the crux eminentia. The expression of both Myo6 (Figure 4.5C,E) and Gfi1 (Figure 4.5C",E") occurred in two distinct patches for each anterior and posterior crista. The non-expressing region between the two patches appeared to be just the width of a few cell bodies, which is approximately the size of the mature crux eminentia (Figure 4.1C-F).

In the horizontal crista, which does not have a crux eminentia and is instead one continuous sensory region, hair cell differentiation appeared to begin towards one side of the sensory region, marked by Sox2 (Figure 4.5D-D"). This side is furthest from the developing cochlea towards the endolymphatic duct and the lateral portion of the head, and is known as

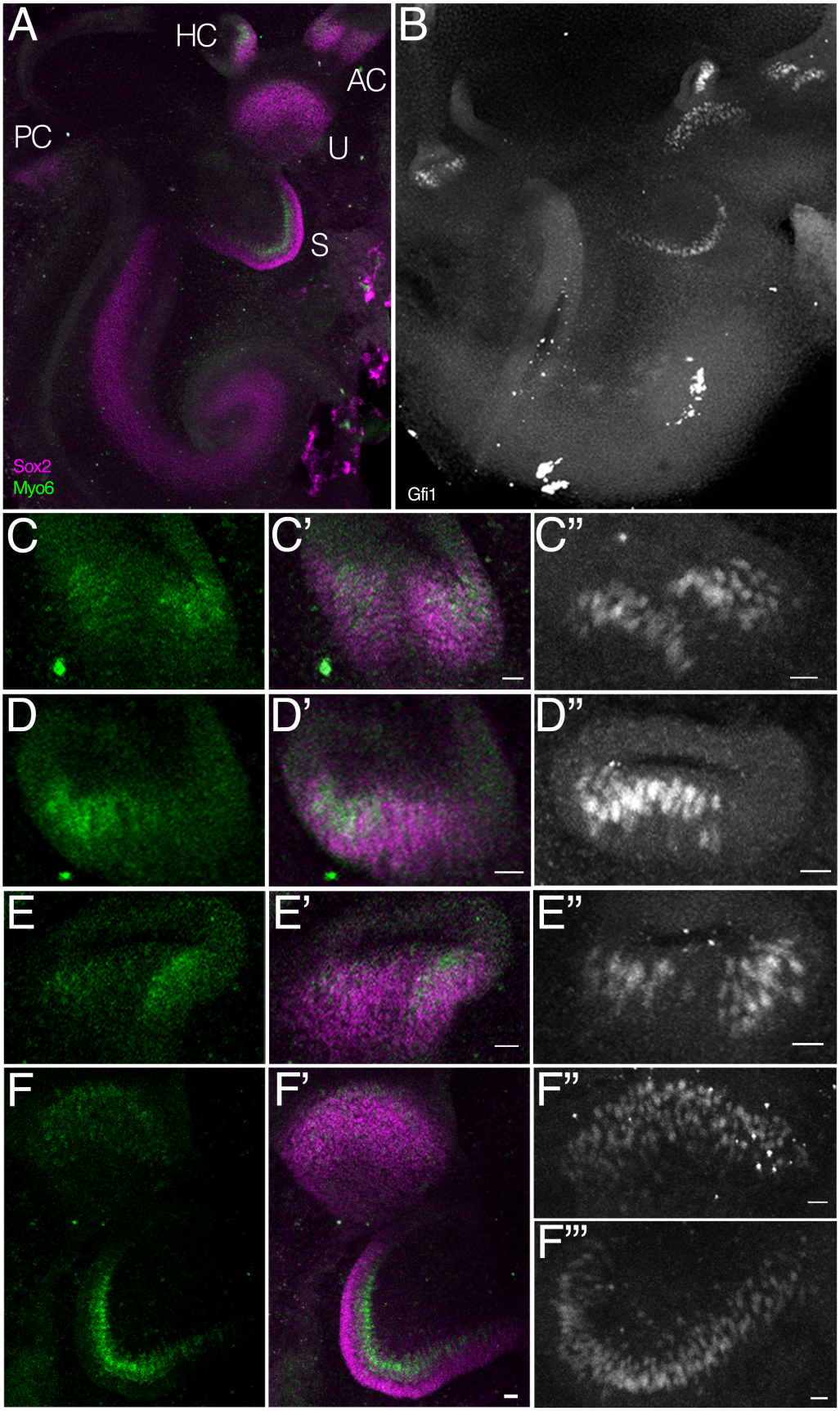
A
HC
AC
PC
U
S
Sox2
Myo6
B
Gfi1
C
C'
C''
D
D'
D''
E
E'
E''
F
F'
F''
F'''

Figure 4.5 Expression of the hair cell markers Myo6 and Gfi1 in the E14.5 inner ear. **A-B**) Maximum intensity projections of E14.5 inner ears labeled in A for hair cells with Myo6 (green) and sensory regions with Sox2 (red) and in B for Gfi1 (white). AC – anterior crista, HC – horizontal crista, PC – posterior crista, U – utricle, S – saccule. **C-F'''**) Zoomed views of the sensory organs stained with Myo6 (green, C,D,E,F), Sox2 (purple, C',D',E',F'), and Gfi1 (white, C'',D'',E'',F'',F''') show the developing anterior crista (C-C''), horizontal crista (D-D''), posterior crista (E-E''), utricle (upper F-F',F''), and saccule (lower F-F',F'''). **C-C''**) In anterior cristae, the hair cells begin differentiating adjacent to the non-sensory crux eminentia. **D-D''**) In horizontal cristae, the hair cells develop as one continuous patch starting on the superior or dorsal half of the cristae (towards the left), consistent with the lack of a crux eminentia in the horizontal cristae. **E-E''**) In posterior cristae, the hair cells also begin differentiating adjacent to the crux eminentia. **F-F'''**) At E14.5, the utricle and saccule have more differentiated hair cells than the cristae. In the saccule, hair cells stained with Myo6 are beginning to show a characteristic hair cell morphology (F-F'). Scale bars – 10 μm.

the superior half of the cristae. This asymmetric pattern of differentiation is consistent with the pattern of hair cell birth along the longitudinal axis for the horizontal cristae (Figure 4.2D and 4.4D).

Overall, the relative expression patterns and levels of Myo6 and Gfi1 agreed with the known order of cell cycle exit and differentiation for the inner ear organs, which from earliest to latest are the saccule, utricle, anterior crista, posterior crista, horizontal crista, and cochlea (Ruben, 1967; Sher, 1971; Sans and Chat, 1982). The saccule had the most Gfi1-positive cells, followed by the utricle, the anterior crista, and the posterior and horizontal cristae (Figure 4.5C",D",E",F",F""). In addition, the Myo6 staining was most distinct in the saccule where the distinctive morphology of hair cells was apparent (Figure 4.5F,F', green). In the utricle, Myo6 appeared to be localized to distinct cells, but these cells did not exhibit a typical hair cell morphology (Figure 4.5F,F', green). In the cristae, the Myo6 expression was diffuse but located within a portion of the Sox2-positive sensory region (Figure 4.5C-E'). The cochlear duct, as expected, was not immunolabeled by either Gfi1 or Myo6 at this age.

4.2.5 SUPPORT CELL BIRTH FOLLOWS A SIMILAR PATTERN

In the above analyses, I demonstrate that hair cell birth and differentiation proceed from the central to peripheral regions of the developing cristae; however, since I hypothesized that the timing of differentiation underlies regenerative competence and hair cell regeneration is driven by the transdifferentiation of support cells, I also analyzed the spatial pattern of development of support cells for E12.5 posterior cristae using immunolabeling for Sox2.

In order to birthdate support cells I used the same methods described above to birthdate hair cells with the exception that BrdU-positive support cells were identified as being positive for BrdU and Sox2 and negative for Myosin7a. Bins were created for both the x-axis and the z-axis as described previously using the list of Myosin7a-positive hair cells, and the number of BrdU-positive support cells was counted for each bin. The data for the

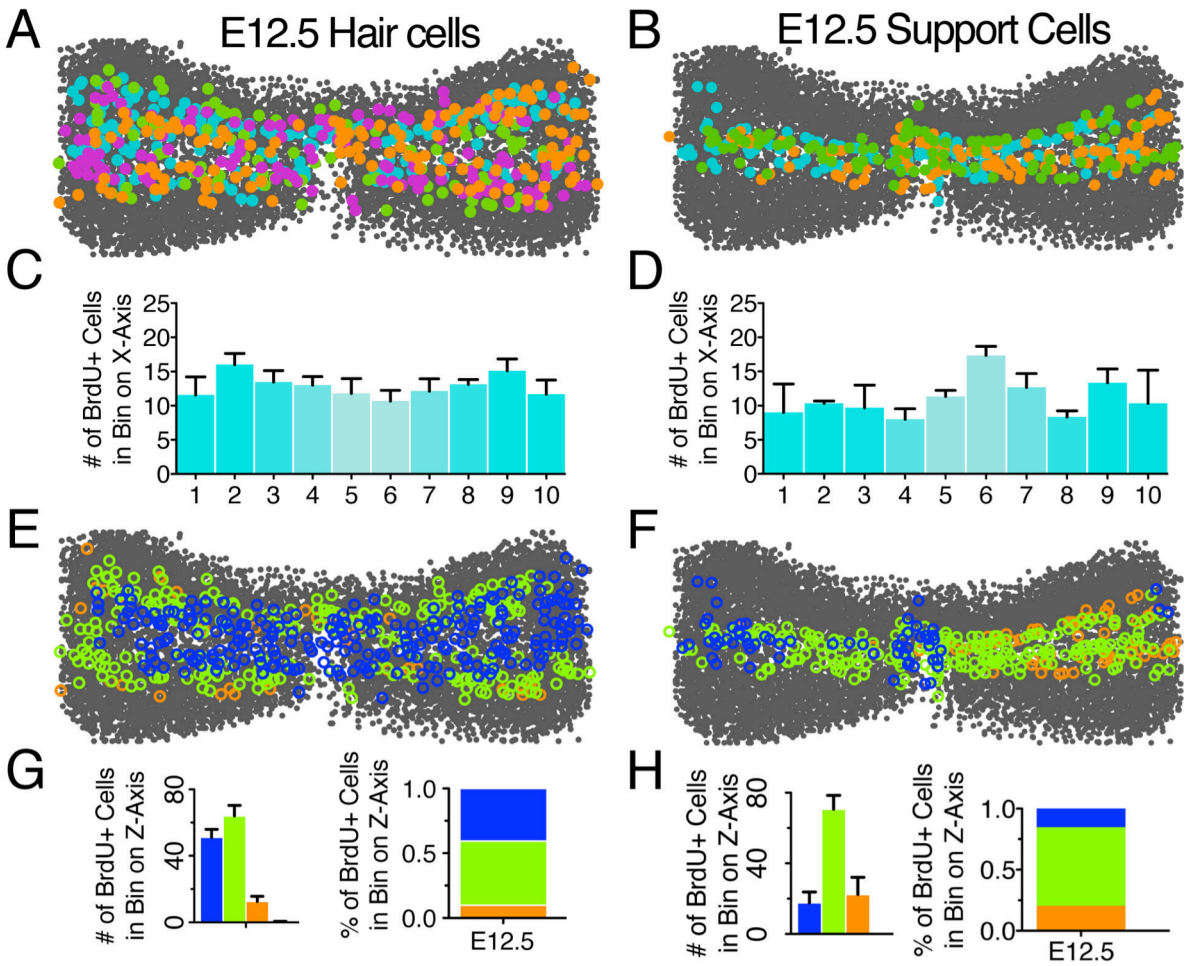

Figure 4.6 Support cells in E12.5 posterior cristae show a similar pattern as hair cells. **A-B)** Support cells that double-labeled for BrdU and Sox2 were analyzed and plotted identically to those shown in the hair cell plot from Figure 4.2A depicting the group data for E12.5 posterior cristae (A). **C-D)** Similar to the hair cells, the BrdU-positive support cells show a fairly even distribution along the x-axis at E12.5. Error bars depict SEM. **E-F)** The same plots as shown in panels A and B here color coded for z-bin in the color order from top to bottom of blue, green, orange, red. **G-H)** Similar to the hair cells, the BrdU-positive support cells are located in the higher, or more medial, z-bins, as seen in graphs of both the number and the percentage of BrdU-positive cells in each z-bin. The greater distribution of support cells in the green bin is due to the support cell nuclei sitting below the hair cells.

support cells (Figure 4.6B,D,F,H) is shown alongside the corresponding data for the hair cells in the E12.5 posterior cristae (Figure 4.6A,C,E,G) shown in previous figures.

In E12.5 posterior cristae, the spatial pattern of support cell development was very similar to that seen for hair cells (Figure 4.6A,B). Both cell types were born in the medial region of the cristae and have a fairly even distribution along the longitudinal axis (Figure 4.6C,D). The exception to this was a slight enrichment in the medial bin 6 for the support cells, which reflects the large number of Sox2-positive non-sensory cells born in the crux eminentia at this age (Figure 4.6B,D). An analysis of the z-axis confirmed that the majority of support cells were born medially (Figure 4.6F,H). This is slightly different than the hair cells, which were found at similar levels in both the blue and green bins (Figure 4.6E,G). However, since the same bins created using the list of Myosin7a-positive hair cells were used for both analyses, this difference is a reflection of the pseudolayering of the sensory epithelium in which support cell nuclei are located beneath the hair cell layer. Overall, these data indicate that hair cells and support cells in the same region exit the cell cycle at similar times.

4.3 DISCUSSION

4.3.1 THE SPATIAL PATTERN OF DEVELOPMENT IN THE CRISTAE

By injecting BrdU into mouse embryos, I determined the spatial pattern of hair cell development throughout the period of hair cell birth in the cristae. My data confirms the previous results from the rat horizontal cristae (Sans and Chat, 1982) demonstrating that hair cell birth largely changes along the medial to lateral axis, occurring early in the central regions and later in the more peripheral edges in all three cristae types. In addition, I found that hair

cell differentiation is coupled to cell cycle exit in the cristae and identified previously unknown patterns of hair cell development in the cristae along the longitudinal axis.

In the cochlea, where the developmental process has been more extensively characterized, cell cycle exit is uncoupled from cellular differentiation. Cells of the cochlear duct are born between E12 and E16 (Ruben, 1967) in a mitotic zone found at the junction of the cochlea and the saccule (Marovitz and Shugar, 1976; Marovitz et al., 1976). As the cochlea elongates, the earliest born cells form the apical turns, whereas later born cells become the more basal turns (Ruben, 1967; Lee et al., 2006). In contrast, the onset of hair cell differentiation begins in the midbasal turn and extends to both the apex and the base between E14.5 and E16.5. Therefore, even though the cells in the apical turn are born first, they are actually the last to differentiate (Sher, 1971; Lim and Anniko, 1985; Lanford et al., 2000; Chen et al., 2002; Woods et al., 2004). This extended period between terminal mitosis and differentiation is fairly unique to the cochlea, as in both the utricle (Zheng and Gao, 1997) and the central nervous system (reviewed in Gotz and Huttner, 2005; Nguyen et al., 2006) most cells begin to differentiate almost immediately after cell cycle exit. My data from the E14.5 embryonic ears and the embryonic BrdU injections suggest that the cristae adhere to the more common mechanism where cellular differentiation occurs shortly after cell cycle exit.

In the posterior and anterior cristae, hair cell birth begins near the crux eminentia in two distinct patches, extends along the entire length of the crista in the medial regions, and then finally shifts to the more lateral edges of the crista between E15.5 and E17.5. Differentiation, as indicated by the expression of Gfi1 and Myo6 at E14.5, begins in the

regions nearest to the medial crux eminentia, even though at E12.5 hair cells exited the cell cycle throughout the entire medial region of the cristae. This suggests that the cells nearest to the crux eminentia are born earlier than those closer to the peripheral planum semilunatum. This is further supported by the "off-wave" of hair cell birth found along the longitudinal axis using embryonic BrdU injections. Although hair cell birth was evenly distributed along the longitudinal axis at E12.5, it decreased first in the regions near the crux eminentia at E15.5 and later in regions near the planum semilunatum at E17.5.

The horizontal cristae, which do not have a crux eminentia, appeared to develop asymmetrically along the longitudinal axis, with hair cell birth beginning in the superior, or more dorsal, half of the cristae. This asymmetric development was seen to a lesser extent in the embryonic posterior and anterior cristae, where sometimes one hemicristae had slightly more Gfi1-expressing hair cells or more Myo6-labeling than the other. This finding is interesting as the superior half of the horizontal cristae is specifically innervated by vestibulocerebellar afferents (Maklad et al., 2010) and the horizontal crista lies along the dorsoventral axis, making it particularly susceptible to the dorsoventral gradients present in the developing inner ear (reviewed in Groves and Fekete, 2012; Wu and Kelley, 2012).

4.3.2 REGIONAL DIFFERENCES IN HAIR CELL REGENERATION

Through the work of many studies, including my own, it is now clear that the mature mammalian inner ear does have a limited capacity for hair cell regeneration through the transdifferentiation of support cells, both spontaneously (Forge*, et al.,* 1993, Warchol*, et al.,* 1993, Rubel*, et al.,* 1995, Tanyeri*, et al.,* 1995, Yamane*, et al.,* 1995, Meza*, et al.,* 1996, Li and Forge*,* 1997, Lopez*, et al.,* 1997, Zheng and Gao*,* 1997, Forge*, et al.,* 1998, Lopez*, et al.,* 1998,

Ogata, *et al.,* 1999, Kirkegaard and Jorgensen, 2000, Walsh, *et al.,* 2000, Berggren, *et al.,* 2003, Lopez, *et al.,* 2003, Oesterle, *et al.,* 2003, Taura, *et al.,* 2006, Kawamoto, *et al.,* 2009, Lin, *et al.,* 2011, Golub, *et al.,* 2012) and through methods such as inhibition of Notch signaling (Hori, *et al.,* 2007, Lin, *et al.,* 2011, Jung, *et al.,* 2013, Mizutari, *et al.,* 2013, Slowik and Bermingham-McDonogh, 2013). However, it remains unclear what is limiting regeneration in the adult and why the majority of support cells do not transdifferentiate, as occurs earlier in all of the developing organs in response to damage and various differentiation protocols including Notch inhibition (Chapter 2.3.4, Figure 2.6)(Lanford, *et al.,* 1999, Zine, *et al.,* 2001, White, *et al.,* 2006, Yamamoto, *et al.,* 2006, Hayashi, *et al.,* 2008, Collado, *et al.,* 2011b, Zhao, *et al.,* 2011, Burns, *et al.,* 2012a, Munnamalai, *et al.,* 2012, Slowik and Bermingham-McDonogh, 2013).

One hypothesis is that the complex cytoskeletal organization and anchorage necessary for the specialized morphologies of the support cells are limiting their ability to transdifferentiate (Davies, *et al.,* 2007, Meyers and Corwin, 2007, Burns, *et al.,* 2008, Collado, *et al.,* 2011a, Collado, *et al.,* 2011b, Burns, *et al.,* 2013, Burns and Corwin, 2014). This is easiest to imagine in the cochlea where these morphologies are the most extreme. However, even in the vestibular organs of mammals, E-cadherin accumulation in the junctions between support cells results in the thickening of the F-actin belts with age, which does not occur in non-mammalian vertebrates. Further, this thickening is inversely correlated with the decrease in regenerative potential with age as the organs mature (Burns, *et al.,* 2008, Collado, *et al.,* 2011b). In postnatal cultured utricles, Collado, *et al.* (2011b) found that the support cells that were able to transdifferentiate, first down-regulated E-cadherin. Conversely, those

support cells that did not transdifferentiate, which accounted for the majority of the support cells, maintained their E-cadherin expression. Therefore, if these specialized junctions are in fact limiting the regenerative potential of these organs, this will be a significant hurdle to inducing robust hair cell regeneration.

Our data demonstrating that hair cell development in the cristae begins in the central regions and shifts to the peripheral edges with age is consistent with the hypothesis that the last regions of the sensory organ to differentiate retain regenerative potential the longest (Figure 4.7). In the cristae, support cells in the peripheral region transdifferentiate in response to inhibition of Notch signaling as shown using lineage tracing with the PLP/CreER mice (Slowik and Bermingham-McDonogh, 2013). The peripheral region is also the only region that maintains expression of the Notch effector, Hes5, in the adult (Hartman et al., 2009).

This relationship between relative maturity and regenerative potential is consistent with the other inner ear organs. In the utricle, hair cell development begins in the striolar region with later addition occurring along the lateral edges (Sans and Chat, 1982; Zheng and Gao, 1997; Burns et al., 2012b). Hair cell regeneration in the utricle has been found

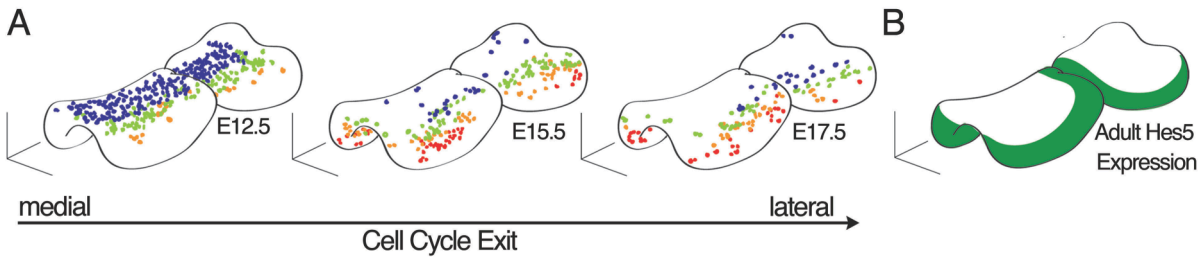

Figure 4.7 Summary of the pattern of cell cycle exit in the cristae. **A)** A cartoon diagram summarizing the changes in the spatial distribution of hair cell birth with age. **B)** A cartoon diagram of the regions in the adult cristae that maintain active Notch signaling and express the downstream Notch effector Hes5. This region correlates with the areas at E17.5 where some of the last hair cells exited the cell cycle.

spontaneously after damage in the lateral extrastriolar region (Golub et al., 2012) and in the posteromedial extrastriolar region using Hes5 siRNA (Jung et al., 2013). In the cochlea, the apical turn is the last region to differentiate and mature (Sher, 1971; Lim and Anniko, 1985; Lanford et al., 2000; Chen et al., 2002; Woods et al., 2004) and is also where the majority of the postnatal regeneration has been found (Zheng and Gao, 2000; Yamamoto et al., 2006; Doetzlhofer et al., 2009; Kelly et al., 2012; Liu et al., 2012; Shi et al., 2013; Bramhall et al., 2014; Cox et al., 2014; Liu et al., 2014; Walters et al., 2014; Li et al., 2015).

Although my data in the cristae and data from other studies in the utricle and cochlea support a link between the regenerative ability of different regions and the relative maturity of those regions, there are several studies in both the utricle and the cristae demonstrating different patterns of hair cell regeneration that suggest that there may be multiple mechanisms for regeneration. Spontaneous hair cell regeneration in the mature chinchilla cristae occurs in a gradient along the longitudinal axis where it is highest near the central crux eminentia and lowest at the periphery near the planum semilunatum (Lopez et al., 1997). This same pattern of regeneration also occurs in cultured postnatal cristae treated with the gamma-secretase inhibitor, DAPT, to inhibit Notch signaling (Slowik and Bermingham-McDonogh, 2013). However, as I show here, the regions nearest to the crux eminentia are actually the first to exit the cell cycle and differentiate. It is possible that regenerative ability in these regions may be modulated through differential gene expression and/or the presence of specific signaling cues. For example, the crux eminentia is the only region in the cristae where the bHLH transcription factor, GATA3, is expressed (Karis et al., 2001). GATA proteins have been shown to act cooperatively with NICD-CSL at the

promoter level (Neves et al., 2007) and in the inner ear, it has been suggested that GATA-3 expression could be important for hair cell regeneration through downstream signaling targets such as Wnt (Alvarado et al., 2009). In the utricle, GATA3 is specifically expressed in the striolar region, which, along with the juxtastriolar region, is where hair cell regeneration has been found in several studies (Collado et al., 2011b; Lin et al., 2011; Burns et al., 2012a).

Although in the cochlea, the potential for regeneration is lost with age, in the vestibular sensory organs, later born regions appear to maintain a low level of regenerative ability into adulthood. This suggests that the link between maturity and regenerative ability is not a developmental phenomenon. Identifying the factors that limit regeneration may come from observations of these regional differences. By further studying these organs, we can better understand the mechanism through which a small subset of support cells is maintaining regenerative competence and develop methods to induce more robust regeneration in the larger quiescent population of support cells and in other non-regenerative neural systems.

C H A P T E R F I V E

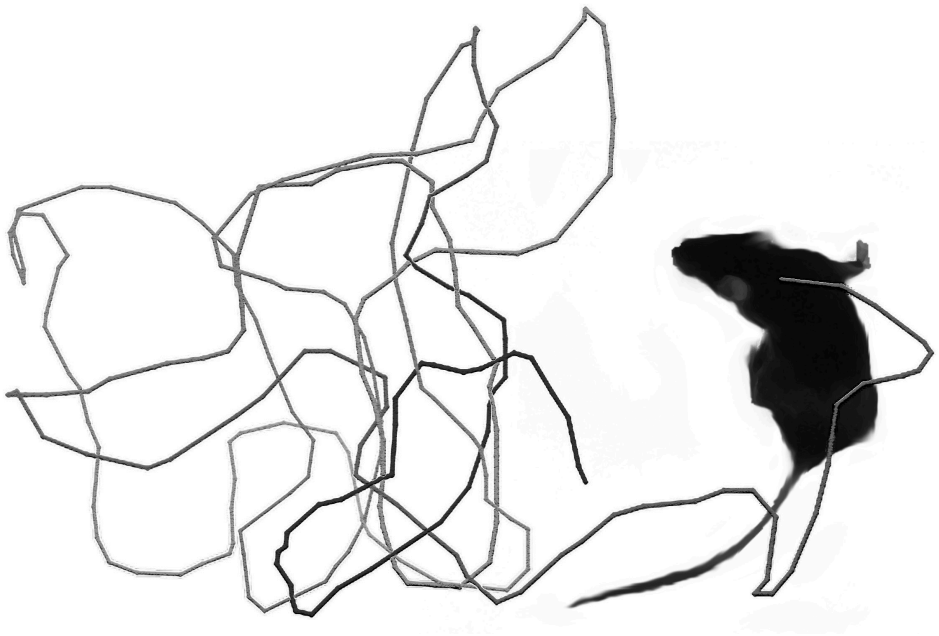

BEHAVIORAL ASSAY OF VESTIBULAR DEFICIT IN MICE

5.1 INTRODUCTION

The hearing loss and vestibular deficits resulting from loss of the sensory hair cells from the inner ear organs are both permanent and debilitating. The loss of hair cells from the auditory system can be partially ameliorated by the use of hearing aids to replace lost outer hair cells and by the use of cochlear implants to replace lost inner hair cells; however, in the vestibular system, the only therapeutic option for severe vestibular deficit is lesioning the organs and allowing for compensation by the other ear and/or cerebellum. While vestibular prostheses similar to cochlear implants are under development to treat vestibular deficit (Dai, et al., 2011, Lewis, et al., 2013, Phillips, et al., 2014), the recent work by myself and others demonstrating low levels of hair cell regeneration through inhibition of Notch signaling (Hori, et al., 2007, Lin, et al., 2011, Jung, et al., 2013, Mizutari, et al., 2013, Slowik and Bermingham-McDonogh, 2013) suggest that regenerative therapies may also be possible in the near future. In fact, it is even possible that the current low levels of regeneration observed are sufficient to restore some meaningful function. In my study, I saw approximately a ten percent increase in total hair cell number following inhibition of Notch signaling *in vitro*. Since, in the cristae, humans lose approximately 30-40% of the hair cells over the course of their lives due to aging (Rauch, et al., 2001, Lopez, et al., 2005), it is possible that a ten percent increase would restore some functionality. To assess this, however, we would need to understand how vestibular function scales with hair cell number. This information would also be helpful in regenerative studies, as it would allow us to estimate the degree of hair cell regeneration based on behavioral output over time.

Here, I present a systematic study describing the effectiveness of standard vestibular tests at different levels of hair cell lesion using the known ototoxin, IDPN. I identified two simple tests, the open field test and the swim test, which together provide distinct and quantifiable behaviors at different levels of hair cell lesion.

5.2 RESULTS

5.2.1 STRAIN DIFFERENCES IN HAIR CELL NUMBER AND EFFICACY OF IDPN LESION

In order to generate a variable number of hair cells, I used the known ototoxin, 3,3'-iminodipropionitrile (IDPN) to lesion the hair cells (Soler-Martin, et al., 2007) in two different strains of mice: CBA/CaJ and C57BL/6. C57BL/6 is the background for many transgenic animals that could be useful for studying the inner ear and regeneration, including: Hes5-eGFP, DCX-CreER, Ai14, Glast-CreER, Otof-Cre, and PLP-CreER. However, C57BL/6 mice have age-related hearing loss with a known mutation in cadherin 23 (Johnson et al., 1997, Noben-Trauth et al., 2003), which is a component of the tip links that are necessary for auditory transduction (Kazmierczak et al., 2007). In C57BL/6 mice, hearing loss begins in the higher frequencies located at the base of the cochlea at 1-2 months of age (Mikaelian, et al., 1974, Henry and Chole, 1980, Shnerson and Pujol, 1981, Willott, 1986, Li and Borg, 1991, White, et al., 2000, Hequembourg and Liberman, 2001, Ison and Allen, 2003). By 3 months of age, C57BL/6 mice show a 75% loss of outer hair cells and a 55% loss of inner hair cells in the base with a further progression of hair cell loss as they age (Spongr, et al., 1997). It is for this reason that many inner ear researchers use the CBA/CaJ mouse strain, which does not show abnormal age-related hearing loss and has no hair cell

loss at 18 months of age (Spongr, et al., 1997). However, since back-crossing lines onto the CBA/CaJ strain is a long process, I wanted to determine if the vestibular system of the C57BL/6 mice also underwent age-related hair cell loss, similar to the auditory system.

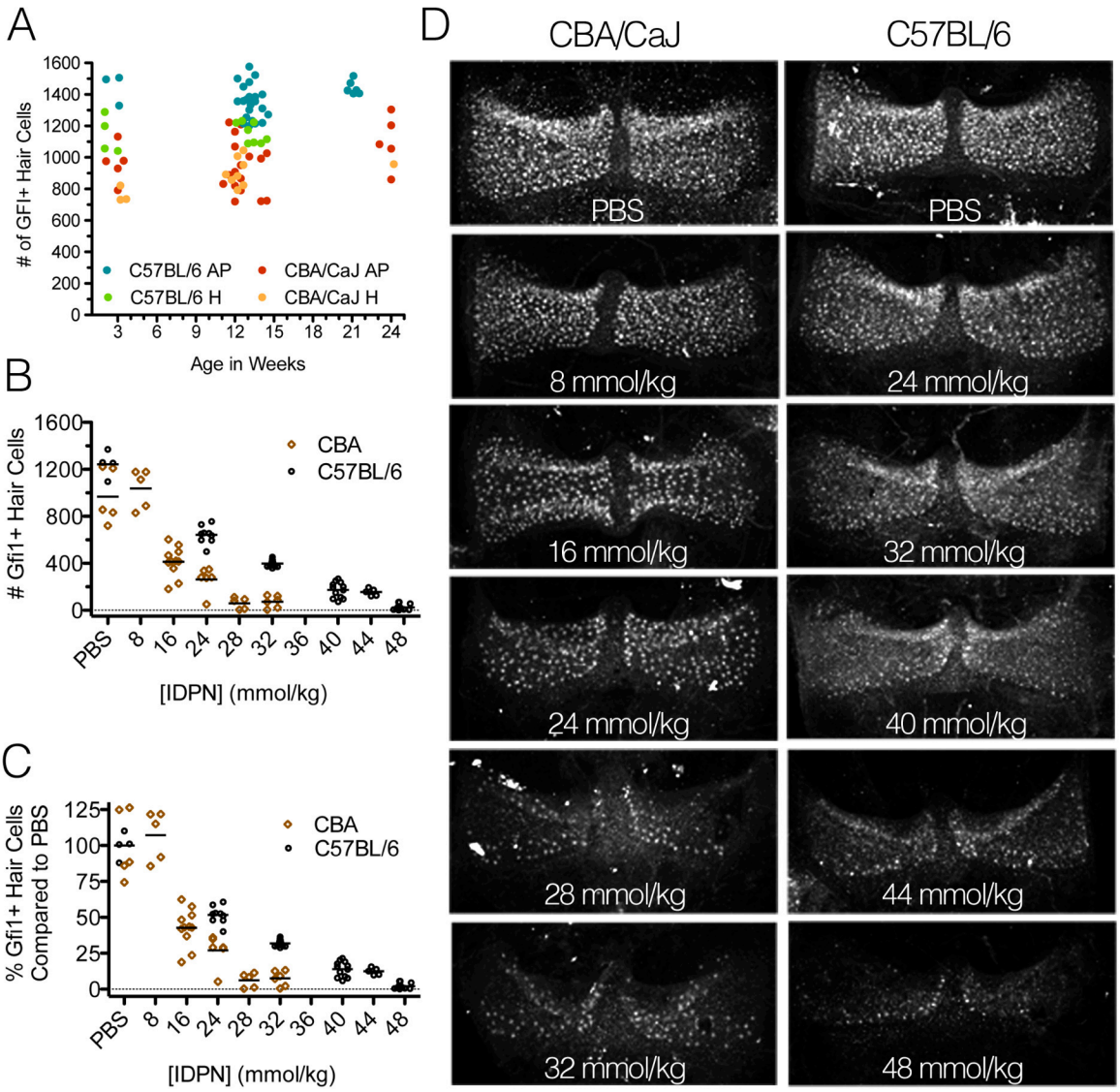

Figure 5.1 Differences in hair cell number and IDPN efficacy in C57BL/6 and CBA/CaJ mice. **A)** The total number of Gfi1+ hair cells is lower in all of the cristae of the CBA/CaJ mice compared o C57BL/6. Both strains show consistent levels of hair cell number between weaning age and 5-6 months of age. AP – data from anterior and posterior cristae. H – data from horizontal cristae. **B-C)** Dose response curves for hair cell lesion with IDPN in CBA/CaJ and C57BL/6 mice show that C57BL/6 require higher doses of IDPN for hair cell lesion shown as both the number (B) and percentage (C) of Gfi1+ hair cells. **D)** Maximum intensity projections of cristae from CBA/CaJ and C57BL/6 mice lesioned with IDPN and immunolabeled with the nuclear hair cell marker Gfi1.

In both the C57BL/6 and CBA/CaJ mouse strains, I did not find any evidence for hair cell loss with age in the cristae (Figure 5.1A). I, with several undergraduates, collected cristae from both strains of mice at several ages, including: weaning, 3 months, and 5 months. The cristae were immunolabeled with Gfi1 to identify hair cell nuclei, imaged as wholemounts, and counted. Although the CBA/CaJ mice consistently had fewer hair cells than the age-matched C57BL/6 mice, both strains had approximately the same average number of Gfi1-positive hair cells at 5 months of age as they had at weaning.

In addition to a difference in hair cell number, I also found that the two strains showed differences in their susceptibility to IDPN lesion. The CBA/CaJ mice showed a similar dose response curve as the CD-1 mice used by Soler-Martin et al. (2007) who originally described the IDPN lesion qualitatively. The C57BL/6 mice, however, required higher doses of IDPN in order to achieve a similar level of lesion as the CBA/CaJ mice (Figure 5.1B-D, brown versus black dots). The higher doses of IDPN required were not due to the higher number of hair cells found in the C57BL/6 mice versus the CBA/CaJ mice

TABLE 5.1

Numerical summary of the number of Gfi1+ hair cells at varying ages in CBA/CaJ and C57BL/6 mice

		ANTERIORS AND POSTERIORS						HORIZONTALS					
		CBA/CaJ			C57BL/6			CBA/CaJ			C57BL/6		
		mean	SEM	n	mean	SEM	n	mean	SEM	n	mean	SEM	n
Age (weeks)	Weanling	2			1496.00		1				1182.00	± 67.57	3
		3	962.00	± 54.43	5	1417.50	± 88.50	2	763.33	± 29.36	3	1041.00	1
	3 months	12	953.67	± 49.44	12				906.75	± 31.18	8		
		13				1361.89	± 26.49	18				1172.50	± 26.73	6
		14	894.60	± 70.06	5	1307.40	± 30.31	5				1103.00	± 13.00	2
	5 months	21				1442.83	± 17.93	6					
		24	1101.60	± 74.90	5				957.00		1		

(Figure 5.1A), as the percentage of Gfi1-positive hair cells in cristae compared to PBS controls was higher for a given dose of IDPN in the C57BL/6 mice versus the CBA/CaJ mice (Figure 5.1C, brown versus black dots).

5.2.2 MEASURING VESTIBULAR DEFICIT IN IDPN-LESIONED MICE: VESTIBULO-OCULAR REFLEX (VOR)

Traditionally, behavioral deficit of the cristae and semicircular canals in humans, primates, and rodents is assayed using the vestibulo-ocular reflex (VOR)(Figure 5.2A). The VOR is primarily used to stabilize images on the retina and relies on input from the vestibular system in order to create compensatory eye movements in response to brief head movements. The pathway for this reflex includes only a few central nuclei, including the vestibular nuclei, abducens nucleus, and oculomotor nucleus. These same nuclei are essential for another visual reflex, the optokinetic nystagmus (OKN)(Figure 5.2B), which uses visual

TABLE 5.2

Numerical summary of the number and percentage of Gfi1+ hair cells at varying IDPN concentrations

		CBA/CaJ				C57BL/6			
		mean [# (%)]		SEM [# (%)]	n	mean [# (%)]		SEM [# (%)]	n
IDPN Concentration (mmol/kg)	PBS	968.20 (100.00)	±	103.79 (10.72)	5	1244.25 (100.00)	±	56.72 (4.56)	4
	8	1038.00 (107.21)	±	74.45 (7.69)	5				
	16	414.18 (42.78)	±	37.89 (3.91)	11				
	24	262.33 (27.10)	±	44.19 (4.56)	6	642.44 (51.63)	±	25.20 (2.03)	9
	28	60.40 (6.24)	±	21.95 (2.27)	5				
	32	72.67 (7.51)	±	20.72 (2.14)	6	397.00 (31.91)	±	8.47 (0.68)	12
	36								
	40					172.58 (13.87)	±	19.31 (1.55)	12
	44					154.80 (12.44)	±	13.79 (1.11)	5
	48					26.25 (2.11)	±	7.25 (0.58)	12

- Number, % - Percentage

input instead of vestibular input and serves as a control for the central components of the VOR. For VOR and OKN testing, mice are fixated using a previously implanted head post (Figure 5.2C,C') and either rotated in the dark or shown a screen with a moving sinusoidal

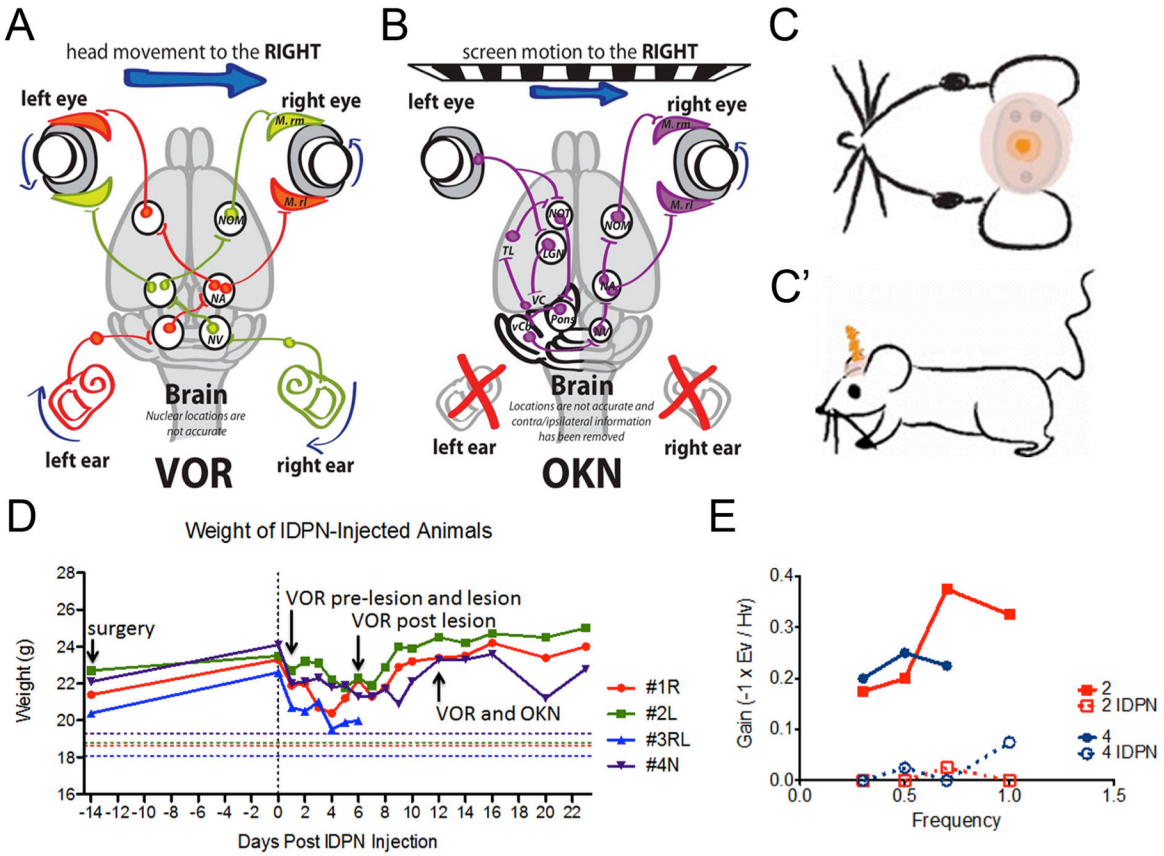

Figure 5.2 Measuring the vestibulo-ocular reflex after IDPN lesion. **A)** The central pathway for the vestibulo-ocular reflex (VOR) includes the vestibular nuclei (NV), the abducens nucleus (NA), and the oculomotor nucleus (NOM). M. rm – medial rectus muscle. M. rl – lateral rectus muscle. **B)** The central pathway for the optokinetic nystagmus (OKN) is very similar to that of the VOR but receives visual input only. NOT – nucleus of the optic tract, LGN – lateral geniculate nucleus, TL – temporal lobe, VC – visual cortex, vCb – vestibular cerebellum. **C-C')** To test for the VOR and OKN, mice must be implanted with a head screw in order to fix their head position during testing. **D)** A diagram of the weight of four mice throughout the testing paradigm. Mice were implanted with headposts two weeks prior to VOR testing and lesion with IDPN. Additional testing was performed 6 days (VOR only) and 12 days after lesion (VOR and OKN). Mouse number 3 was euthanized at day 6 due to complications with the head post implant. **E)** VOR data from mice numbers 2 and 4 show good gain responses that increase with increasing frequency of rotation. After IDPN treatment, these responses are attenuated. Mouse number 2 did not show a VOR response either before or after IDPN lesion.

gradient. If the reflexes are intact, these stimuli will result in stereotyped compensatory eye movements that can be tracked using a camera and later quantified.

To determine if VOR testing can be used in IDPN-lesioned mice, I implanted head posts onto four CBA/CaJ mice. The experimental paradigm is shown in Figure 5.2D overlayed over the weight of the animals. Following IDPN-lesion, it is common for mice to lose weight; however this weight loss is within acceptable parameters (shown by the dotted line) and is recovered within two weeks. Two weeks after the head post surgery, I tested the mice for a VOR reflex and then lesioned their hair cells using a single intraperitoneal injection of 24 mmol/kg IDPN. Out of the four mice tested, only three mice exhibited a VOR response. The mice were tested again for a VOR response six days after lesion and for a VOR and OKN response twelve days after lesion. Due to complications with the head post implant, one mouse had to be euthanized after the VOR testing on the sixth day. For unexplained reasons, one of the remaining mice did not have a VOR response before or after IDPN lesion, which according to our collaborator Dr. Jim Phillips, appears to occur in approximately 25% of mice tested. Although, the last two remaining mice showed robust VOR responses prior to lesion that were attenuated after IDPN lesion (Figure 5.2E, solid versus dotted lines), I was unable to measure a robust OKN response in these mice. The lack of an OKN response suggests that the IDPN lesion may compromise the central pathways necessary for the VOR.

5.2.3 MEASURING VESTIBULAR DEFICIT IN IDPN-LESIONED MICE: OPEN FIELD TEST AND SWIM TEST

The potential spread in hair cell number provided by the expanded dose curve response of the C57BL/6 mice allowed me to measure vestibular behavior at varying degrees of hair cell lesion. Adult C57BL/6 mice were given a single intraperitoneal injection of IDPN in PBS at the following doses: PBS (vehicle control), 16 mmol/kg, 24 mmol/kg, 28 mmol/kg, 32 mmol/kg, 36 mmol/kg, 40 mmol/kg, 44 mmol/kg, and 48 mmol/kg. Since it is unclear whether the VOR testing can be used on IDPN-lesioned mice, I assayed vestibular behavior in the lesioned mice using several other described tests for vestibular deficit including the conical tube test, the open field test, and the swim test. A further advantage of these tests is that they do not require any surgeries or specialized equipment and can easily be used to monitor vestibular behavior over time with minimal stress to the animals.

The conical tube test involves coaxing a mouse into a 50 mL conical falcon tube and flipping the tube so that the mouse is upside down. A mouse with a functioning vestibular system can sense its awry body position and will rotate inside of the tube to correct its position. A mouse with vestibular deficit will either take longer to right itself or will not right itself at all. The open field test was used to assay hyperactivity and circling behavior, which are both permanent and known yet unexplained indicators of vestibular deficit (Porter, et al., 1990, Goddard, et al., 2008, Baek, et al., 2010). The swim test was used to assay swimming ability, which is impaired in mice with vestibular deficits. In water, proprioceptive inputs are reduced and the mice must rely more on their vestibular system to determine their body position. Although each of these tests is used to assay vestibular behavior, the way in which

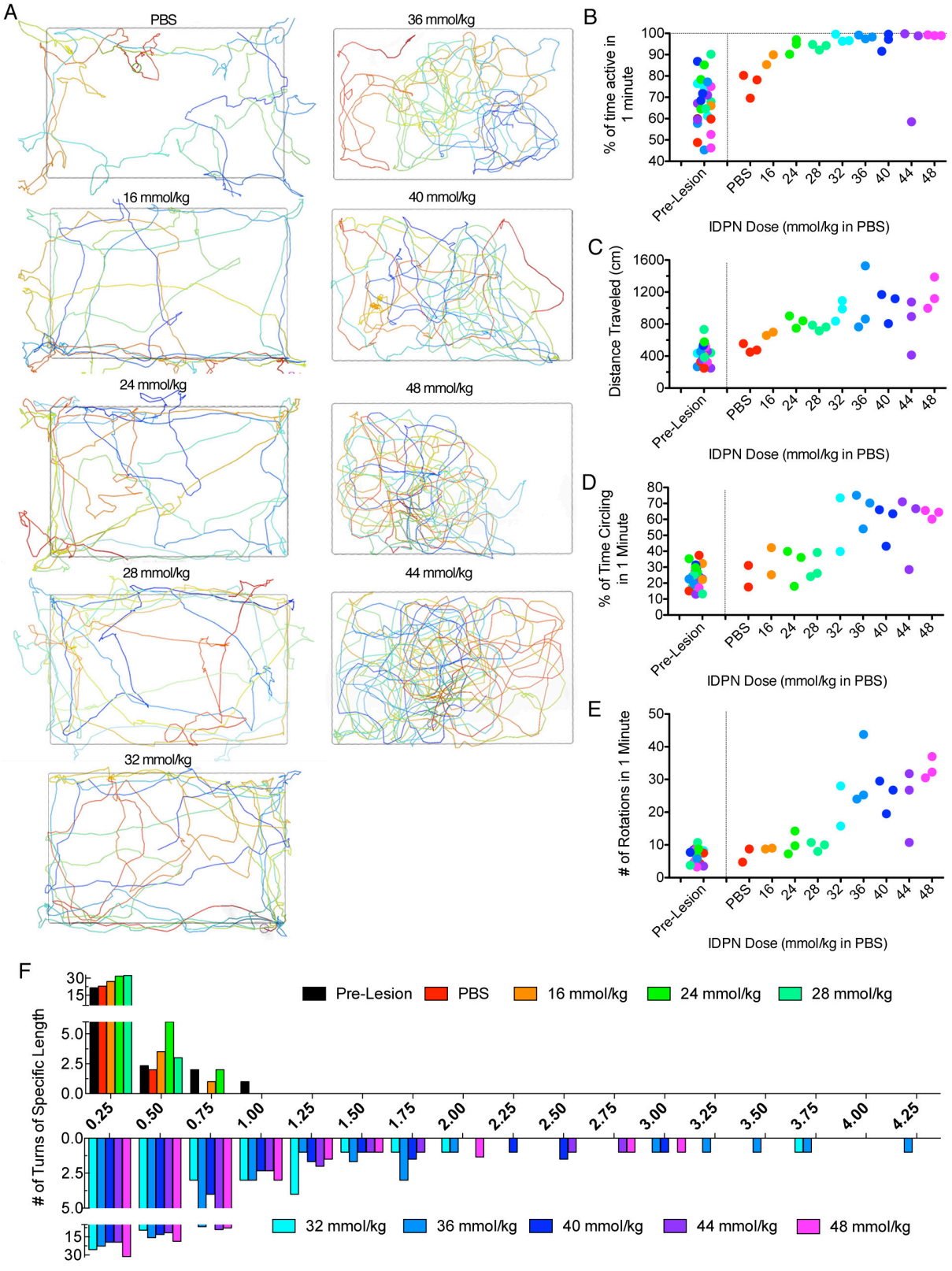
A
PBS
36 mmol/kg
16 mmol/kg
40 mmol/kg
24 mmol/kg
48 mmol/kg
28 mmol/kg
44 mmol/kg
32 mmol/kg
B
% of time active in 1 minute
IDPN Dose (mmol/kg in PBS)
C
Distance Traveled (cm)
IDPN Dose (mmol/kg in PBS)
D
% of Time Circling in 1 Minute
IDPN Dose (mmol/kg in PBS)
E
# of Rotations in 1 Minute
IDPN Dose (mmol/kg in PBS)
Pre-Lesion
PBS
16
24
28
32
36
40
44
48
F
# of Turns of Specific Length
Pre-Lesion
PBS
16 mmol/kg
24 mmol/kg
28 mmol/kg
32 mmol/kg
36 mmol/kg
40 mmol/kg
44 mmol/kg
48 mmol/kg
0.25
0.50
0.75
1.00
1.25
1.50
1.75
2.00
2.25
2.50
2.75
3.00
3.25
3.50
3.75
4.00
4.25

Figure 5.3 Hyperactivity and circling scale with degree of vestibular deficit in the open field test. **A)** Example traces of the mouse's path over a one minute period labeled from beginning to end as blue to red. The black box indicates the location of the cage bottom and traces outside of this box indicate that the mouse was climbing onto the cage edges. Relative to control mice, mice lesioned with up to 32 mmol/kg IDPN show increasing levels of activity. Mice lesioned with more than 32 mmol/kg IDPN showing increasing levels of circling. **B-C)** Both measures of hyperactivity, including percentage of time active (B) and distance traveled (C), increased with the dose of IDPN. Each point represents data from an individual mouse colored based on IDPN dose. Pre-lesion data points are colored based on the IDPN dose the animal eventually received. **D)** Mice treated with less than 32 mmol/kg IDPN spent normal amounts of time turning in the cage, while mice treated with more than 32 mmol/kg IDPN spent more time circling. A turn was quantified if it was at least a quarter turn. **E)** The total length of rotations, summed from all rotations greater than a quarter turn, increased with IDPN dose. **F)** Histograms of the length of individual bouts of rotation are shown. Control mice and mice treated with less than 32 mmol/kg IDPN mostly performed quarter or half turn rotations as part of cage exploration (warm colors, top). Mice treated with more than 32 mmol/kg IDPN had longer bouts of rotations characteristic of vestibular deficit and not part of normal cage exploration (cool colors, bottom).

the output of each test scales with the degree of vestibular deficit is not known as these tests are generally used subjectively to determine whether or not an animal has any degree of vestibular deficit.

The conical tube test was a very sensitive test that saturated in effect at very low doses of IDPN. While this test could be useful for detecting small perturbations in vestibular function, I did not follow up with this test as the lesions used in regenerative studies are generally much more severe.

In the open field test, the lesioned mice exhibited the expected hyperactivity and circling behaviors, which more importantly, appeared to scale with IDPN dose (Figure 5.3A). Control mice explored the cage and spent a lot of time along the edges of the cage. Mice that received a dose of 32 mmol/kg IDPN or less also exhibited this behavior, but showed increasing levels of hyperactivity, measured as the percentage of time active (Figure 5.3B) and the total distance traveled (Figure 5.3C). Mice that received more than 32

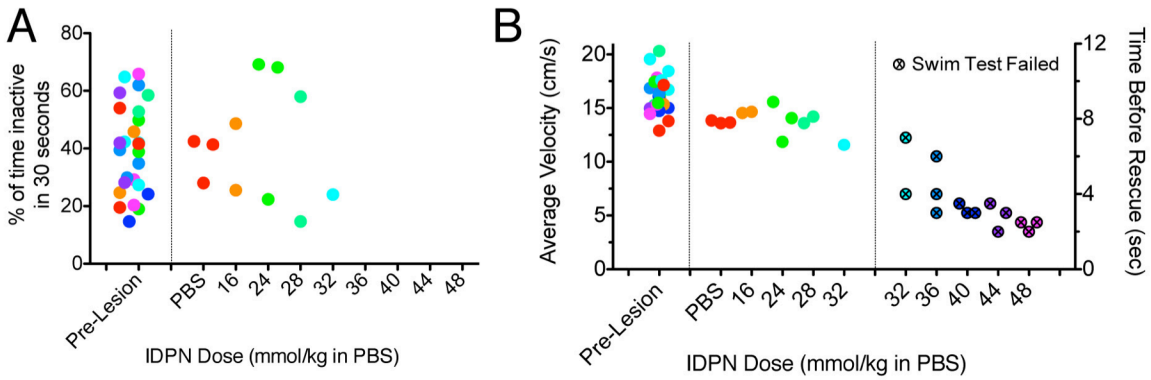

Figure 5.4 Swimming ability decreased with vestibular deficit in a swim test. **A)** Mice subjected to a thirty second swim test spent highly variable amounts of time swimming that did not correlate with vestibular deficit. **B)** Mice lesioned with IDPN showed decreasing swimming ability measured as velocity, compared to control mice with high swimming velocities. At a dose of 32 mmol/kg IDPN and higher, mice had to be rescued from the water. While mice treated with lower doses of IDPN could float and remained in the test for a few seconds, mice treated with higher doses of IDPN had to be rescued immediately.

mmol/kg IDPN exhibited circling behaviors (Figure 5.3D) in addition to signs of hyperactivity. Although their activity level was saturated (Figure 5.3B), the total distance traveled continued to increase with increasing IDPN dose due to an increased velocity (Figure 5.3C). The percentage of time spent circling was similar for all IDPN doses above 32 mmol/kg; however, the total length of all rotations summed scaled with IDPN dose (Figure 5.3E). Individual rotations were counted if they consisted of at least a quarter turn. Control mice and mice that received 32 mmol/kg of IDPN or less performed many quarter and half turns as part of their normal cage exploration (Figure 5.3F, warm colors on top). Mice that received greater than 32 mmol/kg of IDPN performed longer bouts of circling, up to 3-4 rotations in one continuous motion, in addition to the normal turns necessary for cage navigation (Figure 5.3F, cool colors on bottom).

In the swim test, mice showed variable degrees of swimming ability that was best measured with swimming velocity. Due to the stressful nature of this test, mice exhibited highly variable levels of swimming activity that did not correlate with IDPN dose due to the time spent trying to escape the edges by control mice and the time spent floating by the lesioned mice (Figure 5.4A). When the mice did swim, however, their swimming ability was readily apparent as a function of their swimming velocity because the mice with vestibular deficit exhibited barrel rolling (Figure 5.4B). In mice with minor vestibular deficit, this rolling was quickly corrected and only slowed their pace. In mice with intermediate vestibular deficit, this rolling led to bouts of submersion, which the animals controlled by floating. In mice with severe vestibular deficit, the animals could not control the rolling and submersion and had to be rescued. In the animals that had to be rescued, the time to rescue scaled with

IDPN dose, as the mice with more intermediate lesions were still able to partially compensate for their lack of swimming ability by floating prior to needing rescuing (Figure 5.4B).

5.3 DISCUSSION

Here I have quantified the hair cell number with age in two widely used mouse strains and identified two simple tests that can be used to assay varying degrees of vestibular behavior. By analyzing cristae of different ages, I found that CBA/CaJ mice have significantly fewer hair cells than C57BL/6 mice at all ages tested. More importantly, neither of these strains exhibited age-related hair cell loss up to 5 months of age. This is surprising, as C57BL/6 mice are known to have severe age-related hearing loss, with significant hair cell losses beginning at one month of age. In addition to differences in hair cell number, these two strains also showed differences in susceptibility to IDPN-lesion. The mechanism through which IDPN lesions hair cells is currently unknown; however, it is hypothesized that metabolic bioactivation is required. Therefore, differences in metabolic processing of the drug may explain why higher doses of IDPN are required to lesion vestibular hair cells in C57BL/6. These differences in hair cell number and drug susceptibility between mouse strains are important examples of the large variability in mouse strains that must be incorporated into experimental design.

The behavioral tests identified here, the open field test and the swim test, both showed quantifiable behaviors that scale with decreasing hair cell number. These tests do not require any surgical procedures or specialized equipment and can easily be performed in any lab with a recording device (such as a cell phone or video recorder) and the equipment

necessary for normal mouse husbandry. In addition, both tests can be analyzed by tracking the position of the mouse in successive still frames. This positional data can be used to determine activity level, velocity, and circling behavior in an unbiased manner, as compared to the subjective scales traditionally used to quantify vestibular behavior that are difficult to compare between researchers and laboratories.

At present, hair cell number can only be assayed in explanted organs of euthanized animals. My data here, however, suggests that there may be a clear correlation between vestibular behavior and hair cell number that would allow for hair cell number to be estimated based on behavioral assays. This information would be useful for both degenerative and regenerative studies where animals are tracked over time to monitor experimental outcomes. Although the scope of the current study is limited by the use of IDPN lesions, the results of this study are very promising and provide strong support for future studies using other types of hair cell lesion. Of particular concern is the fact that IDPN is a known neurotoxin in addition to an ototoxin. The lack of an OKN response, for example, suggests that this drug may be having an effect on the central nervous system. Since other neurological systems may also be impaired by IDPN, I cannot rule out an effect on vestibular behavior by another system affected by IDPN.

CHAPTER SIX

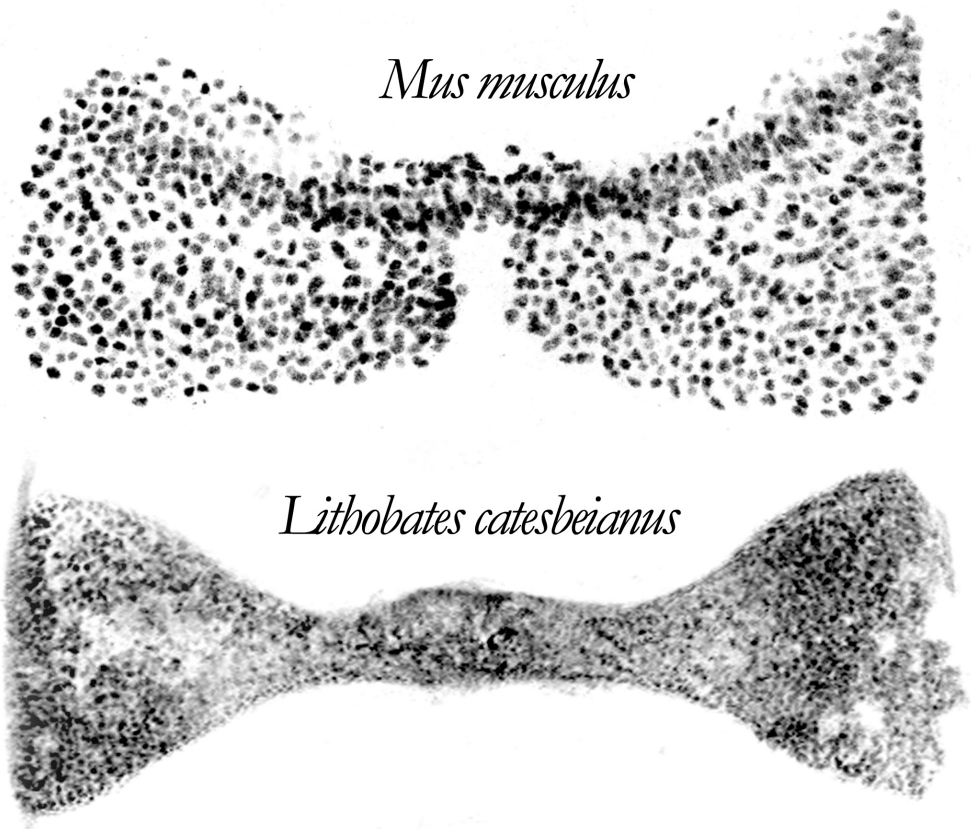

CONCLUSIONS AND FUTURE DIRECTIONS

6.1 PERSPECTIVE

6.1.1 SPONTANEOUS HAIR CELL REGENERATION

During the course of this dissertation, significant strides have been made in the field of hair cell regeneration, such that we now know definitively that the mammalian inner ear retains some regenerative ability into adulthood. At the beginning of this dissertation work, it was unclear whether or not hair cell regeneration occurred in the mature mammalian inner ear. Although many previous studies had shown evidence for spontaneous hair cell regeneration after damage in the vestibular system, the level of regeneration in these studies was very low. Further, these experiments were performed in chinchillas (Tanyeri*, et al.,* 1995, Lopez*, et al.,* 1997, Lopez*, et al.,* 1998, Lopez*, et al.,* 2003), guinea pigs (Forge*, et al.,* 1993, Warchol*, et al.,* 1993, Rubel*, et al.,* 1995, Yamane*, et al.,* 1995, Li and Forge*,* 1997, Forge*, et al.,* 1998, Walsh*, et al.,* 2000), gerbils (Ogata*, et al.,* 1999), bats (Kirkegaard and Jorgensen*,* 2000), and rats (Meza*, et al.,* 1996, Zheng and Gao*,* 1997, Berggren*, et al.,* 2003, Oesterle*, et al.,* 2003, Taura*, et al.,* 2006), where the lack of genetic tools limited the analytical power of these studies. The experimenters largely had to rely on secondary measures to identify regenerating hair cells, such as the presence of immature hair bundles by scanning electron microscopy (SEM), and, using light microscopy on thin sections, the presence of hair cells after a complete lesion and the identification of intermediate transitional morphologies.

Although these were very promising signs of regeneration, many investigators questioned the validity of this evidence as hair cell repair and other changes to the sensory epithelium could have accounted for the observed "regeneration". For example, in the rat

utricle, it was found that a large number of hair cells could survive in the sensory epithelium without stereocilia bundles after lesion with aminoglycoside antibiotics (Zheng*, et al.,* 1999). Further, in the bullfrog saccule, these "bundleless" hair cells could eventually replace their lost stereocilia (Gale*, et al.,* 2002), which was troubling as many previous studies had solely relied on the presence of new hair bundles as evidence for hair cell regeneration.

Another study in the gerbil posterior cristae cautioned against limiting analyses of hair cell number to subsections of the sensory epithelium, as they found that regional changes in hair cell number were not necessarily indicative of a total change in hair cell number throughout the entire sensory organ. This was due to the fact that the organs are asymmetric in shape and drug-susceptibility. Further, damage from aminoglycoside antibiotics causes many changes to the sensory epithelium that do not necessarily indicate hair cell loss or regeneration throughout the entire sensory organ, such as expansion or shrinkage of the sensory epithelium and regional thinning (Polgar*, et al.,* 2001).

These newer studies did not affect some of the evidence for hair cell regeneration, such as the transitional morphologies suggestive of support cell transdifferentiation. However, overall, these studies cast a large shadow of doubt over the field of mammalian hair cell regeneration that highlighted the need for newer and more robust techniques to identify hair cell regeneration in whole sensory organs.

6.1.2 INDUCED HAIR CELL REGENERATION

At the same time that these questions into spontaneous hair cell regeneration were raised, there were many significant advances in our understanding of hair cell development

that shifted the focus away from spontaneous regeneration and raised the possibility of greater levels of hair cell regeneration through other means.

The role of Notch signaling through lateral inhibition in establishing and maintaining the correct ratio of hair cells and support cells was shown in embryonic and early postnatal animals in both the auditory (Lanford*, et al.,* 1999, Zhang*, et al.,* 2000, Zheng*, et al.,* 2000, Zine*, et al.,* 2001, Kiernan*, et al.,* 2005, Brooker*, et al.,* 2006, Yamamoto*, et al.,* 2006, Takebayashi*, et al.,* 2007, Hayashi*, et al.,* 2008, Doetzlhofer*, et al.,* 2009, Zhao*, et al.,* 2011, Du*, et al.,* 2013, Korrapati*, et al.,* 2013, Mizutari*, et al.,* 2013) and the vestibular system (Zheng*, et al.,* 2000, Zine*, et al.,* 2001, Collado*, et al.,* 2011b, Du*, et al.,* 2013) (reviewed in Cotanche and Kaiser*,* 2010, Murata*, et al.,* 2012, Kiernan*,* 2013). In many cases, loss of Notch signaling resulted in a significant increase in supernumerary hair cells through support cell transdifferentiation, which suggested a potential therapeutic role for Notch signaling through its inhibition.

Around this time, the bHLH transcription factor, Atoh1, which is the downstream target of Notch signaling, was also discovered and shown to start the transcriptional cascade necessary for hair cell differentiation (Bermingham*, et al.,* 1999, Chen*, et al.,* 2002). This began the search for reprogramming methods to induce cells to become hair cells through overexpression of Atoh1 (reviewed in Mulvaney and Dabdoub*,* 2012). Since my dissertation work focuses on the use of Notch inhibition to regenerate hair cells, I will focus my discussion to studies involving Notch signaling in mammals.

Many studies attempted to inhibit Notch signaling to induce hair cell regeneration; however, it was found that the organ of Corti loses its ability to generate supernumerary hair

cells in response to Notch inhibition postnatally (Lanford*, et al.,* 1999, Zine*, et al.,* 2001, Murata*, et al.,* 2006, Yamamoto*, et al.,* 2006, Hayashi*, et al.,* 2008, Doetzlhofer*, et al.,* 2009, Hartman*, et al.,* 2009, Basch*, et al.,* 2011, Zhao*, et al.,* 2011) as Notch ligands are down-regulated within the first few days after birth (Hartman*, et al.,* 2007). In addition, a former member of the Bermingham-McDonogh lab found that Notch signaling, as reported by the downstream Notch effector Hes5, was not up-regulated as a result of aminoglycoside damage to the organ (Hartman*, et al.,* 2009), suggesting that Notch signaling was not re-activated after damage as occurs in some other regenerative species.

Together, all of this work suggested that hair cell regeneration, either spontaneously or through inhibition of Notch signaling, was not possible in the cochlea, which was the prevalent perception when I began my dissertation. In addition, the cochlea as I have described it, with the three rows of outer hair cells, one row of inner hair cells, and highly specialized support cells is unique to mammals. It is thought, even today, that this highly specialized morphology of the cells within the mammalian cochlea may in part be responsible for limiting its regenerative ability.

The mammalian vestibular system, on the other hand, has many of the same functions and morphological features as those found in lower vertebrates, which have robust hair cell regeneration (reviewed in Warchol*,* 2011). This, in addition to the earlier work on spontaneous hair cell regeneration led people to hypothesize that the vestibular system may retain some regenerative potential in the adult. More evidence for this came from the same study demonstrating that Notch signaling was not up-regulated in response to damage. In that study, Hartman*, et al.* (2009) also found that the downstream Notch effector Hes5 was

present in the vestibular system of the adult. This was a very exciting finding that fueled my own studies as well as multiple independent investigations into hair cell regeneration in the utricle in other laboratories.

6.2 CONCLUSIONS

For my dissertation work, I wanted to build upon the previous findings in the Bermingham-McDonogh lab showing robust expression of Hes5 in the mature cristae ampullaris by determining if Notch signaling was active in the adult cristae and if it could be inhibited in order to regenerate hair cells. Over the last five years, I have not only accomplished that goal, but have also established the mouse cristae as a viable model for studying hair cell regeneration. More specifically, I showed that treatment with the gamma-secretase inhibitor, DAPT, down-regulates the Notch effectors *Hes1* and *Hes5* and increases the total number of Gfi1-positive hair cells in cultured cristae explanted from one month old mice. Using lineage tracing with PLP/CreER;mTmG mice to label support cells, I showed that support cells undergo transdifferentiation in response to DAPT treatment in mice up to ten weeks of age and that these transdifferentiating support cells can express hair cell markers, translocate to the hair cell layer, take on a hair cell morphology, and even develop a stereocilia bundle with a kinocilium.

In addition, I performed these analyses on whole organs using techniques such as lineage tracing that definitively show whether or not regeneration is occurring. By analyzing the entire organ, I accounted for any possible changes in the shape, structure, or density of the organs and the cells within them that in the past have confounded the evidence regarding

the levels of regeneration observed. Further, by using the Cre-loxp technology to lineage trace support cells, I have bypassed the problems regarding potential hair cell repair prevalent in previous studies and shown unequivocally that at least some hair cells arise through transdifferentiation of support cells following inhibition of Notch signaling *in vitro*.

In order to recapitulate these results *in vivo*, I tested the viability of administering DAPT systemically to adult mice by injecting Hes5-eGFP mice with the maximum allowed dose (set by IACUC) of 90 mg/kg DAPT in DMSO via subcutaneous injection once daily for three consecutive days. In previous *in vitro* experiments, I found that it took three days of DAPT treatment in order to see a significant down-regulation in Hes5-eGFP fluorescence intensity due to the stability of the eGFP protein. However, after the three days of DAPT injections *in vivo,* I was unable to see a significant decrease in Hes5-eGFP fluorescence. Notably, the injected mice did not show any deleterious side effects such as significant weight loss, gastrointestinal distress, or general malaise that has been reported previously using systemic treatment with gamma-secretase inhibitors (Mizutari*, et al.,* 2013). Due to the lack of effect of DAPT treatment, the high cost of these experiments, and the potential for harm to the animals, I did not follow up on these experiments. Instead, future work should focus on administering the DAPT locally through application via the round window as was performed by Mizutari*, et al.* (2013) and many others for administering gamma-secretase inhibitors and other pharmacological agents. This does involve a small surgery, but also allows for injections of significantly smaller amounts of drug and a localized effect of the drug. This would help to limit both the costs and the side effects associated with these experiments.

The remainder of my dissertation was, therefore, focused on expanding our knowledge of how the cristae develop and adding to the collection of tools available for studying the cristae. Thanks to my efforts, we now understand the complex spatial patterns involved in the development of the cristae and how they relate to the regions that display regenerative competence in both postnatal and mature animals. In addition, through my screen of Cre-expressing mouse strains, we now have several options for recombining both hair cells and support cells in the cristae for a variety of studies including lineage tracing, FACS, genetic lesion, etc. Using one of these lines, the Dcx-CreER mice crossed to the Ai14 reporter line (Dcx-CreER;Ai14), I showed in a preliminary *in vivo* experiment that the level of spontaneous hair cell regeneration after aminoglycoside damage is very low in the mature cristae. In fact, the level of spontaneous regeneration I observed through lineage tracing support cells was much lower than that reported by previous studies in the chinchilla (Tanyeri*, et al.,* 1995, Lopez*, et al.,* 1997, Lopez*, et al.,* 1998, Lopez*, et al.,* 2003). As more work is performed on hair cell regeneration using the newer and more robust techniques now available to us, it will be interesting to see what the actual level of hair cell regeneration and what the therapeutic relevance of that regeneration are.

With this in mind, I have also demonstrated, for the first time, a direct relationship between hair cell number and vestibular behavior. More importantly, this data shows that differences of less than 200 hair cells at varying degrees of hair cell lesion can be detected and objectively quantified using a combination of open field and swim tests. This is particularly significant for determining the behavioral relevance and therefore therapeutic

importance of hair cell regeneration, which at present is approximately in this range of one to two hundred hair cells.

6.3 FUTURE WORK

Overall, this work, together with findings from a number of other investigators (Hori*, et al.,* 2007, Lin*, et al.,* 2011, Jung*, et al.,* 2013, Mizutari*, et al.,* 2013), demonstrates that manipulation of Notch signaling, particularly through γ-secretase inhibitors, can stimulate hair cell regeneration through support cell transdifferentiation in the mammalian inner ear. To date, only a single study has demonstrated functional recovery from Notch inhibition *in vivo*, albeit with only modest effects. This was the study in the cochlea where hair cell regeneration after otoacoustic damage resulted in some functional recovery (Mizutari*, et al.,* 2013). It is not known whether inhibition of Notch signaling in the vestibular organs would provide sufficient numbers of new hair cells to provide a functional benefit, but these are clearly the next steps towards a therapy based on this strategy. However, beyond this, we still have many challenges ahead of us as the current levels of regeneration in the mammal, even through modulation of Notch signaling, are far less than those found in non-mammalian vertebrates.

In order to induce robust, sustainable hair cell regeneration we need to not only increase the degree of hair cell regeneration, but also ensure that these hair cells have the appropriate identity and characteristics, such as polarity, for their specific sensory organ and location within that organ. In addition, in order for hair cell regeneration to be sustainable, the "progenitor-like" pool of support cells from which the new hair cells are arising must be

maintained. In the mammal, there appears to be a limited degree of support cell proliferation; however, this is unlikely to be sufficient to maintain the level of hair cell regeneration that will ultimately be required for full functional recovery. Many groups are investigating how to induce more robust support cell proliferation in mammalian organs and have shown some success in mature organs through manipulations such as loss of c-Myc (Burns*, et al.,* 2012) and $p27^{kip1}$ (Lowenheim*, et al.,* 1999, Oesterle*, et al.,* 2011) and through addition of TGF-α and EGF with insulin (Yamashita and Oesterle*,* 1995).

Even if we can induce robust support cell proliferation, we must still be able to convert sufficient amounts of these support cells to transdifferentiate into hair cells. While the methods discussed here have shown promising results, they are only able to generate modest amounts of hair cells. With each of the regenerative methods used, there seems to be a specific competence window for hair cell regeneration. Using Notch overexpression for lateral induction, this time window is very early in otic development and appears to follow the normal developmental timeline for prosensory formation (Hartman*, et al.,* 2010, Pan*, et al.,* 2010, Basch*, et al.,* 2011, Liu*, et al.,* 2012b, Pan*, et al.,* 2013). It is likely that the decreasing competence is linked to the change between the prosensory and lateral inhibition roles that is occurring at this time. Since this change would be necessary for the continued development of the inner ear organs and appears to involve multiple complex regulatory elements, this method of hair cell regeneration may not be feasible or practical for use in mature organs.

The induction of robust hair cell generation from Notch inhibition currently seems to be a more feasible approach since all of the mature mammalian organs of the inner ear have

some regenerative capacity in response to Notch inhibition. While it is not clear whether Notch is required for the normal maintenance of the vestibular organs, Notch signaling does seem to play a role in each of the mouse inner ear organs following damage. More work, however, needs to be done in order to establish the conditions under which Notch signaling is induced after damage, as there is some controversy over whether only certain types or degrees of damage can induce a Notch-mediated regenerative response. Ideally, we would be able to regenerate hair cells under all damage conditions, including drug-induced ototoxicity, noise damage, and varying forms of degeneration.

Even with damage, inhibition of Notch signaling has a limited regenerative response. This was particularly apparent in my own data where almost all of the peripheral support cells down-regulated Notch signaling in response to DAPT treatment, but the majority of these cells did not undergo transdifferentiation. This is also true of the utricle and cochlea, where even though it is more difficult to determine how many of the support cells were expressing Notch components and down-regulated them in response to inhibition, it is clear that only a subset of them are transdifferentiating in response to Notch inhibition.

What then is limiting support cell transdifferentiation in these mature organs? One possibility is that additional signaling factors might interact with the Notch pathway to regulate competence. For example, the expression of Hey2 in the pillar cells of the cochlea prevents their differentiation into hair cells, even after Notch inhibition. In fact, inhibition of both FGF signaling and Notch signaling is required for the down-regulation of Hey2 and subsequent pillar cell transdifferentiation (Doetzlhofer*, et al.,* 2009). Further, the Notch receptor is not the only target for γ-secretase, and therefore Notch might not be the only

pathway whose inhibition is contributing to the regeneration observed through γ-secretase inhibition. The γ-secretase complex is involved in a process called regulated intramembrane proteolysis (RIP) that has over ninety known substrates including Notch receptors and ligands, amyloid precursor protein (APP), Ephs/Ephrins, Interleukin receptors, cadherins, and Erb/Neuregulins (reviewed in Haapasalo and Kovacs, 2011). While Notch inhibition is sufficient for some hair cell regeneration, as shown by Jung, *et al.* (2013) through specific knock down of *Hes5,* it is possible that inhibition of some of these other pathways might be modulating the regenerative response.

The regulation of Atoh1 downstream of Notch signaling is another possibility for limiting transdifferentiation as it has several known enhancer sites (Helms and Johnson, 1998, Helms, *et al.,* 2000) as well as multiple known repressors and activators under the control of multiple signaling pathways (reviewed in Mulvaney and Dabdoub, 2012). This is supported by the fact that overexpression of Atoh1 itself is not able to generate hair cells in the mature inner ear. Interestingly, Liu, *et al.* (2012a) found that the Atoh1-induced transdifferentiation of pillar cells and Deiters' cells in the immature cochlea required activation of endogenous Atoh1, suggesting that a critical level of Atoh1 expression through activation of an autoregulatory feedback mechanism may be required (Helms, *et al.,* 2000).

Beyond these regulatory mechanisms, it is also possible that the specialized morphologies of the support cells are limiting their ability to transdifferentiate, as discussed in Chapter 4.3.2. Even though the vestibular organs do not have specialized morphologies unique to mammals, like the cochlea, they do show differences with age not found in non-mammalian vertebrates such as the accumulation of E-cadherin in the junctions between

support cells and the resulting thickening of the F-actin belts with age (Davies*, et al.,* 2007, Meyers and Corwin*,* 2007, Burns*, et al.,* 2008, Collado*, et al.,* 2011a, Collado*, et al.,* 2011b, Burns*, et al.,* 2013, Burns and Corwin*,* 2014).

Overall, while the recent work investigating the role of Notch inhibition in hair cell regeneration has been very promising and has shown the potential for some therapeutic benefit, we still have many challenges that we must overcome. Ultimately, it appears that we need a better understanding of the different regulatory mechanisms involved in the maturation of the various sensory organs. For example, in order to understand what is limiting the competence of the inner ear for lateral induction, we must understand how the switch between the prosensory and lateral inhibition roles of Notch signaling is occurring. Further, to understand why Notch inhibition does not result in more hair cell transdifferentiation through lateral inhibition, we must understand how Atoh1 is being regulated and mechanistically how it is driving hair cell differentiation. Just as we gained many insights into different ways to use Notch signaling to induce regeneration from studying the role of Notch signaling in development, we must now go back to development to determine how Notch signaling and Atoh1 are being regulated there in order to develop strategies to induce more robust hair cell regeneration.

C H A P T E R S E V E N

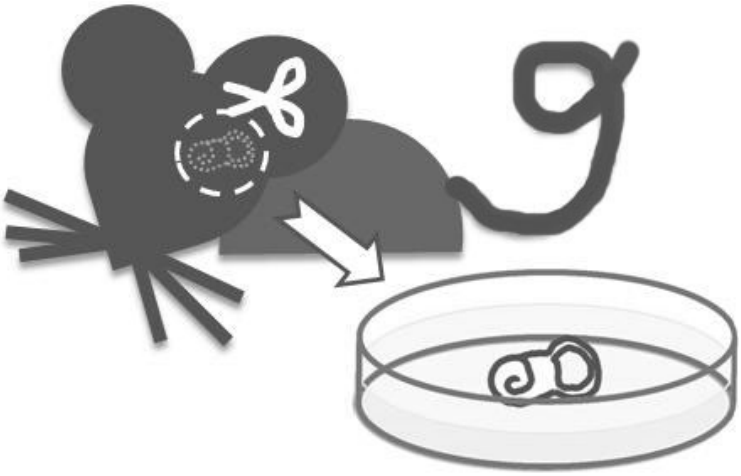

MATERIALS AND METHODS

7.1 ANIMALS AND GENOTYPING

Animal housing and care was provided by the Department of Comparative Medicine at the University of Washington. All procedures were done in compliance with the standards and protocols set forth by the University of Washington Institutional Animal Care and Use

TABLE 7.1

Summary of mouse strains used

	STRAIN	TYPE[1]	STRAIN BACKGROUND	SUPPLIER	STOCK #
	C57BL/6	WT	-	Harlan Laboratories	057
	CBA/CaJ	WT	-	The Jackson Laboratory	000654
	ND4 Swiss Webster	WT	-	Harlan Laboratories	032
Reporters	Ai14	TG	C57BL/6J	The Jackson Laboratory	007914
Reporters	Hes5-eGFP	TG	C57BL/6	Dr. Verdon Taylor	-
Reporters	Math1-nGFP	TG	(C57BL/6 x DBA/2)F1	Dr. Jane Johnson	-
Reporters	R26-mTmG	TG	129X1/SvJ (approximate)	The Jackson Laboratory	007576
Cre-Expressing Strains	Calb2-IRES-Cre	KI	C57BL/6J	The Jackson Laboratory	010774
Cre-Expressing Strains	Cralbp-CreER	TG	C57BL/6 x CBA	Dr. Edward Levine	-
Cre-Expressing Strains	Dcx-CreER	TG	C57BL/6J	MMRRC	032780-MU
Cre-Expressing Strains	Dlx5-CreERT2	KI	C57BL/6J	The Jackson Laboratory	010705
Cre-Expressing Strains	Glast-CreER	KI	129S2/SvPas	Dr. Masato Nakafuku (made by Dr. Magdalena Goetz)	-
Cre-Expressing Strains	Glast-CreER	TG	C57BL/6J	The Jackson Laboratory	012586
Cre-Expressing Strains	Gpr26-Cre	TG	FVB/B6/129/Swiss/CD1	MMRRC	033032-UCD
Cre-Expressing Strains	Grm2-Cre	TG	FVB/N-Crl:CD1(ICR)	MMRRC	036166-UCD
Cre-Expressing Strains	Otof-Cre	KI	C57BL/6	MMRRC	032782-MU
Cre-Expressing Strains	Plp-CreER	TG	C57BL/6J	The Jackson Laboratory	005975
Cre-Expressing Strains	Satb2-Cre	TG	FVB/B6/129/CD1	MMRRC	034813-UCD
Cre-Expressing Strains	Vipr2-Cre	TG	FVB/B6/129/Swiss/CD1	MMRRC	034281-UCD
Cre-Expressing Strains	Wfs1-Tg2-CreERT2	TG	C57BL/6J	The Jackson Laboratory	009614

[1] KI - Knock-in, TG - Transgenic, WT - Wildtype

Committee (IACUC). Unless otherwise noted, both male and female mice were used for experiments and postnatal day 0 (P0) was defined as the day of birth after an assumed gestation period of 19 days. A list of the mouse strains used, including their approximate background strain and supplier information, is summarized in Table 7.1.

Ai14 transgenic mice expressing a floxed-stop tdTomato under the control of the CAG promoter in the *Rosa26* locus (Madisen*, et al.,* 2010) were obtained from Dr. Thomas Reh (University of Washington, Seattle, WA), who originally purchased them from the Jackson Laboratory. These reporter mice were maintained as a homozygous colony and crossed to various mouse lines expressing Cre recombinase for experiments. The inner ears obtained from Dr. Julie Harris (Allen Institute for Brain Science, Seattle, WA) were also crossed to this reporter line. Genotyping was performed according to the supplier's protocols using the following primers: wild-type forward 5'-AAGGGAGCTGCAGTGGAGTA-3', wild-type reverse 5'-CCGAAAATCTGTGGGAAGTC-3', mutant forward 5'-GGCATTAAAGCAGCGTATCC-3', and mutant reverse 5'-CTGTTCCTGTACGGCATGG-3'. These primers generate a wild-type amplicon of 297 bp and a mutant amplicon of 196 bp.

Hes5-eGFP transgenic mice expressing GFP under the control of the *Hes5* promoter (Basak and Taylor*,* 2007) were obtained from Dr. Verdon Taylor (University of Basel, Basel, Switzerland). These mice were maintained as a homozygous colony and not genotyped. Presence of the Hes5-eGFP transgene was determined by immunofluorescence.

Math1-nGFP transgenic mice expressing a nuclear-localized GFP under the control of the *Math1* promoter (Lumpkin*, et al.,* 2003) were obtained from Dr. Jane Johnson

(University of Texas Southwestern, Dallas, TX). These mice were maintained as a homozygous colony and outcrossed to ND4 Swiss Webster mice for experiments. Mice were genotyped for GFP using the following primers: forward 5'-AAGTTCATCTGCACCACCG-3' and reverse 5'-TCCTTGAAGAAGATGGTGCG-3'. These primers generate a mutant amplicon of 200 bp.

R26-mTmG transgenic mice expressing a floxed-membrane-localized tdTomato-stop followed by a membrane-localized GFP under the control of the CAG promoter in the *Rosa26* locus (Muzumdar*, et al.,* 2007) were obtained from the Jackson Laboratory. These mice were maintained as a homozygous colony and crossed to the PLP/CreER mouse line for lineage tracing support cells. Mice were genotyped for the mutant *Rosa26* allele using the following primers: forward 5'-CTCTGCTGCCTCCTGGCTTCT-3', wild-type reverse 5'-CGAGGCGGATCACAAGCAATA-3', and mutant reverse 5'-TCAATGGGCGGGGGTCGTT-3'. These primers generate a wild-type amplicon of 330 bp and a mutant amplicon of 250 bp.

Dcx-CreER transgenic mice expressing an inducible Cre recombinase under the control of the doublecortin promoter were originally generated by Dr. Ulrich Mueller (The Scripps Research Institute, San Diego, CA) and were obtained from the Mutant Mouse Regional Resource Centers (MMRRC). These mice were maintained as a homozygous colony and crossed to the Ai14 reporter mouse line for experiments. Genotyping was performed according to the supplier's protocols for the Cre recombinase element and for the inducible ERT2 element using the following primers: Dcx forward 5'-TGAATGTCGGATAGCTGCAC-3', Cre reverse 5'-GCAAACGGACAGAAGCATTT-3', ERT2 forward 5'-GATTGGTCTCGTCTGGCGCTCC-3', and ERT2 reverse 5'-

ACGGCTAGTGGGCGCATGT-3'. These primers generate a mutant Cre amplicon of 899 bp and a mutant ERT2 amplicon of 502 bp.

The Plp-CreER transgenic mice expressing an inducible Cre recombinase under the control of the Plp promoter (Doerflinger*, et al.,* 2003) were obtained from the Jackson Laboratory. These mice were maintained as a heterozygous colony and crossed to the R26-mTmG reporter mouse line for lineage tracing support cells. Genotyping was performed for Cre recombinase using the following primers: forward 5'- AACATTCTCCCACCGTGAGT-3' and reverse 5'- CATTTGGGCCAGCTAAACCAT-3'. These primers generate a mutant amplicon of 300 bp.

Samples from the Calb2-IRES-Cre, Dlx5-CreERT2, Gpr26-Cre, Grm2-Cre, Otof-Cre, Satb2-Cre, Vipr2-Cre, and Wfs1-Tg2-CreERT2 mouse lines were obtained from Dr. Julie Harris (Allen Institute for Brain Science, Seattle, WA). Samples from the Cralbp-CreER and the Glast-CreER (knock-in and transgenic) mouse lines were obtained from Dr. Thomas Reh (University of Washington, Seattle, WA).

7.2 INJECTIONS OF PHARMACOLOGICAL AGENTS

In order to birthdate hair cells, a single intraperitoneal (IP) injection of 5-bromo-2'-deoxyuridine (BrdU, Sigma, 1.25 mg/25 g mouse) in sterile PBS was administered to time-mated pregnant Swiss Webster females. The age of the embryos at the time of injection was determined by plug date and confirmed by birthdate assuming a gestation period of 19 days.

To lesion hair cells, a single IP injection of 3,3'-Iminodiproprionitrile (IDPN, Acros Organics) in sterile PBS was administered at doses between 8 and 48 mmol/kg. For C57BL/6 mice, a dose of 40 mmol/kg was normally used. For all other strains, a dose of 24

mmol/kg was normally used. Behaviors consistent with a vestibular deficit including head bobbing, circling, and hyperactivity normally began approximately 3-4 days after injection.

To induce recombination in Dcx-CreER mice expressing an inducible Cre recombinase, IP injections of tamoxifen (Sigma, 3.0 mg/25 g mouse) in sterile corn oil (Sigma) were administered once daily for two consecutive days. To dissolve the tamoxifen in the corn oil, tamoxifen was incubated on a nutator overnight at 37°C. For the mice obtained from Dr. Julie Harris (Allen Institute for Brain Science, Seattle, WA), tamoxifen (5.0 mg/25 g mouse) was administered via oral gavage for five consecutive days.

To inhibit Notch signaling, the γ-secretase inhibitor N-[N-(3,5-Difluorophenacetyl)-L-alanyl]- S-phenylglycine t-butyl ester (DAPT, Calbiochem) was administered via subcutaneous injection at a dose of 10-90 mg/kg using either sterile corn oil or DMSO as a vehicle.

7.3 ORGANOTYPIC CRISTAE CULTURES

Mice were euthanized according to approved procedures. Cristae were explanted from the capsule on ice in modified Hank's balanced salts solution without phenol red or sodium bicarbonate (Sigma) supplemented with 5 mM HEPES and 200 U/mL penicillin. The semicircular canals were mechanically separated from the cristae using fine forceps, while the cupula and ampulla were left intact. The cristae were cultured in modified Dulbecco's MEM (DMEM)/F-12 medium [DMEM/F-12, Reh modification without L-Aspartic Acid, L-Glutamic Acid powder (US Biological) with an additional 0.3% D-glucose, 0.8 mM GlutaMAX (Life Technologies), 0.1275% sodium bicarbonate, 5% fetal bovine serum (FBS), 1x N2 supplement, 1x B27 supplement, and 200 U/mL penicillin, at pH 7.4],

with 5% CO_2 at 37°C. Unless otherwise noted, 75% of the media was replaced every three days. Cristae were cultured at the gas-liquid interface on hydrophilic PTFE cell culture inserts with 0.4 μm pores (Millipore) coated with a 2:1 mixture of 0.12% rat-tail collagen and growth-factor reduced Matrigel (BD).

For pharmacological inhibition of Notch signaling, the γ-secretase inhibitor, DAPT, was used at a concentration of 30 μM with an equal volume of DMSO as a vehicle control (concentrations of 1-50 μM DAPT were also used in specific experiments as noted).

To induce recombination in the PLP/CreER;mTmG and Dcx-CreER;Ai14 mice, explants were treated with 5 μM 4-Hydroxytamoxifen (4-OHT; Sigma) for 2 days followed by washing prior to Notch inhibition. For the PLP/CreER;mTmG mice, only one media change containing fresh 4-OHT was given on the first day. For the Dcx-CreER;mTmG mice, two media changes with fresh 4-OHT were given per day.

To assess proliferation, the thymidine analogue Ethynyl deoxyuridine (EdU, Life Technologies) was added to the culture media at a concentration of 5 μM. EdU was visualized using the Click-iT Alexa Fluor 647 Kit (Life Technologies). For experiments using either DAPT or EdU, 75% of the media was replaced daily.

7.4 IMMUNOFLUORESCENCE

Immunostaining of whole mount cristae and cultured cristae were performed almost identically with the differences noted below. For whole mount immunostaining, capsules were removed from the head and bisected using a scalpel to isolate the vestibular system and expose the membranous labyrinth. The capsules were then fixed in cold 4% paraformaldehyde (PFA) overnight (O/N). Cultured cristae were fixed on the culture

membranes in cold 4% PFA for one hour. After fixation, all samples were rinsed in phosphate buffered saline (PBS), permeabilized in 0.5% Triton-X in PBS (PBSTx) for 30 minutes at room temperature (RT), and then blocked at RT. For Chapter 3, 10% fetal bovine serum (FBS) in 0.5% PBSTx was applied for one hour as a blocking solution. For all other experiments, samples were blocked for three hours in a solution containing 10% donkey serum, 4% bovine serum albumin, and 100 mM glycine in 0.5% PBSTx. There was not a significant difference between these two blocking solutions; however, the increased blocking period resulted in a significantly better signal to noise ratio. Blocking solution was used for both primary and secondary antibody solutions and 0.5% PBSTx was used for washing.

Primary antibodies were applied O/N at 4°C and secondary antibodies were applied either O/N at 4°C or for 3 hours at RT. When applicable, Hoechst 33342 (1:10,000) and/or Phalloidin conjugated to Alexa Fluor 647 (1:200) were added to the secondary antibody solution. All genetically encoded fluorescent reporters, including Hes5-eGFP, Math1-nGFP, tdTomato, mTomato, and mGFP, were visualized without additional antibody labeling. To preserve fluorescence, all samples were mounted in Fluoromount-G (SouthernBiotech). Occasionally, for experiments where the curved morphology of the cristae was important, whole mount cristae were mounted using 0.12 mm thick imaging spacers (Sigma). A summary of the antibodies used is presented in Table 7.2, including the host species, concentration used, and the supplier's information.

For mice that received embryonic BrdU injections, antigen retrieval was performed after permeabilization and prior to blocking. For antigen retrieval, cristae were incubated in 2N hydrochloric acid (HCl) for 30 minutes at 37°C followed by two washes in 0.1 M sodium

borate (pH 8.5) for 10 minutes to neutralize the acid. After treatment with sodium borate, cristae were rinsed in PBS and antibody staining proceeded as normal beginning with blocking.

For imaging intact embryonic inner ear capsules, the ears were cleared after immunolabeling using a solution containing five parts methyl salicylate and three parts benzyl benzoate (MSBB) according to the protocol published by MacDonald and Rubel (2008). Prior to immunolabeling but after fixation, inner ears were decalcified in 10% ethylenediamine tetraacetic acid-disodium salt (EDTA) in PBS, pH 7.4, for four days on a

TABLE 7.2

Summary of antibodies used

	ANTIGEN	CONJUGATED	HOST	CONC.	SUPPLIER	PRODUCT #
Primary Antibodies	BrdU (BU1/75)	-	Rat	1:100	Accurate Chemical	OBT-0030
	Calretinin	-	Rabbit	1:2000	Swant	7699/4
	Dcx (C-18)	-	Goat	1:120	Santa Cruz Biotechnology	SC-8066
	Gfi1	-	Guinea Pig	1:1000	Dr. Hugo J. Bellen, Baylor	-
	Myosin6	-	Rabbit	1:1000	Proteus Biosciences	25-6791
	Myosin7a	-	Rabbit	1:500	Proteus Biosciences	25-6790
	Sox2 (Y-17)	-	Goat	1:200	Santa Cruz Biotechnology	SC-17320
	Sox9	-	Rabbit	1:800	Millipore	AB5535
Secondary Antibodies	Goat	Alexa Fluor 488	Donkey	1:400	Jackson ImmunoResearch	705-545-147
	Goat	Alexa Fluor 568	Donkey	1:400	Life Technologies	A11057
	Goat	Alexa Fluor 594	Donkey	1:400	Life Technologies	A11058
	Goat	Alexa Fluor 633	Donkey	1:400	Life Technologies	A21082
	Guinea Pig	DyLight 649	Donkey	1:200	Jackson ImmunoResearch	discontinued
	Rabbit	Alexa Fluor 488	Donkey	1:400	Life Technologies	A21206
	Rabbit	Alexa Fluor 568	Donkey	1:400	Life Technologies	A10042
	Rabbit	Alexa Fluor 594	Donkey	1:400	Life Technologies	A21207
	Rabbit	Alexa Fluor 647	Donkey	1:400	Life Technologies	A31573
	Rat	Alexa Fluor 594	Donkey	1:400	Life Technologies	A21209
	Rat	DyLight 649	Donkey	1:400	Jackson ImmunoResearch	discontinued
	Phalloidin	Alexa Fluor 647	-	1:200	Invitrogen	A22287
	Hoechst 333432	-	-	1:10,000	Life Technologies	H3570

nutator at 4°C. Samples were changed into a new solution of 10% EDTA each day. After four days, the samples were rinsed in PBS.

After immunolabeling, samples were dehydrated in 70% ethanol overnight, followed by 95% ethanol for 30 minutes, and then two incubations with pure ethanol for two hours each. After dehydration, samples were incubated in a 1:1 mixture of MSBB and pure ethanol for four hours. Samples were then cleared using three changes of MSBB for 2 hours, 4 hours, and overnight. Samples were imaged in the MSBB solution on 1 mm thick rubber imaging spacers (Coverwell PCI-A-2.0, Grace Bio-Labs).

7.5 PAINT-FILL OF THE EMBRYONIC INNER EAR

An embryonic day 14.5 (E14.5) inner ear was filled with 0.1% white latex paint in methyl salicylate according to Morsli*, et al.* (1998) and Kiernan (2006).

7.6 IMAGING AND PROCESSING OF IMAGE FILES

All samples were imaged using a Nikon A1R laser scanning confocal mounted on a Nikon TiE inverted microscope. Images were taken in NIS Elements (Nikon) using either a 20x dry CFI Plan Apochromat VC objective with a numerical aperture (NA) of 0.75 or a 60x oil immersion CFI Plan Apochromat VC objective with a NA of 1.4. Unless otherwise noted, z-stacks were taken at a step size of 0.5 μm with the 20x objective and at 0.125 μm with the 60x oil objective.

Maximum intensity projections and slice projections were created using either NIS Elements or ImageJ. On images shown at higher magnification in Chapter 3, blind 3D deconvolutions were performed using AutoQuant X vX2.1.1 (Media Cybernetics). Three-dimensional reconstructions and movies were created using NIS Elements. Images for

figures were compiled in Adobe Photoshop CS4 and all diagrams were made in Adobe Illustrator CS4.

7.7 ANALYSIS OF FLUORESCENT INTENSITY

For the analysis of the fluorescence intensity of Hes5-eGFP, all samples within an experiment (not across ages) were cultured, fixed, stained, imaged, and processed simultaneously using the same intensities and settings in order to preserve the integrity of the intensity comparison. Since it was therefore not appropriate to compare the absolute intensity values across ages I showed these values as only the relative difference between the DAPT-treated cristae and their own age-matched controls.

The fluorescence intensity of the entire sensory epithelium was measured in NIS Elements on maximum intensity projections as the sum fluorescence intensity/μm^2. Since Hes5-eGFP is downregulated by DAPT-treatment, the sensory epithelium region of interest (ROI) was created by outlining the Gfi1 labeling and included the non-sensory crux eminentia. The sum fluorescence intensity/μm^2 was then normalized to the average sum fluorescence intensity of six 30 μm^2 randomly placed squares outside of the sensory region (negative for both Gfi1 and Hes5).

7.8 MANUAL CELL COUNTING

Cells were counted manually in ImageJ using the standard cell counter plugin. Hair cells were counted by continuously scanning through confocal stacks taken at a z-interval of 0.5 μm to avoid double counting or missing cells. The hair cell counts in the control cristae are similar to what has been reported previously in adult mice with optical dissector counting

(Desai*, et al.,* 2005) and in E18.5 mice using confocal slices taken at 6 μm intervals (Fritzsch*, et al.,* 2010).

In Chapter 5, the data on cell counts in whole mount cristae from C57BL/6 and CBA/CaJ mice was collected from multiple people (counters). To standardize counts, all counters were trained on files that had previously been counted until the counts were consistent between counters within an acceptable margin of error (approximately ± 50 cells).

7.9 IDENTIFYING LINEAGE-TRACED HAIR CELLS

In the lineage tracing experiments using PLP/CreER;mTmG mice, lineage traced hair cells were defined as $mGFP^+$ cells expressing the early hair cell marker Gfi1, irrespective of morphology or position. More specifically, the Gfi1 labeling had to be centered within the mGFP labeling in all dimensions to control for support cells "cupping" hair cells as they extend through the hair cell layer. In addition, lineage traced hair cells had to be distinguishable from the surrounding GFP^+ cells. To be counted as a lineage traced hair cell, a cell could not exhibit ambiguity on any of these criteria, which generally resulted in the exclusion of areas of high recombination from this analysis. All $mGFP^+$ cells were analyzed in confocal stacks taken at a z-interval of 0.5 μm. Generally, lineage traced hair cells expressing mGFP had decreased mTomato expression, though this was not a criterion for analysis.

7.10 NORMALIZATION OF CRISTAE POSITION

For the analysis of the spatial pattern of development in the cristae, the position of each crista had to be normalized within the 3-dimensional space. In order to do this, the visual data in the confocal images had to be converted to xyz coordinates. For each confocal

stack, the standard cell counter plugin in ImageJ was used to mark the position of the BrdU-labeled hair cells (double positive for BrdU and Myosin7a) in addition to the position of the majority of Myosin7a+ hair cells. This information was then exported into two separate lists of xyz-coordinates, one containing the BrdU+ hair cells and the other containing the Myo7a+ hair cells for each crista. Once these coordinate lists were obtained, they were run through a python script that normalized the position of the cristae in all three dimensions by rotating all of the coordinates in both lists.

In order to determine the degree of rotation along the z-axis, the script found the median y-value of the cells in a 40 pixel range around the x-coordinates at the 25th and 75th percentiles (approximately 0.56 μm/pixel). The slope of the line between the two median values was calculated and the angle, theta, between this line and a line with a slope of 0 was determined. If theta was greater than +/- 0.07 degrees, then the coordinates in both lists were rotated by theta. Almost identical functions were performed for rotations along the y-axis and the x-axis with the following exceptions. For y-axis rotations, the cutoff value for theta was +/- 0.018 degrees. For x-axis rotations, the range of cells used to determine the two median values was expanded. Here, the hair cells were divided into two halves along the y-axis and the median z-value for each half was calculated. In addition, the cutoff value for theta for rotations along the x-axis was +/- 0.034 degrees. All rotations were visually verified by plotting both the raw coordinates and the rotated coordinates in 2-dimensions by flattening the dimension of rotation.

7.11 ANALYSIS OF SPATIAL PATTERNS OF DEVELOPMENT

To analyze the spatial distribution of the BrdU+ hair cells, a python script was again used in order to divide the hair cells into bins based on their position. For an analysis along the x-axis, hair cells were divided into ten evenly distributed bins based on their position along the x-axis. The total number of BrdU+ hair cells in each bin was then counted and exported. For an analysis along the z-axis, which is equivalent to digitally unfolding the cristae and analyzing the y-axis, hair cells were divided into four evenly distributed bins based on their position along the z-axis. The total number of BrdU+ hair cells in each bin was then counted and exported.

7.12 ANALYSIS OF MOUSE BEHAVIOR USING VIDEO TRACKING

In order to quantify behaviors consistent with a vestibular deficit such as circling and hyperactivity, mice were recorded performing a two minute open field test followed by a one minute swim test in 37°C water. If mice could not swim or float, the swim test was ended prematurely by removing the mouse from the water.

The TrackMate plugin in ImageJ was used to manually track the mice in the video files. For the open field test, one minute of video at 20 frames/second was analyzed. For the swim test, 30 seconds of video at 20 frames/second was analyzed. For each frame, a point was made on the mouse's head between its ears. Points between consecutive frames were linked to generate a continuous path for the entire sequence, or individual bouts of circling within the sequence. A bout of circling was defined as a minimum of a 90° turn by the mouse.

For the open field test, the videos were analyzed for the total distance traveled, the percentage of time active, the percentage of time circling, and the total number of rotations. The distance traveled was defined as the sum of the length of the links between points. This was given in pixels, which was converted to centimeters by measuring the length of the cage in the image in pixels and the length of the actual cage with a ruler.

The percentage of time active was determined by summing the number of frames in which the mouse moved less then 0.2 cm in that frame and less than 0.2 cm in the previous or next frame. The total number of frames multiplied by 0.05 seconds/frame was considered to be the dwell time for the mouse. The percentage of time active was then equal to: (sixty seconds – the dwell time)/60 seconds.

The percentage of time circling was determined by summing the number of frames in which the mouse was turning at least 90°. This number was then divided by 1200, or the

TABLE 7.3

Summary of qPCR primers used

GENE	ACCESSION #	AMP. SIZE	PRIMERS	REFERENCE
eGFP	U55762	372	F: gcaagctgaccctgaagttcatc R: tcaccttgatgccgttcttctg	Li et al (2006). J RNAi and Gene Silencing, 2, 195-204
Gapdh	NM_008084	262	F: ggcattgctctcaatgacaa R: cttgctcagtgtccttgctg	Lamba et al (2008). Dev Dyn, 237, 3016-23
Hes1	NM_008235.2	144	F: ccgagcgtgttggggaaatac R: gttgatctgggtcatgcagttgg	Yamamoto et al (2006). J Mol Med, 84, 37-45
Hes5	NM_010419.4	82	F: gcaccagcccaactccaa R: ggcgaaggctttgctgtgt	Basch et al (2011). J Neuro, 31, 8046-58
Notch1	NM_008714.3	305	F: gacaactcctacctctgcttatgcc R: ttactgttgcactcgttgacctcg	Yamamoto et al (2006). J Mol Med, 84, 37-45

total number of frames analyzed, to determine the percentage of time circling.

The total number of rotations was defined as the sum of all rotations greater than 90°. For example, four individual 90° turns count as one complete rotation, just as two 180° turns also count as one complete rotation. Turns were defined in 90° increments.

7.13 QUANTITATIVE REAL-TIME POLYMERASE CHAIN REACTION

For the cristae cultured with DAPT or DMSO, three independent pools of cDNA were used for each condition and age. Each pool was generated using cultured cristae explanted from 6 to 8 mice (36-48 cristae). For the analysis of uncultured cristae at various ages, only two independent pools of cDNA were used for each age. This was due to the high number of animals needed to successfully extract the RNA as each pool was generated using uncultured cristae from 12-14 mice (72-84 cristae). For all experiments, the pools of cristae were homogenized in 250 μL of TRIzol (Life Technologies), extracted using chloroform supplemented with 10 μg glycogen as a carrier, treated with DNase I (Qiagen), and column purified using the RNeasy Micro kit (Qiagen). cDNA was synthesized using the iScript kit (BioRad). Quantitative RT-PCR (RT-qPCR) was performed using a SYBR Green-based mastermix (Applied Biosystems) on an ABI 7900 384- and 96- well block with TaqMan Low Density Array (Applied Biosystems). For all samples, cycle differences were normalized to the housekeeping gene, *Gapdh* (glyceraldehyde 3-phosphate dehydrogenase), and are reported as either cycle differences to GAPDH (ΔCt) or as fold changes, equal to $2^{\Delta\Delta_{Ct}}$. A list of the primers used is provided in Table 7.3.

7.14 GRAPHS, TABLES, AND STATISTICAL ANALYSES

In Chapter 3, the analyses of hair cell number and fluorescent intensity only include data from anterior and posterior cristae. For all other experiments, all cristae were analyzed.

Microsoft Excel was used to create tables and Prism v5.0c (GraphPad) was used to create graphs and perform statistical analyses. The analyses used include one-or two-tailed unpaired Student's *t*-tests, one- and two-way ANOVAs with either Tukey-Kramer or Bonferroni post-tests, and, Pearson's correlations. Unless otherwise noted, the error bars of graphs depicting means are standard error of the mean (SEM) and the error bars of graphs depicting differences between means are standard error of the difference (SE). SE was calculated using the following formula: SE = square.root[$(sd^2/n_a) + (sd^2/n_b)$], where sd is the standard deviation of each sample group and n_a/n_b are the sizes of the two sample groups, a and b.

For one-tailed unpaired Student's t-tests, significance is denoted as follows: ns for $p>0.025$, * for $p\leq0.025$, ** for $p\leq0.0125$, *** for $p\leq0.00125$, *and* **** for $p\leq0.0001$. Otherwise, significance is denoted as: ns for $p>0.05$, * for $p \leq 0.05$, ** for $p \leq 0.01$, *** for $p \leq 0.001$, and **** for $p \leq 0.0001$. Exact p-values are reported for all cases where $p\geq0.0001$. Otherwise, p-values are reported as $p<0.0001$.

Prism was also used to create the visual representations of the spatial data. In order to visually compare cristae, the cristae were aligned using a python script that created a scaled dataset for each crista with an arbitrary height of 500 pixels and a width of 1000 pixels. These scaled datasets were then plotted as xy points in Prism and colored based on z-depth or to distinguish individual samples.

For the graphs replotted from Ruben (1967), the number of hair cells born at different embryonic ages were extrapolated from the printed graphs in his publication by measuring the height of the data points and relating this to the relative height of the scaled axis. In addition, the analysis by Ruben (1967) had a longer gestational period of 21 days. Therefore, to reconcile and compare the data to my own, I reassigned Ruben's data to a gestational period of 19 days by counting backwards from the day of birth.

BIBLIOGRAPHY

Ables, J.L., Decarolis, N.A., Johnson, M.A., Rivera, P.D., Gao, Z., Cooper, D.C., Radtke, F., Hsieh, J. and Eisch, A.J. (2010). Notch1 is required for maintenance of the reservoir of adult hippocampal stem cells. *J Neurosci* **30**, 10484-10492.

Acampora, D., Merlo, G.R., Paleari, L., Zerega, B., Postiglione, M.P., Mantero, S., Bober, E., Barbieri, O., Simeone, A. and Levi, G. (1999). Craniofacial, vestibular and bone defects in mice lacking the Distal-less-related gene Dlx5. *Development* **126**, 3795-3809.

Adler, H.J. and Raphael, Y. (1996). New hair cells arise from supporting cell conversion in the acoustically damaged chick inner ear. *Neurosci Lett* **205**, 17-20.

Adler, H.J., Komeda, M. and Raphael, Y. (1997). Further evidence for supporting cell conversion in the damaged avian basilar papilla. *Int J Dev Neurosci* **15**, 375-385.

Aguirre, A., Rubio, M.E. and Gallo, V. (2010). Notch and EGFR pathway interaction regulates neural stem cell number and self-renewal. *Nature* **467**, 323-327.

Ahmad, M., Bohne, B.A. and Harding, G.W. (2003). An in vivo tracer study of noise-induced damage to the reticular lamina. *Hear Res* **175**, 82-100.

Alcamo, E.A., Chirivella, L., Dautzenberg, M., Dobreva, G., Farinas, I., Grosschedl, R. and McConnell, S.K. (2008). Satb2 regulates callosal projection neuron identity in the developing cerebral cortex. *Neuron* **57**, 364-377.

Alvarado, D.M., Veile, R., Speck, J., Warchol, M. and Lovett, M. (2009). Downstream targets of GATA3 in the vestibular sensory organs of the inner ear. *Dev Dyn* **238**, 3093-3102.

Anderson, D.H., Neitz, J., Saari, J.C., Kaska, D.D., Fenwick, J., Jacobs, G.H. and Fisher, S.K. (1986). Retinoid-binding proteins in cone-dominant retinas. *Invest Ophthalmol Vis Sci* **27**, 1015-1026.

Andersson, E.R., Sandberg, R. and Lendahl, U. (2011). Notch signaling: simplicity in design, versatility in function. *Development* **138**, 3593-3612.

Andreu-Agullo, C., Morante-Redolat, J.M., Delgado, A.C. and Farinas, I. (2009). Vascular niche factor PEDF modulates Notch-dependent stemness in the adult subependymal zone. *Nat Neurosci* **12**, 1514-1523.

Avallone, B., Porritiello, M., Esposito, D., Mutone, R., Balsamo, G. and Marmo, F. (2003). Evidence for hair cell regeneration in the crista ampullaris of the lizard Podarcis sicula. *Hear Res* **178**, 79-88.

Avallone, B., Fascio, U., Balsamo, G. and Marmo, F. (2008). Gentamicin ototoxicity in the saccule of the lizard Podarcis Sicula induces hair cell recovery and regeneration. *Hear Res* **235**, 15-22.

Baek, J.H., Zheng, Y., Darlington, C.L. and Smith, P.F. (2010). Evidence that spatial memory deficits following bilateral vestibular deafferentation in rats are probably permanent. *Neurobiol Learn Mem* **94**, 402-413.

Baird, R.A., Torres, M.A. and Schuff, N.R. (1993). Hair cell regeneration in the bullfrog vestibular otolith organs following aminoglycoside toxicity. *Hear Res* **65**, 164-174.

Baird, R.A., Steyger, P.S. and Schuff, N.R. (1996). Mitotic and nonmitotic hair cell regeneration in the bullfrog vestibular otolith organs. *Ann N Y Acad Sci* **781**, 59-70.

Baird, R.A., Burton, M.D., Lysakowski, A., Fashena, D.S. and Naeger, R.A. (2000). Hair cell recovery in mitotically blocked cultures of the bullfrog saccule. *Proc Natl Acad Sci U S A* **97**, 11722-11729.

Basch, M.L., Ohyama, T., Segil, N. and Groves, A.K. (2011). Canonical Notch signaling is not necessary for prosensory induction in the mouse cochlea: insights from a conditional mutant of RBPjkappa. *J Neurosci* **31**, 8046-8058.

Bechstedt, S. and Brouhard, G.J. (2012). Doublecortin recognizes the 13-protofilament microtubule cooperatively and tracks microtubule ends. *Dev Cell* **23**, 181-192.

Berggren, D., Liu, W., Frenz, D. and Van De Water, T. (2003). Spontaneous hair-cell renewal following gentamicin exposure in postnatal rat utricular explants. *Hear Res* **180**, 114-125.

Bermingham, N.A., Hassan, B.A., Price, S.D., Vollrath, M.A., Ben-Arie, N., Eatock, R.A., Bellen, H.J., Lysakowski, A. and Zoghbi, H.Y. (1999). Math1: an essential gene for the generation of inner ear hair cells. *Science* **284**, 1837-1841.

Bespalova, I.N., Van Camp, G., Bom, S.J., Brown, D.J., Cryns, K., DeWan, A.T., Erson, A.E., Flothmann, K., Kunst, H.P., Kurnool, P., Sivakumaran, T.A., Cremers, C.W., Leal, S.M., Burmeister, M. and Lesperance, M.M. (2001). Mutations in the Wolfram syndrome 1 gene (WFS1) are a common cause of low frequency sensorineural hearing loss. *Hum Mol Genet* **10**, 2501-2508.

Bird, J.E., Daudet, N., Warchol, M.E. and Gale, J.E. (2010). Supporting cells eliminate dying sensory hair cells to maintain epithelial integrity in the avian inner ear. *J Neurosci* **30**, 12545-12556.

Boettger, T., Hubner, C.A., Maier, H., Rust, M.B., Beck, F.X. and Jentsch, T.J. (2002). Deafness and renal tubular acidosis in mice lacking the K-Cl co-transporter Kcc4. *Nature* **416**, 874-878.

Boettger, T., Rust, M.B., Maier, H., Seidenbecher, T., Schweizer, M., Keating, D.J., Faulhaber, J., Ehmke, H., Pfeffer, C., Scheel, O., Lemcke, B., Horst, J., Leuwer, R., Pape, H.C., Volkl, H., Hubner, C.A. and Jentsch, T.J. (2003). Loss of K-Cl co-transporter KCC3 causes deafness, neurodegeneration and reduced seizure threshold. *EMBO J* **22**, 5422-5434.

Bramhall, N.F., Shi, F., Arnold, K., Hochedlinger, K. and Edge, A.S. (2014). Lgr5-positive supporting cells generate new hair cells in the postnatal cochlea. *Stem Cell Reports* **2**, 311-322.

Breunig, J.J., Silbereis, J., Vaccarino, F.M., Sestan, N. and Rakic, P. (2007). Notch regulates cell fate and dendrite morphology of newborn neurons in the postnatal dentate gyrus. *Proc Natl Acad Sci U S A* **104**, 20558-20563.

Britanova, O., Alifragis, P., Junek, S., Jones, K., Gruss, P. and Tarabykin, V. (2006). A novel mode of tangential migration of cortical projection neurons. *Dev Biol* **298**, 299-311.

Brooker, R., Hozumi, K. and Lewis, J. (2006). Notch ligands with contrasting functions: Jagged1 and Delta1 in the mouse inner ear. *Development* **133**, 1277-1286.

Brown, J.P., Couillard-Despres, S., Cooper-Kuhn, C.M., Winkler, J., Aigner, L. and Kuhn, H.G. (2003). Transient expression of doublecortin during adult neurogenesis. *J Comp Neurol* **467**, 1-10.

Buniello, A., Hardisty-Hughes, R.E., Pass, J.C., Bober, E., Smith, R.J. and Steel, K.P. (2013). Headbobber: a combined morphogenetic and cochleosaccular mouse model to study 10qter deletions in human deafness. *PLoS One* **8**, e56274.

Bunt-Milam, A.H. and Saari, J.C. (1983). Immunocytochemical localization of two retinoid-binding proteins in vertebrate retina. *J Cell Biol* **97**, 703-712.

Burns, J.C., Christophel, J.J., Collado, M.S., Magnus, C., Carfrae, M. and Corwin, J.T. (2008). Reinforcement of cell junctions correlates with the absence of hair cell regeneration in mammals and its occurrence in birds. *J Comp Neurol* **511**, 396-414.

Burns, J.C., Cox, B.C., Thiede, B.R., Zuo, J. and Corwin, J.T. (2012a). In vivo proliferative regeneration of balance hair cells in newborn mice. *J Neurosci* **32**, 6570-6577.

Burns, J.C., On, D., Baker, W., Collado, M.S. and Corwin, J.T. (2012b). Over half the hair cells in the mouse utricle first appear after birth, with significant numbers originating from early postnatal mitotic production in peripheral and striolar growth zones. *J Assoc Res Otolaryngol* **13**, 609-627.

Burns, J.C., Yoo, J.J., Atala, A. and Jackson, J.D. (2012c). MYC gene delivery to adult mouse utricles stimulates proliferation of postmitotic supporting cells in vitro. *PLoS One* **7**, e48704.

Burns, J.C., Collado, M.S., Oliver, E.R. and Corwin, J.T. (2013). Specializations of intercellular junctions are associated with the presence and absence of hair cell regeneration in ears from six vertebrate classes. *J Comp Neurol* **521**, 1430-1448.

Burns, J.C. and Corwin, J.T. (2014). Responses to cell loss become restricted as the supporting cells in mammalian vestibular organs grow thick junctional actin bands that develop high stability. *J Neurosci* **34**, 1998-2011.

Carlen, M., Meletis, K., Goritz, C., Darsalia, V., Evergren, E., Tanigaki, K., Amendola, M., Barnabe-Heider, F., Yeung, M.S., Naldini, L., Honjo, T., Kokaia, Z., Shupliakov, O., Cassidy, R.M., Lindvall, O. and Frisen, J. (2009). Forebrain ependymal cells are

Notch-dependent and generate neuroblasts and astrocytes after stroke. *Nat Neurosci* **12**, 259-267.

Chatterjee, S., Kraus, P. and Lufkin, T. (2010). A symphony of inner ear developmental control genes. *BMC Genet* **11**, 68.

Chen, P., Johnson, J.E., Zoghbi, H.Y. and Segil, N. (2002). The role of Math1 in inner ear development: Uncoupling the establishment of the sensory primordium from hair cell fate determination. *Development* **129**, 2495-2505.

Cheng, X., Li, Y., Huang, Y., Feng, X., Feng, G. and Xiong, Z.Q. (2011). Pulse labeling and long-term tracing of newborn neurons in the adult subgranular zone. *Cell Res* **21**, 338-349.

Chow, L.M., Tian, Y., Weber, T., Corbett, M., Zuo, J. and Baker, S.J. (2006). Inducible Cre recombinase activity in mouse cerebellar granule cell precursors and inner ear hair cells. *Dev Dyn* **235**, 2991-2998.

Collado, M.S., Burns, J.C., Meyers, J.R. and Corwin, J.T. (2011a). Variations in shape-sensitive restriction points mirror differences in the regeneration capacities of avian and mammalian ears. *PLoS One* **6**, e23861.

Collado, M.S., Thiede, B.R., Baker, W., Askew, C., Igbani, L.M. and Corwin, J.T. (2011b). The postnatal accumulation of junctional E-cadherin is inversely correlated with the capacity for supporting cells to convert directly into sensory hair cells in mammalian balance organs. *J Neurosci* **31**, 11855-11866.

Corwin, J.T. (1981). Postembryonic production and aging in inner ear hair cells in sharks. *J Comp Neurol* **201**, 541-553.

Corwin, J.T. (1983). Postembryonic growth of the macula neglecta auditory detector in the ray, Raja clavata: continual increases in hair cell number, neural convergence, and physiological sensitivity. *J Comp Neurol* **217**, 345-356.

Corwin, J.T. (1985). Perpetual production of hair cells and maturational changes in hair cell ultrastructure accompany postembryonic growth in an amphibian ear. *Proc Natl Acad Sci U S A* **82**, 3911-3915.

Cotanche, D.A., Saunders, J.C. and Tilney, L.G. (1987). Hair cell damage produced by acoustic trauma in the chick cochlea. *Hear Res* **25**, 267-286.

Cotanche, D.A. and Dopyera, C.E. (1990). Hair cell and supporting cell response to acoustic trauma in the chick cochlea. *Hear Res* **46**, 29-40.

Cotanche, D.A. and Kaiser, C.L. (2010). Hair cell fate decisions in cochlear development and regeneration. *Hear Res* **266**, 18-25.

Couillard-Despres, S., Winner, B., Schaubeck, S., Aigner, R., Vroemen, M., Weidner, N., Bogdahn, U., Winkler, J., Kuhn, H.G. and Aigner, L. (2005). Doublecortin expression levels in adult brain reflect neurogenesis. *Eur J Neurosci* **21**, 1-14.

Cox, B.C., Liu, Z., Lagarde, M.M. and Zuo, J. (2012). Conditional gene expression in the mouse inner ear using Cre-loxP. *J Assoc Res Otolaryngol* **13**, 295-322.

Cox, B.C., Chai, R., Lenoir, A., Liu, Z., Zhang, L., Nguyen, D.H., Chalasani, K., Steigelman, K.A., Fang, J., Rubel, E.W., Cheng, A.G. and Zuo, J. (2014). Spontaneous hair cell regeneration in the neonatal mouse cochlea in vivo. *Development* **141**, 816-829.

Cristobal, R., Wackym, P.A., Cioffi, J.A., Erbe, C.B., Roche, J.P. and Popper, P. (2005). Assessment of differential gene expression in vestibular epithelial cell types using microarray analysis. *Brain Res Mol Brain Res* **133**, 19-36.

Cryns, K., Thys, S., Van Laer, L., Oka, Y., Pfister, M., Van Nassauw, L., Smith, R.J., Timmermans, J.P. and Van Camp, G. (2003). The WFS1 gene, responsible for low frequency sensorineural hearing loss and Wolfram syndrome, is expressed in a variety of inner ear cells. *Histochem Cell Biol* **119**, 247-256.

D'Souza, B., Meloty-Kapella, L. and Weinmaster, G. (2010). Canonical and non-canonical Notch ligands. *Curr Top Dev Biol* **92**, 73-129.

Dabdoub, A., Puligilla, C., Jones, J.M., Fritzsch, B., Cheah, K.S., Pevny, L.H. and Kelley, M.W. (2008). Sox2 signaling in prosensory domain specification and subsequent hair cell differentiation in the developing cochlea. *Proc Natl Acad Sci U S A* **105**, 18396-18401.

Dai, C., Fridman, G.Y., Davidovics, N.S., Chiang, B., Ahn, J.H. and Della Santina, C.C. (2011). Restoration of 3D vestibular sensation in rhesus monkeys using a multichannel vestibular prosthesis. *Hear Res* **281**, 74-83.

Daudet, N., Gibson, R., Shang, J., Bernard, A., Lewis, J. and Stone, J. (2009). Notch regulation of progenitor cell behavior in quiescent and regenerating auditory epithelium of mature birds. *Dev Biol* **326**, 86-100.

Davies, D., Magnus, C. and Corwin, J.T. (2007). Developmental changes in cell-extracellular matrix interactions limit proliferation in the mammalian inner ear. *Eur J Neurosci* **25**, 985-998.

de Moraes, S.A., Soares, W.J., Rodrigues, R.A., Fett, W.C., Ferriolli, E. and Perracini, M.R. (2011). Dizziness in community-dwelling older adults: a population-based study. *Braz J Otorhinolaryngol* **77**, 691-699.

Dechesne, C.J., Winsky, L., Kim, H.N., Goping, G., Vu, T.D., Wenthold, R.J. and Jacobowitz, D.M. (1991). Identification and ultrastructural localization of a calretinin-like calcium-binding protein (protein 10) in the guinea pig and rat inner ear. *Brain Res* **560**, 139-148.

Dechesne, C.J., Winsky, L., Moniot, B. and Raymond, J. (1993). Localization of calretinin mRNA in rat and guinea pig inner ear by in situ hybridization using radioactive and non-radioactive probes. *Hear Res* **69**, 91-97.

Dechesne, C.J., Rabejac, D. and Desmadryl, G. (1994). Development of calretinin immunoreactivity in the mouse inner ear. *J Comp Neurol* **346**, 517-529.

Depew, M.J., Liu, J.K., Long, J.E., Presley, R., Meneses, J.J., Pedersen, R.A. and Rubenstein, J.L. (1999). Dlx5 regulates regional development of the branchial arches and sensory capsules. *Development* **126**, 3831-3846.

Desai, S.S., Ali, H. and Lysakowski, A. (2005a). Comparative morphology of rodent vestibular periphery. II. Cristae ampullares. *J Neurophysiol* **93**, 267-280.

Desai, S.S., Zeh, C. and Lysakowski, A. (2005b). Comparative morphology of rodent vestibular periphery. I. Saccular and utricular maculae. *J Neurophysiol* **93**, 251-266.

Desmadryl, G. and Dechesne, C.J. (1992). Calretinin immunoreactivity in chinchilla and guinea pig vestibular end organs characterizes the calyx unit subpopulation. *Exp Brain Res* **89**, 105-108.

Doerflinger, N.H., Macklin, W.B. and Popko, B. (2003). Inducible site-specific recombination in myelinating cells. *Genesis* **35**, 63-72.

Doetzlhofer, A., Basch, M.L., Ohyama, T., Gessler, M., Groves, A.K. and Segil, N. (2009). Hey2 regulation by FGF provides a Notch-independent mechanism for maintaining pillar cell fate in the organ of Corti. *Dev Cell* **16**, 58-69.

Driver, E.C., Sillers, L., Coate, T.M., Rose, M.F. and Kelley, M.W. (2013). The Atoh1-lineage gives rise to hair cells and supporting cells within the mammalian cochlea. *Dev Biol* **376**, 86-98.

Du, X., Li, W., Gao, X., West, M.B., Saltzman, W.M., Cheng, C.J., Stewart, C., Zheng, J., Cheng, W. and Kopke, R.D. (2013). Regeneration of mammalian cochlear and vestibular hair cells through Hes1/Hes5 modulation with siRNA. *Hear Res* **304**, 91-110.

Eatock, R.A., Rusch, A., Lysakowski, A. and Saeki, M. (1998). Hair cells in mammalian utricles. *Otolaryngol Head Neck Surg* **119**, 172-181.

Ehm, O., Goritz, C., Covic, M., Schaffner, I., Schwarz, T.J., Karaca, E., Kempkes, B., Kremmer, E., Pfrieger, F.W., Espinosa, L., Bigas, A., Giachino, C., Taylor, V., Frisen, J. and Lie, D.C. (2010). RBPJkappa-dependent signaling is essential for long-term maintenance of neural stem cells in the adult hippocampus. *J Neurosci* **30**, 13794-13807.

Engel, J., Braig, C., Ruttiger, L., Kuhn, S., Zimmermann, U., Blin, N., Sausbier, M., Kalbacher, H., Munkner, S., Rohbock, K., Ruth, P., Winter, H. and Knipper, M. (2006). Two classes of outer hair cells along the tonotopic axis of the cochlea. *Neuroscience* **143**, 837-849.

Espinosa, L., Ingles-Esteve, J., Aguilera, C. and Bigas, A. (2003). Phosphorylation by glycogen synthase kinase-3 beta down-regulates Notch activity, a link for Notch and Wnt pathways. *J Biol Chem* **278**, 32227-32235.

Faucher, K., Aas-Hansen, O., Damsgard, B., Laukli, E. and Stenklev, N.C. (2009). Damage and functional recovery of the Atlantic cod (Gadus morhua) inner ear hair cells following local injection of gentamicin. *Int J Audiol* **48**, 456-464.

Fekete, D.M., Muthukumar, S. and Karagogeos, D. (1998). Hair cells and supporting cells share a common progenitor in the avian inner ear. *J Neurosci* **18**, 7811-7821.

Fettiplace, R. and Hackney, C.M. (2006). The sensory and motor roles of auditory hair cells. *Nat Rev Neurosci* **7**, 19-29.

Forge, A. (1985). Outer hair cell loss and supporting cell expansion following chronic gentamicin treatment. *Hear Res* **19**, 171-182.

Forge, A., Li, L., Corwin, J.T. and Nevill, G. (1993). Ultrastructural evidence for hair cell regeneration in the mammalian inner ear. *Science* **259**, 1616-1619.

Forge, A., Li, L. and Nevill, G. (1998). Hair cell recovery in the vestibular sensory epithelia of mature guinea pigs. *J Comp Neurol* **397**, 69-88.

Fourniol, F.J., Sindelar, C.V., Amigues, B., Clare, D.K., Thomas, G., Perderiset, M., Francis, F., Houdusse, A. and Moores, C.A. (2010). Template-free 13-protofilament microtubule-MAP assembly visualized at 8 A resolution. *J Cell Biol* **191**, 463-470.

Francis, F., Koulakoff, A., Boucher, D., Chafey, P., Schaar, B., Vinet, M.C., Friocourt, G., McDonnell, N., Reiner, O., Kahn, A., McConnell, S.K., Berwald-Netter, Y., Denoulet, P. and Chelly, J. (1999). Doublecortin is a developmentally regulated, microtubule-associated protein expressed in migrating and differentiating neurons. *Neuron* **23**, 247-256.

Fritzsch, B., Dillard, M., Lavado, A., Harvey, N.L. and Jahan, I. (2010). Canal cristae growth and fiber extension to the outer hair cells of the mouse ear require Prox1 activity. *PLoS One* **5**, e9377.

Furness, D.N. and Lehre, K.P. (1997). Immunocytochemical localization of a high-affinity glutamate-aspartate transporter, GLAST, in the rat and guinea-pig cochlea. *Eur J Neurosci* **9**, 1961-1969.

Furness, D.N., Hulme, J.A., Lawton, D.M. and Hackney, C.M. (2002). Distribution of the glutamate/aspartate transporter GLAST in relation to the afferent synapses of outer hair cells in the guinea pig cochlea. *J Assoc Res Otolaryngol* **3**, 234-247.

Furness, D.N. and Lawton, D.M. (2003). Comparative distribution of glutamate transporters and receptors in relation to afferent innervation density in the mammalian cochlea. *J Neurosci* **23**, 11296-11304.

Gale, J.E., Meyers, J.R., Periasamy, A. and Corwin, J.T. (2002). Survival of bundleless hair cells and subsequent bundle replacement in the bullfrog's saccule. *J Neurobiol* **50**, 81-92.

Gale, J.E., Piazza, V., Ciubotaru, C.D. and Mammano, F. (2004). A mechanism for sensing noise damage in the inner ear. *Curr Biol* **14**, 526-529.

Gerfen, C.R., Paletzki, R. and Heintz, N. (2013). GENSAT BAC cre-recombinase driver lines to study the functional organization of cerebral cortical and basal ganglia circuits. *Neuron* **80**, 1368-1383.

Givogri, M.I., de Planell, M., Galbiati, F., Superchi, D., Gritti, A., Vescovi, A., de Vellis, J. and Bongarzone, E.R. (2006). Notch signaling in astrocytes and neuroblasts of the adult subventricular zone in health and after cortical injury. *Dev Neurosci* **28**, 81-91.

Gleeson, J.G., Lin, P.T., Flanagan, L.A. and Walsh, C.A. (1999). Doublecortin is a microtubule-associated protein and is expressed widely by migrating neurons. *Neuron* **23**, 257-271.

Glowatzki, E., Cheng, N., Hiel, H., Yi, E., Tanaka, K., Ellis-Davies, G.C., Rothstein, J.D. and Bergles, D.E. (2006). The glutamate-aspartate transporter GLAST mediates glutamate uptake at inner hair cell afferent synapses in the mammalian cochlea. *J Neurosci* **26**, 7659-7664.

Goddard, M., Zheng, Y., Darlington, C.L. and Smith, P.F. (2008). Locomotor and exploratory behavior in the rat following bilateral vestibular deafferentation. *Behav Neurosci* **122**, 448-459.

Goldman, D. (2014). Muller glial cell reprogramming and retina regeneration. *Nat Rev Neurosci* **15**, 431-442.

Golub, J.S., Tong, L., Ngyuen, T.B., Hume, C.R., Palmiter, R.D., Rubel, E.W. and Stone, J.S. (2012). Hair cell replacement in adult mouse utricles after targeted ablation of hair cells with diphtheria toxin. *J Neurosci* **32**, 15093-15105.

Gomez-Casati, M.E., Murtie, J., Taylor, B. and Corfas, G. (2010a). Cell-specific inducible gene recombination in postnatal inner ear supporting cells and glia. *J Assoc Res Otolaryngol* **11**, 19-26.

Gomez-Casati, M.E., Murtie, J.C., Rio, C., Stankovic, K., Liberman, M.C. and Corfas, G. (2010b). Nonneuronal cells regulate synapse formation in the vestibular sensory epithelium via erbB-dependent BDNF expression. *Proc Natl Acad Sci U S A* **107**, 17005-17010.

Gong, S., Doughty, M., Harbaugh, C.R., Cummins, A., Hatten, M.E., Heintz, N. and Gerfen, C.R. (2007). Targeting Cre recombinase to specific neuron populations with bacterial artificial chromosome constructs. *J Neurosci* **27**, 9817-9823.

Gopinath, B., McMahon, C.M., Rochtchina, E. and Mitchell, P. (2009). Dizziness and vertigo in an older population: the Blue Mountains prospective cross-sectional study. *Clin Otolaryngol* **34**, 552-556.

Gotz, M. and Huttner, W.B. (2005). The cell biology of neurogenesis. *Nat Rev Mol Cell Biol* **6**, 777-788.

Gray, P.A., Fu, H., Luo, P., Zhao, Q., Yu, J., Ferrari, A., Tenzen, T., Yuk, D.I., Tsung, E.F., Cai, Z., Alberta, J.A., Cheng, L.P., Liu, Y., Stenman, J.M., Valerius, M.T., Billings, N., Kim, H.A., Greenberg, M.E., McMahon, A.P., Rowitch, D.H., Stiles, C.D. and Ma, Q. (2004). Mouse brain organization revealed through direct genome-scale TF expression analysis. *Science* **306**, 2255-2257.

Groves, A.K. and Fekete, D.M. (2012). Shaping sound in space: the regulation of inner ear patterning. *Development* **139**, 245-257.

Gubbels, S.P., Woessner, D.W., Mitchell, J.C., Ricci, A.J. and Brigande, J.V. (2008). Functional auditory hair cells produced in the mammalian cochlea by in utero gene transfer. *Nature* **455**, 537-541.

Gyorgy, A.B., Szemes, M., de Juan Romero, C., Tarabykin, V. and Agoston, D.V. (2008). SATB2 interacts with chromatin-remodeling molecules in differentiating cortical neurons. *Eur J Neurosci* **27**, 865-873.

Haapasalo, A. and Kovacs, D.M. (2011). The many substrates of presenilin/gamma-secretase. *J Alzheimers Dis* **25**, 3-28.

Hao, J., Koesters, R., Bouchard, M., Gridley, T., Pfannenstiel, S., Plinkert, P.K., Zhang, L. and Praetorius, M. (2012). Jagged1-mediated Notch signaling regulates mammalian inner ear development independent of lateral inhibition. *Acta Otolaryngol* **132**, 1028-1035.

Hartman, B.H., Hayashi, T., Nelson, B.R., Bermingham-McDonogh, O. and Reh, T.A. (2007). Dll3 is expressed in developing hair cells in the mammalian cochlea. *Dev Dyn* **236**, 2875-2883.

Hartman, B.H., Basak, O., Nelson, B.R., Taylor, V., Bermingham-McDonogh, O. and Reh, T.A. (2009). Hes5 expression in the postnatal and adult mouse inner ear and the drug-damaged cochlea. *J Assoc Res Otolaryngol* **10**, 321-340.

Hartman, B.H., Reh, T.A. and Bermingham-McDonogh, O. (2010). Notch signaling specifies prosensory domains via lateral induction in the developing mammalian inner ear. *Proc Natl Acad Sci U S A* **107**, 15792-15797.

Hasson, T., Heintzelman, M.B., Santos-Sacchi, J., Corey, D.P. and Mooseker, M.S. (1995). Expression in cochlea and retina of myosin VIIa, the gene product defective in Usher syndrome type 1B. *Proc Natl Acad Sci U S A* **92**, 9815-9819.

Hayashi, H. and Kume, T. (2008). Foxc transcription factors directly regulate Dll4 and Hey2 expression by interacting with the VEGF-Notch signaling pathways in endothelial cells. *PLoS One* **3**, e2401.

Hayashi, S. and McMahon, A.P. (2002). Efficient recombination in diverse tissues by a tamoxifen-inducible form of Cre: a tool for temporally regulated gene activation/inactivation in the mouse. *Dev Biol* **244**, 305-318.

Hayashi, T., Kokubo, H., Hartman, B.H., Ray, C.A., Reh, T.A. and Bermingham-McDonogh, O. (2008a). Hesr1 and Hesr2 may act as early effectors of Notch signaling in the developing cochlea. *Dev Biol* **316**, 87-99.

Hayashi, T., Ray, C.A. and Bermingham-McDonogh, O. (2008b). Fgf20 is required for sensory epithelial specification in the developing cochlea. *J Neurosci* **28**, 5991-5999.

Helms, A.W. and Johnson, J.E. (1998). Progenitors of dorsal commissural interneurons are defined by MATH1 expression. *Development* **125**, 919-928.

Helms, A.W., Abney, A.L., Ben-Arie, N., Zoghbi, H.Y. and Johnson, J.E. (2000). Autoregulation and multiple enhancers control Math1 expression in the developing nervous system. *Development* **127**, 1185-1196.

Henry, K.R. and Chole, R.A. (1980). Genotypic differences in behavioral, physiological and anatomical expressions of age-related hearing loss in the laboratory mouse. *Audiology* **19**, 369-383.

Hequembourg, S. and Liberman, M.C. (2001). Spiral ligament pathology: a major aspect of age-related cochlear degeneration in C57BL/6 mice. *J Assoc Res Otolaryngol* **2**, 118-129.

Hertzano, R., Montcouquiol, M., Rashi-Elkeles, S., Elkon, R., Yucel, R., Frankel, W.N., Rechavi, G., Moroy, T., Friedman, T.B., Kelley, M.W. and Avraham, K.B. (2004). Transcription profiling of inner ears from Pou4f3(ddl/ddl) identifies Gfi1 as a target of the Pou4f3 deafness gene. *Hum Mol Genet* **13**, 2143-2153.

Hicks, C., Johnston, S.H., diSibio, G., Collazo, A., Vogt, T.F. and Weinmaster, G. (2000). Fringe differentially modulates Jagged1 and Delta1 signalling through Notch1 and Notch2. *Nat Cell Biol* **2**, 515-520.

Hirose, K., Westrum, L.E., Stone, J.S., Zirpel, L. and Rubel, E.W. (1999). Dynamic studies of ototoxicity in mature avian auditory epithelium. *Ann N Y Acad Sci* **884**, 389-409.

Hirose, K., Westrum, L.E., Cunningham, D.E. and Rubel, E.W. (2004). Electron microscopy of degenerative changes in the chick basilar papilla after gentamicin exposure. *J Comp Neurol* **470**, 164-180.

Holm, P.C., Mader, M.T., Haubst, N., Wizenmann, A., Sigvardsson, M. and Gotz, M. (2007). Loss- and gain-of-function analyses reveal targets of Pax6 in the developing mouse telencephalon. *Mol Cell Neurosci* **34**, 99-119.

Hordichok, A.J. and Steyger, P.S. (2007). Closure of supporting cell scar formations requires dynamic actin mechanisms. *Hear Res* **232**, 1-19.

Horesh, D., Sapir, T., Francis, F., Wolf, S.G., Caspi, M., Elbaum, M., Chelly, J. and Reiner, O. (1999). Doublecortin, a stabilizer of microtubules. *Hum Mol Genet* **8**, 1599-1610.

Hori, R., Nakagawa, T., Sakamoto, T., Matsuoka, Y., Takebayashi, S. and Ito, J. (2007). Pharmacological inhibition of Notch signaling in the mature guinea pig cochlea. *Neuroreport* **18**, 1911-1914.

Huang, Y., Song, N.N., Lan, W., Hu, L., Su, C.J., Ding, Y.Q. and Zhang, L. (2013). Expression of transcription factor Satb2 in adult mouse brain. *Anat Rec (Hoboken)* **296**, 452-461.

Hudspeth, A.J. (2008). Making an effort to listen: mechanical amplification in the ear. *Neuron* **59**, 530-545.

Hume, C.R., Bratt, D.L. and Oesterle, E.C. (2007). Expression of LHX3 and SOX2 during mouse inner ear development. *Gene Expr Patterns* **7**, 798-807.

Hwang, C.H., Simeone, A., Lai, E. and Wu, D.K. (2009). Foxg1 is required for proper separation and formation of sensory cristae during inner ear development. *Dev Dyn* **238**, 2725-2734.

Imayoshi, I., Sakamoto, M., Yamaguchi, M., Mori, K. and Kageyama, R. (2010). Essential roles of Notch signaling in maintenance of neural stem cells in developing and adult brains. *J Neurosci* **30**, 3489-3498.

Inagaki, N., Yoshida, H., Mizuta, M., Mizuno, N., Fujii, Y., Gonoi, T., Miyazaki, J. and Seino, S. (1994). Cloning and functional characterization of a third pituitary adenylate cyclase-activating polypeptide receptor subtype expressed in insulin-secreting cells. *Proc Natl Acad Sci U S A* **91**, 2679-2683.

Ison, J.R. and Allen, P.D. (2003). Low-frequency tone pips elicit exaggerated startle reflexes Jagger, D.J. and Forge, A. (2006). Compartmentalized and signal-selective gap junctional coupling in the hearing cochlea. *J Neurosci* **26**, 1260-1268.

Jagger, D.J. and Forge, A. (2006). Compartmentalized and signal-selective gap junctional coupling in the hearing cochlea. *J Neurosci* **26**, 1260-1268.

Jeon, S.J., Fujioka, M., Kim, S.C. and Edge, A.S. (2011). Notch signaling alters sensory or neuronal cell fate specification of inner ear stem cells. *J Neurosci* **31**, 8351-8358.

Jiang, H., Wang, L., Beier, K.T., Cepko, C.L., Fekete, D.M. and Brigande, J.V. (2013). Lineage analysis of the late otocyst stage mouse inner ear by transuterine microinjection of a retroviral vector encoding alkaline phosphatase and an oligonucleotide library. *PLoS One* **8**, e69314.

Jin, Z.H., Kikuchi, T., Tanaka, K. and Kobayashi, T. (2003). Expression of glutamate transporter GLAST in the developing mouse cochlea. *Tohoku J Exp Med* **200**, 137-144.

Johnson, K.R., Erway, L.C., Cook, S.A., Willott, J.F. and Zheng, Q.Y. (1997). A major gene affecting age-related hearing loss in C57BL/6J mice. *Hear Res* **114**, 83-92.

Jorgensen, J.M. and Mathiesen, C. (1988). The avian inner ear. Continuous production of hair cells in vestibular sensory organs, but not in the auditory papilla. *Naturwissenschaften* **75**, 319-320.

Jung, J.Y., Avenarius, M.R., Adamsky, S., Alpert, E., Feinstein, E. and Raphael, Y. (2013). siRNA Targeting Hes5 Augments Hair Cell Regeneration in Aminoglycoside-damaged Mouse Utricle. *Mol Ther* **21**, 834-841.

Kang, W. and Hebert, J.M. (2012). A Sox2 BAC transgenic approach for targeting adult neural stem cells. *PLoS One* **7**, e49038.

Karis, A., Pata, I., van Doorninck, J.H., Grosveld, F., de Zeeuw, C.I., de Caprona, D. and Fritzsch, B. (2001). Transcription factor GATA-3 alters pathway selection of olivocochlear neurons and affects morphogenesis of the ear. *J Comp Neurol* **429**, 615-630.

Kato, T.M., Kawaguchi, A., Kosodo, Y., Niwa, H. and Matsuzaki, F. (2010). Lunatic fringe potentiates Notch signaling in the developing brain. *Mol Cell Neurosci* **45**, 12-25.

Kawamoto, K., Ishimoto, S., Minoda, R., Brough, D.E. and Raphael, Y. (2003). Math1 gene transfer generates new cochlear hair cells in mature guinea pigs in vivo. *J Neurosci* **23**, 4395-4400.

Kawamoto, K., Izumikawa, M., Beyer, L.A., Atkin, G.M. and Raphael, Y. (2009). Spontaneous hair cell regeneration in the mouse utricle following gentamicin ototoxicity. *Hear Res* **247**, 17-26.

Kazmierczak, P., Sakaguchi, H., Tokita, J., Wilson-Kubalek, E.M., Milligan, R.A., Muller, U. and Kachar, B. (2007). Cadherin 23 and protocadherin 15 interact to form tip-link filaments in sensory hair cells. *Nature* **449**, 87-91.

Kazmierczak, P. and Muller, U. (2012). Sensing sound: molecules that orchestrate mechanotransduction by hair cells. *Trends Neurosci* **35**, 220-229.

Kelly, M.C., Chang, Q., Pan, A., Lin, X. and Chen, P. (2012). Atoh1 directs the formation of sensory mosaics and induces cell proliferation in the postnatal mammalian cochlea in vivo. *J Neurosci* **32**, 6699-6710.

Kiernan, A.E., Ahituv, N., Fuchs, H., Balling, R., Avraham, K.B., Steel, K.P. and Hrabe de Angelis, M. (2001). The Notch ligand Jagged1 is required for inner ear sensory development. *Proc Natl Acad Sci U S A* **98**, 3873-3878.

Kiernan, A.E., Cordes, R., Kopan, R., Gossler, A. and Gridley, T. (2005). The Notch ligands DLL1 and JAG2 act synergistically to regulate hair cell development in the mammalian inner ear. *Development* **132**, 4353-4362.

Kiernan, A.E. (2006). The paintfill method as a tool for analyzing the three-dimensional structure of the inner ear. *Brain Res* **1091**, 270-276.

Kiernan, A.E., Xu, J. and Gridley, T. (2006). The Notch ligand JAG1 is required for sensory progenitor development in the mammalian inner ear. *PLoS Genet* **2**, e4.

Kiernan, A.E. (2013). Notch signaling during cell fate determination in the inner ear. *Semin Cell Dev Biol* **24**, 470-479.

Kil, J., Warchol, M.E. and Corwin, J.T. (1997). Cell death, cell proliferation, and estimates of hair cell life spans in the vestibular organs of chicks. *Hear Res* **114**, 117-126.

Kirkegaard, M. and Jorgensen, J.M. (2000). Continuous hair cell turnover in the inner ear vestibular organs of a mammal, the Daubenton's bat (Myotis daubentonii). *Naturwissenschaften* **87**, 83-86.

Kopan, R. and Ilagan, M.X. (2009). The canonical Notch signaling pathway: unfolding the activation mechanism. *Cell* **137**, 216-233.

Korrapati, S., Roux, I., Glowatzki, E. and Doetzlhofer, A. (2013). Notch signaling limits supporting cell plasticity in the hair cell-damaged early postnatal murine cochlea. *PLoS One* **8**, e73276.

Kroenke, K., Hoffman, R.M. and Einstadter, D. (2000). How common are various causes of dizziness? A critical review. *South Med J* **93**, 160-167; quiz 168.

Lahne, M. and Gale, J.E. (2008). Damage-induced activation of ERK1/2 in cochlear supporting cells is a hair cell death-promoting signal that depends on extracellular ATP and calcium. *J Neurosci* **28**, 4918-4928.

Lahne, M. and Gale, J.E. (2010). Damage-induced cell-cell communication in different cochlear cell types via two distinct ATP-dependent Ca waves. *Purinergic Signal* **6**, 189-200.

Lanford, P.J., Lan, Y., Jiang, R., Lindsell, C., Weinmaster, G., Gridley, T. and Kelley, M.W. (1999). Notch signalling pathway mediates hair cell development in mammalian cochlea. *Nat Genet* **21**, 289-292.

Lanford, P.J., Shailam, R., Norton, C.R., Gridley, T. and Kelley, M.W. (2000). Expression of Math1 and HES5 in the cochleae of wildtype and Jag2 mutant mice. *J Assoc Res Otolaryngol* **1**, 161-171.

Lee, Y.S., Liu, F. and Segil, N. (2006). A morphogenetic wave of p27Kip1 transcription directs cell cycle exit during organ of Corti development. *Development* **133**, 2817-2826.

Leone, D.P., Srinivasan, K., Chen, B., Alcamo, E. and McConnell, S.K. (2008). The determination of projection neuron identity in the developing cerebral cortex. *Curr Opin Neurobiol* **18**, 28-35.

Leone, D.P., Heavner, W.E., Ferenczi, E.A., Dobreva, G., Huguenard, J.R., Grosschedl, R. and McConnell, S.K. (2014). Satb2 Regulates the Differentiation of Both Callosal and Subcerebral Projection Neurons in the Developing Cerebral Cortex. *Cereb Cortex*

Lewis, E.R. and Li, C.W. (1973). Evidence concerning the morphogenesis of saccular receptors in the bullfrog (Rana catesbeiana). *J Morphol* **139**, 351-361.

Lewis, R.F., Haburcakova, C., Gong, W., Lee, D. and Merfeld, D. (2013). Electrical stimulation of semicircular canal afferents affects the perception of head orientation. *J Neurosci* **33**, 9530-9535.

Lewis, R.M., Hume, C.R. and Stone, J.S. (2012). Atoh1 expression and function during auditory hair cell regeneration in post-hatch chickens. *Hear Res* **289**, 74-85.

Leyva-Diaz, E. and Lopez-Bendito, G. (2013). In and out from the cortex: development of major forebrain connections. *Neuroscience* **254**, 26-44.

Li, H.S. and Borg, E. (1991). Age-related loss of auditory sensitivity in two mouse genotypes. *Acta Otolaryngol* **111**, 827-834.

Li, H.S., Niedzielski, A.S., Beisel, K.W., Hiel, H., Wenthold, R.J. and Morley, B.J. (1994). Identification of a glutamate/aspartate transporter in the rat cochlea. *Hear Res* **78**, 235-242.

Li, L., Nevill, G. and Forge, A. (1995). Two modes of hair cell loss from the vestibular sensory epithelia of the guinea pig inner ear. *J Comp Neurol* **355**, 405-417.

Li, L. and Forge, A. (1997). Morphological evidence for supporting cell to hair cell conversion in the mammalian utricular macula. *Int J Dev Neurosci* **15**, 433-446.

Li, M., Tian, Y., Fritzsch, B., Gao, J., Wu, X. and Zuo, J. (2004). Inner hair cell Cre-expressing transgenic mouse. *Genesis* **39**, 173-177.

Li, W., Wu, J., Yang, J., Sun, S., Chai, R., Chen, Z.Y. and Li, H. (2015). Notch inhibition induces mitotically generated hair cells in mammalian cochleae via activating the Wnt pathway. *Proc Natl Acad Sci U S A* **112**, 166-171.

Lickiss, T., Cheung, A.F., Hutchinson, C.E., Taylor, J.S. and Molnar, Z. (2012). Examining the relationship between early axon growth and transcription factor expression in the developing cerebral cortex. *J Anat* **220**, 201-211.

Lillevali, K., Haugas, M., Matilainen, T., Pussinen, C., Karis, A. and Salminen, M. (2006). Gata3 is required for early morphogenesis and Fgf10 expression during otic development. *Mech Dev* **123**, 415-429.

Lim, D.J. and Anniko, M. (1985). Developmental morphology of the mouse inner ear. A scanning electron microscopic observation. *Acta Otolaryngol Suppl* **422**, 1-69.

Lin, H.W. and Bhattacharyya, N. (2012). Balance disorders in the elderly: epidemiology and functional impact. *Laryngoscope* **122**, 1858-1861.

Lin, V., Golub, J.S., Nguyen, T.B., Hume, C.R., Oesterle, E.C. and Stone, J.S. (2011). Inhibition of Notch activity promotes nonmitotic regeneration of hair cells in the adult mouse utricles. *J Neurosci* **31**, 15329-15339.

Liu, Z., Dearman, J.A., Cox, B.C., Walters, B.J., Zhang, L., Ayrault, O., Zindy, F., Gan, L., Roussel, M.F. and Zuo, J. (2012a). Age-dependent in vivo conversion of mouse cochlear pillar and Deiters' cells to immature hair cells by Atoh1 ectopic expression. *J Neurosci* **32**, 6600-6610.

Liu, Z., Owen, T., Fang, J., Srinivasan, R.S. and Zuo, J. (2012b). In vivo Notch reactivation in differentiating cochlear hair cells induces Sox2 and Prox1 expression but does not disrupt hair cell maturation. *Dev Dyn* **241**, 684-696.

Liu, Z., Owen, T., Fang, J. and Zuo, J. (2012c). Overactivation of Notch1 signaling induces ectopic hair cells in the mouse inner ear in an age-dependent manner. *PLoS One* **7**, e34123.

Liu, Z., Fang, J., Dearman, J., Zhang, L. and Zuo, J. (2014). In vivo generation of immature inner hair cells in neonatal mouse cochleae by ectopic Atoh1 expression. *PLoS One* **9**, e89377.

Lopez, I., Honrubia, V., Lee, S.C., Schoeman, G. and Beykirch, K. (1997). Quantification of the process of hair cell loss and recovery in the chinchilla crista ampullaris after gentamicin treatment. *Int J Dev Neurosci* **15**, 447-461.

Lopez, I., Honrubia, V., Lee, S.C., Li, G. and Beykirch, K. (1998). Hair cell recovery in the chinchilla crista ampullaris after gentamicin treatment: a quantitative approach. *Otolaryngol Head Neck Surg* **119**, 255-262.

Lopez, I., Ayala, C. and Honrubia, V. (2003). Synaptophysin immunohistochemistry during vestibular hair cell recovery after gentamicin treatment. *Audiol Neurootol* **8**, 80-90.

Lopez, I., Ishiyama, G., Tang, Y., Tokita, J., Baloh, R.W. and Ishiyama, A. (2005). Regional estimates of hair cells and supporting cells in the human crista ampullaris. *J Neurosci Res* **82**, 421-431.

Loponen, H., Ylikoski, J., Albrecht, J.H. and Pirvola, U. (2011). Restrictions in cell cycle progression of adult vestibular supporting cells in response to ectopic cyclin D1 expression. *PLoS One* **6**, e27360.

Lowenheim, H., Furness, D.N., Kil, J., Zinn, C., Gultig, K., Fero, M.L., Frost, D., Gummer, A.W., Roberts, J.M., Rubel, E.W., Hackney, C.M. and Zenner, H.P. (1999). Gene disruption of p27(Kip1) allows cell proliferation in the postnatal and adult organ of corti. *Proc Natl Acad Sci U S A* **96**, 4084-4088.

Lugert, S., Basak, O., Knuckles, P., Haussler, U., Fabel, K., Gotz, M., Haas, C.A., Kempermann, G., Taylor, V. and Giachino, C. (2010). Quiescent and active hippocampal neural stem cells with distinct morphologies respond selectively to physiological and pathological stimuli and aging. *Cell Stem Cell* **6**, 445-456.

Lumpkin, E.A., Collisson, T., Parab, P., Omer-Abdalla, A., Haeberle, H., Chen, P., Doetzlhofer, A., White, P., Groves, A., Segil, N. and Johnson, J.E. (2003). Math1-driven GFP expression in the developing nervous system of transgenic mice. *Gene Expr Patterns* **3**, 389-395.

Lutz, E.M., Sheward, W.J., West, K.M., Morrow, J.A., Fink, G. and Harmar, A.J. (1993). The VIP2 receptor: molecular characterisation of a cDNA encoding a novel receptor for vasoactive intestinal peptide. *FEBS Lett* **334**, 3-8.

Ma, E.Y., Rubel, E.W. and Raible, D.W. (2008). Notch signaling regulates the extent of hair cell regeneration in the zebrafish lateral line. *J Neurosci* **28**, 2261-2273.

MacDonald, G.H. and Rubel, E.W. (2008). Three-dimensional imaging of the intact mouse cochlea by fluorescent laser scanning confocal microscopy. *Hear Res* **243**, 1-10.

Machold, R. and Fishell, G. (2005). Math1 is expressed in temporally discrete pools of cerebellar rhombic-lip neural progenitors. *Neuron* **48**, 17-24.

Madisen, L., Zwingman, T.A., Sunkin, S.M., Oh, S.W., Zariwala, H.A., Gu, H., Ng, L.L., Palmiter, R.D., Hawrylycz, M.J., Jones, A.R., Lein, E.S. and Zeng, H. (2010). A robust and high-throughput Cre reporting and characterization system for the whole mouse brain. *Nat Neurosci* **13**, 133-140.

Maklad, A., Kamel, S., Wong, E. and Fritzsch, B. (2010). Development and organization of polarity-specific segregation of primary vestibular afferent fibers in mice. *Cell Tissue Res* **340**, 303-321.

Marovitz, W.F. and Shugar, J.M. (1976). Single mitotic center for rodent cochlear duct. *Ann Otol Rhinol Laryngol* **85**, 225-233.

Marovitz, W.F., Shugar, J.M. and Khan, K.M. (1976). Spiral migration theory of organ of Corti development. *Ann Otol Rhinol Laryngol* **85**, 1-19.

Marsh, R.R., Xu, L.R., Moy, J.P. and Saunders, J.C. (1990). Recovery of the basilar papilla following intense sound exposure in the chick. *Hear Res* **46**, 229-237.

Matei, V., Pauley, S., Kaing, S., Rowitch, D., Beisel, K.W., Morris, K., Feng, F., Jones, K., Lee, J. and Fritzsch, B. (2005). Smaller inner ear sensory epithelia in Neurog 1 null mice are related to earlier hair cell cycle exit. *Dev Dyn* **234**, 633-650.

Matsui, J.I., Oesterle, E.C., Stone, J.S. and Rubel, E.W. (2000). Characterization of damage and regeneration in cultured avian utricles. *J Assoc Res Otolaryngol* **1**, 46-63.

Meiteles, L.Z. and Raphael, Y. (1994). Scar formation in the vestibular sensory epithelium after aminoglycoside toxicity. *Hear Res* **79**, 26-38.

Mendel, B., Bergenius, J. and Langius-Eklof, A. (2010). Dizziness: A common, troublesome symptom but often treatable. *J Vestib Res* **20**, 391-398.

Merchant, S.N., Velazquez-Villasenor, L., Tsuji, K., Glynn, R.J., Wall, C., 3rd and Rauch, S.D. (2000). Temporal bone studies of the human peripheral vestibular system. Normative vestibular hair cell data. *Ann Otol Rhinol Laryngol Suppl* **181**, 3-13.

Meyers, J.R. and Corwin, J.T. (2007). Shape change controls supporting cell proliferation in lesioned mammalian balance epithelium. *J Neurosci* **27**, 4313-4325.

Meza, G., Bohne, B., Daunton, N., Fox, R. and Knox, J. (1996). Damage and recovery of otolithic function following streptomycin treatment in the rat. *Ann N Y Acad Sci* **781**, 666-669.

Mikaelian, D.O., Warfield, D. and Norris, O. (1974). Genetic progressive hearing loss in the C57-b16 mouse. Relation of behavioral responses to chochlear anatomy. *Acta Otolaryngol* **77**, 327-334.

Millimaki, B.B., Sweet, E.M., Dhason, M.S. and Riley, B.B. (2007). Zebrafish atoh1 genes: classic proneural activity in the inner ear and regulation by Fgf and Notch. *Development* **134**, 295-305.

Mizutari, K., Fujioka, M., Hosoya, M., Bramhall, N., Okano, H.J., Okano, H. and Edge, A.S. (2013). Notch inhibition induces cochlear hair cell regeneration and recovery of hearing after acoustic trauma. *Neuron* **77**, 58-69.

Montcouquiol, M., Valat, J., Travo, C. and Sans, A. (1998). A role for BDNF in early postnatal rat vestibular epithelia maturation: implication of supporting cells. *Eur J Neurosci* **10**, 598-606.

Monzack, E.L. and Cunningham, L.L. (2013). Lead roles for supporting actors: critical functions of inner ear supporting cells. *Hear Res* **303**, 20-29.

Moores, C.A., Perderiset, M., Francis, F., Chelly, J., Houdusse, A. and Milligan, R.A. (2004). Mechanism of microtubule stabilization by doublecortin. *Mol Cell* **14**, 833-839.

Moraes, F., Novoa, A., Jerome-Majewska, L.A., Papaioannou, V.E. and Mallo, M. (2005). Tbx1 is required for proper neural crest migration and to stabilize spatial patterns during middle and inner ear development. *Mech Dev* **122**, 199-212.

Moretti, J. and Brou, C. (2013). Ubiquitinations in the notch signaling pathway. *Int J Mol Sci* **14**, 6359-6381.

Mori, T., Tanaka, K., Buffo, A., Wurst, W., Kuhn, R. and Gotz, M. (2006). Inducible gene deletion in astroglia and radial glia--a valuable tool for functional and lineage analysis. *Glia* **54**, 21-34.

Morsli, H., Choo, D., Ryan, A., Johnson, R. and Wu, D.K. (1998). Development of the mouse inner ear and origin of its sensory organs. *J Neurosci* **18**, 3327-3335.

Morton, N.E. (1991). Genetic epidemiology of hearing impairment. *Ann N Y Acad Sci* **630**, 16-31.

Mulvaney, J. and Dabdoub, A. (2012). Atoh1, an essential transcription factor in neurogenesis and intestinal and inner ear development: function, regulation, and context dependency. *J Assoc Res Otolaryngol* **13**, 281-293.

Munnamalai, V., Hayashi, T. and Bermingham-McDonogh, O. (2012). Notch prosensory effects in the Mammalian cochlea are partially mediated by Fgf20. *J Neurosci* **32**, 12876-12884.

Murata, J., Tokunaga, A., Okano, H. and Kubo, T. (2006). Mapping of notch activation during cochlear development in mice: implications for determination of prosensory domain and cell fate diversification. *J Comp Neurol* **497**, 502-518.

Murata, J., Ikeda, K. and Okano, H. (2012). Notch signaling and the developing inner ear. *Adv Exp Med Biol* **727**, 161-173.

Muzumdar, M.D., Tasic, B., Miyamichi, K., Li, L. and Luo, L. (2007). A global double-fluorescent Cre reporter mouse. *Genesis* **45**, 593-605.

Nacher, J., Crespo, C. and McEwen, B.S. (2001). Doublecortin expression in the adult rat telencephalon. *Eur J Neurosci* **14**, 629-644.

Neuhauser, H.K., Radtke, A., von Brevern, M., Lezius, F., Feldmann, M. and Lempert, T. (2008). Burden of dizziness and vertigo in the community. *Arch Intern Med* **168**, 2118-2124.

Neves, A., English, K. and Priess, J.R. (2007). Notch-GATA synergy promotes endoderm-specific expression of ref-1 in C. elegans. *Development* **134**, 4459-4468.

Nguyen, L., Besson, A., Roberts, J.M. and Guillemot, F. (2006). Coupling cell cycle exit, neuronal differentiation and migration in cortical neurogenesis. *Cell Cycle* **5**, 2314-2318.

Noben-Trauth, K., Zheng, Q.Y. and Johnson, K.R. (2003). Association of cadherin 23 with polygenic inheritance and genetic modification of sensorineural hearing loss. *Nat Genet* **35**, 21-23.

Oesterle, E.C., Cunningham, D.E., Westrum, L.E. and Rubel, E.W. (2003). Ultrastructural analysis of [3H]thymidine-labeled cells in the rat utricular macula. *J Comp Neurol* **463**, 177-195.

Oesterle, E.C., Campbell, S., Taylor, R.R., Forge, A. and Hume, C.R. (2008). Sox2 and JAGGED1 expression in normal and drug-damaged adult mouse inner ear. *J Assoc Res Otolaryngol* **9**, 65-89.

Oesterle, E.C., Chien, W.M., Campbell, S., Nellimarla, P. and Fero, M.L. (2011). p27(Kip1) is required to maintain proliferative quiescence in the adult cochlea and pituitary. *Cell Cycle* **10**, 1237-1248.

Ogata, Y., Slepecky, N.B. and Takahashi, M. (1999). Study of the gerbil utricular macula following treatment with gentamicin, by use of bromodeoxyuridine and calmodulin immunohistochemical labelling. *Hear Res* **133**, 53-60.

Ozaki, H., Nakamura, K., Funahashi, J., Ikeda, K., Yamada, G., Tokano, H., Okamura, H.O., Kitamura, K., Muto, S., Kotaki, H., Sudo, K., Horai, R., Iwakura, Y. and Kawakami, K. (2004). Six1 controls patterning of the mouse otic vesicle. *Development* **131**, 551-562.

Pan, W., Jin, Y., Stanger, B. and Kiernan, A.E. (2010). Notch signaling is required for the generation of hair cells and supporting cells in the mammalian inner ear. *Proc Natl Acad Sci U S A* **107**, 15798-15803.

Pan, W., Jin, Y., Chen, J., Rottier, R.J., Steel, K.P. and Kiernan, A.E. (2013). Ectopic expression of activated notch or SOX2 reveals similar and unique roles in the development of the sensory cell progenitors in the mammalian inner ear. *J Neurosci* **33**, 16146-16157.

Phillips, C., Ling, L., Oxford, T., Nowack, A., Nie, K., Rubinstein, J.T. and Phillips, J.O. (2014). Longitudinal performance of an implantable vestibular prosthesis. *Hear Res*

Polgar, R., Collison, T., Slepecky, N.B. and Wanamaker, H.H. (2001). Anatomic and morphometric changes to gerbil posterior cristas following transtympanic administration of gentamicin and streptomycin. *J Assoc Res Otolaryngol* **2**, 147-158.

Popper, A.N. and Hoxter, B. (1984). Growth of a fish ear: 1. Quantitative analysis of hair cell and ganglion cell proliferation. *Hear Res* **15**, 133-142.

Popper, A.N. and Hoxter, B. (1990). Growth of a fish ear. II. Locations of newly proliferated sensory hair cells in the saccular epithelium of Astronotus ocellatus. *Hear Res* **45**, 33-40.

Porter, J.D., Pellis, S.M. and Meyer, M.E. (1990). An open-field activity analysis of labyrinthectomized rats. *Physiol Behav* **48**, 27-30.

Rao, M.S. and Shetty, A.K. (2004). Efficacy of doublecortin as a marker to analyse the absolute number and dendritic growth of newly generated neurons in the adult dentate gyrus. *Eur J Neurosci* **19**, 234-246.

Raphael, Y. and Altschuler, R.A. (1991). Reorganization of cytoskeletal and junctional proteins during cochlear hair cell degeneration. *Cell Motil Cytoskeleton* **18**, 215-227.

Raphael, Y., Adler, H.J., Wang, Y. and Finger, P.A. (1994). Cell cycle of transdifferentiating supporting cells in the basilar papilla. *Hear Res* **80**, 53-63.

Rauch, S.D., Velazquez-Villasenor, L., Dimitri, P.S. and Merchant, S.N. (2001). Decreasing hair cell counts in aging humans. *Ann N Y Acad Sci* **942**, 220-227.

Reiner, O. (2013). LIS1 and DCX: Implications for Brain Development and Human Disease in Relation to Microtubules. *Scientifica (Cairo)* **2013**, 393975.

Richter, E. (1980). Quantitative study of human Scarpa's ganglion and vestibular sensory epithelia. *Acta Otolaryngol* **90**, 199-208.

Rivers, L.E., Young, K.M., Rizzi, M., Jamen, F., Psachoulia, K., Wade, A., Kessaris, N. and Richardson, W.D. (2008). PDGFRA/NG2 glia generate myelinating oligodendrocytes and piriform projection neurons in adult mice. *Nat Neurosci* **11**, 1392-1401.

Roberson, D.F., Weisleder, P., Bohrer, P.S. and Rubel, E.W. (1992). Ongoing production of sensory cells in the vestibular epithelium of the chick. *Hear Res* **57**, 166-174.

Rogers, J.H. (1989). Two calcium-binding proteins mark many chick sensory neurons. *Neuroscience* **31**, 697-709.

Roux, I., Safieddine, S., Nouvian, R., Grati, M., Simmler, M.C., Bahloul, A., Perfettini, I., Le Gall, M., Rostaing, P., Hamard, G., Triller, A., Avan, P., Moser, T. and Petit, C. (2006). Otoferlin, defective in a human deafness form, is essential for exocytosis at the auditory ribbon synapse. *Cell* **127**, 277-289.

Rubel, E.W., Dew, L.A. and Roberson, D.W. (1995). Mammalian vestibular hair cell regeneration. *Science* **267**, 701-707.

Ruben, R.J. (1967). Development of the inner ear of the mouse: a radioautographic study of terminal mitoses. *Acta Otolaryngol* Suppl 220:221-244.

Saari, J.C. and Crabb, J.W. (2005). Focus on molecules: cellular retinaldehyde-binding protein (CRALBP). *Exp Eye Res* **81**, 245-246.

Sage, C., Huang, M., Vollrath, M.A., Brown, M.C., Hinds, P.W., Corey, D.P., Vetter, D.E. and Chen, Z.Y. (2006). Essential role of retinoblastoma protein in mammalian hair cell development and hearing. *Proc Natl Acad Sci U S A* **103**, 7345-7350.

Sans, A. and Chat, M. (1982). Analysis of temporal and spatial patterns of rat vestibular hair cell differentiation by tritiated thymidine radioautography. *J Comp Neurol* **206**, 1-8.

Savary, E., Sabourin, J.C., Santo, J., Hugnot, J.P., Chabbert, C., Van De Water, T., Uziel, A. and Zine, A. (2008). Cochlear stem/progenitor cells from a postnatal cochlea respond to Jagged1 and demonstrate that notch signaling promotes sphere formation and sensory potential. *Mech Dev* **125**, 674-686.

Schug, N., Braig, C., Zimmermann, U., Engel, J., Winter, H., Ruth, P., Blin, N., Pfister, M., Kalbacher, H. and Knipper, M. (2006). Differential expression of otoferlin in brain, vestibular system, immature and mature cochlea of the rat. *Eur J Neurosci* **24**, 3372-3380.

Sher, A.E. (1971). The embryonic and postnatal development of the inner ear of the mouse. *Acta Otolaryngol Suppl* **285**, 1-77.

Shi, F., Hu, L. and Edge, A.S. (2013). Generation of hair cells in neonatal mice by beta-catenin overexpression in Lgr5-positive cochlear progenitors. *Proc Natl Acad Sci U S A* **110**, 13851-13856.

Shnerson, A. and Pujol, R. (1981). Age-related changes in the C57BL/6J mouse cochlea. I. Physiological findings. *Brain Res* **254**, 65-75.

Shou, J., Zheng, J.L. and Gao, W.Q. (2003). Robust generation of new hair cells in the mature mammalian inner ear by adenoviral expression of Hath1. *Mol Cell Neurosci* **23**, 169-179.

Simeone, A., Acampora, D., Pannese, M., D'Esposito, M., Stornaiuolo, A., Gulisano, M., Mallamaci, A., Kastury, K., Druck, T., Huebner, K. and et al. (1994). Cloning and characterization of two members of the vertebrate Dlx gene family. *Proc Natl Acad Sci U S A* **91**, 2250-2254.

Slowik, A.D. and Bermingham-McDonogh, O. (2013a). Hair cell generation by notch inhibition in the adult Mammalian cristae. *J Assoc Res Otolaryngol* **14**, 813-828.

Slowik, A.D. and Bermingham-McDonogh, O. (2013b). Notch signaling in mammalian hair cell regeneration. *Trends Dev Biol* **7**, 73-89.

Soler-Martin, C., Diez-Padrisa, N., Boadas-Vaello, P. and Llorens, J. (2007). Behavioral disturbances and hair cell loss in the inner ear following nitrile exposure in mice, guinea pigs, and frogs. *Toxicol Sci* **96**, 123-132.

Somma, G., Alger, H.M., McGuire, R.M., Kretlow, J.D., Ruiz, F.R., Yatsenko, S.A., Stankiewicz, P., Harrison, W., Funk, E., Bergamaschi, A., Oghalai, J.S., Mikos, A.G., Overbeek, P.A. and Pereira, F.A. (2012). Head bobber: an insertional mutation causes inner ear defects, hyperactive circling, and deafness. *J Assoc Res Otolaryngol* **13**, 335-349.

Soucek, S., Michaels, L. and Frohlich, A. (1987). Pathological changes in the organ of Corti in presbyacusis as revealed by microslicing and staining. *Acta Otolaryngol Suppl* **436**, 93-102.

Spiess, A.C., Lang, H., Schulte, B.A., Spicer, S.S. and Schmiedt, R.A. (2002). Effects of gap junction uncoupling in the gerbil cochlea. *Laryngoscope* **112**, 1635-1641.

Spongr, V.P., Flood, D.G., Frisina, R.D. and Salvi, R.J. (1997). Quantitative measures of hair cell loss in CBA and C57BL/6 mice throughout their life spans. *J Acoust Soc Am* **101**, 3546-3553.

Srinivasan, K., Leone, D.P., Bateson, R.K., Dobreva, G., Kohwi, Y., Kohwi-Shigematsu, T., Grosschedl, R. and McConnell, S.K. (2012). A network of genetic repression and derepression specifies projection fates in the developing neocortex. *Proc Natl Acad Sci U S A* **109**, 19071-19078.

Srinivasan, R.S., Geng, X., Yang, Y., Wang, Y., Mukatira, S., Studer, M., Porto, M.P., Lagutin, O. and Oliver, G. (2010). The nuclear hormone receptor Coup-TFII is required for the initiation and early maintenance of Prox1 expression in lymphatic endothelial cells. *Genes Dev* **24**, 696-707.

Stankovic, K., Rio, C., Xia, A., Sugawara, M., Adams, J.C., Liberman, M.C. and Corfas, G. (2004). Survival of adult spiral ganglion neurons requires erbB receptor signaling in the inner ear. *J Neurosci* **24**, 8651-8661.

Steyger, P.S., Burton, M., Hawkins, J.R., Schuff, N.R. and Baird, R.A. (1997). Calbindin and parvalbumin are early markers of non-mitotically regenerating hair cells in the bullfrog vestibular otolith organs. *Int J Dev Neurosci* **15**, 417-432.

Stone, J.S. and Cotanche, D.A. (1992). Synchronization of hair cell regeneration in the chick cochlea following noise damage. *J Cell Sci* **102 (Pt 4)**, 671-680.

Stone, J.S., Choi, Y.S., Woolley, S.M., Yamashita, H. and Rubel, E.W. (1999). Progenitor cell cycling during hair cell regeneration in the vestibular and auditory epithelia of the chick. *J Neurocytol* **28**, 863-876.

Stone, J.S. and Rubel, E.W. (1999). Delta1 expression during avian hair cell regeneration. *Development* **126**, 961-973.

Stump, G., Durrer, A., Klein, A.L., Lutolf, S., Suter, U. and Taylor, V. (2002). Notch1 and its ligands Delta-like and Jagged are expressed and active in distinct cell populations in the postnatal mouse brain. *Mech Dev* **114**, 153-159.

Sugawara, M., Corfas, G. and Liberman, M.C. (2005). Influence of supporting cells on neuronal degeneration after hair cell loss. *J Assoc Res Otolaryngol* **6**, 136-147.

Szemes, M., Gyorgy, A., Paweletz, C., Dobi, A. and Agoston, D.V. (2006). Isolation and characterization of SATB2, a novel AT-rich DNA binding protein expressed in development- and cell-specific manner in the rat brain. *Neurochem Res* **31**, 237-246.

Takebayashi, S., Yamamoto, N., Yabe, D., Fukuda, H., Kojima, K., Ito, J. and Honjo, T. (2007). Multiple roles of Notch signaling in cochlear development. *Dev Biol* **307**, 165-178.

Takumi, Y., Matsubara, A., Danbolt, N.C., Laake, J.H., Storm-Mathisen, J., Usami, S., Shinkawa, H. and Ottersen, O.P. (1997). Discrete cellular and subcellular localization of glutamine synthetase and the glutamate transporter GLAST in the rat vestibular end organ. *Neuroscience* **79**, 1137-1144.

Tanaka, T., Serneo, F.F., Tseng, H.C., Kulkarni, A.B., Tsai, L.H. and Gleeson, J.G. (2004). Cdk5 phosphorylation of doublecortin ser297 regulates its effect on neuronal migration. *Neuron* **41**, 215-227.

Taniguchi, H., He, M., Wu, P., Kim, S., Paik, R., Sugino, K., Kvitsiani, D., Fu, Y., Lu, J., Lin, Y., Miyoshi, G., Shima, Y., Fishell, G., Nelson, S.B. and Huang, Z.J. (2011). A resource of Cre driver lines for genetic targeting of GABAergic neurons in cerebral cortex. *Neuron* **71**, 995-1013.

Tanyeri, H., Lopez, I. and Honrubia, V. (1995). Histological evidence for hair cell regeneration after ototoxic cell destruction with local application of gentamicin in the chinchilla crista ampullaris. *Hear Res* **89**, 194-202.

Taura, A., Kojima, K., Ito, J. and Ohmori, H. (2006). Recovery of hair cell function after damage induced by gentamicin in organ culture of rat vestibular maculae. *Brain Res* **1098**, 33-48.

Taylor, R.R. and Forge, A. (2005). Hair cell regeneration in sensory epithelia from the inner ear of a urodele amphibian. *J Comp Neurol* **484**, 105-120.

Tian, Y., Li, M., Fritzsch, B. and Zuo, J. (2004). Creation of a transgenic mouse for hair-cell gene targeting by using a modified bacterial artificial chromosome containing Prestin. *Dev Dyn* **231**, 199-203.

Tritsch, N.X., Yi, E., Gale, J.E., Glowatzki, E. and Bergles, D.E. (2007). The origin of spontaneous activity in the developing auditory system. *Nature* **450**, 50-55.

Tritsch, N.X. and Bergles, D.E. (2010). Developmental regulation of spontaneous activity in the Mammalian cochlea. *J Neurosci* **30**, 1539-1550.

Tsukada, M., Prokscha, A., Oldekamp, J. and Eichele, G. (2003). Identification of neurabin II as a novel doublecortin interacting protein. *Mech Dev* **120**, 1033-1043.

Tsukada, M., Prokscha, A., Ungewickell, E. and Eichele, G. (2005). Doublecortin association with actin filaments is regulated by neurabin II. *J Biol Chem* **280**, 11361-11368.

Tsukada, M., Prokscha, A. and Eichele, G. (2006). Neurabin II mediates doublecortin-dephosphorylation on actin filaments. *Biochem Biophys Res Commun* **343**, 839-847.

Uno, A., Nagai, M., Sakata, Y., Moriwaki, K. and Kato, T. (2001). [Statistical observation of vertigo and dizziness patients]. *Nihon Jibiinkoka Gakkai Kaiho* **104**, 1119-1125.

Vazquez-Chona, F.R., Clark, A.M. and Levine, E.M. (2009). Rlbp1 promoter drives robust Muller glial GFP expression in transgenic mice. *Invest Ophthalmol Vis Sci* **50**, 3996-4003.

Visel, A., Thaller, C. and Eichele, G. (2004). GenePaint.org: an atlas of gene expression patterns in the mouse embryo. *Nucleic Acids Res* **32**, D552-556.

Wallis, D., Hamblen, M., Zhou, Y., Venken, K.J., Schumacher, A., Grimes, H.L., Zoghbi, H.Y., Orkin, S.H. and Bellen, H.J. (2003). The zinc finger transcription factor Gfi1, implicated in lymphomagenesis, is required for inner ear hair cell differentiation and survival. *Development* **130**, 221-232.

Walsh, R.M., Hackney, C.M. and Furness, D.N. (2000). Regeneration of the mammalian vestibular sensory epithelium following gentamicin-induced damage. *J Otolaryngol* **29**, 351-360.

Walters, B.J., Liu, Z., Crabtree, M., Coak, E., Cox, B.C. and Zuo, J. (2014). Auditory hair cell-specific deletion of p27Kip1 in postnatal mice promotes cell-autonomous generation of new hair cells and normal hearing. *J Neurosci* **34**, 15751-15763.

Wang, G.P., Chatterjee, I., Batts, S.A., Wong, H.T., Gong, T.W., Gong, S.S. and Raphael, Y. (2010). Notch signaling and Atoh1 expression during hair cell regeneration in the mouse utricle. *Hear Res* **267**, 61-70.

Wang, W., Chan, E.K., Baron, S., Van de Water, T. and Lufkin, T. (2001). Hmx2 homeobox gene control of murine vestibular morphogenesis. *Development* **128**, 5017-5029.

Wang, Y., Rattner, A., Zhou, Y., Williams, J., Smallwood, P.M. and Nathans, J. (2012). Norrin/Frizzled4 signaling in retinal vascular development and blood brain barrier plasticity. *Cell* **151**, 1332-1344.

Warchol, M.E., Lambert, P.R., Goldstein, B.J., Forge, A. and Corwin, J.T. (1993). Regenerative proliferation in inner ear sensory epithelia from adult guinea pigs and humans. *Science* **259**, 1619-1622.

Warchol, M.E. (2011). Sensory regeneration in the vertebrate inner ear: differences at the levels of cells and species. *Hear Res* **273**, 72-79.

Weisleder, P. and Rubel, E.W. (1993). Hair cell regeneration after streptomycin toxicity in the avian vestibular epithelium. *J Comp Neurol* **331**, 97-110.

Wharton, K.A., Johansen, K.M., Xu, T. and Artavanis-Tsakonas, S. (1985). Nucleotide sequence from the neurogenic locus notch implies a gene product that shares homology with proteins containing EGF-like repeats. *Cell* **43**, 567-581.

White, J.A., Burgess, B.J., Hall, R.D. and Nadol, J.B. (2000). Pattern of degeneration of the spiral ganglion cell and its processes in the C57BL/6J mouse. *Hear Res* **141**, 12-18.

White, P.M., Doetzlhofer, A., Lee, Y.S., Groves, A.K. and Segil, N. (2006). Mammalian cochlear supporting cells can divide and trans-differentiate into hair cells. *Nature* **441**, 984-987.

Willott, J.F. (1986). Effects of aging, hearing loss, and anatomical location on thresholds of inferior colliculus neurons in C57BL/6 and CBA mice. *J Neurophysiol* **56**, 391-408.

Woods, C., Montcouquiol, M. and Kelley, M.W. (2004). Math1 regulates development of the sensory epithelium in the mammalian cochlea. *Nat Neurosci* **7**, 1310-1318.

Wright, A., Davis, A., Bredberg, G., Ulehlova, L. and Spencer, H. (1987). Hair cell distributions in the normal human cochlea. *Acta Otolaryngol Suppl* **444**, 1-48.

Wright, T.J. and Mansour, S.L. (2003). Fgf3 and Fgf10 are required for mouse otic placode induction. *Development* **130**, 3379-3390.

Wu, D.K. and Kelley, M.W. (2012). Molecular mechanisms of inner ear development. *Cold Spring Harb Perspect Biol* **4**, a008409.

Yamamoto, N., Tanigaki, K., Tsuji, M., Yabe, D., Ito, J. and Honjo, T. (2006). Inhibition of Notch/RBP-J signaling induces hair cell formation in neonate mouse cochleas. *J Mol Med (Berl)* **84**, 37-45.

Yamamoto, N., Chang, W. and Kelley, M.W. (2011). Rbpj regulates development of prosensory cells in the mammalian inner ear. *Dev Biol* **353**, 367-379.

Yamane, H., Nakagawa, T., Iguchi, H., Shibata, S., Takayama, M., Nishimura, K. and Nakai, Y. (1995). In vivo regeneration of vestibular hair cells of guinea pig. *Acta Otolaryngol Suppl* **520 Pt 1**, 174-177.

Yamashita, H. and Oesterle, E.C. (1995). Induction of cell proliferation in mammalian inner-ear sensory epithelia by transforming growth factor alpha and epidermal growth factor. *Proc Natl Acad Sci U S A* **92**, 3152-3155.

Yang, H., Gan, J., Xie, X., Deng, M., Feng, L., Chen, X., Gao, Z. and Gan, L. (2010a). Gfi1-Cre knock-in mouse line: A tool for inner ear hair cell-specific gene deletion. *Genesis* **48**, 400-406.

Yang, H., Xie, X., Deng, M., Chen, X. and Gan, L. (2010b). Generation and characterization of Atoh1-Cre knock-in mouse line. *Genesis* **48**, 407-413.

Yang, L., Zhang, H., Hu, G., Wang, H., Abate-Shen, C. and Shen, M.M. (1998). An early phase of embryonic Dlx5 expression defines the rostral boundary of the neural plate. *J Neurosci* **18**, 8322-8330.

Yin, M., Ishikawa, K., Wong, W.H. and Shibata, Y. (2009). A clinical epidemiological study in 2169 patients with vertigo. *Auris Nasus Larynx* **36**, 30-35.

Yokoyama, S., Ito, Y., Ueno-Kudoh, H., Shimizu, H., Uchibe, K., Albini, S., Mitsuoka, K., Miyaki, S., Kiso, M., Nagai, A., Hikata, T., Osada, T., Fukuda, N., Yamashita, S., Harada, D., Mezzano, V., Kasai, M., Puri, P.L., Hayashizaki, Y., Okado, H., Hashimoto, M. and Asahara, H. (2009). A systems approach reveals that the myogenesis genome network is regulated by the transcriptional repressor RP58. *Dev Cell* **17**, 836-848.

Young, K.M., Mitsumori, T., Pringle, N., Grist, M., Kessaris, N. and Richardson, W.D. (2010). An Fgfr3-iCreER(T2) transgenic mouse line for studies of neural stem cells and astrocytes. *Glia* **58**, 943-953.

Young, T.L., Ives, E., Lynch, E., Person, R., Snook, S., MacLaren, L., Cater, T., Griffin, A., Fernandez, B., Lee, M.K. and King, M.C. (2001). Non-syndromic progressive hearing loss DFNA38 is caused by heterozygous missense mutation in the Wolfram syndrome gene WFS1. *Hum Mol Genet* **10**, 2509-2514.

Zhang, L., Song, N.N., Chen, J.Y., Huang, Y., Li, H. and Ding, Y.Q. (2012). Satb2 is required for dendritic arborization and soma spacing in mouse cerebral cortex. *Cereb Cortex* **22**, 1510-1519.

Zhang, N., Martin, G.V., Kelley, M.W. and Gridley, T. (2000). A mutation in the Lunatic fringe gene suppresses the effects of a Jagged2 mutation on inner hair cell development in the cochlea. *Curr Biol* **10**, 659-662.

Zhao, L.D., Guo, W.W., Lin, C., Li, L.X., Sun, J.H., Wu, N., Ren, L.L., Li, X.X., Liu, H.Z., Young, W.Y., Gao, W.Q. and Yang, S.M. (2011). Effects of DAPT and Atoh1 overexpression on hair cell production and hair bundle orientation in cultured Organ of Corti from neonatal rats. *PLoS One* **6**, e23729.

Zheng, J.L. and Gao, W.Q. (1997). Analysis of rat vestibular hair cell development and regeneration using calretinin as an early marker. *J Neurosci* **17**, 8270-8282.

Zheng, J.L., Keller, G. and Gao, W.Q. (1999). Immunocytochemical and morphological evidence for intracellular self-repair as an important contributor to mammalian hair cell recovery. *J Neurosci* **19**, 2161-2170.

Zheng, J.L. and Gao, W.Q. (2000). Overexpression of Math1 induces robust production of extra hair cells in postnatal rat inner ears. *Nat Neurosci* **3**, 580-586.

Zheng, J.L., Shou, J., Guillemot, F., Kageyama, R. and Gao, W.Q. (2000). Hes1 is a negative regulator of inner ear hair cell differentiation. *Development* **127**, 4551-4560.

Zine, A., Aubert, A., Qiu, J., Therianos, S., Guillemot, F., Kageyama, R. and de Ribaupierre, F. (2001). Hes1 and Hes5 activities are required for the normal development of the hair cells in the mammalian inner ear. *J Neurosci* **21**, 4712-4720.

Zuccotti, A., Kuhn, S., Johnson, S.L., Franz, C., Singer, W., Hecker, D., Geisler, H.S., Kopschall, I., Rohbock, K., Gutsche, K., Dlugaiczyk, J., Schick, B., Marcotti, W., Ruttiger, L., Schimmang, T. and Knipper, M. (2012). Lack of brain-derived neurotrophic factor hampers inner hair cell synapse physiology, but protects against noise-induced hearing loss. *J Neurosci* **32**, 8545-8553.

A P P E N D I X O N E

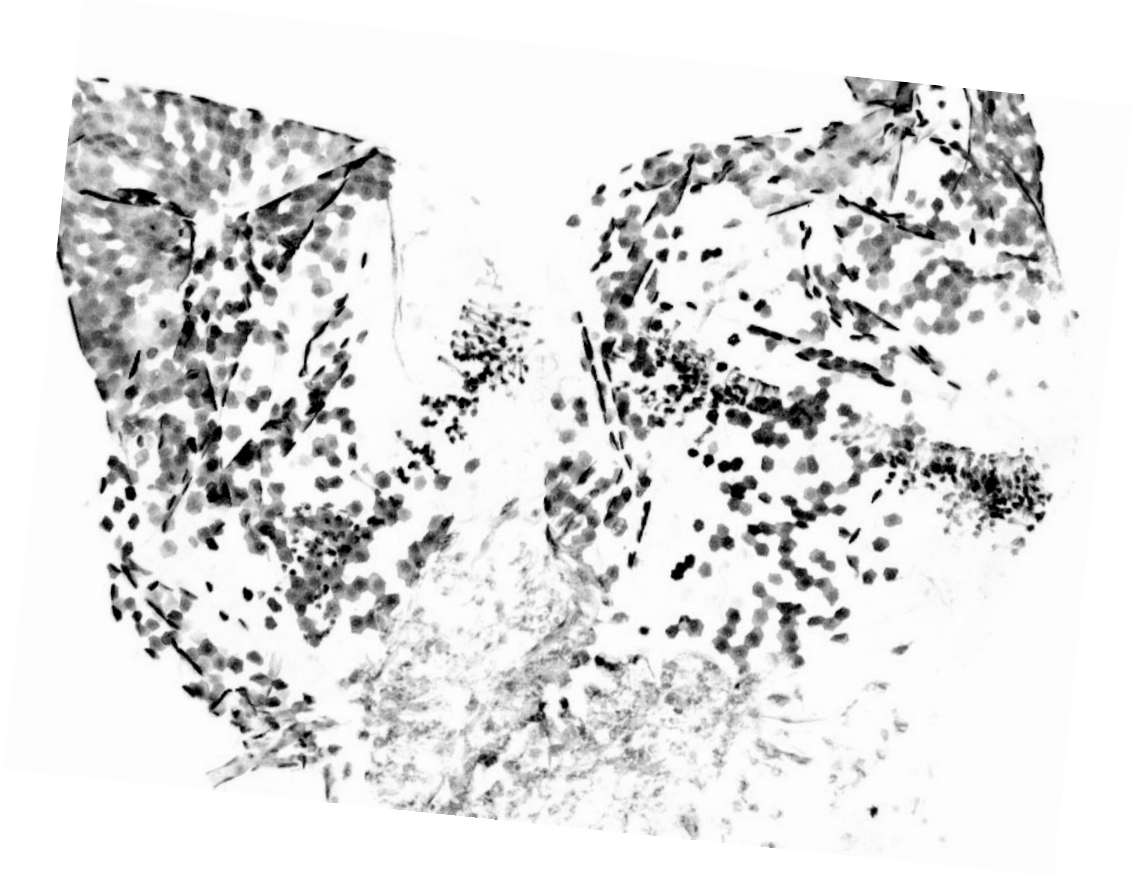

SCREEN FOR CRE RECOMBINASES EXPRESSED IN THE INNER EAR

A1.1 SCREEN FOR CRE RECOMBINASES EXPRESSED IN THE INNER EAR

Mouse lines with known expression of Cre recombinase in the nervous system were screened for expression of Cre recombinase in the mature inner ear. Samples were provided by Dr. Julie Harris at the Allen Institute for Brain Science and more information on the screen can be found in Chapter 3.2.1. A summary of the results of the screen is shown in

TABLE A1.1

Summary of the cellular expression of various Cre recombinase Mouse Lines

		CRISTAE						COCHLEA				
		Central		Peripheral		Crux	Other	HCs		SCs	SGNs	Other
		HCs	SCs	HCs	SCs	-	-	IHCs	OHCs	-	-	-
Non-Inducible Cre Recombinases	Vipr2-Cre (Transgenic)	X	XXX	X	XXX	XXX	XX	--	X	XX	XX	XX
	Satb2-Cre (Transgenic)	--	XX	X	XX	XX	XXX	XX	--	XX	XXX	--
	Gpr26-Cre (Transgenic)	--	--	--	X	--	X	X	--	X	X	--
	Calb2-IRES-Cre (Knockin)	XXX	--	XXX	--	--	X	XXX	X	--	X	X
	Otof-Cre (Knockin)	XXX	--	XXX	--	--	--	XXX	X	--	--	--
	Grm2-Cre (Transgenic)	--	--	X	--	--	X	--	--	--	--	--
Inducible Cre Recombinases	Dlx5-CreERT2 (Knockin)	--	--	--	X	XXX	XXX	--	--	--	XX	X
	Dcx-CreER (Transgenic)	--	XX	--	XX	--	X	--	--	--	XXX	--
	Wfs1-Tg2-CreERT2 (Transgenic)	X	XXX	X	XXX	--	X	--	--	X	--	X
	Glast-CreER (Transgenic)	--	--	--	X	--	X					
	Glast-CreER (Knockin)	--	--	--	X	--	X					
	Plp-CreER (Transgenic)	--	--	--	XXX	--	XXX					
	Cralbp-CreER (Transgenic)	--	XX	--	--	--	XX					

HCs: Hair cells
SCs: Support cells
SGNs: Spiral ganglion neurons
IHCs: Inner hair cells
OHCs: Outer hair cells
--: Not expressed by these cells
X: Expressed by a few cells
XX: Expressed by many cells
XXX: Expressed by most cells

Table 3.1, which indicates if the Cre recombinase was a transgene or knocked-in to the native locus, if the Cre recombinase was inducible or non-inducible, and in what cell types the Cre recombinase was expressed. Two Cre-expressing lines, Vipr2-Cre and Satb2-Cre, showed almost ubiquitous expression in both the cochlea and the cristae (Figure A1.1). Three lines, Dlx5-CreERT2, Gpr26-Cre, and Grm2-Cre showed specific and interesting patterns of expression in the cristae that are, however, not immediately useful (Figure A1.2). More importantly, two lines, Calb2-IRES-Cre and Otof-Cre, showed specific expression in hair cells (Figure A1.3), and five lines showed expression mainly in support cells, including Wfs1-Tg2-CreERT2, Glast-CreER (transgenic and knock-in), Cralbp-CreER, and Dcx-CreER (Figure A1.4).

A1.1.1 CRE RECOMBINASES EXPRESSED UBIQUITOUSLY

Vipr2-Cre transgenic mice (GENSAT)(Gong*, et al.,* 2007, Gerfen*, et al.,* 2013) express a non-inducible Cre recombinase under the vasoactive intestinal peptide receptor 2 (Vipr2) promoter. In the adult cochlea, recombined cells include many spiral ganglion neurons, some support cells and hair cells, and many other non-sensory cells (Figure A1.1A). In the cristae, recombined cells include most support cells, some hair cells, and many non-sensory epithelial cells, including those found in the ampulla and in the crux eminentia (Figure A1.1B,C). Vipr2 was originally identified in the pituitary (Lutz*, et al.,* 1993, Inagaki*, et al.,* 1994) and has no known role in the inner ear, including no expression at E14.5 as assayed by *in situ* hybridization (Visel*, et al.,* 2004).

Satb2-Cre transgenic mice (GENSAT)(Gong, *et al.,* 2007, Gerfen, *et al.,* 2013) express a non-inducible Cre recombinase under the special AT-rich sequence-binding protein 2 (Satb2) promoter. In the adult cochlea, recombined cells include many spiral ganglion neurons (Figure A1.1D), inner hair cells, and support cells, including pillar cells (Figure

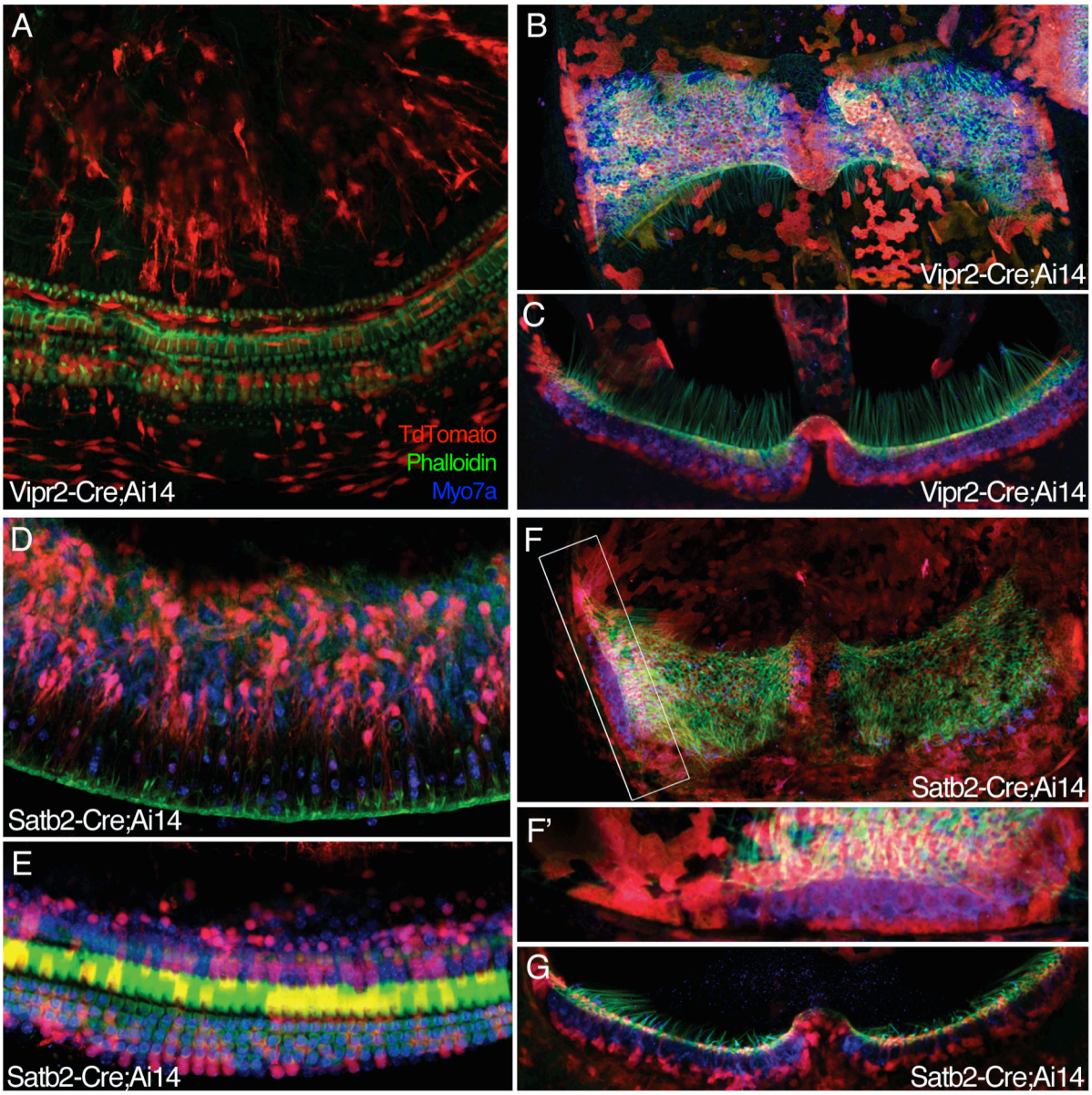

Figure A1.1 Cre recombinase strains ubiquitously expressed in the inner ear. **A-C)** Adult Vipr2-Cre;Ai14 mice show recombination in most cell types of the inner ear in both the cochlea (A) and the cristae (B,C). **D-G)** Adult Satb2-Cre;Ai14 also mice show recombination in most cell types of the inner ear in both the cochlea (D,E) and the cristae (F,F',G).

A1.1E). In the adult cristae, recombined cells include most non-sensory epithelial cells (Figure A1.1F) in addition to some hair cells (Figure A1.1F') and most support cells (Figure A1.1G). Satb2 is a transcription factor thought to mediate long-term epigenetic changes in chromatin configuration (reviewed in Leyva-Diaz and Lopez-Bendito, 2013). When assayed by *in situ* hybridization, Satb2 was not found in E13.5 or early postnatal ears (Gray, *et al.,* 2004); however, Satb2 does have a well-characterized role in the development of callosal projection neurons in the cortex (Britanova, *et al.,* 2006, Szemes, *et al.,* 2006, Holm, *et al.,* 2007, Alcamo, *et al.,* 2008, Gyorgy, *et al.,* 2008, Leone, *et al.,* 2008, Lickiss, *et al.,* 2012, Srinivasan, *et al.,* 2012, Zhang, *et al.,* 2012, Huang, *et al.,* 2013, Leone, *et al.,* 2014).

A1.1.2 CRE RECOMBINASES WITH INTERESTING EXPRESSION

Dlx5-CreERT2 knock-in mice (NIH Blueprint and Josh Huang, Cold Spring Harbor Laboratory) express an inducible Cre recombinase in the distal-less homeobox 5 (Dlx5) native locus. In the adult cochlea, recombined cells include the spiral ganglion neurons and other non-sensory cells (Figure A1.2A). In the adult cristae, almost all non-sensory epithelial cells recombine (Figure A1.2B), in addition to some support cells (Figure A1.2C). Normally, Dlx5, assayed by *in situ* hybridization, is expressed throughout inner ear development including in the otic placode at E8.5 and in the postnatal ear (Simeone, *et al.,* 1994, Yang, *et al.,* 1998, Depew, *et al.,* 1999, Wang, *et al.,* 2001, Wright and Mansour, 2003, Gray, *et al.,* 2004, Ozaki, *et al.,* 2004, Visel, *et al.,* 2004, Moraes, *et al.,* 2005, Lillevali, *et al.,* 2006, Hwang, *et al.,* 2009, Yokoyama, *et al.,* 2009). In addition, Dlx5 is critical for the development of the vestibular organs, including the cristae, canals, and endolymphatic duct, with a lesser effect

on the maculae (Acampora*, et al.,* 1999, Depew*, et al.,* 1999) (reviewed in Chatterjee*, et al.,* 2010).

Gpr26-Cre transgenic mice (GENSAT)(Gerfen*, et al.,* 2013) express a non-inducible Cre recombinase under the G-protein-coupled receptor 26 (Gpr26) promoter. In the adult

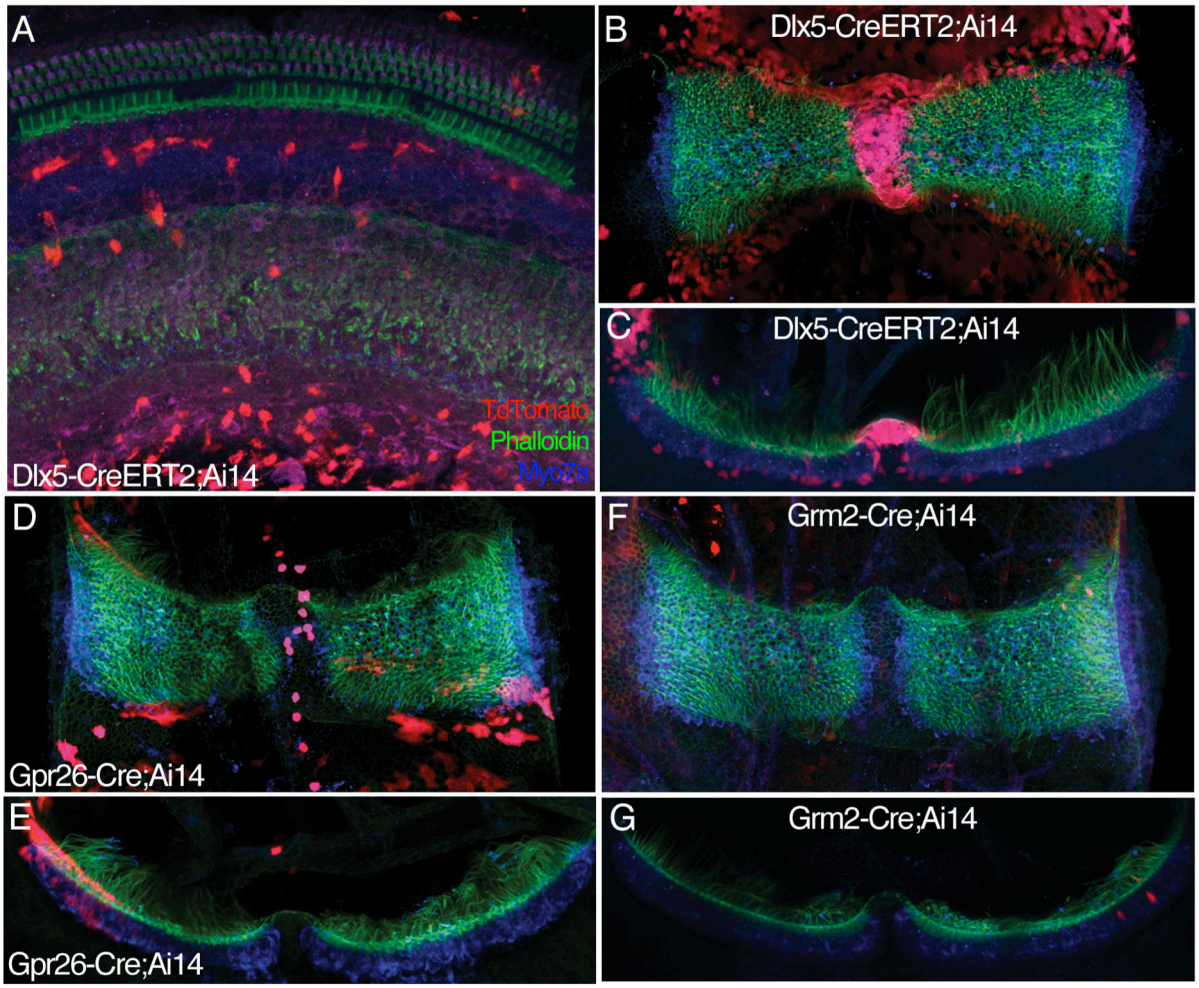

Figure A1.2 Cre recombinase strains with interesting expression patterns. **A)** Adult Dlx5-CreERT2;Ai14 mice show recombination in the cochlea in the spiral ganglion, as well as in some other non-sensory cells. **B-C)** In the cristae, Dlx5-CreERT2;Ai14 mice show recombination in some support cells as well as in every other non-sensory epithelial cell including in the crux eminentia. **D-E)** Adult Gpr26-Cre;Ai14 mice show recombination in only a few cells, including some support cells in a small region of peripheral cristae, some non-sensory epithelial cells, and a scattering of cells along the midline of the ampulla parallel to the axis of the semicircular canal. **F-G)** Adult Grm2-Cre;Ai14 mice have almost no recombination in the inner ear. Interestingly though, they consistently show recombination in less than a handful of hair cells per cristae in approximately the same region.

cochlea, there was very little recombination overall with tdTomato expression in only a few inner hair cells, inner phalangeal cells, and spiral ganglion neurons (data not shown). In the adult cristae, expression was also fairly low, with recombination in some peripheral support cells and non-sensory epithelial cells (Figure A1.2D,E). Though many cells do not express the Gpr26 transgene, there was a scattering of recombined cells along the midline of the ampulla parallel to the axis of the semicircular canal, which was interesting but not particularly useful (Figure A1.2D). Normally, Gpr26 is expressed in the spiral ganglion and fibrocytes of the inner ear at P5 and is one of three candidate genes for the headbobber mice (Buniello*, et al.,* 2013). Headbobber mice have vestibular and hearing impairment at two weeks of age (Somma*, et al.,* 2012) and morphologically lack semicircular canals and cristae, have fused maculae, and have severe cochlear abnormalities (Buniello*, et al.,* 2013). Based on the severity of the phenotype of the headbobber mice, it is surprising that the Gpr26 transgene is not expressed in more cells; however, it is possible that the Gpr26 transgene is not faithfully reporting on the endogenous expression of Gpr26 or that Gpr26 is not the causative gene for the headbobber phenotype.

Grm2-Cre transgenic mice (GENSAT)(Gerfen*, et al.,* 2013) express a non-inducible Cre recombinase under the metabotropic glutamate receptor 2 (Grm2) promoter. This transgene was not expressed in the cochlea and in the cristae was only expressed in a couple of hair cells per crista (Figure A1.2F,G). Interestingly, these hair cells were found in all of the cristae screened and were located in the same region in similar numbers in each crista. However, since only a few cells in the sensory organs express this transgene, it is not very useful and unlikely to be playing an important role in the inner ear.

A1.1.3 CRE RECOMBINASES EXPRESSED IN HAIR CELLS

Calb2-IRES-Cre knock-in mice (NIH Blueprint and Josh Huang, Cold Spring Harbor Laboratory)(Taniguchi*, et al.,* 2011) express a non-inducible Cre recombinase in the Calretinin (also known as Calbindin 2) native locus. The expression of Calretinin in the inner ear is well described and is mostly recapitulated in these knock-in mice. In the cochlea,

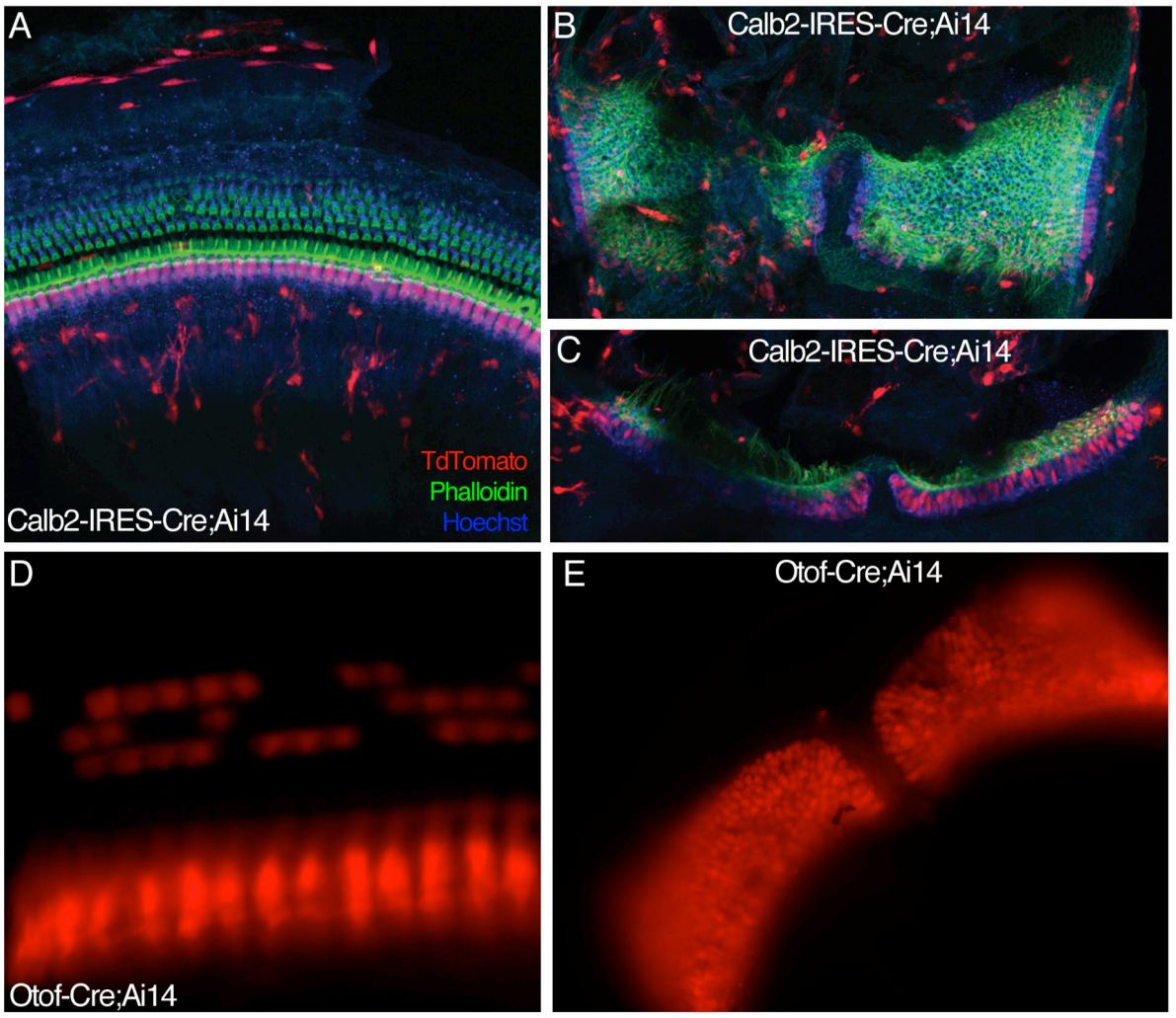

Figure A1.3 Cre recombinase strains expressed in hair cells. **A)** Adult Calb2-IRES-Cre;Ai14 mice show recombination in all inner hair cells in the cochlea in addition to in some ganglion cells and non-sensory cells. **B-C)** In the cristae, adult Calb2-IRES-Cre;Ai14 mice show recombination in almost all hair cells (dark area in C is shadowed by pigment) as well as in some non-sensory cells. **D)** Adult Otof-Cre;Ai14 show recombination in all inner hair cells and in a random pattern of outer hair cells in all three hair cell rows. **E)** In the cristae, adult Otof-Cre;Ai14 mice show recombination in all hair cells.

recombined cells include the inner hair cells, outer hair cells, some non-sensory cells, and some ganglion cells, as expected (Figure A1.3A) (Rogers, 1989, Dechesne, *et al.,* 1991, Desmadryl and Dechesne, 1992, Dechesne, *et al.,* 1993, Dechesne, *et al.,* 1994). In the cristae, most of the recombined cells were hair cells in addition to some non-sensory cells and neuronal like cells (Figure A1.3B,C). While this expression is in agreement with previous studies (Dechesne, *et al.,* 1994), these mice lack recombination in the calyces of the afferent nerve fibers, which is the characteristic expression pattern for Calretinin in the mature cristae and utricle (Rogers, 1989, Dechesne, *et al.,* 1991, Desmadryl and Dechesne, 1992, Dechesne, *et al.,* 1993, Dechesne, *et al.,* 1994).

Otof-Cre knock-in mice (NIH Blueprint and Ulrich Mueller, The Scripps Research Institute) express a non-inducible Cre recombinase in the Otoferlin native locus. Like Calretinin, the expression of Otoferlin in the inner ear is well characterized and mostly recapitulated in these knock-in mice. In the cochlea, recombined cells included all inner hair cells and a smattering of outer hair cells located in all three hair cell rows (Figure A1.3D). In the cristae, only the hair cells underwent recombination (Figure A1.3E), consistent with the endogenous expression previously described (Schug, *et al.,* 2006). In the cochlea, Otoferlin is endogenously expressed in inner hair cells, a subset of low frequency outer hair cells, and some auditory nerve fibers (Engel, *et al.,* 2006, Roux, *et al.,* 2006).

A1.1.4 CRE RECOMBINASES EXPRESSED IN SUPPORT CELLS

Wfs1-TG2-CreERT2 transgenic mice (Theresa Zwingman and Ed Lein, Allen Institute for Brain Science) express an inducible Cre recombinase under the Wolfram

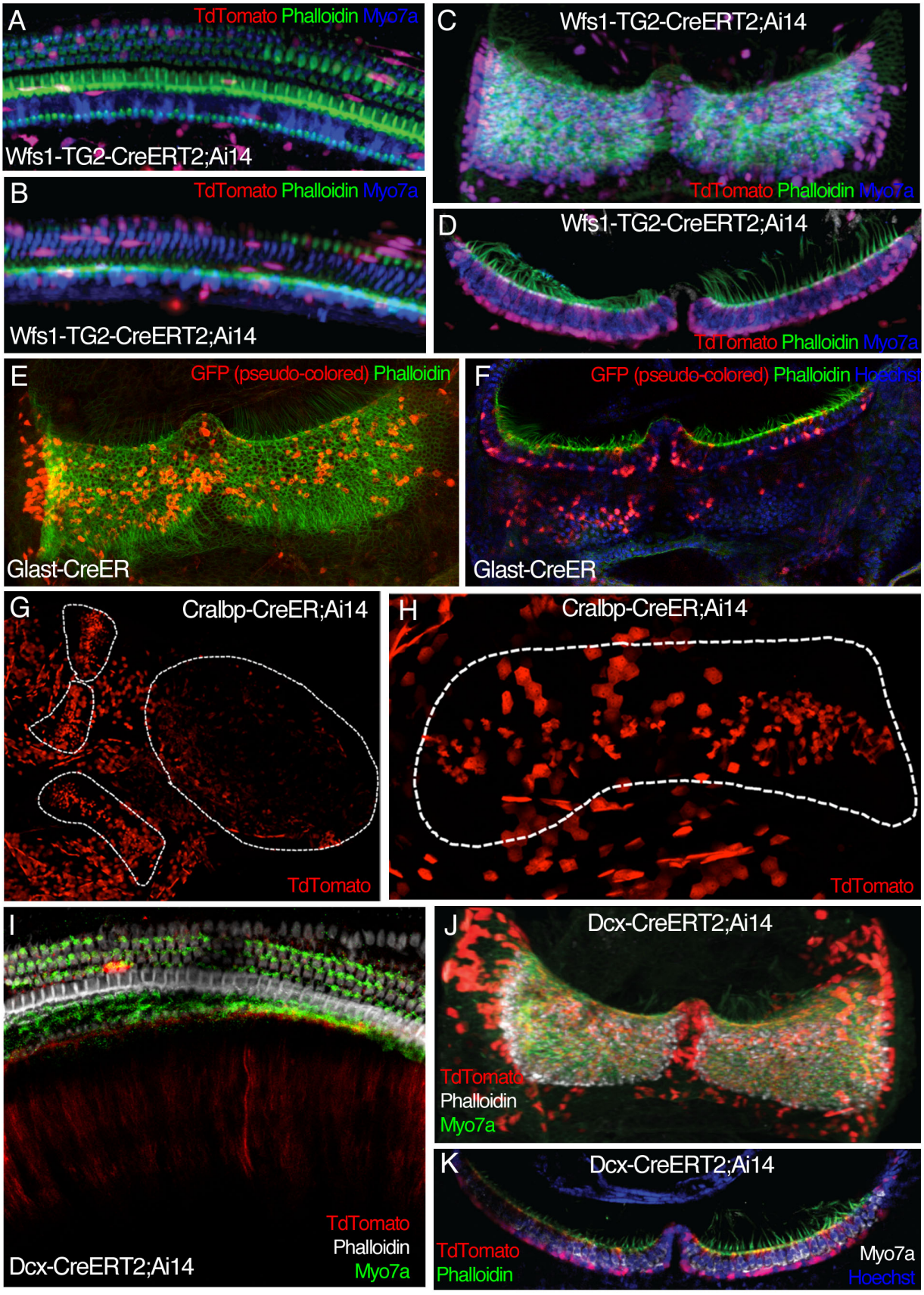
A
TdTomato Phalloidin Myo7a
Wfs1-TG2-CreERT2;Ai14
B
TdTomato Phalloidin Myo7a
Wfs1-TG2-CreERT2;Ai14
C
Wfs1-TG2-CreERT2;Ai14
TdTomato Phalloidin Myo7a
D
Wfs1-TG2-CreERT2;Ai14
TdTomato Phalloidin Myo7a
E
GFP (pseudo-colored) Phalloidin
Glast-CreER
F
GFP (pseudo-colored) Phalloidin Hoechst
Glast-CreER
G
Cralbp-CreER;Ai14
TdTomato
H
Cralbp-CreER;Ai14
TdTomato
I
TdTomato
Phalloidin
Myo7a
Dcx-CreERT2;Ai14
J
Dcx-CreERT2;Ai14
TdTomato
Phalloidin
Myo7a
K
Dcx-CreERT2;Ai14
TdTomato
Phalloidin
Myo7a
Hoechst

Figure A1.4 Cre recombinase strains expressed in support cells. **A,B)** Adult Wfs1-TG2-CreERT2;Ai14 mice show recombination in the cochlea in some support cells and non-sensory cells. **C,D)** In the cristae, Wfs1-TG2-CreERT2;Ai14 mice show recombination mainly in support cells, but also in some hair cells and non-sensory cells. **E,F)** Adult Glast-CreER knock-in mice show recombination in a scattering of support cells throughout the sensory epithelium. **G,H)** P14 Cralbp-CreER;Ai14 mice show recombination in many non-sensory cells of the ampulla and canals, with less recombination occurring around the utricle. In addition, they show recombination in many support cells located in the central zone of the cristae. White dotted lines indicate the location of the sensory epithelia, including the two cristae and the utricle. **I)** Adult Dcx-CreERT2;Ai14 mice show the expected pattern of recombination in the cochlea with recombination mainly in the nerve fibers of the spiral ganglion neurons. **J,K)** In the cristae, however, adult Dcx-CreERT2;Ai14 mice show recombination almost exclusively in the support cells.

syndrome 1 homolog (Wfs1) promoter. In the cochlea, the identity of recombined cells was varied, including support cells and several other types of non-sensory cells (Figure A1.4A,B). In the cristae, support cells throughout the entire sensory epithelium were labeled almost exclusively (Figure A1.4C,D). If not for the presence of some recombined hair cells, this transgenic line would be excellent for support cell lineage tracing. Even with some hair cell recombination, these mice may still be useful for experiments involving fluorescence-activated cell sorting (FACS). In humans, mutations in Wfs1 are associated with Wolfram syndrome and non-syndromic progressive low-frequency sensorineural hearing impairment (Bespalova*, et al.,* 2001, Young*, et al.,* 2001). In the adult cochlea, Wfs1 is normally expressed in many cells, including inner and outer hair cells, spiral ganglion neurons, Deiters' cells, Hensen cells, Claudius cells, and cells in the interdental region, Reissner's membrane, and the spiral ligament (Cryns*, et al.,* 2003). In the vestibular system, Wfs1 is normally expressed in both hair cells and support cells (Cryns*, et al.,* 2003).

Both Glast-CreER transgenic (Wang*, et al.,* 2012) and knock-in mice (Mori*, et al.,* 2006) express an inducible Cre recombinase under the glutamate aspartate transporter (Glast) promoter. I did not analyze the cochlea of the Glast-CreER mice, but found in the cristae of both the transgenic and the knock-in mice that recombination exclusively occurred in a smattering of support cells found throughout the sensory epithelium (Figure A1.4E,F). This pattern of expression makes Glast a good candidate for lineage tracing support cells; however, the efficiency of recombination in both the transgenic and the knock-in mice is low. Endogenously, Glast is expressed in the support cells of the vestibular system, the support cells surrounding inner and outer hair cells, and in satellite cells ensheathing type I

spiral ganglion neurons (Li*, et al.,* 1994, Furness and Lehre*,* 1997, Takumi*, et al.,* 1997, Furness*, et al.,* 2002, Jin*, et al.,* 2003).

Cralbp-CreER transgenic mice (Vazquez-Chona*, et al.,* 2009) express an inducible Cre recombinase under the Retinaldehyde binding protein 1 (Rlbp1/Cralbp) promoter. I only analyzed the vestibular system, where recombination occurred in many non-sensory epithelial cells around the cristae, including in the ampulla and the semicircular canals. In addition, support cells recombined specifically in the central region of the cristae, where the type I hair cells that receive calyx afferent nerve innervation are located (Figure A1.4G,H). Very little recombination occurred in the utricle and its surrounding tissues (Figure A1.4G). Based on the expression in the cristae, this transgenic line would be very useful for lineage tracing support cells in the central region. Endogenously, Cralbp has no known function or expression in the inner ear, but is expressed by Müller glia in the retina (Bunt-Milam and Saari*,* 1983, Anderson*, et al.,* 1986) (reviewed in Saari and Crabb*,* 2005). Müller glia are very similar to support cells and serve similar functions in the retina as support cells in the inner ear, including acting as the progenitor cell that undergoes reprogramming during regeneration in lower vertebrates (reviewed in Goldman*,* 2014).

Dcx-CreER transgenic mice (Cheng*, et al.,* 2011) express an inducible Cre recombinase under the Doublecortin (Dcx) promoter. In the cochlea, Dcx transgenic mice show recombination in the nerve fibers extending from the spiral ganglion to the cochlea, as well as in the bouton afferents innervating the inner and outer hair cells (Figure A1.4I). In the cristae, however, Dcx transgenic mice show recombination primarily in the support cells throughout the entire sensory epithelium. In addition, the efficiency of recombination is

higher than that in the Glast-CreER mice (Figure A1.4E,F), making the Dcx-CreER mice a better candidate for support cell lineage tracing. Endogenously, Dcx is expressed in neurons during development (Francis*, et al.,* 1999, Gleeson*, et al.,* 1999, Tanaka*, et al.,* 2004) and in regions of the adult brain where there is ongoing neurogenesis, including the subventricular zone and the subgranular zone (Nacher*, et al.,* 2001, Brown*, et al.,* 2003, Rao and Shetty*,* 2004, Couillard-Despres*, et al.,* 2005). In neurons, Dcx mainly associates with microtubules (Francis*, et al.,* 1999, Gleeson*, et al.,* 1999, Horesh*, et al.,* 1999), but has also been shown to interact with actin (Tsukada*, et al.,* 2003, Tsukada*, et al.,* 2005, Tsukada*, et al.,* 2006). More specifically, Dcx promotes the nucleation, assembly, and stability of microtubules (Moores*, et al.,* 2004, Fourniol*, et al.,* 2010) and decreases the dissociation of other nearby molecules from the microtubules (Bechstedt and Brouhard*,* 2012) (reviewed in Reiner*,* 2013).

A P P E N D I X T W O

SUPPLEMENTAL MOVIES

MOVIE 1.1

The inner ear contains six distinct sensory organs: The cochlea, utricle, saccule, posterior cristae, horizontal cristae, and anterior cristae. These organs be seen in an intact E15.5 inner ear labeled for the sensory regions with Sox2 (white) and in a color coded model of the position of the Sox2-labeled sensory organs created by 3-dimensionally rendering tracings of the Sox2 regions in the individual confocal slices.

MOVIE 2.1

Cristae are highly three-dimensional, composed of two saddle-shaped hemicristae separated by the eminentia cruciatum. Sox9 (red) labels support cells as well as non-sensory cells in the eminentia cruciatum and throughout the ampulla and semicircular canals. Gfi1 (white) labels all hair cells in the sensory epithelium. Hes5-GFP is expressed in a subset of support cells in the Calretinin-negative peripheral zone. Note that while the overall structure of the sensory epithelium was preserved, the normally dome-like $Sox9^+$ ampulla flattened onto the sensory epithelium. Dimensions in μm (w x h x d) - 544.9 x 272.5 x 75.5.

MOVIE 2.2

An example of a lineage traced transitional cell from the mTmG mouse (see Figure 7B-B"). The GFP^+ cell expressed Gfi1, but had an elongated body similar to a support cell. The nucleus was lifting off of the basement membrane and the apical part of the cell had an unusual appearance unlike a normal hair cell or support cell. There was also another GFP^+ support cell that spans the sensory epithelium as well as several non-sensory cells in view. Dimensions in μm (w x h x d) – 36.4 x 61.2 x 6.9.

MOVIE 2.3

An example of a lineage traced transitional cell from the mTmG mouse (see Fig. 7C-C"). The GFP$^+$ cell expresses Gfi1 and overall has a normal appearance for a hair cell, except for a thin foot-like projection that extends to the basement membrane. Also in view are two support cells, one of which is directly next to the hair cell. Dimensions in μm (w x h x d) – 43.3 x 52.6 x 13.0.

MOVIE 2.4

An example of a lineage traced hair cell with a kinocilium from the mTmG mouse (see Fig. 7D-D"). The GFP$^+$ cell expressed Gfi1 (red) and had a flask shape with a rounded bottom and a thin neck. A long kinocilium extended up from the apical surface. Nuclei are labeled with Hoechst 33342 (white) and had prominent nucleoli at this fluorescent intensity. Also in view were a couple of GFP$^+$ support cells and a non-sensory cell. Dimensions in μm (w x h x d) – 28.7 x 64.2 x 13.5.

CURRICULUM VITAE

AMBER D. SLOWIK

EDUCATION

[JUNE 2015 – JUNE 2016] **Seattle Pacific University** [Seattle, WA]
Masters in Teaching Math and Science

[SEPT 2009 – JUNE 2015] **University of Washington** [Seattle, WA]
PhD Candidate, Neuroscience
GPA: 3.80/4.0
Thesis Advisor: Olivia Bermingham-McDonogh
Thesis Project: "Hair cell regeneration in the cristae of the adult mouse"

Related Course Work:

- [-] Developmental Neurobiology
- [-] Applied Biostatistics I
- [-] hESCs & Regenerative Medicine
- [-] Signal Transduction
- [-] Development
- [-] Modeling Proteomes

[AUG 2011] **Marine Biological Laboratory** [Woods Hole, MA]
Biology of the Inner Ear Course

[AUG 2005 - MAY 2009] **Rensselaer Polytechnic Institute** [Troy, NY]
BS, Bioinformatics and Molecular Biology, *magna cum laude*
BS, Biochemistry and Biophysics, *magna cum laude*
Major GPA: 3.91/4.0
GPA: 3.77/4.0

Related Course Work:

- [-] Molecular Biology Lab
- [-] Genetic Engineering with Lab
- [-] Comp. Biology and Bioinformatics
- [-] Computer Science I and II
- [-] Data Structures and Algorithms
- [-] Database Systems

RESEARCH EXPERIENCE AND FELLOWSHIPS

[JUL 2013 – JUNE 2015] **University of Washington** [Seattle, WA]
Neurobiology Training Grant Fellowship

[JUL 2010 – JUN 2013] **University of Washington** [Seattle, WA]
Cellular and Molecular Biology Training Grant Fellowship

[JUL 2006 - MAY 2009] **Rensselaer Polytechnic Institute** [Troy, NY]
Funding awarded by the Undergraduate Research Program
Research Advisor: Russell J Ferland
Research Project: "The role of Ahi1 in primary cilium function and genesis"

Determine the effect of loss of Ahi1, a novel gene implicated in the neurodevelopmental disorder Joubert Syndrome, in the function and generation of primary cilia in cell cultures using siRNA and in the kidneys of mice deficient in Ahi1 using immunocytochemistry, immunohistochemistry, and western blotting. Determine possible mechanisms for primary cilium regulation using molecular cloning techniques, overexpression, and coimmunoprecipitation.

PUBLICATIONS

1. **Slowik, AD** and Bermingham-McDonogh, O (in review). A medial to lateral wave in cell cycle exit and hair cell differentiation in the developing mouse cristae.
2. **Slowik, AD** and Bermingham-McDonogh, O (**2013**). Notch signaling in hair cell regeneration (review). *Trends Dev Biol*, 7, 73-89.
3. **Slowik, AD** and Bermingham-McDonogh, O (**2013**). Hair cell generation by notch inhibition in the adult mammalian cristae. *JARO*, 14, 813-28.
4. Hayashi T, Lamba DA, **Slowik A**, Reh TA, Bermingham-McDonogh O (**2010**). A method for stabilizing RNA for transfection that allows control of expression duration. *Dev Dyn,* 239, 2034-40.
5. Doering JD, Kane K, Hsiao YC, Yao C, Shi B, **Slowik AD**, Dhagat B, Scott DD, Ault JG, Page-McCaw PS, Ferland RJ (**2008**). Species differences in the expression of Ahi1, a protein implicated in the neurodevelopmental disorder Joubert syndrome, with preferential accumulation to stigmoid bodies. *J Comp Neurol,* 511, 238-56.

TALKS

1. **Slowik, AD**, Bermingham-McDonogh O. A spatial analysis of hair cell development in the mouse cristae. 37th Midwinter Meeting of the Association for Research in Otolaryngology (ARO), San Diego, CA, February 22-26, 2014.
2. **Slowik, AD**, Bermingham-McDonogh O. Hair cell regeneration in the cristae of the mouse. 2012 NW Auditory and vestibular research meeting, Portland, OR, October 25-26, 2012.
3. **Slowik, AD**. Ear development and regeneration. Session: Gene Networks and Endless Things Most Beautiful in Cell, Developmental and Evolutionary Biology. SACNAS, Seattle, WA, October 10-14, 2012.
4. **Slowik AD**, Bermingham-McDonogh O. Hair cell transdifferentiation in the cristae of the postnatal to adult mouse. 2012 Northwest Developmental Biology (NWDB) Conference, Friday Harbor, WA, March 14-17, 2012.
5. **Slowik AD**, Hartman, B, Bermingham-McDonogh O. Hair cell regeneration in the cristae of the adult mouse. University of Washington Institute for Stem Cell and Regenerative Medicine 2012 Symposium, Seattle, WA, January 12, 2012.

POSTERS

1. **Slowik AD** and Bermingham-McDonogh O. A spatial analysis of hair cell development in the mouse crista. 73rd Annual Meeting of the Society for Developmental Biology (SDB), Seattle, WA, July 17-21, 2014.
2. **Slowik AD**, Hartman B, Bermingham-McDonogh O. Hair cell transdifferentiation in the cristae of the postnatal to adult mouse. 35th Midwinter Meeting of the Association for Research in Otolaryngology (ARO), San Diego, CA, February 25-29, 2012.
3. **Slowik AD**, Hartman B, Bermingham-McDonogh O. Hair cell regeneration in the cristae of the adult mouse. University of Washington South Lake Union Group Research Symposium, Seattle, WA, May 25, 2011.
4. **Slowik AD**, Hartman B, Sudar S, Bermingham-McDonogh O. A method for culturing cristae *in vitro*. Poster presentation at the Northwest Auditory Vestibular Research Meeting, Seattle, WA, October 22-23, 2010.

Technical Experience

Mice Husbandry, genotyping, breeding (including crosses for Cre/lox, Tet-on/off).

Dissection Embryonic, postnatal, and adult inner ear (embryonic and postnatal cochlea; embryonic, postnatal and adult utricle; postnatal and adult cristae).

Cell Culture Dissociated cell culture, primary organotypic culture, DNA transfection, DNA and RNA electroporation.

Molecular Biology PCR/RT-qPCR, DNA purification and amplification, subcloning, cloning from genomic DNA and cDNA libraries, primer design, *in vitro* transcription.

Imaging Confocal, multi-photon, epifluorescence, light, and phase contrast microscopy.

Biochemistry Western blotting and co-immunoprecipitation pull-down assay.

Histology Sample sectioning (cryostat and paraffin) and general tissue staining methods.

Other Prism, ImageJ, Photoshop, Illustrator, Microsoft Office suite, and working knowledge of C^{++} and Python programming languages.

Teaching Experience

[Spring 2014] **University of Washington** [Seattle, WA]
Teaching Instructor
Current Research Literature in Neurobiology

[Winter 2011] **University of Washington** [Seattle, WA]
Teaching Intern
Introduction to Cellular and Molecular Neurobiology (Lab)

Honors and Awards

[Mar 2012] **Northwest Developmental Biology Conference** [Friday Harbor, WA]
Genesis Award

[Oct 2007] **Rensselaer Polytechnic Institute** [Troy, NY]
Founder's Award of Excellence